THE DEVELOPMENT OF ANALYTICAL METHODS TO ELUCIDATE THE CHEMICAL FORMS OF Cu, Zn, Cd AND Pb IN SOIL CONTAMINATED BY SEWAGE SLUDGE AND OTHER EFFLUENTS.

JOHN SCOTT PARK

A thesis submitted in partial fulfilment of the
requirements of the Council for National Academic Awards
for the degree of Doctor of Philosophy

July 1990

Robert Gordons Institute of Technology
Aberdeen

To Mum and Dad

ACKNOWLEDGEMENT

Firstly, I would like to thank both my Supervisors, Dr. A.R. Morrisson and Dr. B.L. Sharp for the excellent supervision and encouragement provided throughout this project. I would like to thank Dr. M.L. Berrow (Macaulay Land Use Research Institute, Aberdeen) for his help during the sampling stages and for providing much background knowledge about some of the sampling sites visited during this work. Special thanks go to Mrs. M. Mitchell for her technical assistance and to Mrs. L. Keddie for typing this thesis.

My thanks to the Science and Engineering Research Council for funding this research project and the Macaulay Land Use Research Institute for providing the facilities and expertise that made this project possible.

Finally, I thank my wife, Violet who has been a constant source of encouragement throughout my research.

ABSTRACT

The contents of this thesis describes the development of an analytical method to determine the chemical speciation of heavy metals in soils contaminted by sewage sludge and distillery wastes.

Chapter one serves as an introduction discussing the various heavy metal species that can occur in soils. The chapter also contains a review of the analytical methods that have already been used in speciation studies and discusses their suitability for this particular problem.

Chapter two is mainly concerned with the derivation of a relationship between the electrical conductivity and ionic strength of soil solutions.

Chapter three describes the development of suitable sampling techniques for the study of chemical speciation in soils.

Chapter four describes the development of the Size Exclusion Chromatography (SEC) separation technique chosen to separate the species of interest. The chapter also describes how this technique was interfaced to Graphite Furnace Atomic Absorption Spectrometry in order to detect the copper content of the various soil solution species.

Chapter five extends the above technique to the study of the long term partioning of copper in water extracts of sewage sludge and distillery waste polluted soils and compares the results with those obtained from previous studies on the same sampling sites.

Chapter six investigates the possibility of utilizing Inductively Coupled Plasma Optical Emission Spectrometry as a detector for the SEC separation technique.

Chapter seven contains suggestions for future research.

I N D E X

ACKNOWLEDGEMENT i

ABSTRACT ii

1.0 *INTRODUCTION* 2

1.1 *THE REACTIONS OF HEAVY METALS IN SOILS* 3

1.2 *THE IMPORTANCE OF HUMIC MATERIAL IN SOILS* 3

1.2.1 *Complexation of metal ions with humic material* 5

1.3 *THE COMPLEXATION OF HEAVY METALS WITH LOW MOLECULAR WEIGHT LIGANDS* 8

1.4 *THE INORGANIC SPECIATION OF Cu, Zn, Cd AND Pb IN SOILS* 8

1.4.1 *Inorganic solution equilibria* 8

1.4.1.1 Equilibrium constants 8

1.4.1.2 Activity Coefficients 9

1.4.1.3 Ionic strength 9

1.4.1.4 Debye-Hückel equations 10

1.4.2 *Copper* 11

1.4.3 *Zinc* 12

1.4.4 *Cadmium* 13

1.4.5 *Lead* 14

1.5 *AVAILABILITY AND TOXICITY OF HEAVY METAL SPECIES IN SOILS* 15

1.6 *ANALYTICAL METHODS FOR THE DETERMINATION OF HEAVY METAL SPECIATION* 16

1.6.1 *Thermodynamic calculation of metal speciation* 16

1.6.2 *Experimental determination of metal speciation in solution* 17

1.6.2.1 Physical properties 18

1.6.2.2 Chemical Properties 22

1.7 *CONCLUSIONS* 26

REFERENCES 27

2.1 *BACKGROUND* 31

2.2 *THE VARIATION OF CONDUCTIVITY WITH IONIC STRENGTH FOR SIMPLE ELECTROLYTES* 32

2.2.1 *Apparatus* 32

2.2.2 *Procedure* 32

2.2.3 *RESULTS* 32

2.3 *DISCUSSION* 38

2.4 *MEASUREMENT OF THE ELECTRICAL CONDUCTIVITY OF MODEL SOLUTIONS PERTAINING TO SOIL WATERS* 41

2.4.1 *Background* 41

2.4.2 *Ion-pair concentrations* 42

2.4.3 *Calculation of ion-pair concentrations* 44

2.4.4 *Mixed electrolyte solutions* 46

2.4.5 *Determination of the relationship between ionic strength and conductivity* 47

2.4.5.1 Experimental 48

2.4.5.2 Results 48

2.4.5.3 Discussion 48

2.5 *APPLICATION OF THE IONIC STRENGTH v's CONDUCTIVITY RELATIONSHIP TO MODEL SOLUTIONS OF THE SOIL SITES OF INTEREST* 51

2.5.1 *Sample collection* 51

2.5.2 *Sample preparation* 52

2.5.3 *Chemical analysis* 54

2.5.4 *Cation analysis* 54

2.5.4.1 Inductively coupled plasma optical emission spectroscopy (ICP-OES) 54

2.5.4.2 Atomic Absorption Spectroscopy 54

2.5.5 *Techniques for the analysis of anions* 55

2.5.5.1 High performance ion chromatography (HPIC) for the determination of Cl^-, NO_3^-, SO_4^{2-} 55

2.5.5.2 Colorimetry 57

2.5.5.3 pH measurement 58

2.5.6 *Results* 58

2.5.7 *Discussion* 58

2.5.8 *Modification of IPC in order that the concentration of phosphate ion-pairs can be taken into account* 64

2.5.9 *Correlation of ionic strength and conductivity* 65

2.5.10 *Results* 65

2.5.11 *Conclusion* 67

REFERENCES 68

APPENDIX 2.1 69

APPENDIX 2.2 73

3.1 *INTRODUCTION* 78

3.2 *FIELD SAMPLING PROCEDURE* 78

3.3 *INITIAL EXTRACTION AND ANALYSIS OF SOIL SOLUTIONS* 79

3.3.1 *Apparatus* 79

3.3.2 *Reagents* 79

3.3.3 *Procedure* 80

3.3.4 *Analysis* 80

3.4 *ANALYSIS OF SOIL SOLUTION* 84

3.4.1 *Cationic Analysis of Soil Solutions* 85

3.4.2 *Anionic analysis of soil solutions* 86

3.4.2.1 Apparatus 86

3.4.2.2 Results 86

3.4.3 *Moisture Content* 87

3.4.4 *pH and Conductivity* 87

3.4.4.1 Apparatus 87

3.4.4.2 Results 87

3.5 *SAMPLING TRIP 2* 88

3.5.1 *Sampling and Analysis* 88

3.5.2 *Results and Discussion* 88

3.6 *SAMPLING TRIP 3* 88

3.6.1 *Sampling and Analysis* 88

3.6.2 *Results and discussion* 90

3.7 *SUBSEQUENT SAMPLING TRIPS* 90

3.7.1 *Sampling* 90

3.7.2 *Results and Discussion* 90

3.8 *THE CORRELATION OF THE IONIC STRENGTH ESTIMATED FROM CONDUCTIVITY MEASUREMENTS WITH THE EXPERIMENTALLY DETERMINED IONIC STRENGTH* 93

3.8.1 *Procedure* 93

3.8.2 *Discussion* 93

3.9 *THE CORRELATION OF IONIC CONCENTRATIONS WITH MOISTURE CONTENT* . . 95

3.9.1 *Procedure* 95

3.9.2 *Results* 95

3.9.2.1 Anions 95

3.9.2.2 Cations 95

3.9.2.3 Copper 95

3.9.2.4 Ionic Strength 105

3.9.3 *Discussion* 105

REFERENCES 107

4.1 *INTRODUCTION* 109

4.2 *PRINCIPLES OF SIZE EXCLUSION CHROMATOGRAPHY* 110

4.3 *THEORY OF SIZE EXCLUSION CHROMATOGRAPHY* 111

4.3.1 *The distribution coefficient* 111

4.3.2 *Calibration Curves for SEC* 112

4.4 *THE EFFECTS OF IONIC STRENGTH ON THE ELUTION VOLUME OF ORGANIC LIGANDS PERTAINING TO SOIL SOLUTIONS* 114

4.4.1 *Apparatus* 114

4.4.2 *Reagents* 114

4.4.3 *Experimental* 115

4.4.4 *Results and Discussion* 116

4.5 *THE SIZE EXCLUSION CHROMATOGRAPHY OF SOIL SOLUTIONS* 130

4.5.1 *Apparatus* 130

4.5.2 *Experimental* 130

4.5.3 *Results and Discussion* 130

4.6 *THE MOLECULAR WEIGHT PROFILE OF ORGANNOCOPPER SPECIES IN SOIL SOLUTIONS* 138

4.6.1 *Apparatus* 138

4.6.2 *Experimental* 138

4.6.3 *Results and Discussion* 138

REFERENCES 141

APPENDIX 4.1 142

5.1 *INTRODUCTION* 144

5.2 *SAMPLING AND EXTRACTION OF SOILS* 144

5.3 *THE ANALYSIS OF LUDDINGTON WATER EXTRACTS FOR CU BY AAS* . . 145

5.3.1 *Experimental* 145

5.3.2 *Results and Discussion* 145

5.4 *THE SEC/GFAAS ANALYSIS OF LUDDINGTON WATER EXTRACTS* 146

5.4.1 *Experimental* 147

5.4.2 *Results and Discussion* 147

5.5 *MODIFICATION OF THE ANALYTICAL METHOD TO IMPROVE RESOLUTION AND SENSITIVITY* 157

5.5.1 *Experimental* 157

5.5.2 *Results and Discussion* 162

5.6 *COMPARISON OF CU SPECIATION RESULTS WITH OTHER LONG TERM STUDIES CONDUCTED AT THIS SITE* 173

5.6.1 *Introduction* 173

5.6.2 *Results and Discussion* 173

5.7 *THE STUDY OF CU SPECIATION IN SOILS CONTAMINATED WITH DISTILLERY WASTE* 175

5.7.1 *Introduction* 175

5.7.2 *Experimental* 176

5.7.3 *Results and Discussion* 176

5.8 *SUMMARY AND CONCLUSIONS* 182

REFERENCES 184

6.1 *INTRODUCTION* 186

6.2 *NEBULISERS AND SPRAY CHAMBERS COMMONLY USED IN ICP-OES* . . 188

6.2.1 *Pneumatic Nebulisers* 190

6.2.2 *Spray Chambers* 190

6.3 *THE TESTING OF LINEAR CONESPRAY PROTOTYPES WITH VARIOUS SPRAY CHAMBER DESIGNS* 190

6.3.1 *Design of the Linear Conespray Nebuliser* 190

6.3.2 *The evaluation of the Total Transport Efficiency (TTE) of a Meinhard TR-30-C2 nebuliser in a 100 mm double pass spray chamber* 198

6.3.2.1 Experimental 198

6.3.2.2 Results and Discussion 198

6.3.3 *The TTE of a Prototype Linear Conespray in a 100 mm glass bulb recirculatory spray chamber* 199

6.3.3.1 Preparation of prototype Linear Conespray and Recirculatory Spray Chamber 199

6.3.4 *The testing of a new prototype with an improved recirculatory spray chamber* 205

6.3.4.1 Experimental 207

6.3.4.2 Results and Discussion 207

6.4 *THE USE OF A HEATED IMPACT BEAD IN ICP-OES* 209

6.4.1 *The temperature calibration of the Ta strip* 211

6.4.1.1 Thermal Crayons 211

6.4.1.2 Optical Pyrometer 213

6.4.1.3 Thermocouple 213

6.4.2 *The total transport efficiency of the Heated Impact Bead (HIB) spray chamber* 216

6.4.2.1 Experimental 216

6.4.2.2 Results and Discussion 220

6.4.3 *The analytical performance of the heated impact bead spray chamber* 228

6.5 *CONCLUSIONS* 231

REFERENCES 233

7.1 *SUGGESTIONS FOR FURTHER WORK* 235

CHAPTER ONE

INTRODUCTION

1.0 *INTRODUCTION*

In recent years there has been considerable concern regarding the disposal of sewage sludges and other effluents to agricultural land. Farmers are usually keen to have sludge applied to their land as an inexpensive alternative to fertilizer, because the sludge often contains levels of N and P that are beneficial to plant growth. This method of sludge disposal looks set to increase in importance, especially in the light of new government legislation to end the dumping of sewage sludge at sea by 1998. Sludge disposal on land is probably the cheapest alternative especially when compared with the high costs of incineration.

A major problem with this method of sludge disposal is that sludges produced in urban and industrial areas often contain elevated concentrations of potentially toxic heavy metals e.g. Cu, Zn, Cd and Pb which are often present in such effluents [1]. In the North-east of Scotland a similar use is made of distillery waste [2]. These distillery wastes often contain elevated copper concentrations and are potentially toxic to plant life.

At the moment regulatory agencies have defined upper limits for the loading of soils in terms of the extractable contents, using classical diagnostic reagents to determine the total concentration of heavy metals in soils [3]. The problem with this approach is that the toxicity or plant availability of heavy metals is not simply related to their total concentration in the soil. Indeed it is possible for a soil with a high total heavy metal concentration to be less toxic than another soil with a much lower metal concentration [4]. This is because the plant availability of heavy metals in soils is dependant on their

physico-chemical form or "speciation".

1.1 *THE REACTIONS OF HEAVY METALS IN SOILS*

Heavy metals can undergo many reactions with the variety of ligands present in soils (Fig. 1.1). As a result a particular metal can exist as a wide range of species. Metal species exist along a size spectrum ranging from dissolved through colloidal to particulate species [5]. The diversity of species formed depends upon the complexation properties of the metal in question. In the case of copper the majority of the copper will be in the form of organo-copper complexes due to the ability of copper to form very stable complexes with organic ligands [6]. At the other end of the scale zinc tends to predominate as inorganic species due to the low stability of organo-zinc complexes.

The diversity and poorly defined properties of naturally occurring aqueous organic material still constitutes a major drawback in speciation studies. A division between the low molecular weight organic substances and diversified high molecular weight substances (the so called humic substances) is perhaps the clearest division that can be made [7].

1.2 *THE IMPORTANCE OF HUMIC MATERIAL IN SOILS*

By far the most abundant organic material present in soils is the humic material. These substances have been recently defined as "a general category of naturally occurring, biogenic, heterogeneous organic substances that can generally be characterised as being yellow to black in colour, of high molecular weight and refactory" [7]. Although there is much controversy about the actual structure of humic substances it is generally accepted that they consist of an aliphatic/aromatic carbon skeleton and that the predominating metal ion

Fig. 1.1 The reactions of heavy metals in soils

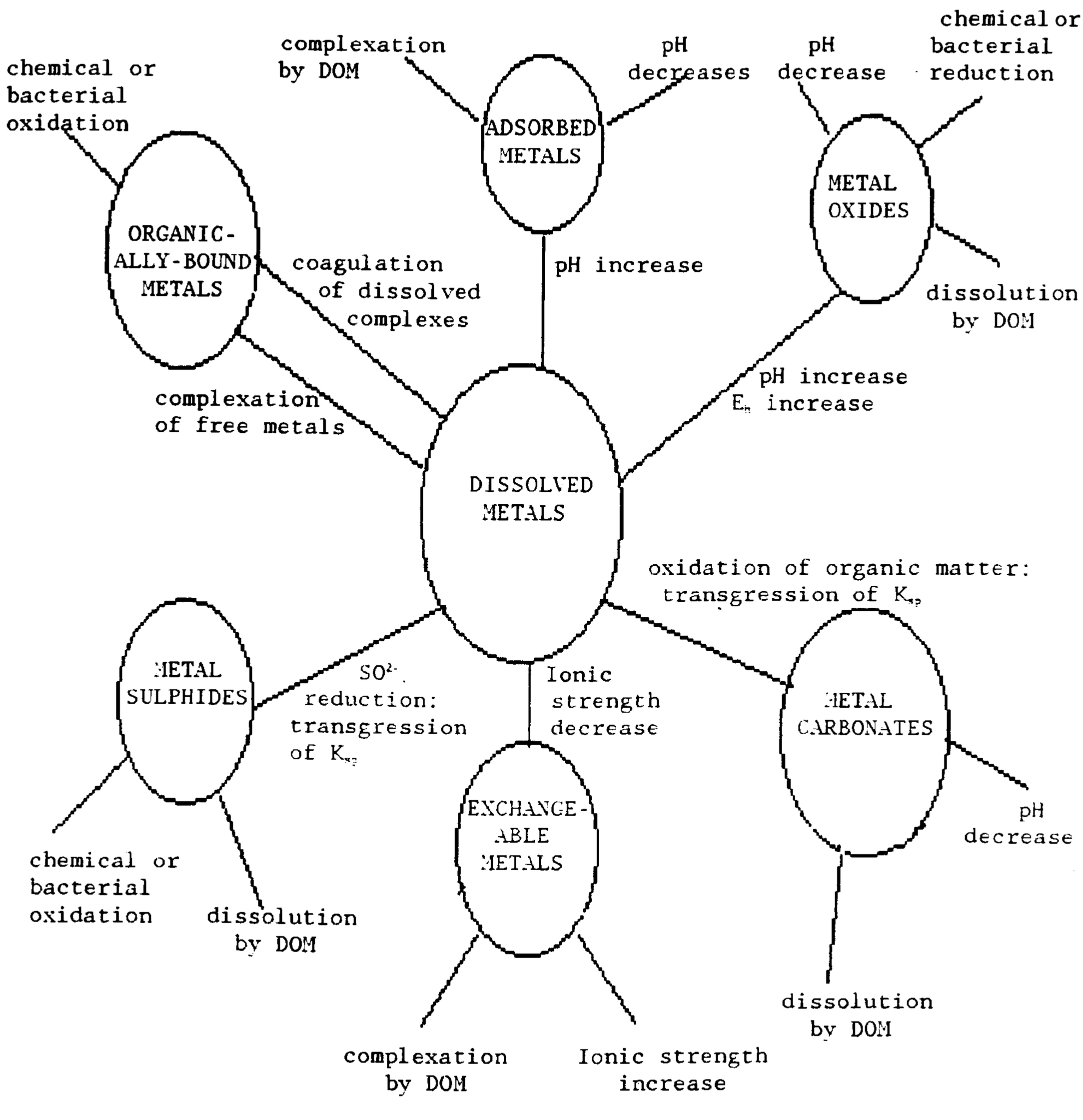

complexation sites are carboxylic acids, phenolic and hydroxyl groups as well as suitably placed carbonyl and quinionic groups [8]. The humic substances can be split into two categories, fulvic acid which is soluble in both dilute acid and alkali and humic acid which is only soluble in dilute alkali. Schnizer and his co-workers have concluded that the fulvic acid structure may typically be represented in part by Fig. 1.2 [8].

As is the case with other polyelectrolytes e.g. polyacrylic acids, both soluble and crosslinked humic acid fractions complex heavy metal ions [9].

1.2.1 *Complexation of metal ions with humic material*

Gamble and Schnizer [8] have investigated the complexation sites of the Cu^{2+} complex. The three types of functional group that influence any metal ion-fulvic acid complexing are:

(a) Phenolic OH groups, which remain unneutralized except by prolonged reaction with concentrated strong base [10];

(b) Type I carboxyl groups defined as those ortho- to the phenolic groups;

(c) All of the other ionizable functional groups, probably including some carboxyl groups meta to the phenolic OH groups, which contribute to the buffering effect.

The complexation behaviour of Cu^{2+} with both salicylic and phthalic acid [8] suggest the following two reactions are both possible with humic acids (Fig. 1.3):

By heavily loading fulvic acid with Fe^{3+} and Al^{3+} Schnizer and Skinner

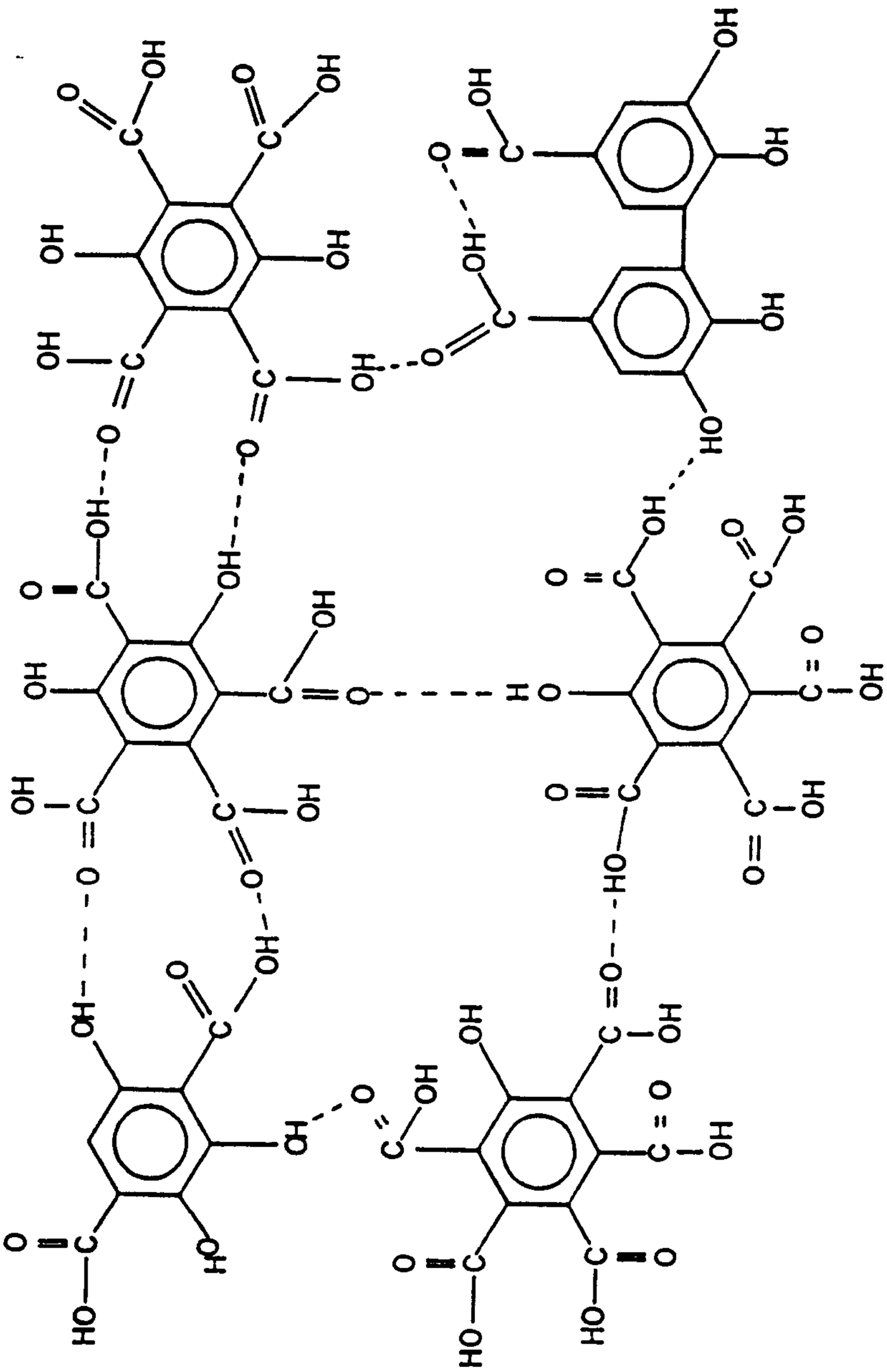

Fig 1.2 A possible structure for fulvic acid (8).

(I)

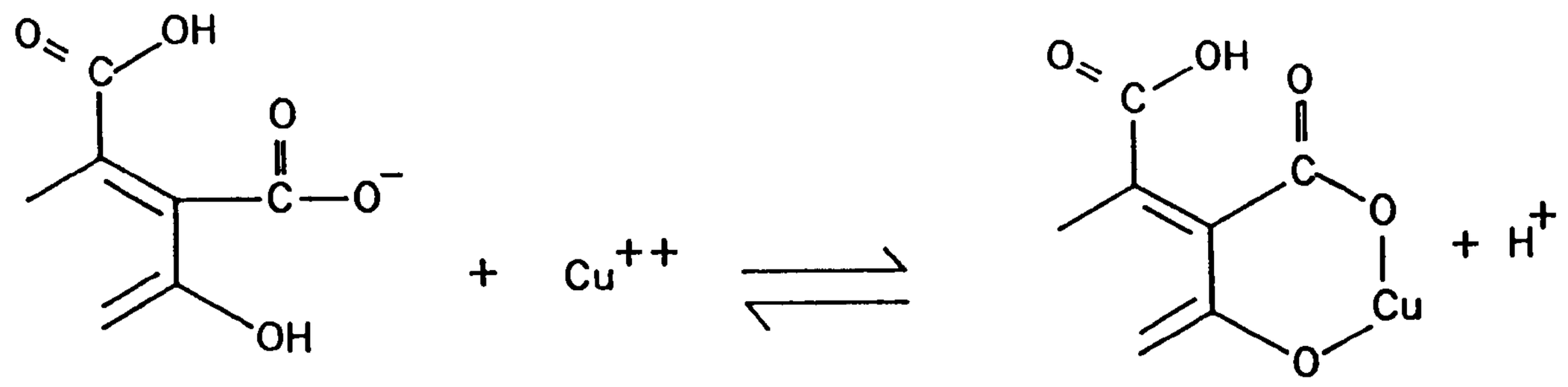

(II)

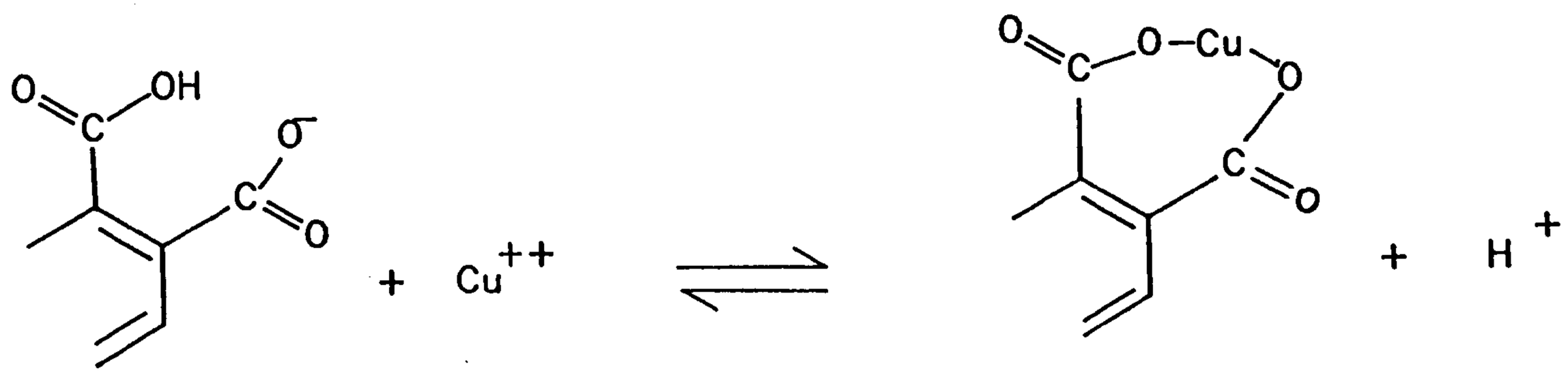

Fig 1.3 The complexation of Cu(II) by fulvic acid (8).

complexed more metal ion per gram of fulvic acid than could have been accounted for by reaction I [8]. Therefore it was concluded that reaction II must have occurred either alone or together with reaction I. The available evidence suggests that under natural conditions reaction I will occur because the trace concentrations of Cu normally found will not cause such loading as to allow reaction II to occur. It may be the case though in polluted soils that the metal loading is such that reaction II will apply.

1.3 *THE COMPLEXATION OF HEAVY METALS WITH LOW MOLECULAR WEIGHT LIGANDS*

Although the majority of heavy metals will be complexed with humic and fulvic acids a significant amount may also be in the form of low molecular weight complexes. There are many low molecular weight ligands present in soils but the most stable complexes are formed with the low molecular weight acids e.g. citric and lactic acids [11]. Some metals may also form complexes with amino acids or low molecular weight polysaccharides but in general the organic acids are of most importance.

1.4 *THE INORGANIC SPECIATION OF Cu, Zn, Cd AND Pb IN SOILS*

The final group of metal species are the inorganic species. These may be simply the free metal ion or simple complexes with carbonate, sulphate, bicarbonate, hydroxyl etc. [12].

1.4.1 *Inorganic solution equilibria* [13]

1.4.1.1 **Equilibrium constants**

Consider the reaction A + B ⟶ AB

This reaction can be expressed in terms of its equilibrium constant K

where

$$K = \frac{[AB]}{[A][B]}$$ where [ ] denotes concentration ..... (1)

Equilibrium constants can also be expressed in terms of activities i.e.

$$K = \frac{(AB)}{(A)(B)}$$ where ( ) denotes activity ..... (2)

and in this case they are true constants which hold for solutions of all ionic strengths. These constants, however, have the disadvantage that many reactants and products consist of specific ionic or molecular species whose activities are difficult or impossible to measure. In these cases concentration constants are often used.

1.4.1.2 **Activity Coefficients**

Only in infinitely dilute solutions are activities and concentrations equal. The ratio of the activity of an ion, a_i, to its concentration, C_i, is called its activity coefficient

$$\gamma_i = \frac{a_i}{C_i}$$ ..... (3)

Knowing γ_i, we are able to convert from concentrations to activities and vice versa. At infinitely dilute solution $a_i = C_i$ and $\gamma_i = 1$. Generally as ionic strength increases, ions of opposite charge interact in such a way that their effective concentration or activity decreases.

1.4.1.3 **Ionic strength**

Ionic strength is defined as

$$I = \tfrac{1}{2} \Sigma C_i Z_i^2$$ ..... (4)

Where I is the ionic strength, C_i is the concentration in Moldm^{-3} of ion i, Z_i is the valency of ion i, and Σ indicates the summation of the product of $C_i Z_i^2$ for each ion present in solution.

1.4.1.4 **Debye-Hückel equations**

The Debye-Hückel theory allows the estimation of activity based on the laws of electrostatics and thermodynamics. The assumption is made that all ions behave as point charges in a continuous medium with dielectric constants equal to that of the solvent. The resulting equation for calculating the activity coefficient of simple ions in an aqueous solution is

$$\log \gamma_i = -AZ_i^2 I^{\frac{1}{2}} \quad \ldots\ldots (5)$$

where A = 0.509 for water at 25°C. Comparison of calculated activity coefficients using the above equation with those determined experimentally show close agreement up to ionic strengths of 0.001 $Moldm^{-3}$. Above this concentration the calculated activity coefficients are generally smaller than those determined experimentally.

Extension of of the Debye-Hückel theory to account for the ionic size of hydrated ions means a more precise equation can be obtained, i.e.

$$\log \gamma_i = -AZ^2 \frac{I^{\frac{1}{2}}}{1 + Bd_i I^{\frac{1}{2}}} \quad \ldots\ldots (6)$$

where $B = 0.328 \times 10^8$ for water at 25°C and d_i is the effective distance of closest approach measured in cm and corresponds roughly to the effective size of the hydrated ion. Values of d_i for selected ions as calculated by Kielland[14] are shown in Table 1.1.

In general the extended Debye-Hückel equation holds up fairly well in solutions of ionic strength up to 0.2 $Moldm^{-3}$. At higher concentrations ionic interactions are difficult to predict and many activity coefficients become larger than unity due to the repulsion of ions.

1.4.2 *Copper*

The hydrolysis reactions of copper have been calculated on the basis of thermodynamics. The predominant ion below pH 6.9 is Cu^{2+} while $Cu(OH)_2^\circ$ is the major solution species above this pH. The hydrolysis species $CuOH^+$ becomes slightly significant near pH 7 whereas $Cu(OH)_3^-$, $Cu(OH)_4^{2-}$, and $Cu_2(OH)_2^{2+}$ are insignificant in soils.

Table 1.1

Individual ion-size parameters, a_i, in angstrom units for the Debye-Huckle equation for single-ion activity coefficients

Ion	a_i value
H^+, Al^{3+}, Fe^{3+}	9
Mg^{2+}	8
Li^+, Ca^{2+}, Cu^{2+}, Zn^{2+}, Mn^{2+}, Fe^{2+}	6
Sr^{2+}, Ba^{2+}	5
Na^+, CO_3^{2-}, HCO_3^-, $H_2PO_4^-$	4.5
SO_4^{2-}, HPO_4^{2-}, PO_4^{3-}	4
OH^-, F^-	3.5
K^+, Cl^-, NO_3^-	3
Rb^+, Cs^+, NH_4^+	2.5

The inorganic complexes of greatest importance in soils are $CuSO_4^\circ$ and $CuCO_3^\circ$. Other complexes that may contribute more than 1% to total concentration in solution include $CuHCO_3^+$ at high CO_2 and neutral pH, $CuHPO_4^\circ$ at high phosphate and neutral pH. complexes such as $CuNO_3^+$, $Cu(NO_3)_2^\circ$, $CuH_2PO_4^+$, $Cu(CO_3)_2^{2-}$, $CuCl^+$, $CuCl_2$ and $CuCl_3^-$ do not contribute significantly to total copper at the concentration level of anions normally found in soils.

Total inorganic copper in soil solution [Cu_{inorg}] can be fairly well represented by the equation

$$[Cu_{inorg}] = [Cu^{2+}] + [CuSO_4^\circ] + [Cu(OH)_2^\circ] + [CuCO_3^\circ] \quad \ldots\ldots (7)$$

substituting activities gives

$$[Cu_{inorg}] = \frac{(Cu^{2+})}{\gamma Cu^{2+}} + (CuSO_4^\circ) + (Cu(OH)_2^\circ) + (CuCO_3^\circ) \quad \ldots\ldots (8)$$

When each term on the right of this equation is expanded in terms of its equilibrium constant [15] the above can be rearranged to give

$$(Cu^{2+}) = \frac{[Cu_{inorg}]}{\frac{1}{\gamma Cu^{2+}} + 10^{2.36}(SO_4^{2-}) + \frac{10^{-13.78}}{(H^+)^2} + \frac{10^{-11.43}CO_{2(g)}}{(H^+)^2}} \quad \ldots\ldots (9)$$

Thus the activity of Cu^{2+} can be estimated from this equation with measurements of (1) total inorganic copper in solution, (2) pH, (3) ionic strength, (4) the activity of SO_4^{2-}, and (5) the partial pressure of $CO_{2(g)}$.

1.4.3 *Zinc*

In terms of hydrolysis species the most important zinc species in solution below pH 7.7 is Zn^{2+}, although $ZnOH^+$ is more prevalent above this pH. The neutral species $Zn(OH)_2^\circ$ is the major species above pH 9.11, whereas $Zn(OH)_3^-$ and $Zn(OH)_4^{2-}$ are never major solution species in the pH range of soils.

Zinc also forms complexes with chloride, phosphate, nitrate and sulphate.

The complexes $ZnNO_3^+$, $Zn(NO_3)_2^\circ$, $ZnCl^+$, $ZnCl_2$, $ZnCl_3^-$, $ZnCl_4^{2-}$ and $ZnH_2PO_4^+$ do not contribute significantly to the total zinc in solution. In neutral and calcareous soils the species $ZnHPO_4^\circ$ may be significant depending upon pH and the activity of phosphate.

The zinc species contributing significantly to total inorganic zinc in solution [Zn_{inorg}] are

$$[Zn_{inorg}] = [Zn^{2+}] + [ZnSO_4^\circ] + [ZnOH^+] + [Zn(OH)_2^\circ] + [ZnHPO_4^\circ] \quad \ldots (10)$$

substituting activities gives

$$[Zn_{inorg}] = \frac{(Zn^{2+})}{\gamma Zn^{2+}} + (ZnSO_2^\circ) + \frac{(ZnOH^+)}{\gamma ZnOH^+} + (Zn(OH)_2^\circ) + (ZnHPO_4^\circ) \quad \ldots (11)$$

When the terms on the right hand side of the equation are expanded in terms of the equilibrium constants taken from [13] the above can be rearranged to give

$$(Zn^{2+}) = \frac{[Zn_{inorg}]}{\frac{1}{\gamma Zn^{2+}} + 10^{2.33}(SO_4^{2-}) + \frac{10^{-7.69}}{\gamma ZnOH^+(H^+)} + \frac{10^{-16.80}}{(H^+)^2} + \frac{10^{-3.90}(H_2PO_4^-)}{(H^+)}} \quad \ldots\ldots (12)$$

Thus the activity of Zn^{2+} can be estimated from the above equation when the following are known:

(1) Total inorganic zinc

(2) pH

(3) Ionic strength

(4) SO_4^{2-} activity

(5) $H_2PO_4^-$ activity

If there are any other complexes that contribute significantly to soluble zinc, then they must also be included in the equations above.

1.4.4 *Cadmium*

None of the hydrolysis species contribute significantly to total cadmium in solution except possibly $CdOH^+$ and $Cd(OH)_2^\circ$ above pH 7.5. The halide complexes of Cd^{2+} all have similar stabilities, which decrease

slightly in the order $I^- > Br^- > Cl^-$. At approximately 10^{-2} mol dm^{-3} halide activities the complexes of CdI^+, $CdBr^+$ and $CdCl^+$ are about equal to Cd^{2+}. At lower halide activities, the complexes become less important whereas at higher activities they become more important. The ammonia complexes are less important than the halide complexes but they increase with pH when the NH_4^+ ion is used as the reacting species. Unless the NH_4^+ activity is very high ($>10^{-2}$ mol dm^{-3}), the cadmium ammonia complexes are not significant in soils.

One of the most abundant cadmium species is $CdSO_4^\circ$, which equals that of Cd^{2+} at $10^{-2.45}$ mol dm^{-3} SO_4^{2-}. The next most significant species is $CdHCO_3^+$, which approaches the activity of Cd^{2+} near pH 8 and increasing $CO_{2(g)}$ increased the relative importance of $CdHCO_3^+$. Also the $CdCO_3^\circ$ complex becomes important near pH 8 and increases with increasing $CO_{2(g)}$.

The $CdNO_3^+$ and $Cd(NO_3)_2^\circ$ complexes can be ignored in soils as their formation would require nitrate in the order of 10^{-2} mol dm^{-3}. The $CdHPO_4^\circ$ ion pair approaches significance only in alkaline soils only when $H_2PO_4^-$ is greater than 10^{-5} mol dm^{-3}, otherwise it can be ignored.

1.4.5 ***Lead***

Below pH 8.0 only Pb^{2+} and $PbOH^+$ contribute significantly to the total lead in solution. Since soils seldom attain pH values above 9, $Pb(OH)_2^\circ$ and $Pb(OH)_3^-$ barely approach significance even at high pH.

In general the halide complexes have similar stabilities but similarly to Cd decrease slightly in the order $PbI^+ > PbBr^+ > PbCl^+ > PbF^+$. At halide activities 10^{-4} mol dm^{-3}, all of these complexes begin to contribute significantly to total lead in solution. In the halide range $> 10^{-2}$ to $10^{-1.5}$ the halide complexes are approximately equal to free Pb^{2+}.

Only in the halide activity range of $10^{-1.3}$ mol dm^{-3} do the higher order complexes such as PbI_2°, PbI_3^-, PbI_4^{2-}, $PbBr_2^\circ$ and $PbCl_2^\circ$ exceed the simple 1:1 complexes. In general the halide complexes of Pb^{2+} are not highly significant in soils.

The $PbSO_4^\circ$ complex is significant and equals that of Pb^{2+} at $10^{-2.62}$ mol dm^{-3} SO_4^{2-}. The $Pb(SO_4)_2^{2-}$ species become significant only as SO_4^{2-} increases above 10^{-3} mol dm^{-3}. The $PbNO_3^+$ complex becomes slightly significant as NO_3^- increases above 10^{-3} mol dm^{-3} while the $Pb(NO_3)_2^\circ$ can be ignored so long as $NO_3 < 10^{-2}$ mol dm^{-3}. The $PbH_2PO_4^+$ complex is not significant in the phosphate range generally encountered in soils while the $PbHPO_4^\circ$ ion pair is significant above pH 7.

1.5 *AVAILABILITY AND TOXICITY OF HEAVY METAL SPECIES IN SOILS*

The plant availability and resultant toxicity of heavy metals in soils is very much dependant upon the metal speciation. Some species may have very high toxicities due to them being readily available to plants, whilst other non-available species may be of very low toxicity. This is best illustrated by referring to copper (Table 1.2) as it has the ability to form a wide range of species all of varying toxicity.

Table 1.2 The Relative Toxicity of Some Copper Species

Species	Relative Toxicity
Cu^{2+}	High
$CuCl_2$	High
$CuCO_3$	Low
Cu^{2+} - fulvic acid	Low
Cu^{2+}/humic acid. Fe_2O_3	Medium
Cu^{2+} - DMP	High

DMP = 2,9 - dimethyl - 1,10, - Phenanthroline

In the case of copper the majority of the metal will be present as complexes with humic material and these complexes are of low → medium toxicity. Indeed, it has been shown that the addition of fulvic acid to a polluted soil causes a decrease in the plant available Cu [16].

Although there is considerable evidence that the free metal ion is the most toxic the situation is not completely clear [13]. Some studies suggest that other species such as the Cu-hydroxy complex [17], and the Cu complexes of citrate and ethylenediamene [18] are also toxic.

1.6 *ANALYTICAL METHODS FOR THE DETERMINATION OF HEAVY METAL SPECIATION*

1.6.1 *Thermodynamic calculation of metal speciation*

Over the years a number of computer based models have been developed which calculate the equilibrium speciation of cationic elements among organic and inorganic ligands [19]. The user simply has to input the total concentration of each metal and ligand in the system and the model computes the eqilibrium concentrations of the species of interest. The calculation usually involves an iterative procedure which attempts to minimise the free energy of the system. The main limitations of such an approach are as follows:

(i) Lack of reliable thermodynamic data. In the case of trace metals, published stability constants for a given species may differ by one or more orders of magnitude. Another cause for concern is that many of these stability constants were determined under conditions differing greatly from those prevailing in the natural systems of interest, i.e. temperature, and the temperature dependence of these constants is rarely known.

(ii) Inconsistencies and inadequacies in the equations used to correct ionic activity coefficients for ionic strength.

(iii) Lack of kinetic data for many chemical and biological processes.

(iv) Difficulties in characterising the organic ligands present in soil solutions. This is probably the main disadvantage of computer modelling. Two of the major complexing agents present in soil water were mentioned earlier i.e. humic and fulvic acids, but the complexation behaviour of these acids is poorly understood. Conditional stability constants have been derived for a "mean fulvic acid unit" [20-21], but true thermodynamic constants for metal-fulvic acid and proton-fulvic acid equilibria are not available. Incorporation of fulvic acids into computer models has therefore been very difficult and historically most authors have adopted the "mixture model" approach used by Sposito [16]. In this approach a set of monomeric organic acids is selected whose reactions with metal ions is well characterised, and whose functional groups are known to exist in the Dissolved Organic Matter (DOM) pool. The distribution of the individual acids is then adjusted to simulate the acid base and metal complexing behaviour of the natural DOM. As a consequence computer models are only of real use when the soil is well characterised in terms of DOM.

1.6.2 *Experimental determination of metal speciation in solution*

Due to the large number of equilibria that exist in soil solutions

it is very important that any analytical method chosen should exert a minimal disruptive effect on such equilibria. This will ensure that the results obtained are relevant to the system under study and not simply a figment of the analytical procedure.

Analytical techniques have improved by orders of magnitude in recent years and it is now possible to make reliable determinations of the metal ion contents of specific fractions of a sample. The usual method of analysis is to carry out a physico-chemical separation followed by subsequent analysis using a suitable elemental technique.

The problem with such an approach is that if the sample equilibria is to be maintained the separation technique must be more or less instant, otherwise transfers due to reaction kinetics will occur [7]. The experimental determination of metal speciation can either make use of the physical properties or chemical reactivity of metal species in order that their separation may be achieved.

1.6.2.1 Physical properties

Size exclusion techniques. involving such techniques as filtration, ultrafiltration, dialysis or size exclusion chromatography, are often used as a preliminary separation stage in a metal speciation procedure [24]. A separation based purely on physical size is useful in that it does yield information about the potential toxicity of metal species. It was pointed out by Bately [25] that the available metals are likely to be those found in the smallest size categories. Although these techniques seem attractive there are associated problems.

In the case of filtration, ultrafiltration and dialysis there are problems with metal losses due to adsorption on to the membrane surface [5]. Dialysis can often cause the dissociation of metal species at the membrane surface due to the large concentration gradient that exists

there.

Size exclusion chromatography also has its own associated drawbacks [26-28]. The traditional Sephadex gels used in such a technique often exhibit the adsorption of organic material, in particular humic acids and the resulting peak shapes obtained are far from satisfactory. The adsorption process is often overcome by the use of high salt concentration eluents e.g. 0.1 Mol dm^{-3} NaCl. Such high salt concentrations are of little use in speciation studies due to the disruptive effect that they would have on soil equilibria.

New size exclusion columns have been developed for use with High Performance Liquid Chromatography (HPLC) Apparatus [29-31]. These packings do not suffer from the adsorption problems associated with Sephadex columns but do exhibit some repulsion of ionic species. This is known as colombic repulsion. Again this has been overcome by the use of high salt concentrations which are unsuitable for soil solution studies. The use of such chromatographic procedures involves the development of a suitable interface between the HPLC column and a suitable elemental detector. The subject of chemical interfacing was recently reviewed by Ebdon [32] and many such interfaces have been developed.

There are many element specific detectors suitable for the determination of the metal content of heavy metal species. The detection technique chosen has to satisfy a number of criteria:

- It must have suitable limits of detection for the species under study.

- The development of an interface between the separation technique and the detector must be feasible e.g. AAS will not tolerate flow rates of the order of 0.1 ml min^{-1}, often used in SEC, without a serious loss in detection limits.
- The analysis should not be too time consuming.
- Ease of automation and operation.

Atomic Absorption Spectrometry AAS

Flame atomic absorption spectrometry was one of the first reported element specific detectors used in combination with High Performance Liquid Chromatography (HPLC) [33]. The construction of such interfaces is relatively simple and usually involves a straight connection of the HPLC outlet to the inlet of the AAS nebulizer. Problems arise due to the incompatibilities in flow rates between the two techniques i.e. typically 5 ml min^{-1} for AAS and 1 ml min^{-1} for HPLC. This is overcome by utilizing the AAS nebuliser in a starved mode of operation. This is a simple operation and involves cutting a small hole in the tubing connecting the HPLC to the AAS nebulizer. The nebulizer then makes up the difference in flow by sucking in air from the atmosphere. The main problem with such an interface is that it results in much poorer limits of detection. This is a major problem with AAS detectors in that they just do not have sufficiently low detection limits for speciation studies.

Graphite Furnace Atomic Absorption Spectrometry (GFAAS)

The use of a graphite furnace for atomisation in AAS has improved detection limits by an order of magnitude but it is much more difficult to interface directly to HPLC. This is because GFAAS has a much longer analysis time. Perhaps the easiest way to use GFAAS as an HPLC detector

is to collect fractions of the HPLC eluent in a fraction collector and carry out subsequent analysis of each fraction by GFAAS [34]. A major problem here is that samples with similar retention times will often be collected in the same fraction thereby defeating the chromatographic separation. This offline analysis of the eluent is a time consuming process and many attempts have been made to improve this. Perhaps the easiest way is to make use of a flow-through cell as used by Brinkman [35]. In this case the HPLC eluent is passed through a flow through cell and is sampled on each cycle of the furnace program.

A major disadvantage of discontinuous sampling is that it is possible to miss a very sharp chromatographic peak during the analysis of the previous sample. The resolution of the technique depends on the speed of the GFAAS cycling time and flow rate of the HPLC. However the technique is rapid because it requires a minimum of method development since the analyst must only develop the chromatographic conditions to separate the compounds that are of interest as the GFAAS will respond only to the compounds which contain the analyte of interest.

Inductive Coupled Plasma Optical Emission Spectrometry (ICP-OES)

The ICP is probably by far the most useful detector for HPLC separation of heavy metal species. The multi-element capability of this technique means that a wealth of speciation results can be obtained for a particular sample. The uptake rate of an ICP nebuliser is similar to that used in many HPLC separations. This means that the construction of an interface is a relatively simple process. Like AAS it simply involves the connection of the HPLC outlet to the ICP nebulizer. The main problem with ICP is that it does not have as good detection limits as GFAAS and this may be a problem when dealing with environmental samples. The weak link in an ICP is the nebulizer. Typical nebulizers

can only achieve an analyte transport efficiency of 1-2%. If however, this could be improved, the potential use of an ICP as a detector in environmental speciation studies would be enormous.

1.6.2.2 Chemical Properties

The determination of chemical speciation using chemical methods will by its very nature have a disruptive effect on the sample equilibria. Some of the chemical methods that have been used are listed below, along with their associated problems [5].

Perhaps the most widely used method in the analysis of soil chemistry is that of solvent extraction. Such methods involve the use of a chelating agent e.g. diethylenetiaminepentaacetic acid DTPA to provide a measure of the bio-available trace metals [22]. As shown in Table 1.3 the correlation of uptake with DTPA-extractable metal (a commonly used extractant) may sometimes not be much better than that with the total metal concentration, and is often not as good as the metal content of the soil solution itself. This may be due to a redistribution of the sample equilibria during the extraction procedure. Some workers [23] have made use of a sequential extraction procedure using different extractants in a stepwise procedure as an attempt to classify metals into different groups of species. It seems obvious that there will be a redistribution of the sample equilibria between each stage in the extraction procedure. This will result in unreliable speciation data.

Table 1.3

Correlations between the metal content of clover and various metal fractions, for four soils treated with sewage sludge [22]

	Correlation Coefficient		
Metal measure	Zn	Cu	Ni
Soil solution	0.94 ***	0.50 ***	0.93 ***
DTPA extraction	0.60 ***	0.54 ***	0.67 ***
Total concentration	0.44 **	0.53 ***	0.51 *

Significance levels *** 0.001, ** 0.01, * 0.05

(1) Electrochemical determinations e.g. Anodic Stripping Voltammetry (ASV), Ion Selective Electrodes (ISE).

One of the first speciation schemes developed was that proposed by Florence [4] (Fig. 1.4). This method has many disadvantages, most notably the fact that it is a stepwise process suggests that there will be substantial redistribution of equilibria between each subsequent stage. The ASV measurements were carried out in a 2 Mol dm^{-3} acetate buffer pH 4.7. Such a high ionic strength buffer would have an effect on the equilibrium distribution of the metal species. Another problem is due to the tendency of natural Dissolved Organic Matter (DOM) to adsorb onto the working electrode [5] this makes distinguishing between metal-DOM interactions in solution and adsorption artifacts at the electrode/solution interface difficult. Finally, the method was unable to identify individual species which is obviously the goal of any speciation scheme.

Fig. 1.4

The speciation scheme developed by Florence and Batley [6]

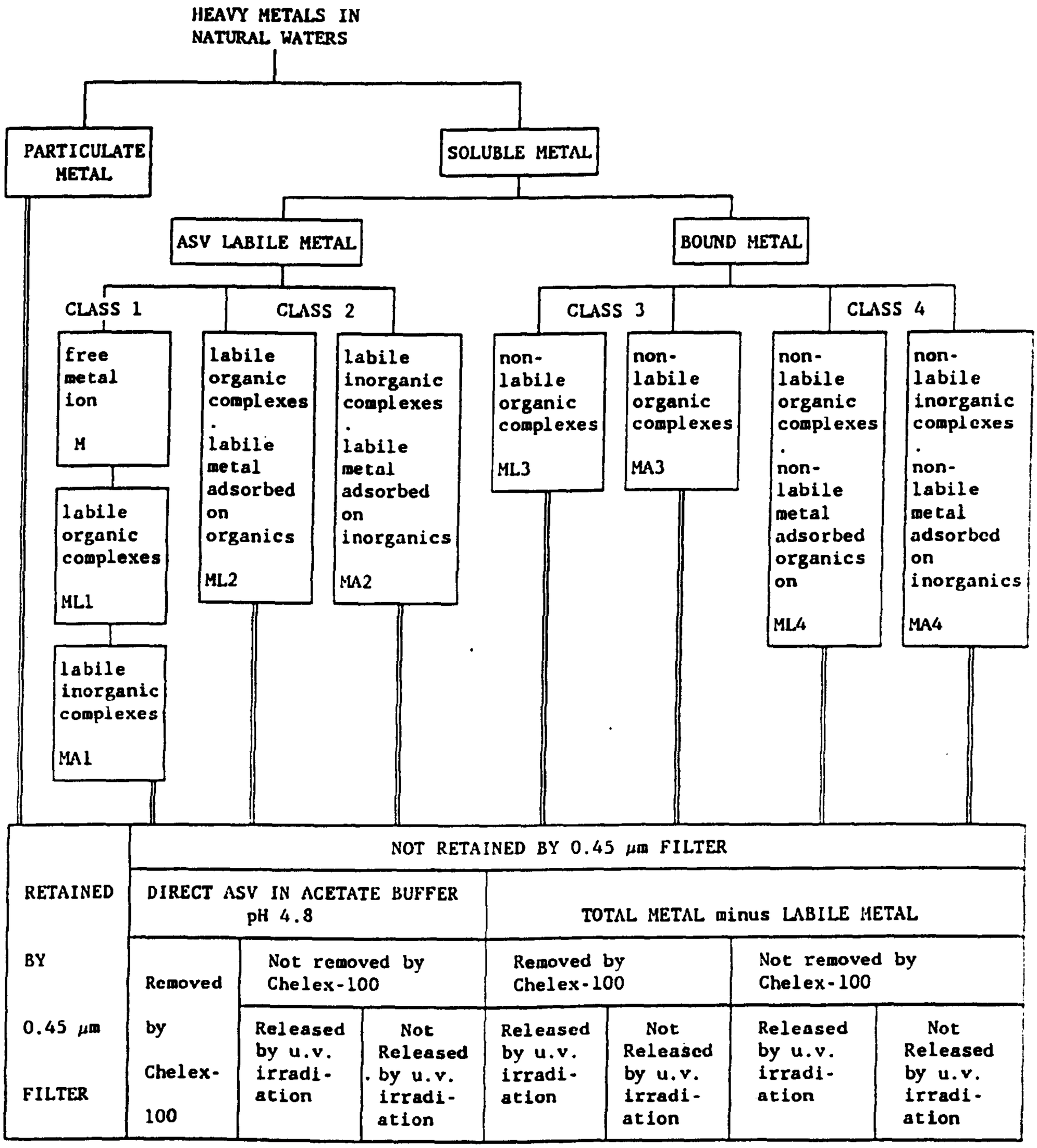

(2) Ion exchange.

Again, this method does not yield information about individual species but will only give an estimation of the percentage of the metal in neutral, cationic or anionic forms [5]. This gives no indication of the potential availability of the metal.

(3) Adsorption - e.g. XAD Sep Pak cartridges [36].

Such methods have been used in an attempt to separate out the humic and fulvic acid fractions from the rest of the metal species. The metal content of such species is then determined by e.g. Atomic Absorption Spectrometry (AAS).The problem with such methods is that although they do adsorb humic substances, by nature they will also adsorb low molecular weight organic acids e.g. citric acid. The presence of residual ion exchange groups on the resin surface complicates the use of these materials, however, unless the critical adsorption step is followed by dilution with a suitable solvent e.g. methanol to distinguish between inorganic and organic metal forms (only the latter are eluted). Florence [37] has attempted to produce resins which have similar functional groups to the biological surfaces used by plants in their uptake of heavy metals. If a resin was devised which could imitate these biological membranes then it would be very useful in the assessment of plant available heavy metals. However, there have been problems due to the instability of thiol based materials.

1.7 *CONCLUSIONS*

The ideal analytical method would be instantaneous. This would minimise changes in sample equilibria due to reaction kinetics. Techniques such as NMR and ESR would allow this but are not applicable to this particular situation. The best one can hope to achieve is to try to ensure that the ionic strength and pH of the samples are maintained during analysis. The maintenance of both these factors would hopefully result in a minimal disruption of sample equilibria.

REFERENCES

(1) Burridge, J.C. and Berrow, M.L., Proc. Int. Conf. Environmental Contamination, London, July 1984. CEP consultants Ltd., Edinburgh, 1984, 215-224.

(2) Reith, J.W.S., Berrow M.L. and Burridge, J.C., Proc. Int. Conf. Management and Control of Heavy Metals in the Environment, London, 1979, CEP Consultants Ltd., Edinburgh 1979, 537-540.

(3) Department of the Environment, 1989. Code of Practice for Agricultural Use of Sewage Sludge. HMSO, London.

(4) Florence, T.M. and Batley, G.E., Talanta, 1977, **24**, 151-158.

(5) Campbell, P.G.C. and Tessier, A.T., in "Metals Speciation Separation and Recovery", Eds. Patterson, J.W. and Passino, R., 1987, Lewis, Michigan, 201-242.

(6) Florence, T.M. and Batley, G.E., CRC Crit. Rev. in Anal. Chem., 1980, **9**, 219-296.

(7) Ohman, L. and Sjöberg, S. in "Metal Speciation: Theory, Analysis and Practice", Eds. Kramer, J.R. and Allen, H.E., 1988, Lewis, Michigan.

(8) Gamble, D.S. and Schnizer, M. in "Iron metals and metal organic interactions in natural waters", Ed. Singer, P.C., 1973, Ann Arbor, 265-301.

(9) Mandel, M., Leyte, J.C. and Stadhouder, M.G., 1967, J. Phys. Chem., **71**, 603-627.

(10) Schnizer, M. and Desjardins, J.G., Soil Sci. Am. Proc., 1962, **26**, 362.

(11) Brown, L., Haswell, S.J., Rhead, M.M., O'Neill, P. and Bancroft, K.C.C., Analyst, 1983, **108**, 1511-1520.

(12) Florence, T.M., Talanta, 1982, **29**, 345-364.

(13) Lindsay, W.L., Chemical Equilibrium in Soils, 1979, Wiley-Interscience, New York, pp 11-33.

(14) Kielland, J., J. Am. Chem. Soc., 1937, **59**, 1675-1678.

(15) Adams, F., Soil Sci. Soc. Am. Proc., 1971, **35**, 420-426.

(16) Piccolo, A., Sci. Tot. Env., 1989, **81-82**, 507-614.

(17) Magnuson, V.R., Harriss, D.K., Sun. M.S. and Taylor, D.K., in "Chemical Modelling in Aqueous Systems", Ed. Jenne, E.A., ACS Symposium Series No. 93, Am. Chem. Soc., Washington DC, 1979, 635.

(18) Guy, R.D. and Kean, A.R., Water Res., 1980, 14, 891.

(19) Nordstrom, D.K., Plummer, L.N., Wigler, T.M.L., Wolery, T.J., Ball, J.W., Jenne, E.A., Bassett, R.L., Crerar, D.A., Florence, T.M., Fritz, B., Hoffman, M., Holdren, G.R., Lafon, G.M., Mattigod, S.V., Mcduff, r.E., Morel, F., Reddy, M.M., Sposito, G. and Thrailkill, J., in "Chemical Modeling in Aqueous Systems", Ed. Jenne, E.A., ACS Symposium Series No. 93, Am. Chem. Soc., Washington DC, 1979, 858-891.

(20) Mantoura, R.F.C., Dickson, A. and Riley, J.P., Estuar. Coast. Mar. Sci., 1978, 6, 387-408.

(21) Sposito, G., Environ. Sci. Technol., 1981, 15, 396-403.

(22) Lindsay, W.L. and Norvell, W.A., J. Soil Sci. Soc. Am., 1978, 42, 421-428.

(23) McLaren, R.G. and Crawford, D.V., J. Soil Sci., 1973, 24, 172-181.

(24) Steinnes, E. in "Trace Element Speciation in Surface Waters and its Ecological Implications", Ed. Leppard, G.G., Plenum Press, New York, 1984, 37-47.

(25) Batley, G.E. in "Trace Element Speciation in Surface Waters and its Ecological Implications", Ed. Leppard, G.G., Plenum Press, New York, 1984, 17-36.

(26) Hine, P.T. and Bursill, D.B., Water Res., 1984, 18, 1461-1465.

(27) Sterrit, R.M. and Lester, J.N., Environ. Pollution (Series A), 1982, 27, 37-44.

(28) Swift, R.S. and Postner, A.M., J. Soil Sci., 1971, 22, pp 237-249.

(29) Adamic, M.L. and Bartak, D.E., Anal. Chem., 1985, 57, 279-283.

(30) Gardner, W.S., Landrum, P.F. and Yates, D.A., Anal. Chem., 1982, 54, 1196-1198.

(31) Saito, Y. and Hayano, S., J. Chrom., 1979, 177, 390-392.

(32) Ebdon, L., Hill, S. and Ward, R.W., Analyst, 1987, 112, 1-15.

(33) Manham, S.E. and Jones, D.R., Anal. Lett., 1973, 6, 745.

(34) Hadieshi, K.H.T. and Mclaughlin, R.D., Anal. Chem., 1978, **50**, 1700-1701.

(35) Brinkman, F.E., Jewett, K.L., Inverson, W.P., Irgolic, K.J., Ehrhardt, K.C. and Stockton, R.A., J. Chrom., 1980, **191**, 31-46.

(36) Miwa, T., Murakami, M. and Mitzuike, A., Anal. Chim. Acta, 1989, **219**, 1-8.

(37) Florence, T.M., Anal. Chim. Acta, 1982, **141**, 73-94.

CHAPTER TWO

AN INVESTIGATION INTO THE RELATIONSHIP BETWEEN THE TOTAL IONIC STRENGTH AND ELECTRICAL CONDUCTIVITY OF SOIL SOLUTIONS

2.1 *BACKGROUND*

In this work the behaviour of various ligands and their ability to complex metals in soil solutions was studied and this was achieved by the use of both chemical and computer models. Computer models of natural systems are often based on thermodynamic functions and require an estimate of the solution ionic strength, from this activity coefficients of pertinent solution species can be calculated. The determination of ionic strength requires either a total ionic analysis of the solution or it is necessary to make certain assumptions about the ionic composition of the solution. A knowledge of ionic strength is also required in speciation studies as it is of the utmost importance that the ionic strength of the sample be maintained during any subsequent analysis. This is due to the fact that in a soil sample there are very complex equilibria taking place which are dependent on both pH and ionic strength. Any change in ionic strength results in disruption of the sample equilibria which leads to erroneous speciation results. In order to maintain the sample equilibria during analysis by HPLC it is necessary to use a column eluent that has the same ionic strength as that present in the sample.

Both Ponnamperuma [1] and Griffin [2] have proposed linear relationships between the electrical conductivity of a solution and its ionic strength. If such a relationship exists then this would provide a rapid accurate method for the determination of ionic strength at all electrolyte concentrations. This would eliminate the need for an extensive chemical analysis and thus provide a knowledge of the ionic strength of the sample enabling a suitable column eluent to be prepared.

2.2 *THE VARIATION OF CONDUCTIVITY WITH IONIC STRENGTH FOR SIMPLE ELECTROLYTES*

2.2.1 *Apparatus*

All conductivities were carried out using a conductivity meter (Model 34, WPSA Ltd., Bracknell, UK) and electrode Kent EIL 2000 electrolytic conductivity cell (Kent Industrial Measurements Ltd., St. Neots, UK). All measurements were carried out in a water bath at 298K.

2.2.2 *Procedure*

A solution of KCl (0.01 Mol dm^{-3}) was prepared in order to obtain the cell constant of the electrode. From standard tables the conductance of 0.01 Mol dm^{-3} KCl was found to be = 1.413 mS cm^{-1} at 298K and from this the cell constant was calculated from equation (1).

Cell Constant = Specific Conductance (mS cm^{-1})/
Observed Conductivity (mS) ..... (1)

Cell Constant = 1.413/1.403 cm^{-1}

= 1.0071 cm^{-1}

The Cell constant was assumed to be = 1 cm^{-1}

2.2.3 *RESULTS*

The following results were obtained for KCl and are shown in Table 2.1.

The results were plotted and a linear regression was carried out on them (graph 2.1), this gave a line the equation of which was,

$I = -5.9 \times 10^{-4} + 7.9 \times 10^{-3}EC$ ..... (2)

r = 0.9999 (r = correlation coefficient).

Where I = Ionic strength (Mol dm^{-3}) and EC = Electrical Conductivity (ms cm^{-1}).

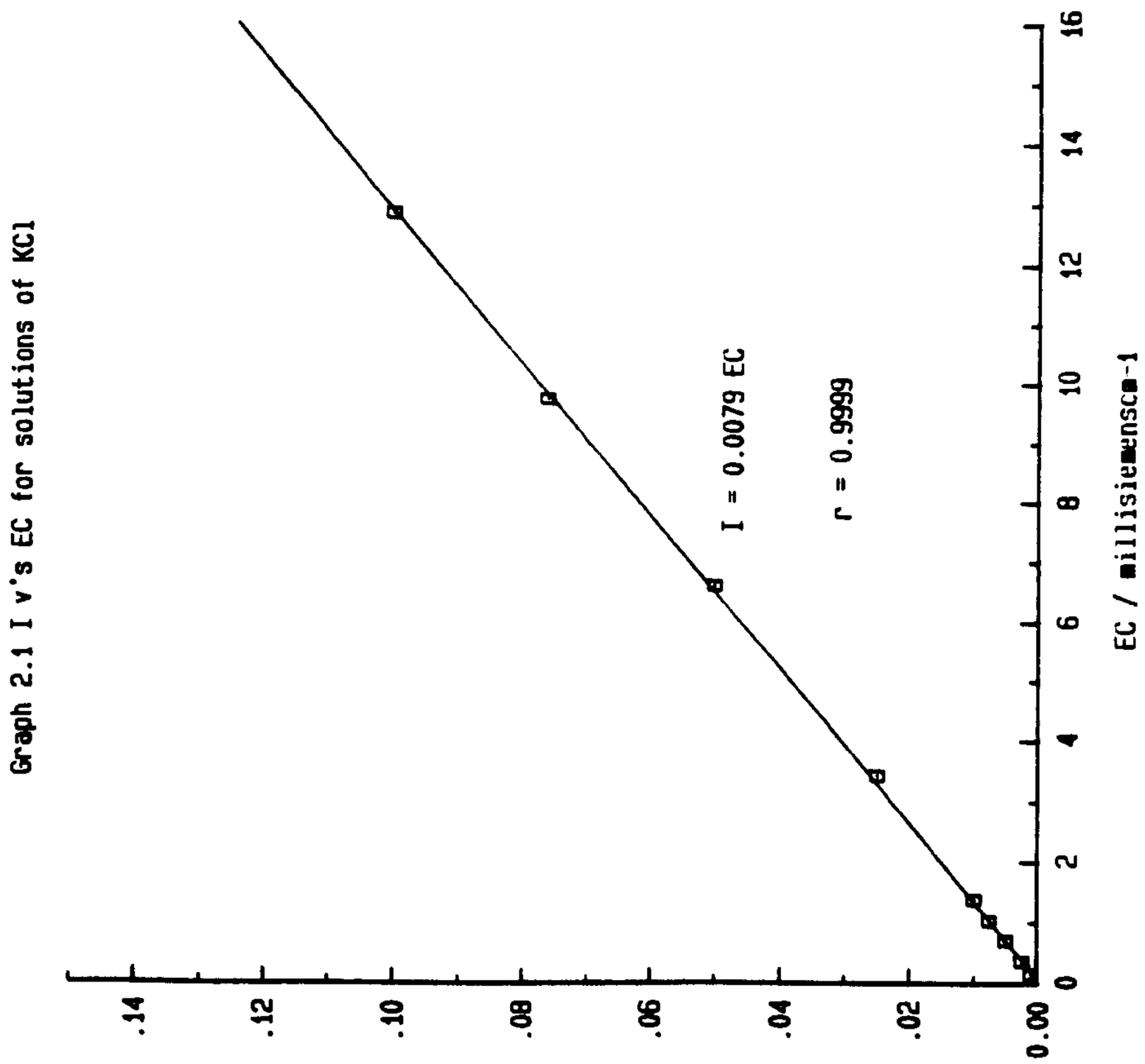
Graph 2.1 I v's EC for solutions of KCl
I = 0.0079 EC
r = 0.9999
EC / millisiemens cm-1
Ionic strength / mol dm-3
0
2
4
6
8
10
12
14
16
.14
.12
.10
.08
.06
.04
.02
0.00

Table 2.1

Conc/ Mol dm^{-3}	Conductivity mS cm^{-1}
1.03×10^{-3}	0.15
2.5×10^{-3}	0.37
5.0×10^{-3}	0.72
7.6×10^{-3}	1.04
0.010	1.40
0.025	3.42
0.050	6.61
0.076	9.75
0.10	12.88

It can be seen that there is a clear cut linear relationship between ionic strength and conductivity. This was repeated for solutions of NaCl and HCl of similar concentrations. The results are shown in Tables 2.2 and 2.3, respectively.

Linear regression was carried out on both sets of data (graphs 2.2 and 2.3). The lines had the following equations:

For NaCl $I = -9.4 \times 10^{-4} + 9.73 \times 10^{-3}EC$ ..... (3)

$r = 0.9987$

For HCl $I = 1.88 \times 10^{-6} + 2.59 \times 10^{-3}EC$ ..... (4)

$r = 0.9997$

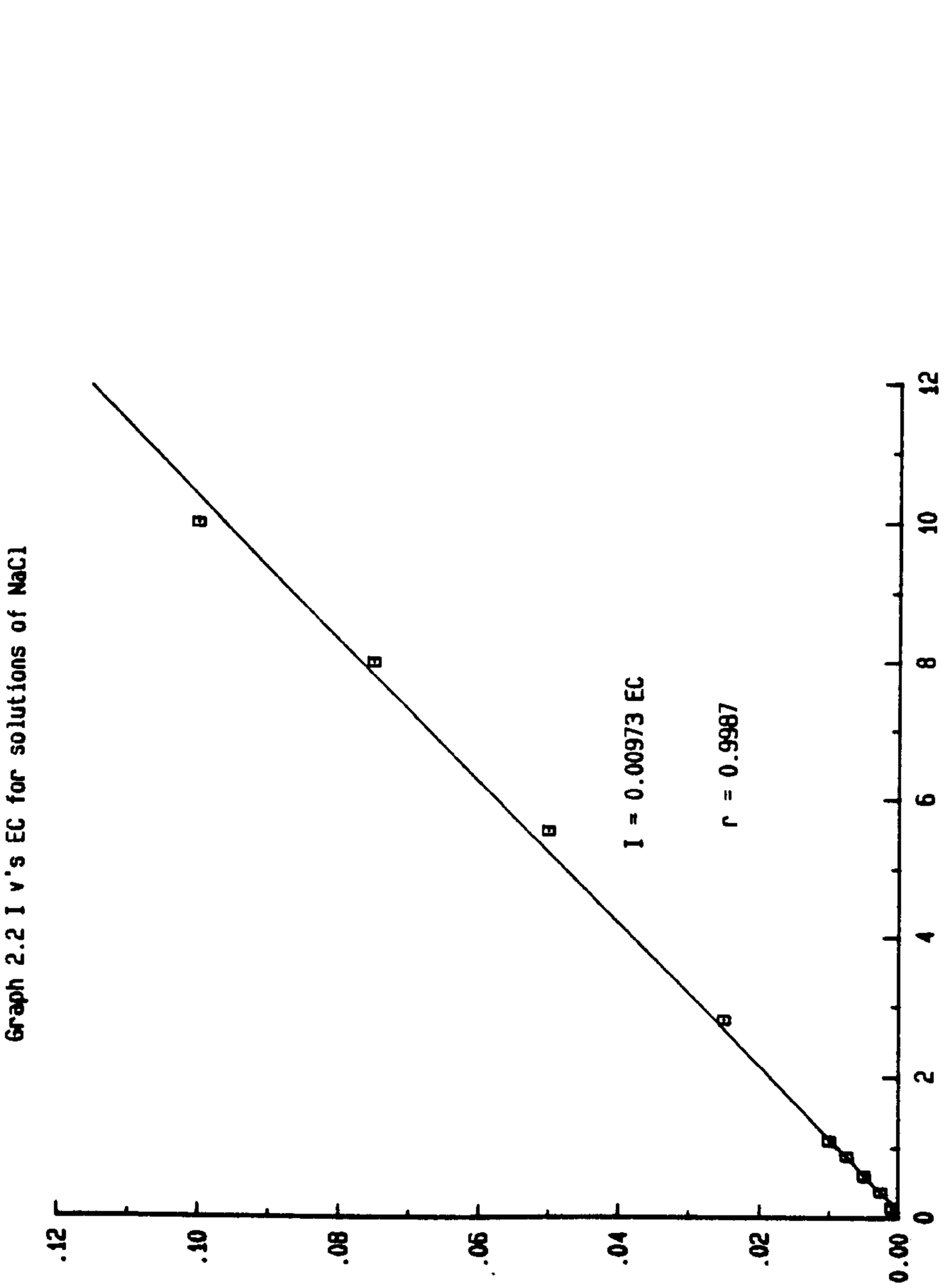
Graph 2.2 I v's EC for solutions of NaCl
I = 0.00973 EC
r = 0.9987
Ionic strength / mol dm-3
EC / millisiemens cm-1
0.00
.02
.04
.06
.08
.10
.12
0
2
4
6
8
10
12

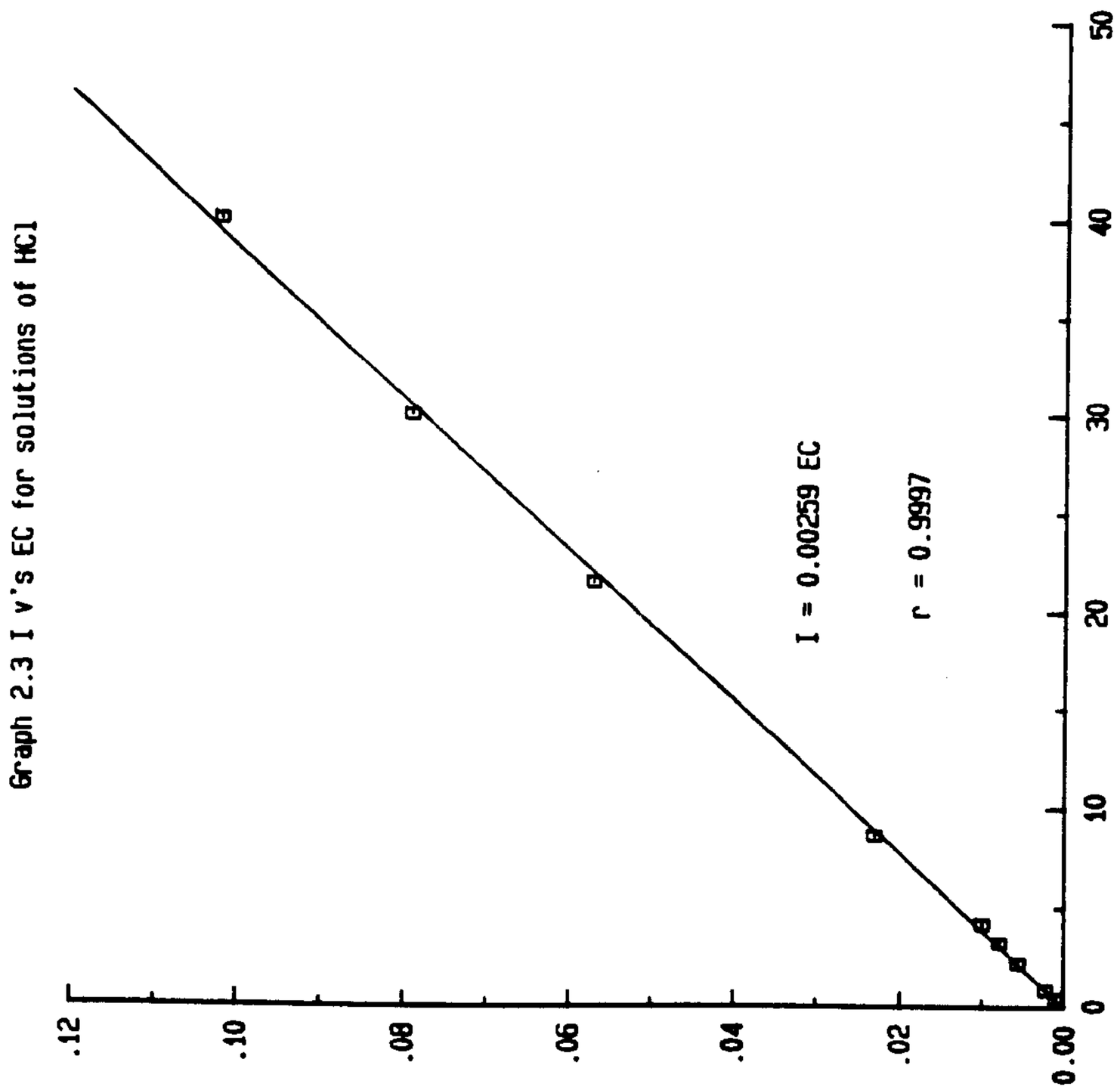
Graph 2.3 I v's EC for solutions of HCl
I = 0.00259 EC
r = 0.9997
Ionic strength / moldm-3
EC / millisiemenscm-1
0.00
.02
.04
.06
.08
.10
.12
0
10
20
30
40
50

Table 2.2

Conc/ Mol dm^{-3}	Conductivity mS cm^{-1}
1.03×10^{-3}	0.13
2.62×10^{-3}	0.37
4.98×10^{-3}	0.60
7.50×10^{-3}	0.88
0.010	1.10
0.025	2.80
0.050	5.55
0.075	8.00
0.100	10.00

Table 2.3

Conc/ Mol dm^{-3}	Conductivity mS cm^{-1}
1.02×10^{-3}	0.44
2.27×10^{-3}	0.88
5.66×10^{-3}	2.25
7.93×10^{-3}	3.25
0.010	4.20
0.023	8.60
0.057	21.50
0.079	30.05
0.102	40.05

2.3 *DISCUSSION*

It can be seen from these results that the gradients are very different. This was not unexpected as it is well known that different electrolytes have different molar conductivities. This is due to the ions having different mobilities. The main factors governing ionic mobility are:

(1) The viscosity of the solution.

(2) The size of the ion.

The mobilities of Na^+, K^+ and H^+ are shown in Table 2.4 [3].

Table 2.4

Ion	Mobility (298K) $u/10^{-4}cm^2s^{-1}V^{-1}$
H^+	36.23
Na^+	5.19
K^+	7.62

It can be seen that the gradients of the Ionic Strength (I) v's Conductivity (EC) plot decrease in the order $H^+ > K^+ > Na^+$ which is in agreement with the above mobility data. Therefore it is apparent that for single component solutions there is no unique empirical relationship between I and EC but rather, the gradient depends on the mobility of the ion [3].

Mobilities are given by

$$u = s/E \qquad \ldots\ldots (5)$$

where u = mobility, s = drift speed and E = electric field of magnitude E.

Ions in solution are subject to a variety of forces, but since these occur in random direction they do not result in net motion if the solution is uniform. In an electric field they also experience an electric force. When two electrodes at a distance 1 apart are at a potential difference ϕ, there is a uniform electric field of magnitude $E=\phi/1$ between them. An ion of charge Ze (where Z = valence of the ion and e = electronic charge) experiences a force of magnitude,

$$f = ZeE = Ze\phi/1 \qquad \ldots\ldots (6)$$

A cation responds by accelerating in the direction of the negative electrode and an anion accelerates towards the positive electrode. As the ion moves through the solvent a frictional force f' retards it with a strength that increases with its speed. If we assume that the Stokes formula ($f'=fs$, $f=6\pi na$) for a sphere of radius a and speed s applies even on a microscopic scale (and independent evidence from magnetic resonance suggests that it often gives at least the right order of magnitude), then a terminal speed, the drift speed, is reached when the accelerating force ($f=ZeE$) is balanced by the viscous drag ($f=fs$). This occurs when

$$s=ZeE/f \qquad \ldots\ldots (7)$$

Since the drift velocity governs the rate at which charge is transported, it follows that we might expect the conductivity to decrease with,

(a) increasing solution viscosity and

(b) increasing ion size.

From the results presented earlier this would not seem to be the case as K^+ although of larger radius than Na^+ it has a higher mobility. This discrepancy is resolved when we realise that the radius in the Stokes formula is the hydrodynamic radius of the ion, i.e. its effective radius taking into account the solvent molecules it carries. Small ions give rise to stronger electric fields than large ones (it is as a result of this that the electric field at the surface of a sphere of radius R is proportional to Ze/R^2) and so the smaller the radius the stronger the field. Therefore smaller ions are more extensively solvated than larger ions. This means that an ion of small ionic radius has a large hydrodynamic radius because it drags many solvent molecules through the solution as it migrates. Therefore, it also has a lower molar conductivity than a larger ion of the same charge. The proton, however, although it is very small, has a very high molar conductivity. This is because it conducts by a mechanism (the Grotthus mechanism, Fig. 2.1) that does not involve its actual motion through the solution, it is believed [3] that there is an effective motion of a proton which involves the rearrangement of bonds through a long chain of water molecules and the conductivity is governed by the rate at which the water molecule can rotate into orientations in which they can accept or donate protons.

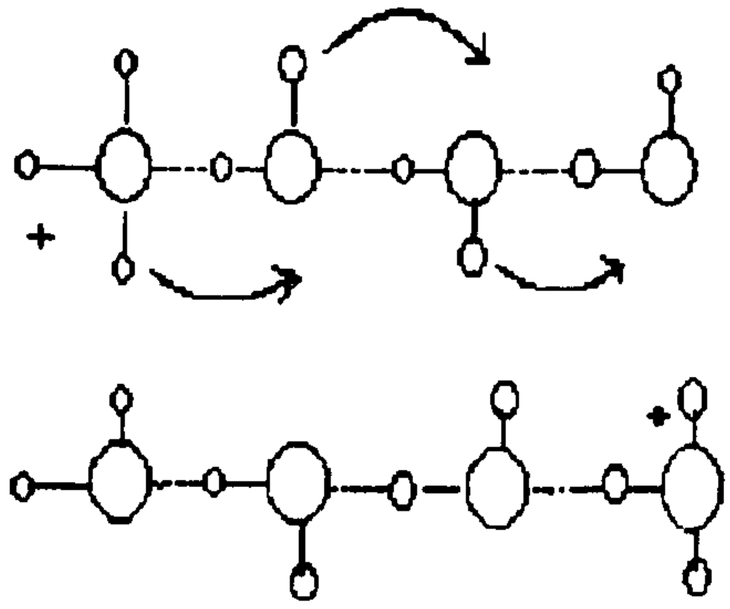

Fig. 2.1

The mechanism of conduction in water. Because protons can be transferred between molecules, the current is transported very rapidly down a chain by an effective, not an actual, migration of proton as each H_2O molecule passes one on to the next.

2.4 *MEASUREMENT OF THE ELECTRICAL CONDUCTIVITY OF MODEL SOLUTIONS PERTAINING TO SOIL WATERS*

2.4.1 *Background*

The work by Griffin and Jurinak [2] was carried out by analyzing various soil extracts and natural water samples for the major cations and anions namely Na^+, K^+, Ca^{2+}, Mg^{2+}, HCO_3^-, CO_3^{2-}, SO_4^{2-} and Cl^-. This data was then used to calculate the total ionic strength of the sample. It is however necessary in the case of such samples to correct the ionic strength in order that ion-pair formation can be taken into account. This can be done very rapidly through the use of the microcomputer. This type of ion-pair correction has also been carried out by Adams [4], Garrels and Thompson [5], Marion and Babcock [6] and Oster and McNeal [7]. The procedure for

ion-pair correction is carried out as follows.

2.4.2 *Ion-pair concentrations*

Although complete ion association can apply to many electrolyte solutions, it is not a rule of universal validity. What may occur in strong electrolyte solutions is that the cations and anions are so attracted to one another that in solution they behave as if unionized. Ions associated in this way are referred to as "ion-pairs". If the ions are equally charged e.g. Ca^{2+} and SO_4^{2-} then the resulting ion-pair will have no net charge ($CaSO_4^\circ$). However if the ions are unequally charged the ion-pair will have a charge e.g. K^+ and SO_4^{2-} in the form KSO_4^-. The extent to which free ions associate in solution is expressed by the traditional method for presenting the dissociation of weak electrolytes. Thus the ion-pair $CaSO_4^\circ$ dissociation reaction is written as,

$$CaSO_4 \quad Ca^{2+} + SO_4^{2-} \qquad \ldots\ldots (8)$$

$$\text{therefore } K = \frac{(Ca^{2+})(SO_4^{2-})}{(CaSO_4)} \qquad \ldots\ldots (9)$$

where parenthesis denote activity. The activity of the ion-pair is generally assumed to be unity. The equilibrium constants for several ion-pairs in aqueous solution at 298K and extrapolated to zero ionic strength are listed in Table 2.5.

As a result of ion-pairing, a soil solution component may actually be present as several different solution species. For example soil solution Ca may be present as Ca^{2+}, $CaSO_4^\circ$, $CaHPO_4^\circ$ or $CaHCO_3^+$. However the analytical methods for the determination of solution Ca make no distinction between the above species so that the "measured Ca" is actually the sum of $Ca^{2+} + CaSO_4^\circ + CaHPO_4^\circ + CaHCO_3^+$. Since the

Table 2.5

Equilibrium constants for selected ion pairs [8-9]

Ion-Pair			K
$CaSO_4^\circ$	⟶	$Ca^{2+} + SO_4^{2-}$	5.25×10^{-3}
$CaHPO_4^\circ$	⟶	$Ca^{2+} + HPO_4^{2-}$	1.98×10^{-3}
$CaH_2PO_4^+$	⟶	$Ca^{2+} + H_2PO_4^-$	9.3×10^{-2}
$CaCO_3^\circ$	⟶	$Ca^{2+} + CO_3^{2-}$	5.3×10^{-4}
$CaHCO_3$	⟶	Ca^{2+} HCO_3^-	5.5×10^{-3}
$MgSO_4^\circ$	⟶	$Mg^{2+} + SO_4^{2-}$	4.88×10^{-3}
$MgHPO_4^\circ$	⟶	$Mg^{2+} + HPO_4^{2-}$	3.16×10^{-3}
$MgH_2PO_4^+$	⟶	$Mg^{2+} + H_2PO_4^-$	1.0×10^{-1}
$MgCO_3^\circ$	⟶	$Mg^{2+} + CO_3^{2-}$	4.0×10^{-4}
$MgHCO_3^+$	⟶	$Mg^{2+} + HCO_3^-$	6.9×10^{-2}
$NaSO_4^-$	⟶	$Na^+ + SO_4^{2-}$	2.4×10^{-1}
KSO_4^-	⟶	$K^+ + SO_4^{2-}$	1.1×10^{-1}

measured Ca concentration of a soil solution, then, is actually the combined total of the Ca species in solution, the actual concentration of the Ca^{2+} ion *per se* must be calculated. The following general principles [4] apply to ion-pairing of common soil solutions cations and anions.

(i) There is no ion-pairing of cations with Cl^-.

(ii) Ion-pairing of cations with NO_3^- is so small that it can be ignored.

(iii) Ion-pairing with SO_4^{2-} is general; it is slight for univalent cations but is extensive for multivalent cations.

(iv) Ion-pairing with $H_2PO_4^-$ and HPO_4^{2-} is only slight for univalent cations and can be ignored; ion-pairing between $H_2PO_4^-$ and multivalent cations is significant but not extensive; ion-pairing between HPO_4^{2-} and univalent cations is insignificant; ion-pairing of multivalent cations with HCO_3^- is significant at high pH or at above normal CO_2 pressure.

2.4.3 *Calculation of ion-pair concentrations*

An analysis of the soil of interest must be carried out in order to determine the concentrations of all the cations and anions that affect ionic strength and also those of special interest. In order to illustrate the calculation procedure it is easier to consider a simple 0.01 Mol dm^{-3} solution of $CaSO_4$. In this case the actual ionic concentration of the solution will differ significantly from the measured value because Ca^{2+} and SO_4^{2-} pair extensively in solution. The pairing for these ions is defined by the following equation:

$$\frac{(Ca^{2+})(SO_4^{2-})}{[CaSO_4^{\circ}]} = 5.25 \times 10^{-3} \qquad \ldots\ldots (10)$$

where parenthesis denote activity, brackets denote concentration and the activity coefficient of $CaSO_4$ is unity. In this case, ionic strength and activity coefficients cannot be calculated directly. This is because ionic strength can only be calculated after $[Ca^{2+}]$ and $[SO_4^{2-}]$ are determined; $[Ca^{2+}]$ and $[SO_4^{2-}]$ can only be determined after $[CaSO_4^{\circ}]$ is ascertained; $[CaSO_4^{\circ}]$ is determined after (Ca^{2+}) and (SO_4^{2-}) are known. Calculation of (Ca^{2+}) and (SO_4^{2-}) values require known γCa^{2+} and γSO_4^{2-}; γCa^{2+} and γSO_4^{2-} are

determined from the ionic strength which was the original unknown. Thus the cycle of iterated unknowns has been completed without finding a solution for any of them. The problem is solved by the use of successive approximations. The first approximation assumes that measured $[Ca^{2+}]$ and $[SO_4^{2-}]$ values are the actual concentrations. Ionic strength can then be calculated from equation (11)

$$I = 1/2 \Sigma C_i Z_i^2 \quad \ldots\ldots (11)$$

therefore $I = 1/2[(0.01 \times 4) + (0.01 \times 4)]$

$= 0.04$

With $I = 0.04$, γCa^{2+} and γSO_4^{2-}, according to equation (12) are 0.51 and 0.47 respectively.

$$\log \gamma_i = -AZ^2 \frac{I^n}{1+Bd_i I^n} \quad \ldots\ldots (12)$$

Calculation of ionic activity then gives $(Ca^{2+}) = 5.1$ mMol dm^{-3} and $(SO_4^{2-}) = 4.7$ mMol dm^{-3}. These values permit the calculation of $[CaSO_4^\circ]$, according to equation (10) as

$$[CaSO_4^\circ] = \frac{(5.1)(4.7)}{5.25 \times 10^{-3}}$$

$= 4.56$ mMol dm^{-3}

This first approximation yields values that are too large for I, $[Ca^{2+}]$, $[SO_4^{2-}]$ and $[CaSO_4^\circ]$. Using the first approximation of $[CaSO_4^\circ]$, the second approximation of $[Ca^{2+}]$ is 10.00 - 4.56 = 5.44 mMol dm^{-3}. Similarly the

second estimate of [SO_4^{2-}] and [$CaSO_4^\circ$] are 5.44 mMol dm^{-3} instead of the original 10.00 mMol dm^{-3} the other second estimates are I = 0.022 Mol dm^{-3}, γCa^{2+} = 0.58, γSO_4^{2-} = 0.56, (Ca^{2+}) = 3.16 mMol dm^{-3}, (SO_4^{2-}) = 3.05 mMol dm^{-3} and [$CaSO_4^\circ$] = 1.83 mMol dm^{-3} . This second approximation underestimates, I, [Ca^{2+}] and [$CaSO_4^\circ$]. This process is repeated until there is no change in successive values. As this process is rather tedious an Amstrad PC1512 and a Turbo Basic software package was used in order to carry out these calculations. After iteration of these equations the actual [Ca^{2+}] and [SO_4^{2-}] values in a 10 mMol dm^{-3} solution of $CaSO_4$ are calculated to be 7.17 mMol dm^{-3} and [$CaSO_4^\circ$] = 2.83 mMol dm^{-3} . Other final values are I = 0.029 mMol dm^{-3}, (Ca^{2+}) = 3.94 mMol dm^{-3}, (SO_4^{2-}) = 3.73 mMol dm^{-3}. Without this correction for ion-pairs (Ca^{2+}) and (SO_4^{2-}) would have been calculated according to the Debye-Huckel equation to be 5.10 mMol dm^{-3} and 4.7 mMol dm^{-3} respectively.

2.4.4 *Mixed electrolyte solutions*

The above is also applicable to mixed electrolyte solutions. The number of equations that must be solved is greater and the number of iterations may be more numerous, but the basic procedure is the same. This was carried out by the computer program IPC.

Step 1: Ionic concentrations and ionic strength

Each measured concentration was assumed to be the actual ionic concentration. The concentrations of Cl^- and NO_3^- were summed and listed as the Cl^- concentration. This is because neither of these ions undergo any significant complexation in soil solutions. The phosphate concentration was initially ignored but was built into the program in a later section. The ionic strength was then calculated according to equation (11).

Step 2: Ionic activities

The activity of each ion was then calculated by multiplying its concentration by its activity coefficient.

Step 3: Ion-pair concentrations

Ion-pair calculations were calculated for the following ion-pairs. $CaSO_4^\circ$, $CaCO_3^\circ$, $CaHCO_3^+$, $MgHCO_3^+$, $MgSO_4^\circ$, $MgCO_3^\circ$, $NaSO_4^-$ and KSO_4^-. The dissociation constants for each ion-pair were listed earlier in Table 2.5.

Step 4: Revised ionic concentrations and ionic strength

A second estimate of ionic strength was obtained by subtracting ion-pair concentrations from the appropriate "measured" ionic concentrations, e.g. second approximation of $[Ca^{2+}]$.

$$[Ca^{2+}] = \text{Measured Ca} - ([CaSO_4^\circ] + [CaCO_3^\circ] + [CaHCO_3^+]) \quad \ldots\ldots (13)$$

$$[HCO_3^-] = \text{Measured } HCO_3^- - ([CaHCO_3^+] + [MgHCO_3^+]) \quad \ldots\ldots (14)$$

This was repeated for all cations and anions, the ionic strength was recalculated and the whole process was repeated until subsequent calculations of ionic strength yielded values of ionic strength that were within 1% of each other. This value was then taken as the corrected ionic strength. A listing of the program used is given in Appendix 1. This program was written in Turbo Basic which is a compilable form of basic and is therefore very fast to run. The program was tested using the ionic strength data of Griffin and Jurinak [2] and gave excellent agreement with their corrected ionic strength values.

2.4.5 *Determination of the relationship between ionic strength and conductivity*

When this relationship has been investigated in the past it has always been carried out on real environmental samples, where the

concentrations of the major cations and anions have been determined by the usual analytical methods [2, 4]. The total ionic strength was then corrected for ion-pair formation. It was decided to repeat this work using model solutions containing similar ionic concentrations to those investigated previously. It was hoped that this would provide a more accurate indication of the ionic strength-conductivity relationship, as the concentrations of all the ionic species would be accurately known.

2.4.5.1 **Experimental**

Solutions of the relevant concentrations were made up using the following chemicals, $CaCl_2$, $CaCO_3$, NaCl, $NaHCO_3$, Na_2SO_4, K_2SO_4, KCl, $MgCl_2$. All chemicals used were "Analar" grade (BDH Chemicals Ltd., Poole, UK). The ionic strength of each model solution was corrected for the formation of the following ion-pairs ($CaSO_4^\circ$, $CaCO_3^\circ$, $CaHCO_3^+$, $MgSO_4^\circ$, $MgHCO_3^+$, $NaSO_4^-$, KSO_4^-, $MgCO_3^\circ$), by using the program IPC. All conductivity measurements were carried out as before.

2.4.5.2 **Results**

The results for 18 model solutions are listed in Table 2.6 and a linear regression was carried out plotting ionic strength v's conductivity which is shown in graph 2.4.

2.4.5.3 **Discussion**

From the graph it is evident that there is in fact a clear cut relationship between ionic strength and conductivity. The relationship was found to be

$$I = 0.01113\ EC \qquad \ldots\ldots (15)$$

$$r = 0.9993$$

where I = Ionic strength (mMol dm^{-3}) and EC = Electrical Conductivity (mS cm^{-1}).

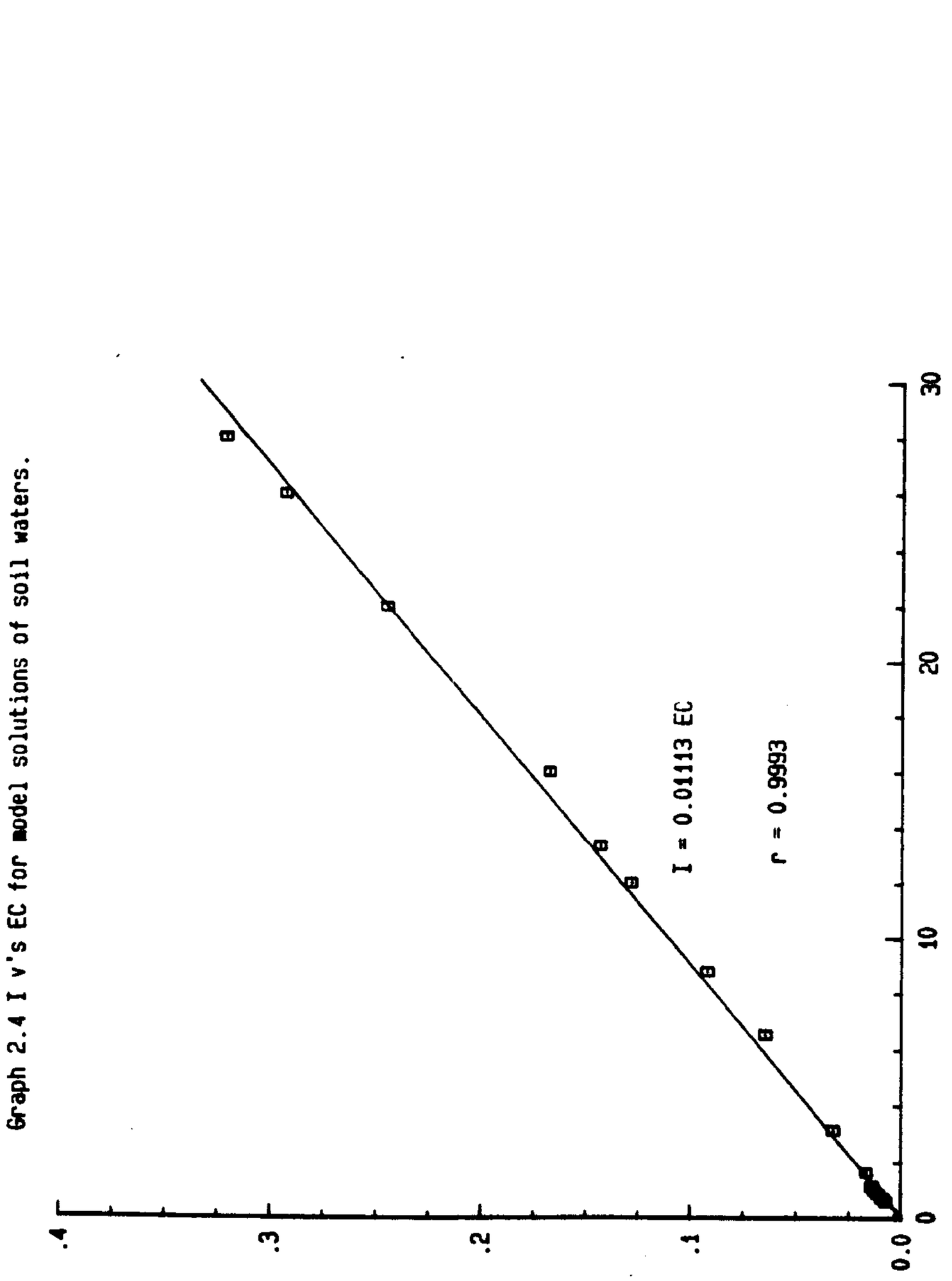
Graph 2.4 I v's EC for model solutions of soil waters.
I = 0.01113 EC
r = 0.9993
Ionic strength / moldm-3
EC / millisiemenscm-1
0.0
.1
.2
.3
.4
0
10
20
30

Table 2.6

Solution No	Conc millimol dm^{-3}									
	Ca^{2+}	Mg^{2+}	Na^{+}	K^{+}	HCO_3^{-}	CO_3^{-}	SO_4^{2-}	Cl^{-}	EC	I
1.	1.64	0.42	1.74	1.33	1.74	0.06	0.66	3.97	0.76	9.33
2.	2.07	0.46	2.99	2.02	2.90	0.09	1.01	4.90	1.04	12.71
3.	1.61	0.49	3.01	1.58	3.01	0.09	0.79	4.03	0.89	10.98
4.	0.89	0.20	3.63	1.54	3.63	0.13	0.77	1.93	0.72	8.82
5.	0.43	0.09	7.45	3.22	5.12	0.08	1.61	3.43	1.17	13.73
6.	0.36	0.09	10.50	1.01	7.04	0.20	1.53	2.00	1.15	14.14
7.	0.34	0.03	27.40	1.46	4.42	0.07	2.72	19.59	3.15	32.20
8.	2.39	0.30	115.80	2.92	1.92	0.05	3.50	115.08	12.00	128.00
9.	3.68	0.51	149.75	3.24	1.91	0.02	3.47	152.48	16.00	167.20
10.	2.29	0.61	3.00	1.00	3.00	0.24	0.50	5.32	0.98	12.39
11.	0.60	0.19	2.84	1.66	2.17	0.38	0.83	1.49	0.59	7.30
12.	0.46	0.22	12.17	1.70	2.17	0.12	0.85	11.12	1.65	16.50
13.	3.16	2.75	116.91	6.06	1.83	0.06	6.67	119.50	13.33	142.90
14.	7.32	8.80	265.55	4.46	2.03	-	15.43	269.36	28.00	321.00
15.	1.95	1.30	74.92	5.00	4.20	-	3.81	74.36	8.75	91.50
16.	1.21	0.34	55.10	3.20	1.30	0.11	2.01	55.88	6.50	64.30
17.	5.75	5.19	204.30	4.84	0.98	0.07	9.12	213.64	22.00	244.60
18.	6.58	7.07	245.90	4.16	0.82	0.04	12.15	252.20	26.00	292.60

This is significantly different to that found by Griffin [2] which is shown below,

$$I = 0.013\ EC \qquad \ldots\ldots (16)$$

$$r = 0.996$$

This could be accounted for as follows. In their work the concentrations of cations and anions were determined by standard methods e.g. metals by flame atomic absorption spectrometry (AAS). The resulting data obtained would only give the total concentration of a particular metal in the sample not the ionic fraction which is the fraction of particular interest, as this is the fraction that would contribute to the ionic strength. The total concentration as measured by flame AAS would include particulate metal, metal adsorbed on to organic or inorganic colloids and organically complexed metal. None of these forms would contribute to the total ionic strength of as any metal in these forms would be effectively removed from the solution. This means that by using the total metal concentration determined by flame AAS in the calculation of ionic strength would result in a higher value for ionic strength than is actually the case. The results from this work yielded a significantly higher correlation coefficient than those obtained by Griffin. It is also likely that the results obtained here are more reliable in that the concentrations of all cations and anions are accurately known.

2.5 *APPLICATION OF THE IONIC STRENGTH v's CONDUCTIVITY RELATIONSHIP TO MODEL SOLUTIONS OF THE SOIL SITES OF INTEREST*

2.5.1 *Sample collection*

The analysis began with sampling which, like all other stages of an analytical procedure may be subject to both random and systematic error.

Sampling was carried out on a site at Laverockbrae Farm, Aberdeen, on 19th January 1988 and then again on 24th March. Samples were taken from a control field which was situated next to the contaminated field and hence were used as a comparison. The field of interest has had at least six applications of sewage sludge from the Persley sewage treatment plant over the past ten years. Surface water from the various areas was collected using a syringe with a one metre length of tubing attached.

2.5.2 *Sample preparation*

Preparation of the soil samples for extraction and chemical analysis of the interstitial water involved weighing out 200 g portions of soil, minus any stones, into sample bottles. The variation in weight was kept to within 0.500 g in order to keep the centrifuge balanced. The sample bottles were each placed into the centrifuge, with the lid secured and the centrifuge set at the desired speed. The centrifuge speed used was relatively low in order that only the free soil water would be extracted, any water that was tightly bound in the smaller pores would therefore not be extracted. In order to find the optimum conditions for the extraction of water, the first sample was spun at various speeds for different periods of time. This process of weighing and spinning was carried out several times using the same weights of soil in clean sample bottles. To the samples from the upper section of the sludge-treated field and to the control field, 20 ml of surface water was added as a displacent, since no water was extracted by simply spinning these soils. The total amounts of soil and surface water are shown in Table 2.7.

Table 2.7

Lab No	Total Weight of Soil/(g)	Volume of surface water added/(ml)
1	2400	240
1D	2400	240
2	1400	-
2D	1400	-
2(X)	1000	100
2-D(X)	1000	100

In order for the surface water to displace the interstitial water, it was added and allowed to equilibrate through the soil overnight, after which the soils were spun and the extracted water separated into the chosen sample containers. This procedure was continued until no more water was extracted and eventually the soils were discarded. For lab 2, that is the samples from the lower section of the sludge treated field, when no more water could be extracted the above procedure of adding a displacent was carried out and the resulting extracted solution labelled lab 2(X) and 2-d(X) for the duplicate. Finally, the eight solutions of interstitial water were filtered separately into clean vials through a millipore membrane filter using an all glass funnel.

NOTE:

1) The extracted samples and surface waters were stored in a cold room (T = 4°C) until required for analysis.

2) Yields of interstitial water from soils at field capacity are typically 20-50% of the total water present.

2.5.3 *Chemical analysis*

2.5.4 *Cation analysis*

The cation concentrations were determined by the use of atomic spectroscopy, primarily Inductively Coupled Plasma Optical Emission Spectroscopy (ICP-OES), but also flame AAS.

2.5.4.1 **Inductively coupled plasma optical emission spectroscopy (ICP-OES)**

An ICP-OES linked to a DEC PDP 11/03 minicomputer was calibrated for the following elements using a simple two point calibration, taking the blank as zero point plus one standard point: (figures in parenthesis are the wavelength (nm) followed by the standard concentration used for calibration (ppm)): Cu (324.75, 0.1); Na (588.9, 10.0); Mn (257.61, 0.1); P (213.62, 0.1). The standard used contained Ca, Mg, Na, K, P, Fe, Cu and Al and also 0.01 M EDTA, when analyzing for copper. The calibrations were carried out using acidified standards. The samples used were also acidified, since the capillary tubing attached to the nebuliser was rinsed with acid between each sample. Blanks and standards were checked at intervals to allow corrections to be made for any slight, within run, instrumental drift. Measured concentrations were based on the average of two integrations for every sample analysed by ICP-OES.

2.5.4.2 **Atomic Absorption Spectroscopy**

The analysis of the remainder of the cations was carried out using unacidified samples. For the analysis of Ca and Mg, atomic absorption spectrometers were used, namely a Varian Techtron AA-1275 using a nitrous oxide-acetylene flame for Ca and a Perkin-Elmer 560 AAS for Mg. For the analysis of Ca and Mg, the soil solutions and surface water samples were

each made up into a solution containing 2500 ppm Sr. This was carried out by adding 5 ml of 12500 ppm Sr plus 19 ml of distilled water to each 1 ml sample of soil extract and similarly to the surface waters, using a pipette. This was then made equivalent to 2500 ppm by a 25 times dilution with distilled water. For the analysis of Ca and Mg, standards containing Sr, as a releasing agent, were used in the concentrations given in Table 2.8.

Table 2.8

Standard	Concentration/ppm Mg	Ca
Blank	-	-
1	6.0	1.2
2	2.4	0.6
3	1.2	0.3
4	0.6	0.15

2.5.5 *Techniques for the analysis of anions*

2.5.5.1 High performance ion chromatography (HPIC) for the determination of Cl^-, NO_3^-, SO_4^{2-}

A widely used analytical technique for the determination of all types of ions, ion chromatography is a liquid chromatographic technique often used in conjunction with suppressed conductivity detection. This technique can achieve the separation and determination of anions and cations [10]. A Dionex HPIC system linked to an autoanalyser was used for the determination of Cl^-, NO_3^- and SO_4^{2-} concentrations simultaneously. The surface water and soil water samples were poured into separate cups which

each held approximately 4 ml of solution. The sample cups were then placed on an automated turntable and the autoanalyser set to analyse the number of samples present. The standards and bulk solution were run initially and again at the end of the analysis. The results of the chromatographic separation were displayed on a strip chart recorder. From the chromatogram, peak heights were measured and the data used to calculate the concentrations by the computer program "Water analysis" which compensates for any linear drift with time between two sets of standards.

Table 2.9

HPIC Conditions

Eluent:	72 mMol dm^{-3} Na_2CO_3/69 mMol dm^{-3} $NaHCO_3$
Flow rate:	1.8 ml/min
Regenerant acid:	0.0125 mMol dm^{-3} H_2SO_4 2 ml/min pumping under 5 psi
Detection:	Conductivity 10 μs
Injection volume:	50 μl

Table 2.10

HPIC Standards

Anion Concentration/ppm	Standard 1	2	3	4
Cl^-	25	50	125	250
F^-	1	2	5	10
NH_4^+	1	2	5	10
PO_4^{3-}	2	4	10	20
NO_3^-	4	8	20	40
SO_4^{2-}	10	20	40	100

Table 2.11

Contents of bulk water solution

Element	Concentration/ppm
NH_4-N	1
NO_3^-	1
K	10
Mg	2
Na	5.2
PO_4-P	0.25
Cl^-	16.77
S	2.64

2.5.5.2 **Colorimetry**

Analysis for the bicarbonate concentration was carried out using a laboratory built colorimeter linked to an autoanalyser. This method is not applicable to coloured or turbid samples, nor samples with a pH lower than 3.1. The method typically covers a total alkalinity range of 0.5 to 100 mg dm^{-3} of $CaCO_3$. The sample was segmented with air and then mixed with a weakly buffered solution of methyl orange, as can be seen from Figure 2.2.

Figure 2.2

Manifold for colorimetric analysis

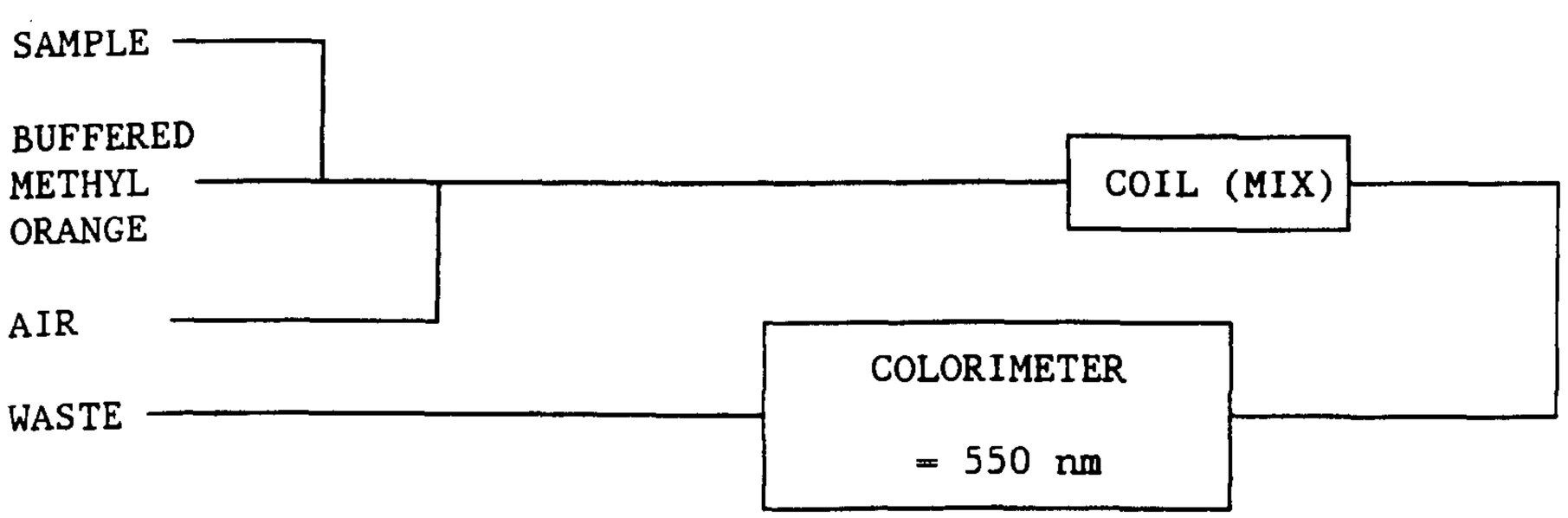

The resulting colour change was measured at 550 nm by means of a continuous flow colorimeter. The samples were placed in the sample cups and on to the automated turntable. Once the baseline had settled the autoanalyser was wet and the samples and standards run. The results were dealt with in the same way as the HPIC results.

2.5.5.3 **pH measurement**

The pH of each sample was measured using buffer solutions of pH 7.00 and 4.00 for standardisation.

2.5.6 ***Results***

The results are shown in Tables 2.12-2.14.

2.5.7 ***Discussion***

The sampling site at Laverockbrae Farm was chosen for this study because it had been treated with seven applications of sewage sludge since 1977, giving rise to increased levels of heavy metals in the soil. The heavy metal content of the applied sewage was as shown in Table 2.15.

Table 2.12

SOIL EXTRACT CONCENTRATIONS

SPECIES	CONCENTRATION ppm $x10^{-3}$ moldm^{-3}					
SURFACE WATERS	Cl^-	HCO_3^-	NO_3^-	PO_4^{2-}	SO_4^{2-}	Ca^{2+}
LAB 1	38.132 1.074	39.101 0.641	16.713 0.269	0.205 0.00216	8.073 0.0841	1.1948 0.0298
LAB 1-D	27.538 0.776	34.9 0.57	26.733 0.431	0.198 0.0021	11.97 0.124	2.093 0.0523
LAB 2	35.465 0.999	12.86 0.211	28.429 0.458	0.155 0.00163	7.31 0.076	2.330 0.0583
LAB 2-D	29.2 0.823	12.86 0.211	21.879 0.353	0.113 0.00119	8.6 0.089	2.998 0.0749
LAB 2(X)	29.77 0.839	24.91 0.408	15.215 0.245	0.104 0.00109	10.35 0.108	1.506 0.0377
LAB 2-D (X)	28.13 0.792	59.03 0.968	18.789 0.303	0.101 0.00106	12.49 0.130	2.344 0.0586
LAB C	23.31 0.657	49.77 0.816	8.574 0.141	0.0073 0.00076	4.510 0.047	0.96 0.024
LAB C-D	22.19 0.625	36.61 0.600	16.85 0.272	0.142 0.00149	14.23 0.252	1.10 0.0275

cont .....

Table 2.12 cont.

SOIL EXTRACT CONCENTRATIONS

SPECIES SURFACE WATERS	Cu^{2+}	K^{+}	Mg^{2+}	Mn^{2+}	Na^{+}
LAB 1	0.0313 0.000489	2.253 0.0577	0.16 0.0067	0.0041 0.000075	24.26 1.0547
LAB 1-D	0.0178 0.000278	1.994 0.0511	0.17 0.00709	0.0067 0.000122	16.29 0.708
LAB 2	0.02 0.000313	2.399 0.0615	0.10 0.00417	0.0184 0.000335	10.67 0.464
LAB 2-D	0.0375 0.000586	2.82 0.0723	0.05 0.00208	0.0098 0.000178	14.10 0.613
LAB2(X)	0.0179 0.000279	2.54 0.0651	0.06 0.0025	0.0087 0.000158	13.98 0.608
LAB 2-D (X)	0.0238 0.000372	2.25 0.0577	0.12 0.005	0.00824 0.000149	11.74 0.510
LAB C	0.0157 0.000245	1.15 0.0295	0.06 0.0025	0.023 0.000418	16.04 0.697
LAB C-D	0.045 0.000703	0.905 0.0232	0.06 0.0025	0.034 0.000618	16.96 0.737

Table 2.13

SURFACE WATER CONCENTRATIONS

	ppm x10^{-3} CONCENTRATION moldm^{-3}					
SPECIES						
SURFACE WATERS	Cl^-	HCO_3^-	NO_3^-	PO_4^{2-}	SO_4^{2-}	Ca^{2+}
LAB C	25.18	33.09	1.501	0.252	4.144	0.65
SW C	0.709	0.542	0.00242	0.00265	0.0432	0.0163
LAB C	24.98	36.119	0.852	0.290	3.551	0.57
SW C	0.703	0.592	0.00137	0.0031	0.0369	0.0143
LAB C	26.033	41.989	3.043	0.293	4.631	0.61
SW C-D	0.733	0.688	0.00491	0.00308	0.0482	0.0153
LAB C	27.876	31.238	3.576	0.28	3.989	0.62
SW C-D	0.785	0.512	0.00577	0.00295	0.0455	0.0155

SPECIES					
SURFACE WATERS	Cu^{2+}	K^+	Mg^{2+}	Mn^{2+}	Na^+
LAB C	0.0095	8.95	0.08	0.0039	10.43
SW C	0.00015	0.229	0.0033	7.09×10^{-5}	0.45
LAB C	0.0088	9.2	0.07	0.00415	10.28
SW C	0.00015	0.235	0.0029	7.55×10^{-5}	0.447
LAB C	0.0098	10.39	0.09	0.0029	11.45
SW C-D	0.00015	0.265	0.0038	5.32×10^{-5}	0.498
LAB C	0.0087	10.19	0.09	0.00199	11.33
SW C-D	0.00014	0.261	0.0038	3.62×10^{-5}	0.493

Table 2.14

Soil Extract	pH
Lab 1	7.38
Lab 1-d	6.83
Lab 2	6.49
Lab 2-d	6.74
Lab 2(X)	6.75
Lab 2-d(X)	6.81
Lab-c	5.22
Lab c-d	4.6

Table 2.15

Persley Sewage Sludge, results from approximately 30 analyses over a period of 10 years

Metal	Concentration mg/kg dry mass
Cadmium	22
Copper	200
Manganese	130
Zinc	430

Samples were taken from the control field, as a comparison, in order to find out how far the actual Cu levels have increased, due to treatment. However due to the similarity of the results from the three areas, it

appears that there must have been some contamination of the control field. This is quite a logical assumption since the treated field is on a slight hill. Hence any run-off caused by a rainfall event would naturally go into this control field, giving rise to similar analytical results to those in the treated field. The day of sampling was carefully chosen so that the soil was at field capacity as a result of the overnight rainfall. This was in the hope that rainwater would have percolated through the soil collecting any contaminants that were present. The actual surface of the field was very wet, with bodies of water lying in the lower area (Lab 2), of the treated field where it tended to collect. Also, on collection of the soil samples, it was observed that there was some frosting on the top soil, which may also have had an effect on some of the results e.g. moisture content. One point was very apparent from the results i.e. the very low copper concentrations in each of the samples. This was very surprising due to the fact that this field had seven applications of sewage sludge with a copper content of 200 ppm. The reason for this may be that the copper is very strongly bound to organic ligands in the very small pores and the relatively low speed of centrifugation was apparently not high enough to extract copper bound in this way. When we look at the results as a whole they indicate that there are increased ionic concentrations in the surface water from Lab 2, i.e. the lower part of the field when compared to those taken at the upper part (Lab 1). However, the opposite is true of the soil extracts. This would tend to suggest that at Lab 1, the rainfall will percolate through the soil but there is also a run-off down to Lab 2 where large amounts of water have collected and have had no time to percolate through the soil. The contaminant levels of Cu

2.5.8 *Modification of IPC in order that the concentration of phosphate ion-pairs can be taken into account*

Although the concentration of phosphate was very low it was decided to modify the computer model in order to take account of the following ion-pairs, $CaHPO_4^\circ$, $CaH_2HPO_4^+$, $MgHPO_4^\circ$ and $MgH_2HPO_4^+$. For this lines were written to allow pH and $[PO_4^{3-}]$ to be input. The equations for calculation of single ion activity coefficients γH^+, $\gamma H_2PO_4^-$ and γHPO_4^{2-} were added and for this the relevant ionic activities were calculated. This was carried out by combining the following equations:

$$\text{Total Phosphate} = [H_2PO_4^-] + [HPO_4^{2-}] \quad \ldots\ldots (17)$$

$$= (H_2PO_4^-) + (HPO_4^{2-}) \quad \ldots\ldots (18)$$

$$\frac{}{\gamma H_2PO_4^-} \qquad \frac{}{\gamma HPO_4^{2-}}$$

$$\text{and } 6.3 \times 10^{-8} = \frac{(H^+)(HPO_4^{2-})}{(H_2PO_4^-)} \quad \ldots\ldots (19)$$

$$\text{to give } (HPO_4^{2-}) = \frac{[H_2PO_4^-] + [HPO_4^{2-}]}{[(H^+)/6.23 \times 10^{-8}\gamma H_2PO_4^-] + 1/\gamma HPO_4^{2-}} \quad \ldots\ldots (20)$$

where (HPO_4^{2-}) is the only unknown. After (HPO_4^{2-}) was calculated according to equation (20), $(H_2PO_4^-)$ was found by use of equation (19). The mass balance equations were modified to take the 4 new ion-pairs into consideration. The following relationship was used to calculated the second estimate of ionic phosphate concentrations.

$$[H_2PO_4^-] + [HPO_4^{2-}] = \text{Measured } [PO_4^{3-}] - ([CaHPO_4^\circ] + [CaH_2HPO_4^+] + [MgHPO_4^\circ] + [MgH_2HPO_4^+]) \quad \ldots\ldots (21)$$

The phosphate was assumed to be completely in the form of $H_2PO_4^-$ for the computation of ionic strength (3). The revised version of the program is shown in Appendix 2.

2.5.9 ***Correlation of ionic strength and conductivity***

Synthetic solutions were prepared which had similar ionic concentrations to the polluted field soil extracts. These were prepared by the appropriate dilution of the following stock solutions, 0.0398 M $CaCl_2$, 0.010M $MgCl_2$, 0.0252M K_2SO_4, 0.0256M Na_2SO_4, 0.0048M Na_2HPO_4, 0.1M $NaHCO_3$, 0.2013M NaCl. All chemicals used were "Analar" grade.

2.5.10 ***Results***

The results for five model solutions of the soil extracts are shown in Table 2.16.

Table 2.16

Results

	Conc Millimol dm^{-3}										
Soil Extract	Ca^{2+}	Mg^{2+}	Na^+	K^+	HCO_3^-	PO_4^{3-}	Cl^-	SO_4^{2-}	pH	EC	I
Lab 1	0.03	0.007	1.75	0.06	0.64	0.0022	1.07	0.084	7.5	0.212	2.0
Lab 2	0.06	0.004	0.7	0.06	0.21	0.0016	0.53	0.07	7.0	0.104	1.0
Lab2-d(X)	0.038	0.0025	0.98	0.065	0.41	0.0011	0.5	0.11	7.2	0.13	1.28
Lab 1-d	0.052	0.007	1.17	0.051	0.57	0.0021	0.52	0.12	7.9	0.15	1.75
Lab c	0.024	0.002	1.18	0.03	0.82	0.0008	0.353	0.047	7.7	0.13	1.34

These points were added to the earlier data in Table 2.4 and a linear regression analysis was carried out. This is shown in graph 2.5. The resulting relationship between I and EC is shown in equation (22).

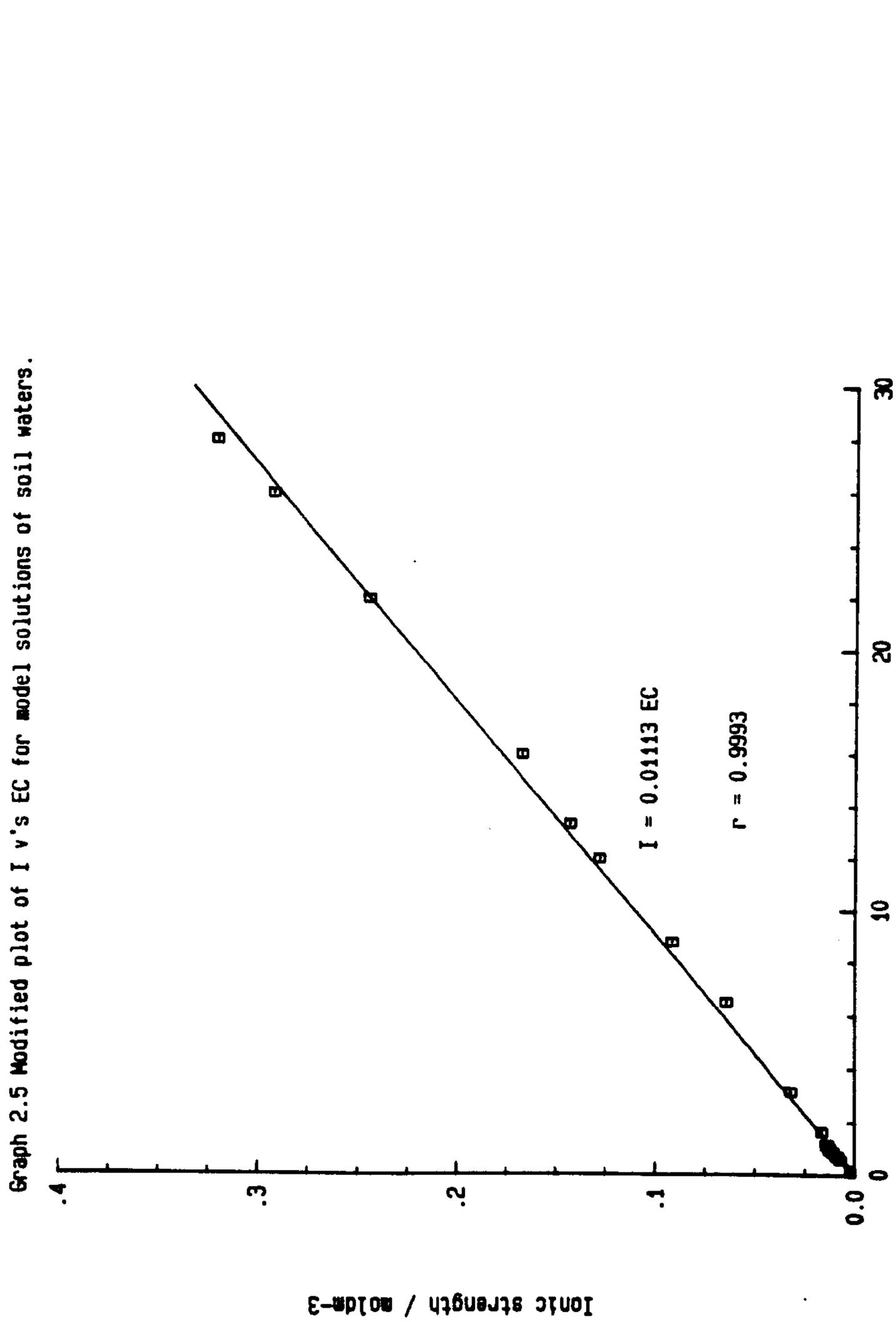
Graph 2.5 Modified plot of I v's EC for model solutions of soil waters.
I = 0.01113 EC
r = 0.9993
Ionic strength / moldm-3
EC / millisiemenscm-1
0.0
.1
.2
.3
.4
0
10
20
30

$$I = 0.01113\ EC \qquad \ldots\ldots (22)$$

$$r = 0.9993$$

Again the degree of correlation is higher than that found by Griffin and it would suggest that the relationship is valid.

2.5.11 ***Conclusion***

From this work it has been shown that a linear relationship exists between Ionic Strength and Electrical conductivity of soil solutions. This will enable HPLC eluents to be prepared with similar ionic strengths to that of a soil sample to be prepared without the need for any prior ionic analysis.

REFERENCES

1. Ponnamperuma, F.N., Tianco, E.M. and Loy, T.A. (1966), Soil Sci, **102**, 408-413.

2. Griffin, R.A. and Jurinak, J.J. (1973), Soil Sci., **116**, 26-30.

3. Atkins P.W., (1987), Physical Chemistry, Oxford University Press, Oxford, Chapter 27.

4. Adams, F. (1971), Soil Sci. Am. Proc., **35**, 420-426.

5. Garrels, R.M. and Christ, C.H., (1965), Solutions Minerals and Equilibria. Harper and Row, New York, Chapter 2.

6. Marion, G.M. and Babcock, K.L. (1976), Soil Sci., **122**(4), 181-187.

7. Oster, J.D. and McNeal, B.L. (1971), **35**, 436-442.

8. Davies, C.W. (1962), in "Ion association", Butterworth, Washington, D.C., 190 p.

9. Sillen, L.G. and Martell, A.E., (1964), Stability constants of metal-ion complexes, The Chemical Society, London, 754 p.

10. Skoog, D.A. (1985), Principles of instrumental analysis, CBS College Publishing, Japan, 817-824.

APPENDIX 2.1

IPC

```
'THIS IS A PROGRAM WHICH CONVERTS IONIC STRENGTH DATA
'IN ORDER THAT ION-PAIRS MAY BE TAKEN INTO ACCOUNT
'(1) INPUT OF DATA
10 CLS
PRINT"PLEASE INPUT THE CONCENTRATIONS (mmoles/litre) OF THE FOLLOWING "
PRINT"CATIONS AND ANIONS EACH SEPARATED BY A COMMA."
PRINT"Ca,Mg,Na,K,Sulphate,Carbonate,Bicarbonate,Chloride."
INPUT CA#,MG#,NA#,K#,S#,CO#,BI#,CL#
CLS
PRINT
PRINT
PRINT"HERE IS THE INPUTED DATA (mmoles/litre)"
PRINT
PRINT"CALCIUM CONCENTRATION        = ",CA#
PRINT
PRINT"MAGNESIUM CONCENTRATION      = ",MG#
PRINT
PRINT"SODIUM CONCENTRATION         = ",NA#
PRINT
PRINT"POTASSIUM CONCENTRATION      = ",K#
PRINT
PRINT"SULPHATE CONCENTRATION       = ",S#
PRINT
PRINT"CARBONATE CONCENTRATION      = ",CO#
PRINT
PRINT"BICARBONATE CONCENTRATION    = ",BI#
PRINT
PRINT"CHLORIDE CONCENTRATION       = ",CL#
PRINT
CA#=CA#*1E-3:MG#=MG#*1E-3:NA#=NA#*1E-3:K#=K#*1E-3
S#=S#*1E-3:CO#=CO#*1E-3:BI#=BI#*1E-3:CL#=CL#*1E-3
INPUT"IS THIS DATA CORRECT Y/N ",X$
IF X$="N" GOTO 10,
'CALCULATION OF IONIC STRENGTH
'
N%=0
I#=0.5*((CA#*4)+(MG#*4)+NA#+K#+(S#*4)+(CO#*4)+BI#+CL#)
CC#=CA#:CM#=MG#:CN#=NA#:CK#=K#:CS#=S#
CCO#=CO#:CBIC#=BI#:CCL#=CL#
```

```
20
N%=N%+1
'
' (2) Calculation of single ion activity coefficients
'
'
A#=0.509: B#=0.329 :Y#=A#*SQR(I#):Z#=B#*SQR(I#)
C#=(4*Y#)/(1+(6*Z#))              'Ca
D#=(4*Y#)/(1+(8*Z#))              'Mg
E#=(Y#)/(1+(4.5*Z#))              'Na
F#=(Y#)/(1+(3*Z#))                'K
G#=(4*Y#)/(1+(4*Z#))              'SO4
H#=(4*Y#)/(1+(4.5*Z#))            'CO3
J#=(Y#)/(1+(4.5*Z#))              'HCO3
'
FC#=EXP10(-C#):FM#=EXP10(-D#)
FS#=EXP10(-E#):FK#=EXP10(-F#)
FSO#=EXP10(-G#):FCO#=EXP10(-H#)
FBI#=EXP10(-J#)
'
'
'(3) CALCULATION OF IONIC ACTIVITIES
'
AC#=FC#*CC#: AM#=FM#*CM# : ANA#=FS#*CN#
AK#=FK#*CK#    : ASO#=FSO#*CS# : ACO#=FCO#*CCO#
ABIC#=FBI#*CBIC#
'
' (4) CALCULATION OF EQUILIBRIUM CONCENTRATIONS
'
'
CASO4#=(AC#*ASO#)/5.25E-003
CACO3#=(AC#*ACO#)/6.3E-004
CBI#=(AC#*ABIC#)/5.5E-002
CMS#=(AM#*ASO#)/5.88E-003
CMB#=AM#*ABIC#)/6.9E-002
CNS#=(ANA#*ASO#)/2.4E-001
CPS#=(AK#*ASO#)/1.1E-001
CMC#=(AM#*ACO#)/4E-004
'
'
'(5) MASS BALANCE EQUATIONS
'
'
CC#=CA#-(CASO4#+CACO3#+CBI#): CM#=MG#-(CMS#+CMC#+CMB#)
CK#=K#-(CPS#): CN#=NA#-(CNS#)
CCO#=CO#-(CMC#+CACO3): CBIC#=BI#-(CBI#+CMB#)
CS#=S#-(CASO4#+CMS#+CNS#+CPS#)
```

```
IF CC#<0 THEN CC#=(CC#+CA#)/2          '       THESE LINES PREVENT
IF CM#<0 THEN CM#=(CM#+MG#)/2          '
IF CK#<0 THEN CK#=(CK#+K#)/2           '       NEGATIVE CONCENTRATION
IF CN#<0 THEN CN#=(CN#+NA#)/2          '
IF CCO#<0 THEN CCO#=(CCO#+CO#)/2       '       VALUES FROM
IF CBIC#<0 THEN CBIC#=(CBIC#+BI#)/2    '
IF CS#<0 THEN CS#=(CS#+S#)/2           '       OCCURRING
'
'
'
IO#=0.5*((CC#*4)+(CM#*4)+CN#+CK#+(CS#*4)+(CCO#*4)+CBIC#+CL#)
IF N%> 500 GOTO 50
IF (I#/IO#),0.99 OR (I#/IO#).1.01 THEN GOTO 25
IF 0.99<(I#/IO#),1.01 THEN GOTO 30
25 I=IO# :GOTO 20
'
'
'
30 CLS
'
' (6) OUTPUT OF DATA
PRINT "THE IONIC STRENGTH OF THIS SOLUTION AFTER CORRECTION FOR"
PRINT
PRINT "ION PAIRS (mmoles/litre) =  " USING ###.###";    IO#*1E3
PRINT
PRINT "THIS CALCULATION TOOK ,",N%," ITERATION(S)"
PRINT
INPUT "DO YOU WISH TO SEE THE INDIVIDUAL FREE ION CONCENTRATIONS Y/N ",B$
IF B$="N" THEN GOTO 40
PRINT
PRINT "FREE ION     CONC(mmoles/litre)"
PRINT
PRINT "[Ca]  =      " USING "###.##";CC#*1E3
PRINT "[Mg]  =      " USING "###.##";CM#*1E3
PRINT "[K]   =      " USING "###.##";CK#*1E3
PRINT "[Na]  =      " USING "###.##";CN#*1E3
PRINT "[CO3] =      " USING "###.##;CCO#*1E3
PRINT "[HCO3]=      " USING "###.##;CBIC#*1E3
PRINT "[SO4] =      " USING "###.##";CS#*1E3
PRINT "[Cl]  =      " USING "###.##";CL#*1E3
PRINT
INPUT "DO YOU WISH TO SEE THE CONCS OF EACH ION PAIR Y/N ",C$
IF C$="N" THEN GOTO 40
CLS
PRINT
PRINT "ION-PAIR     CONC(mmoles/litre)"
PRINT
```

```
PRINT "[CaSO4] -    " USING "###.##";CASO4#*1E3
PRINT "[CaCO3] -    " USING "###.##";CACO3#*1E3
PRINT "[CaHCO3]-    " USING "###.##";CBI#*1E3
PRINT "[MgSO4] -    " USING "###.##";CMS#*1E3
PRINT "[MgCO3] -    " USING "###.##";CMC#*1E3
PRINT "[MgHCO3]-    " USING "###.##";CMB#*1E3
PRINT "[NaSO4] -    " USING "###.##";CNS#*1E3
PRINT "[KSO4]  -    " USING "###.##";CPS#*1E3
PRINT
40 INPUT "DO YOU WISH TO RUN MORE DATA? Y/N ",D$
IF D$="U" THEN GOTO 10
END
'
'
50 CLS
PRINT
PRINT
PRINT
PRINT
PRINT
PRINT
PRINT
PRINT
PRINT
PRINT
PRINT "THIS FAILED TO CONVERGE AFTER ",N% ," ITERATIONS.
```

APPENDIX 2.2

IPC2

```
'THIS IS A PROGRAM WHICH CONVERTS IONIC STRENGTH DATA
'IN ORDER THAT ION-PAIRS MAY BE TAKEN INTO ACCOUNT
'(1) INPUT OF DATA
10 CLS
PRINT"PLEASE INPUT THE CONCENTRATIONS (mmoles/litre) OF THE FOLLOWING "
PRINT"CATIONS AND ANIONS EACH SEPARATED BY A COMMA."
PRINT"Ca,Mg,Na,K,Sulphate,Carbonate,Bicarbonate,Chloride,Phosphate"
INPUT CA#,MG#,NA#,K#,S#,CO#,BI#,CL#,PO#
CLS
PRINT
PRINT
PRINT"HERE IS THE INPUTED DATA (mmoles/litre)"
PRINT
PRINT"CALCIUM CONCENTRATION        = ",CA#
PRINT
PRINT"MAGNESIUM CONCENTRATION      = ",MG#
PRINT
PRINT"SODIUM CONCENTRATION         = ",NA#
PRINT
PRINT"POTASSIUM CONCENTRATION      = ",K#
PRINT
PRINT"SULPHATE CONCENTRATION       = ",S#
PRINT
PRINT"CARBONATE CONCENTRATION      = ",CO#
PRINT
PRINT"BICARBONATE CONCENTRATION    = ",BI#
PRINT
PRINT"CHLORIDE CONCENTRATION       = ",CL#
PRINT
PRINT"TOTAL PHOSPHATE              = ",PO#
PRINT
PRINT"HYDROGEN ION CONCENTRATION   = ",CH#*1E3
PRINT
'
'CONVERT DATA INTO MOLES/LITRE
'
CA#=CA#*1E-3:MG#=MG#*1E-3:NA#=NA#*1E-3:K#=K#*1E-3
S#=S#*1E-3:CO#=CO#*1E-3:BI#=BI#*1E-3:CL#=CL#*1E-3:PO#=PO#*1E-3
INPUT"IS THIS DATA CORRECT Y/N ",X$
IF X$="N" OR X$="n" GOTO 10,
'
CALCULATION OF IONIC STRENGTH
'
'
N%=0
```

```
I#=0.5*((CA#*4)+(MG#*4)+NA#+K#+(S#*4)+(CO#*4)+BI#+CL#)
CC#=CA#:CM#=MG#:CN#=NA#:CK#=K#:CS#=S#
CCO#=CO#:CBIC#=BI#:CCL#=CL#:CPO#=PO#
'
'
'
'
20
N%=N%+1
'
' (2) Calculation of single ion activity coefficients
'
'
A#=0.509: B#=0.329 :Y#=A#*SQR(I#):Z#=B#*SQR(I#)
C#=(4*Y#)/(1+(6*Z#))            'Ca
D#=(4*Y#)/(1+(8*Z#))            'Mg
E#=(Y#)/(1+(4.5*Z#))            'Na
F#=(Y#)/(1+(3*Z#))              'K
G#=(4*Y#)/(1+(4*Z#))            'SO4
H#=(4*Y#)/(1+(4.5*Z#))          'CO3
J#=(Y#)/(1+(4.5*Z#))            'HCO3
L1#=(Y#)/(1+(4.5*Z))         'H2PO4-
L2#=(4*Y#)/(1+(4*Z#))           'HPO42-
H1#=(Y#)/(1+(9*Z#))             'H+
'
FC#=EXP10(-C#):FM#=EXP10(-D#)
FS#=EXP10(-E#):FK#=EXP10(-F#)
FSO#=EXP10(-G#):FCO#=EXP10(-H#)
FBI#=EXP10(-J#):FL1#=EXP10(-L1#)
FL2#=EXP10(-L2#):FH#=EXP10(-H1#)
'
'
'(3) CALCULATION OF IONIC ACTIVITIES
'
AC#=FC#*CC#: AM#=FM#*CM# : ANA#=FS#*CN#
AK#=FK#*CK#    : ASO#=FSO#*CS# : ACO#=FCO#*CCO# :AH#=FH#*CH#
ABIC#=FBI#*CBIC#:BT#=(AH#/(6.23E-008*FL1#))+(1/FL2#)
AL2#=(CPO#)/BT#:AL1#=(AH*AL2#)/6.3E-008
'
' (4) CALCULATION OF EQUILIBRIUM CONCENTRATIONS
'
'
CASO4#=(AC#*ASO#)/5.25E-003
CACO3#=(AC#*ACO#)/6.3E-004
CBI#=(AC#*ABIC#)/5.5E-002
CMS#=(AM#*ASO#)/5.88E-003
CMB#=AM#*ABIC#)/6.9E-002
CNS#=(ANA#*ASO#)/2.4E-001
CPS#=(AK#*ASO#)/1.1E-001
CMC#=(AM#*ACO#)/4E-004
COP#=(AC#*AL2#)/1.98E-003
CDP#=(AC#*AL1#)/8.3E-002
```

```
MOP#=(AM#*AL2#)/3.16E-003
MDP#=(AM#*AL1#)/1E-001
'
'
'(5) MASS BALANCE EQUATIONS'
'
CC#=CA#-(CASO4#+CACO3#+CBI#+COP#+CDP#): CM#=MG#-(CMS#+CMC#+CMB#+MOP#+MDP#)
CK#=K#-(CPS#): CN#=NA#-(CNS#)
CCO#=CO#-(CMC#+CACO3): CBIC#=BI#-(CBI#+CMB#)
CS#=S#-(CASO4#+CMS#+CNS#+CPS#)
CPO#=PO#-(COP#+CDP#+MOP#+MDP#)
IF CC#<0 THEN CC#=(CC#+CA#)/2          '      THESE LINES PREVENT
IF CM#<0 THEN CM#=(CM#+MG#)/2          '
IF CK#<0 THEN CK#=(CK#+K#)/2           '      NEGATIVE CONCENTRATION
IF CN#<0 THEN CN#=(CN#+NA#)/2          '
IF CCO#<0 THEN CCO#=(CCO#+CO#)/2       '      VALUES FROM
IF CBIC#<0 THEN CBIC#=(CBIC#+BI#)/2    '
IF CS#<0 THEN CS#=(CS#+S#)/2           '      OCCURRING
IF COP#,0 THEN CPO#=(CPO#+PO#)/2
'
'
'
IO#=0.5*((CC#*4)+(CM#*4)+CN#+CK#+(CS#*4)+(CCO#*4)+CBIC#+CL#+CPO#)
IF N%> 1000 GOTO 50
IF (I#/IO#),<0.99 OR (I#/IO#)>1.01 THEN GOTO 25
IF 0.99<(I#/IO#),1.01 THEN GOTO 30
25 I=IO# :GOTO 20
'
'
'
30 CLS
'
'OUTPUT OF DATA
PRINT "THE IONIC STRENGTH OF THIS SOLUTION AFTER CORRECTION FOR"
PRINT
PRINT "ION PAIRS (mmoles/litre) =  " USING "###.###";   IO#*1E3
PRINT
PRINT "THIS CALCULATION TOOK ,",N%," ITERATION(S)"
PRINT
INPUT "DO YOU WISH TO SEE THE INDIVIDUAL FREE ION CONCENTRATIONS Y/N ",B$
IF B$="N" OR B$="n" THEN GOTO 40
PRINT
PRINT "FREE ION     CONC(mmoles/litre)"
PRINT
PRINT "[Ca]  =      " USING "###.####";CC#*1E3
PRINT "[Mg]  =      " USING "###.####";CM#*1E3
PRINT "[K]   =      " USING "###.####";CK#*1E3
PRINT "[Na]  =      " USING "###.####";CN#*1E3
PRINT "[CO3] =      " USING "###.####;CCO#*1E3
PRINT "[HCO3]=      " USING "###.####;CBIC#*1E3
PRINT "[SO4] =      " USING "###.####";CS#*1E3
PRINT "[Cl]  =      " USING "###.####";CL#*1E3
```

```
PRINT "[HPO4]-      " USING "###.#####";(AL2#/FL2#)*1E3
PRINT "[H2PO4]-     " USING "###.#####";(AL1#/FL1#)*1E3
PRINT
INPUT "DO YOU WISH TO SEE THE CONCS OF EACH ION PAIR Y/N ",C$
IF C$="N" OR C$="n" THEN GOTO 40
CLS
PRINT
PRINT "ION-PAIR      CONC(mmoles/litre)"
PRINT
PRINT "[CaSO4] =    " USING "###.####";CASO4#*1E3
PRINT "[CaCO3] =    " USING "###.####";CACO3#*1E3
PRINT "[CaHCO3]=    " USING "###.####";CBI#*1E3
PRINT "[MgSO4] =    " USING "###.####";CMS#*1E3
PRINT "[MgCO3] =    " USING "###.####";CMC#*1E3
PRINT "[MgHCO3]=    " USING "###.####";CMB#*1E3
PRINT "[NaSO4] =    " USING "###.####";CNS#*1E3
PRINT "[KSO4]  =    " USING "###.####";CPS#*1E3
PRINT "[CaHPO4]=    " USING "###.#####";COP#*1E3
PRINT "[CaH2PO4]=   " USING "###.#####";CDP#*1E3
PRINT "[MgHPO4]=    " USING "###.#####";MOP#*1E3
PRINT "[MgH2PO4]=   " USING "###.#####";MDP#*1E3
PRINT
40 INPUT "DO YOU WISH TO RUN MORE DATA? Y/N ",D$
IF D$="Y" OR D$="y" THEN GOTO 10
END
'
50 CLS
PRINT
PRINT
PRINT
PRINT
PRINT
PRINT
PRINT
PRINT
PRINT
PRINT
PRINT "THIS FAILED TO CONVERGE AFTER ",N% ," ITERATIONS.
```

CHAPTER THREE

THE SAMPLING AND ANALYSIS OF SOIL SOLUTIONS

3.1 *INTRODUCTION*

The first step in any environmental analysis is that of sampling. It is undoubtedly one of the most critical stages of any environmental analysis but is often ignored or relegated to a minor role. Any errors incurred during the sampling stage will be carried throughout the analytical procedure and it is therefore of the utmost importance that the sample taken is truly representative of the material of interest [1]. It was hoped that sampling the chosen field over a period of months would give some indication of the temporal changes in the soil copper concentration as well as the major cation and anion concentrations.

3.2 *FIELD SAMPLING PROCEDURE*

It was felt that the sampling procedure used in the previous chapter could be vastly improved. The centrifuge technique was very crude and particularly prone to experimental errors. It was therefore decided to undertake a sampling trip on 24/1/89. The field is situated on a slope and because of this samples were taken along a transect halfway down the field. This was because on previous sampling trips it was noticed that rainfall falling on the upper part of the field was running off without having time to equilibrate with the soil. Conversely at the bottom of the field the rainwater tended to collect, and as a result, the soil was saturated to near field capacity. It was felt that the water extracted from sampling sites halfway down the slope would have had ample time to equilibrate with the soil.

Three equidistant sampling sites were chosen along the transect and a duplicate sample was taken at each site. The sampling sites were labelled lab 1-A, lab 1-AD (duplicate), lab 1-B, lab 1-BD, lab 1-C and

lab 1-CD. Soil blocks were taken from the Ap horizon i.e. 0-30 cm and taken back to the Macaulay Institute in polythene bags. The samples were stored in a cold room T=4°C until required for analysis. The characteristics of the soil are shown in Fig. 3.1.

Fig. 3.1 Laverock Brae Soil - NJ 921111 Map Ref.

Parent material	- glacial till	) Till derived from mixed acid)- igneous, acid metamorphic and) basic igneous rocks
Soil Association	- Tarves	)
Soil Series	- Thistlyhill	)- Brown forest soil)
Drainage	- Imperfect	
Vegetation	- Rotational by pasture based on ryegrass	

3.3 *INITIAL EXTRACTION AND ANALYSIS OF SOIL SOLUTIONS*

3.3.1 *Apparatus*

Soils were centrifuged using a MSE Mistral 3000 (Fisons Scientific Equipment, Loughborough UK) centrifuge. The resultant solutions were analysed for cationic content by flame emission spectrometry (Na, K) using a Corning 400 photometer (Corning Ltd. Halstead, UK) and by atomic absorption spectrometry (Ca, Mg, Cu) on either a Varian 1275 (Varian Associates Ltd., Walton on Thames, UK) or a Perkin Elmer 560 (Perkin Elmer, Ltd., Beaconsfield, UK).

3.3.2 *Reagents*

All chemicals used were "Analar" grade (BDH, Ltd.) and all glassware was soaked in 5% Decon overnight. The glassware was rinsed and then washed

with 1:4 HNO_3 and finally rinsed with distilled water. All the glassware used in this study was new and therefore its laboratory history was known.

3.3.3 ***Procedure***

Each bag of soil was thoroughly mixed and from each bag 2 x 250 g samples were taken. The soil samples were then placed in the centrifuge tubes as shown in Fig. 3.2. The tubes used were of a similar design to those used by Elkhatib [2]. The tubes were then placed in the centrifuge and spun under the following conditions:

Table 3.1 Centrifuge Conditions

Speed	3000 rpm ≃ 2000 g
Temperature	21°C
Time	60 mins
Brake rate	5

After spinning, the base of the centrifuge tube was removed and the plastic bag cut open. The soil solution was then decanted into a polythene sample tube. These tubes were then stored in a cold room until required for analysis

3.3.4 ***Analysis***

This initial extraction was used in order to determine the ratios of the major cations so that suitable standards could be prepared with a similar matrix to the soil solutions under study.

5.00 cm^3 of each soil solution was withdrawn and to this 1.25 cm^3 of 12500 ppm Sr was added to act as a releasing agent. The samples were then analysed for Ca, Mg, Na and K using a set of mixed standards prepared

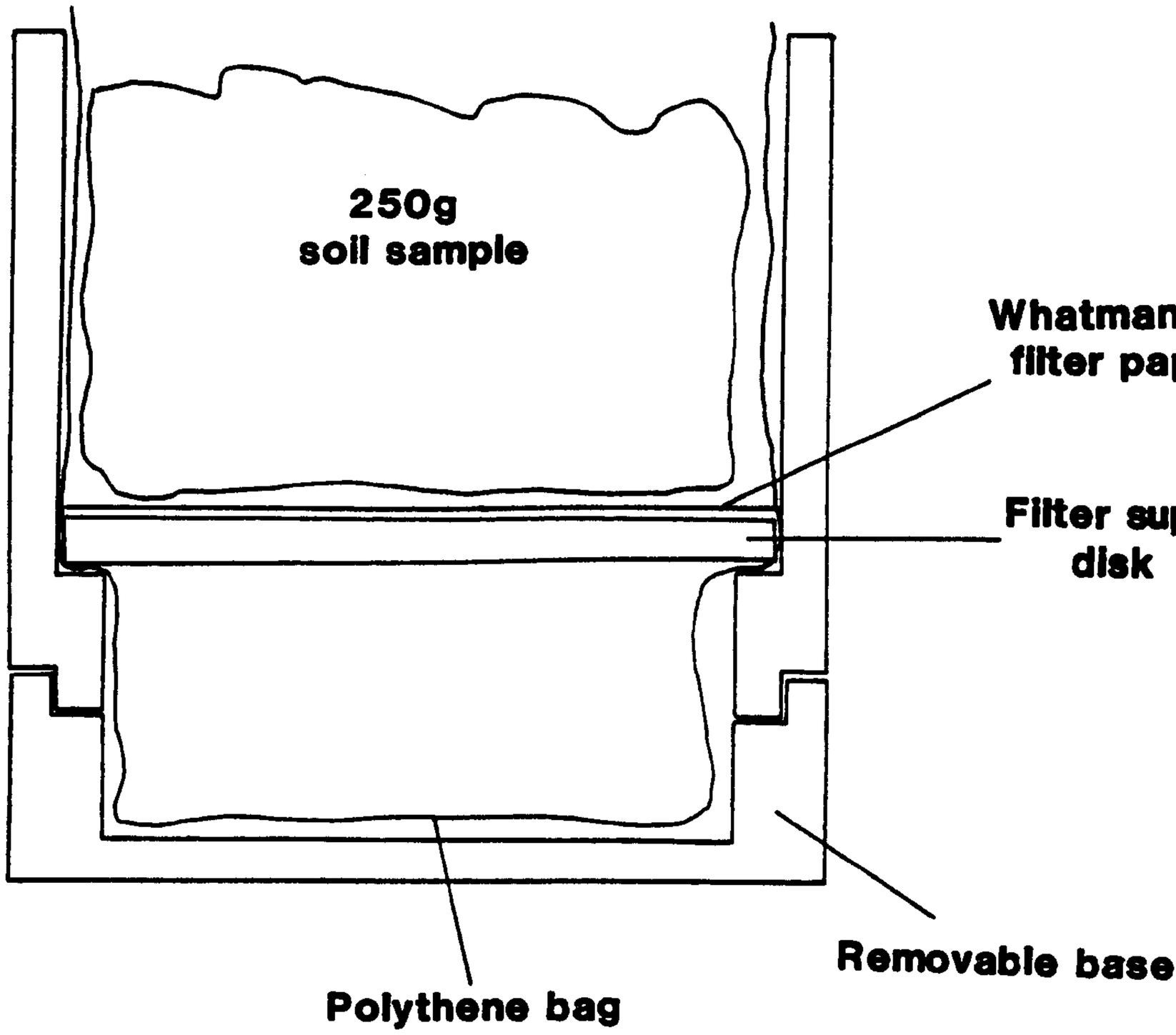

Fig 3.2 The centrifuge tubes used to extract soil solutions.

in a 0.06 Mol dm^{-3} HCl matrix commonly used in the Macaulay Institute for soil analysis. The standards used were as follows:

Table 3.2 Cationic Concentrations in Macaulay Z Standards

Std No	Conc/ppm			
	Na	K	Mg	Ca
1	50	10	6.0	1.2
2	25	5	2.4	0.6
3	10	2	1.2	0.3
4	5	1	0.6	0.15

+ Blank (0.06 mol dm^{-3} HCl)

The results obtained from this initial extraction are shown below:

Table 3.3 Cation Results from the Initial Extraction

Sample site	Element Conc/ppm			
	Na	K	Mg	Ca
Lab 1-A	11.69	2.43	1.91	20.00
Lab 1-AD	10.29	2.06	1.76	20.00
Lab 1-B	11.37	4.50	2.96	28.75
Lab 1-BD	9.87	2.81	2.65	30.00
Lab 1-C	16.62	2.19	4.42	48.75
Lab 1-CD	13.62	3.37	2.74	25.00

It was decided that the cation ratios of sample Lab 1-C would be used as a basis for the preparation of suitable standard.

The ratios of the major cations were as follows:

	Ca		Mg		Na		K
	49		4.5		16.7		2.19
≃	11	:	1	:	4	:	0.5

For ease of standard preparation this was approximated to:

Ca		Mg		Na		K
10	:	2	:	5	:	2

A stock standard solution was prepared with the following concentrations:

Ca	Mg	Na	K
100 ppm	20 ppm	50 ppm	20 ppm

From this stock solution the following standards were prepared:

Table 3.4 Standards Prepared for Laverock Brae farm Samples

Std No	Conc/ppm			
	Ca	Mg	Na	K
1	10	2	5	2.0
2	7.5	1.5	3.75	1.5
3	5.0	1	2.5	1.0
4	2.5	0.5	1.25	0.5
5	1.0	0.2	0.5	0.2
6	0.5	0.1	0.25	0.1
7	0.25	0.05	0.125	0.05

+ Blank (2500 ppm Sn)

each standard also contained 2500 ppm Sr as a releasing agent.

When these standard are compared with the standards used previously it can be seen that not only is the sample matrix different H_2O c.f. 0.06 Mol dm^{-3} HCl but that the cationic ratios are completely different.

3.4 *ANALYSIS OF SOIL SOLUTION*

The soils were again centrifuged but this time as well as being thoroughly mixed in the bags the samples were coned and quartered to hopefully obtain a more representative sample. Each sampling site was extracted in duplicate in an attempt to check for errors introduced in the extraction procedure.

This meant that 4 x 250 g samples were centrifuged and the soil solution obtained was bulked into groups of two. The volume of soil solution extracted was measured.

Table 3.5 Volume of Water Extracted from each Sampling Site

Sampling Site	Vol extracted ml/500 g spin
Lab 1-A	21.00
Lab 1-A(x)	21.25
Lab 1-AD	21.40
Lab 1-AD(x)	20.25
Lab 1-B	26.00
Lab 1-B(x)	25.00
Lab 1-BD	24.00
Lab 1-BD(x)	23.00
Lab 1-C	18.75*
Lab 1-C(x)	20.25
Lab 1-CD	21.50
Lab 1-CD(x)	22.00

x - denotes duplicate
* - some soil solution escaped when the plastic bag burst

It can be seen that the amount of soil solution obtained from duplicate extractions was remarkably consistent.

3.4.1 *Cationic Analysis of Soil Solutions*

The solutions extracted were then analysed after the necessary dilutions had been carried out for Ca, Mg, Na, K. The results obtained are shown in the table below.

Table 3.6 Cationic Analysis of Soil Solutions

Sample site	conc/ppm			
	Na	Ca	K	Mg
Lab 1-A	17.75	52.5	4.95	3.80
Lab 1-A(x)	17.75	52.5	4.70	3.80
Lab 1-AD	14.50	42.5	2.50	7.90
Lab 1-AD(x)	14.50	43.8	2.60	2.90
Lab 1-B	15.50	54.8	4.40	4.60
Lab 1-B(x)	15.50	54.8	4.30	4.60
Lab 1-BD	14.00	59.0	2.40	4.40
Lab 1-BD(x)	14.00	56.0	2.30	4.40
Lab 1-C	20.00	75.5	2.70	5.90
Lab 1-C(x)	20.00	74.7	2.70	6.00
Lab 1-CD	15.00	34.8	1.90	4.65
Lab 1-CD(x)	14.00	34.2	1.45	4.65

It can be seen from the results that the reproducibility of subsequent extractions was extremely good. the soil solutions were also analysed for Cu using flame AAS. The results obtained are shown below.

Table 3.7 Cu Analysis of Soil Solutions

Sample site	Conc/ppb
Lab 1-A	43
Lab 1-A(x)	49
Lab 1-AD	33
Lab 1-AD(x)	33
Lab 1-B	37
Lab 1-B(x)	37
Lab 1-BD	49
Lab 1-BD(x)	49
Lab 1-C	43
Lab 1-C(x)	43
Lab 1-CD	43
Lab 1-CD(x)	43

Again the reproducibility was extremely good.

3.4.2 *Anionic analysis of soil solutions*

3.4.2.1 **Apparatus**

Anions were determined by High Performance Ion Chromatography, HPLC (Cl^-, SO_4^{2-}) on a Dionex 4000 chromatograph (Dionex U.K. ltd., Camberely, UK) and by flow injection colorimetry (HCO_3^-, NO_3^-, PO_4^{3-}) on a Tecator FIAstar 510 instrument (Peristorp Analytical, Bristol, UK).

3.4.2.2 **Results**

All results are shown in Table 3.8.

Table 3.8 Anionic Content of Soil Solutions

Sample Site	NO_3^-	SO_4^{2-}	Cl^-	HCO_3^-
Lab 1-A	48.5	5.9	20.3	6.3
Lab 1-AD	37.9	10.1	13.2	5.2
Lab 1-B	58.4	12.6	13.4	5.2
Lab 1-BD	55.6	10.7	7.3	3.7
Lab 1-C	60.8	18.8	25.3	1.9
Lab 1-CD	50.7	9.4	20.2	1.9

3.4.3 *Moisture Content*

150 g portions of soil were air dried over a period of 3 weeks until the weight loss stabilized. This enable the % moisture content of the soils to be calculated. The results are shown in Table 3.9.

Table 3.9 Moisture Content

Sample Site	Moisture Content % Weight
Lab 1-A	23.4
Lab 1-AD	24.5
Lab 1-B	22.1
Lab 1-BD	22.9
Lab 1-C	24.4
Lab 1-CD	24.1

3.4.4 *pH and Conductivity*

3.4.4.1 **Apparatus**

Jenway 3020 pH meter and 4020 conductivity meter (Jenway Ltd., Felstead, Gt. Dunmow, Essex, UK).

3.4.4.2 **Results**

The results obtained are shown in Table 3.10.

Table 3.10 pH and Conductivity Results

Sample Site	pH	Conductivity/ mS cm^{-1}
Lab 1-A	5.83	0.416
Lab 1-AD	5.54	0.327
Lab 1-B	5.77	0.417
Lab 1-BD	4.71	0.413
Lab 1-C	4.60	0.568
Lab 1-CD	4.30	0.423

3.5 *SAMPLING TRIP 2*

3.5.1 *Sampling and Analysis*

A second sampling trip was undertaken on 22/2/89. Sampling sites were selected that were as close as possible to the sites selected on the previous trip.

During the centrifugation procedure problems arose due to the increased moisture content of the soil (See Section 3.5.2) in that some soil particles were carried around the polythene filter by the soil solution into the collection bag. These soil particles were removed by re-centrifugation of the soil solutions in conventional centrifuge tubes followed by decantation of the soil solution. The soil solutions were then analysed as before.

3.5.2 *Results and Discussion*

During sampling it was noticed that the soil was much wetter than on the previous trip. The soil solution analysis results are shown in Tables 3.11-3.14 There was very little change in the copper concentrations although there were slight decreases in the major cation and anion concentrations. This was most likely due to the higher rainfall, resulting in a higher soil moisture content and consequently lower anion and cation concentrations.

3.6 *SAMPLING TRIP 3*

3.6.1 *Sampling and Analysis*

The sampling trip took place on 5/5/89 and the sampling and analysis was carried out as described in earlier sections.

Table 3.11 Cation Concentrations Sampled 22/2/89

Sample site	conc/ppm			
	Ca	K	Na	Mg
Lab 1-A	53.7	8.2	17.4	2.47
Lab 1-AD	43.4	6.2	16.7	2.47
Lab 1-B	39.2	2.4	11.4	3.12
Lab 1-BD	49.5	2.9	13.3	3.12
Lab 1-C	39.7	1.1	11.4	1.82
Lab 1-CD	45.5	1.5	13.6	1.90

Table 3.12 Cu Concentrations Sampled 22/2/89

Sample site	Conc/ppb
Lab 1-A	42.7
Lab 1-AD	60.3
Lab 1-B	36.9
Lab 1-BD	54.5
Lab 1-C	56.2
Lab 1-CD	53.6

Table 3.13 Anion Concentrations Sampled 22/2/89

Sample Site	NO_3^-	SO_4^{2-}	Cl^-	HCO_3^-
Lab 1-A	27.2	13.8	24.9	13.1
Lab 1-AD	30.3	14.2	6.7	23.9
Lab 1-B	28.5	11.9	10.1	5.3
Lab 1-BD	26.3	24.1	8.4	5.6
Lab 1-C	21.9	9.6	11.9	6.3
Lab 1-CD	21.4	10.8	16.2	11.2

Table 3.14 pH, Conductivity and Moisture Content Sampled 22/2/89

Sample Site	pH	Conductivity mS cm^{-1}	Moisture Content % Weight
Lab 1-A	5.98	0.418	25.0
Lab 1-AD	6.41	0.374	25.2
Lab 1-B	5.96	0.310	23.1
Lab 1-BD	6.03	0.407	39.0
Lab 1-C	5.95	0.268	37.5
Lab 1-CD	6.39	0.304	22.3

3.6.2 *Results and discussion*

The results are shown in Tables 3.15-3.18. Although the moisture content of the soil was lower there was little overall change in the Cu concentrations or the concentrations of the major anions and cations.

3.7 *SUBSEQUENT SAMPLING TRIPS*

3.7.1 *Sampling*

Another sampling trip took place on 4/7/89 but the dry summer months resulted in a very low soil moisture content.

It was decided to add 20 cm^3 of distilled water to each 250 g portion of soil to be centrifuged so that sufficient soil solution could be obtained for analysis. the soil was stored for 2 days in a cold room to inhibit microbial activity and allow equilibration of the soil with the added water before centrifugation.

3.7.2 *Results and Discussion*

There was only sufficient sample to allow the cationic analysis by ICP. From the results in Table 3.19 it can be clearly seen that the concentrations of all the major cations in the soil solution had increased. This was also the case for the soil solution copper. It seems apparent that the addition of water to these dry soils had resulted in a mobilization of some hitherto unavailable cations. A similar phenomenon occurs when distilled water is added to air dried soils [3]. The most likely cause of this mobilization of cations is that of microbial flush. It is well known that the drying of soils results in a decrease in their microbial biomass due to the killing of micro-organisms in the soil. These dead micro-organisms can release N and P into the soil when moisture is

Table 3.15 Cation Concentrations Sampled 5/5/89

Sample site	conc/ppm			
	Ca	K	Na	Mg
Lab 1-A	58.8	8.8	27.4	4.4
Lab 1-AD	41.9	6.4	19.9	3.0
Lab 1-B	28.8	1.2	11.1	1.5
Lab 1-BD	31.9	0.5	12.4	1.9
Lab 1-C	49.4	1.1	20.0	3.2
Lab 1-CD	62.6	3.3	19.3	4.7

Table 3.16 Cu Concentrations Sampled 5/5/89

Sample site	Conc/ppb
Lab 1-A	52.5
Lab 1-AD	58.4
Lab 1-B	58.4
Lab 1-BD	46.6
Lab 1-C	44.7
Lab 1-CD	45.4

Table 3.17 Anion Concentrations Sampled 5/5/89

Sample Site	NO_3^-	SO_4^{2-}	Cl^-	HCO_3^-
Lab 1-A	32.7	31.9	15.3	9.0
Lab 1-AD	22.2	9.5	9.4	8.7
Lab 1-B	10.5	6.7	8.6	12.2
Lab 1-BD	10.9	5.8	12.5	4.3
Lab 1-C	24.9	18.9	10.4	13.2
Lab 1-CD	31.1	14.3	16.5	16.4

Table 3.18 pH, Conductivity and Moisture Content Sampled 5/5/89

Sample Site	pH	Conductivity mS cm^{-1}	Moisture Content % Weight
Lab 1-A	5.5	0.464	20.1
Lab 1-AD	5.5	0.341	23.0
Lab 1-B	6.2	0.212	23.0
Lab 1-BD	5.9	0.238	20.5
Lab 1-C	6.2	0.390	19.3
Lab 1-CD	6.6	0.464	19.8

Table 3.19 ICP Analysis of Wetted Soil Extracts

Sample site	Conc ppm				
	Ca	Na	K	Mg	Cu
Lab 1-A	134.42	43.16	17.73	9.30	0.192
Lab 1-AD	81.06	33.16	6.48	4.79	0.159
Lab 1-B	100.74	32.97	4.68	6.37	0.169
Lab 1-BD	109.65	32.34	4.55	8.12	0.156
Lab 1-C	139.81	47.93	7.59	6.97	0.159
Lab 1-CD	99.77	24.96	3.81	4.16	0.113

added. It seems likely that similar trends would be observed for some of the major cations present in soils. Sparling and Berrow [4] investigated the effects of air drying, γ-irradiation and chloroform fumigation of soil on the extractabilities of trace elements. They found that the above process had very little effect on the amounts of trace elements extracted by acetic acid or ammonium acetate. They concluded that the amounts of readily exchangeable elements in the surface soils were relatively high and that the contribution of the microbial biomass was comparatively small. This is not unexpected as such extractants would have mobilized

much larger concentrations of cations into solution than would have been originally present in the soil solutions.

This work has concentrated on soil solutions and in such cases the concentrations of cations are much smaller than those that would be extractable by the above reagents. Therefore in soil solutions the microbial flush during dry periods could cause significant increases in ionic concentrations. Addition of water to such a soil would cause a mobilization of such elements and hence account for the increase in soil solution concentrations.

3.8 *THE CORRELATION OF THE IONIC STRENGTH ESTIMATED FROM CONDUCTIVITY MEASUREMENTS WITH THE EXPERIMENTALLY DETERMINED IONIC STRENGTH*

3.8.1 *Procedure*

The ionic concentrations for the first three sampling trips were entered into IPC2 and the ionic strength of the soil solution was corrected for ion-pair formation. An estimate of ionic strength was obtained from the electrical conductivities of the soil solution using the relationship obtained in the previous chapter. A linear regression analysis was then carried out and is shown in Graph 3.1.

3.8.2 *Discussion*

If I_{calc} (I determined from the ionic analysis) and I_{exp} (I estimated from EC) were the same then a slope of unity would result. Graph 3.1 shows that this is clearly the case and that the correlation between I_{exp} and I_{calc} is very good indeed.

From this it can be deduced that in this particular soil all the major cations and anions are present in an ionic form that contributes to

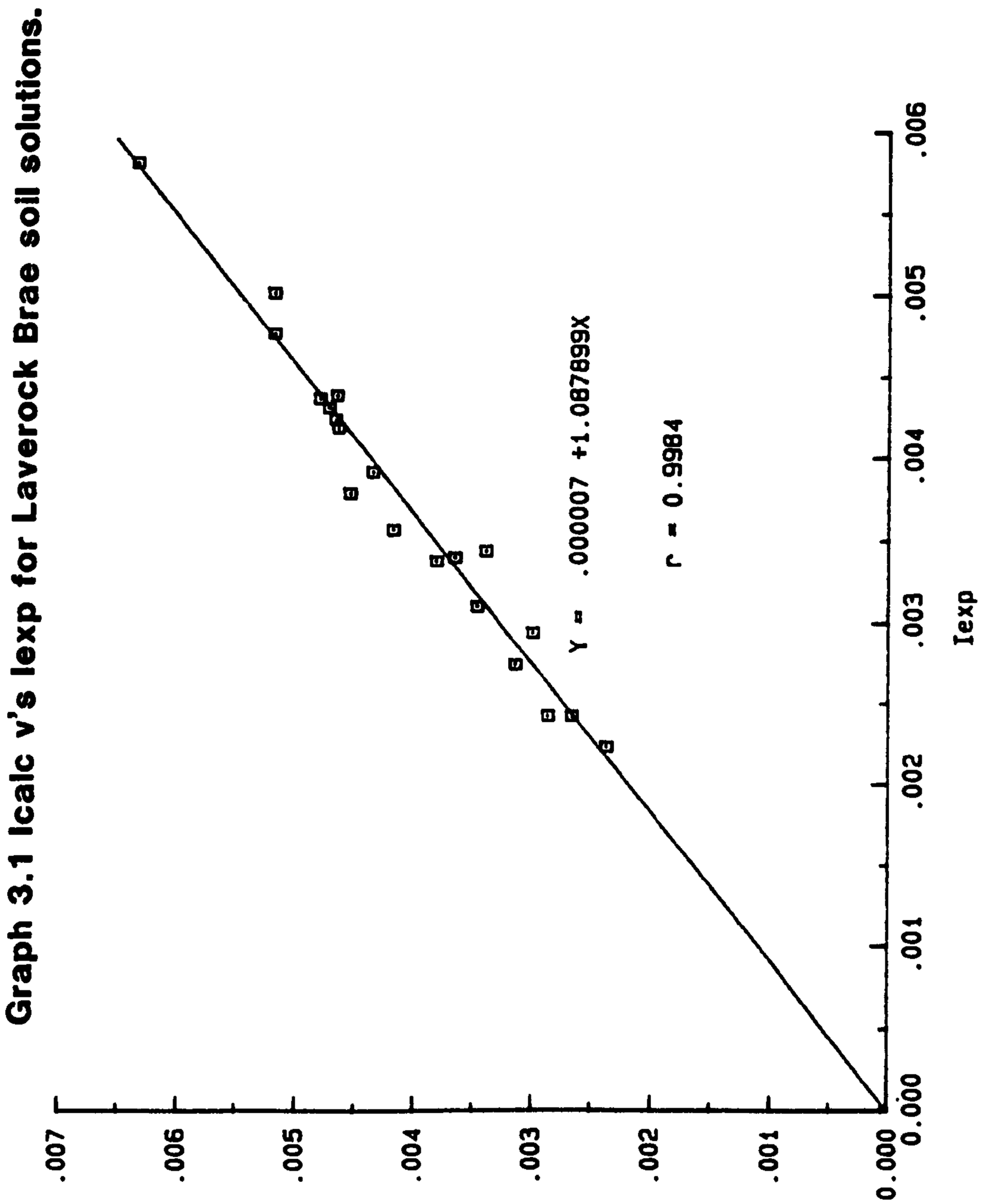
Graph 3.1 Icalc v's Iexp for Laverock Brae soil solution
Y = .000007 +1.087899X
r = 0.9984
Icalc
Iexp
0.000
.001
.002
.003
.004
.005
.006
.007

the electrical conductivity of the soil solution. This means that the ionic strength of this soil can be reliably estimated from its electrical conductivity.

3.9 *THE CORRELATION OF IONIC CONCENTRATIONS WITH MOISTURE CONTENT*

It was decided to investigate whether or not there was any relationship between the anionic and cationic concentrations in soil solutions and the percentage moisture content of the soil. This would give some indication as to whether or not the soil solution was ionically saturated as well as the importance of ion-exchange with the solid phase.

3.9.1 *Procedure*

Graphs of ionic concentration were plotted against the % moisture content of the site from which they were taken. This was carried out for each ion analysed and also for the total ionic strength of the soil solutions.

3.9.2 *Results*

3.9.2.1 **Anions**

The graphs of % moisture content v's concentration (ppm) can be seen in Graphs 3.2 to 3.5. They clearly show that there is no correlation between the anionic concentrations and % moisture content.

3.9.2.2 **Cations**

The results can be seen in Graphs 3.6 to 3.9 and again show no correlation.

3.9.2.3 **Copper**

This is shown in Graph 3.10 and again no relationship is apparent.

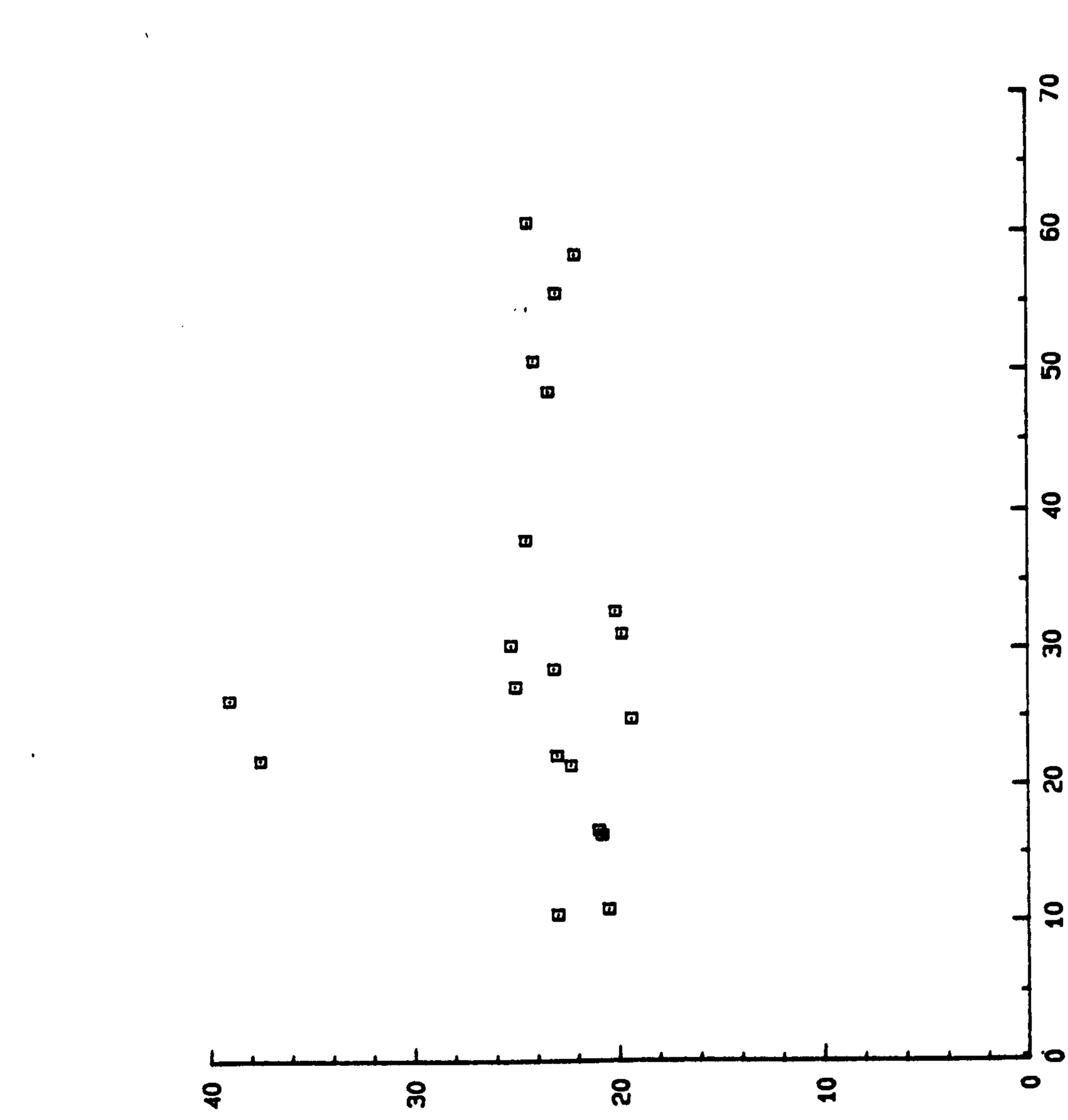

Graph 3.2 % Moisture v's nitrate concentration.

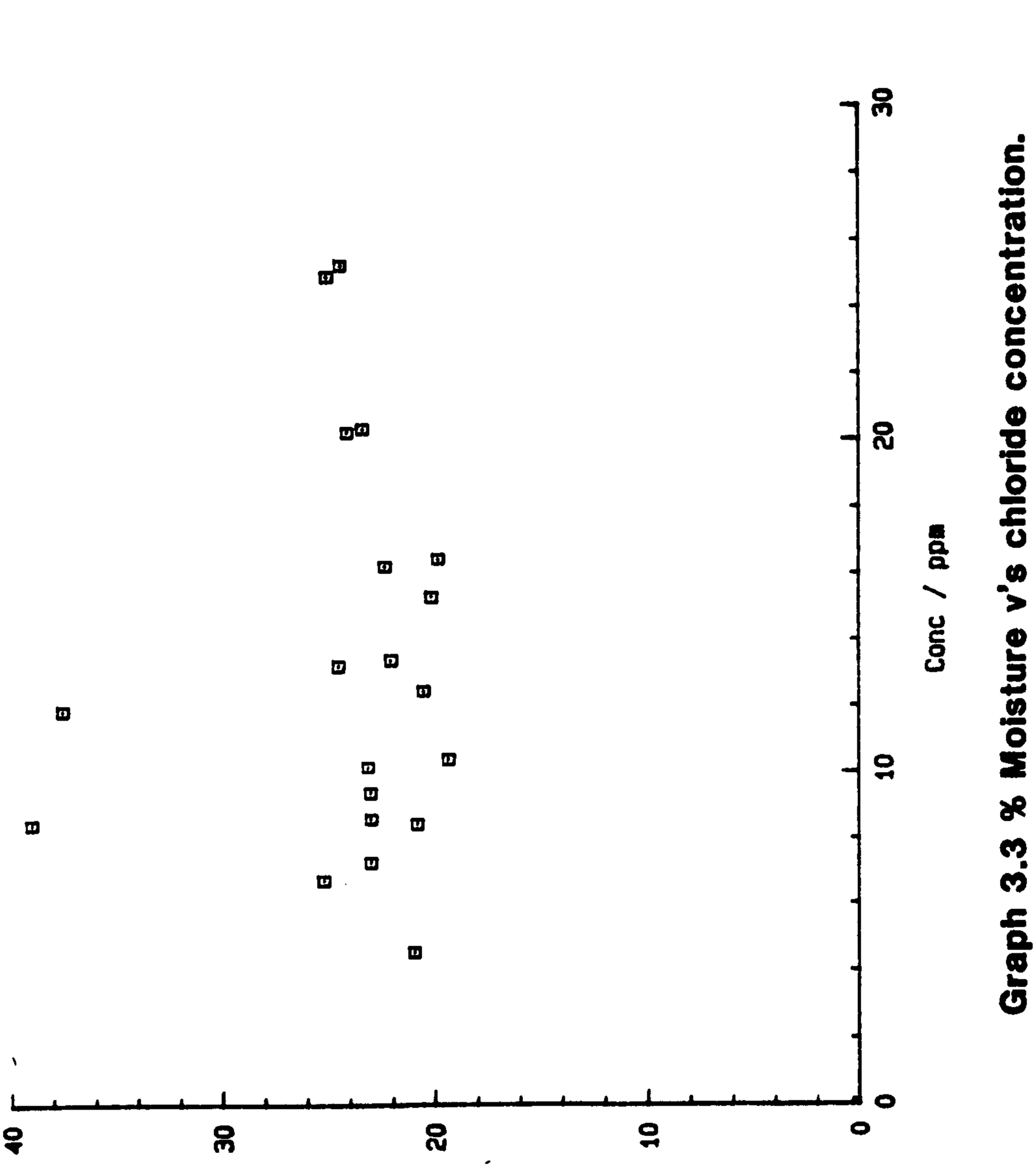

Graph 3.3 % Moisture v's chloride concentration.

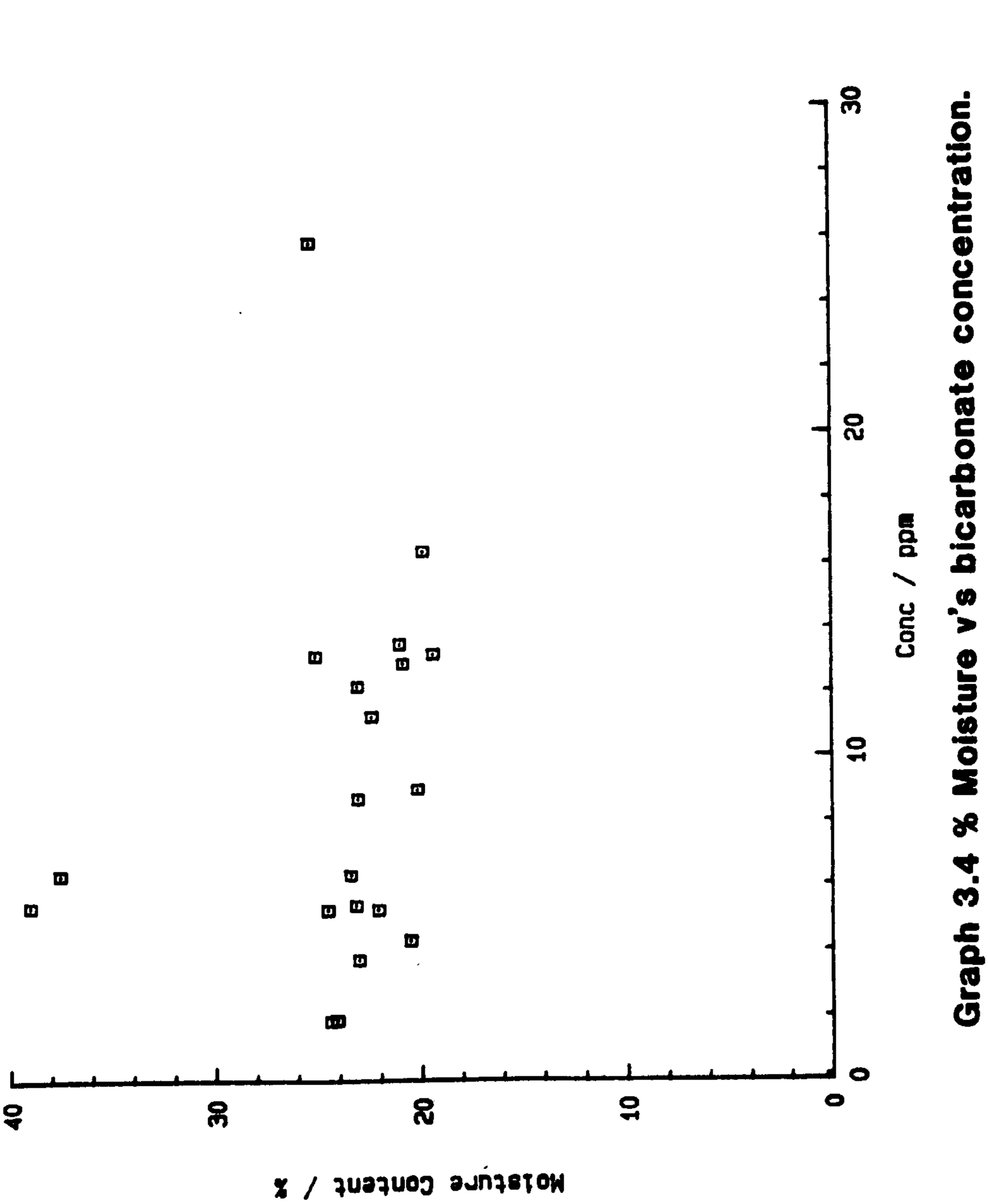

Graph 3.4 % Moisture v's bicarbonate concentration.

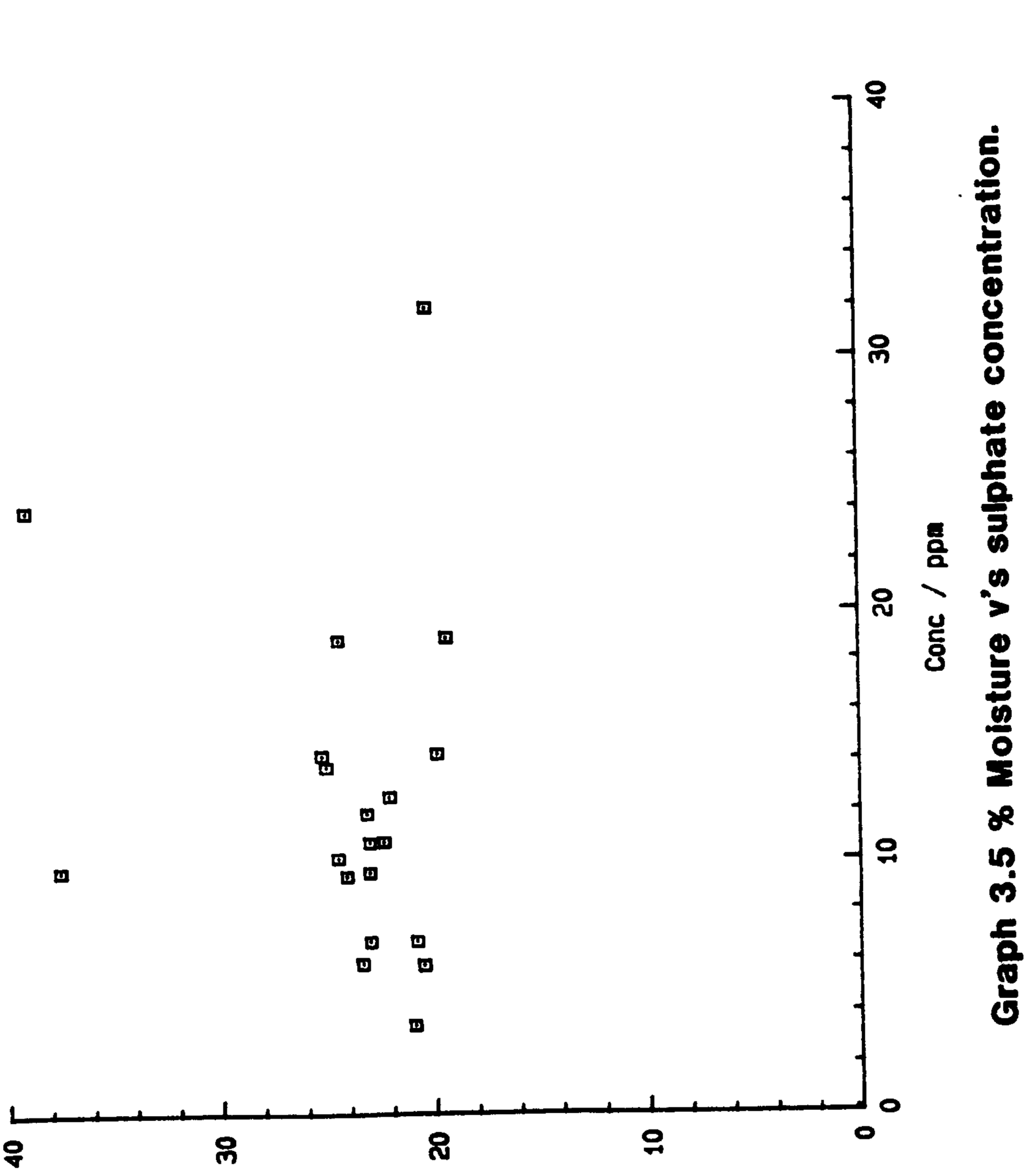

Graph 3.5 % Moisture v's sulphate concentration.

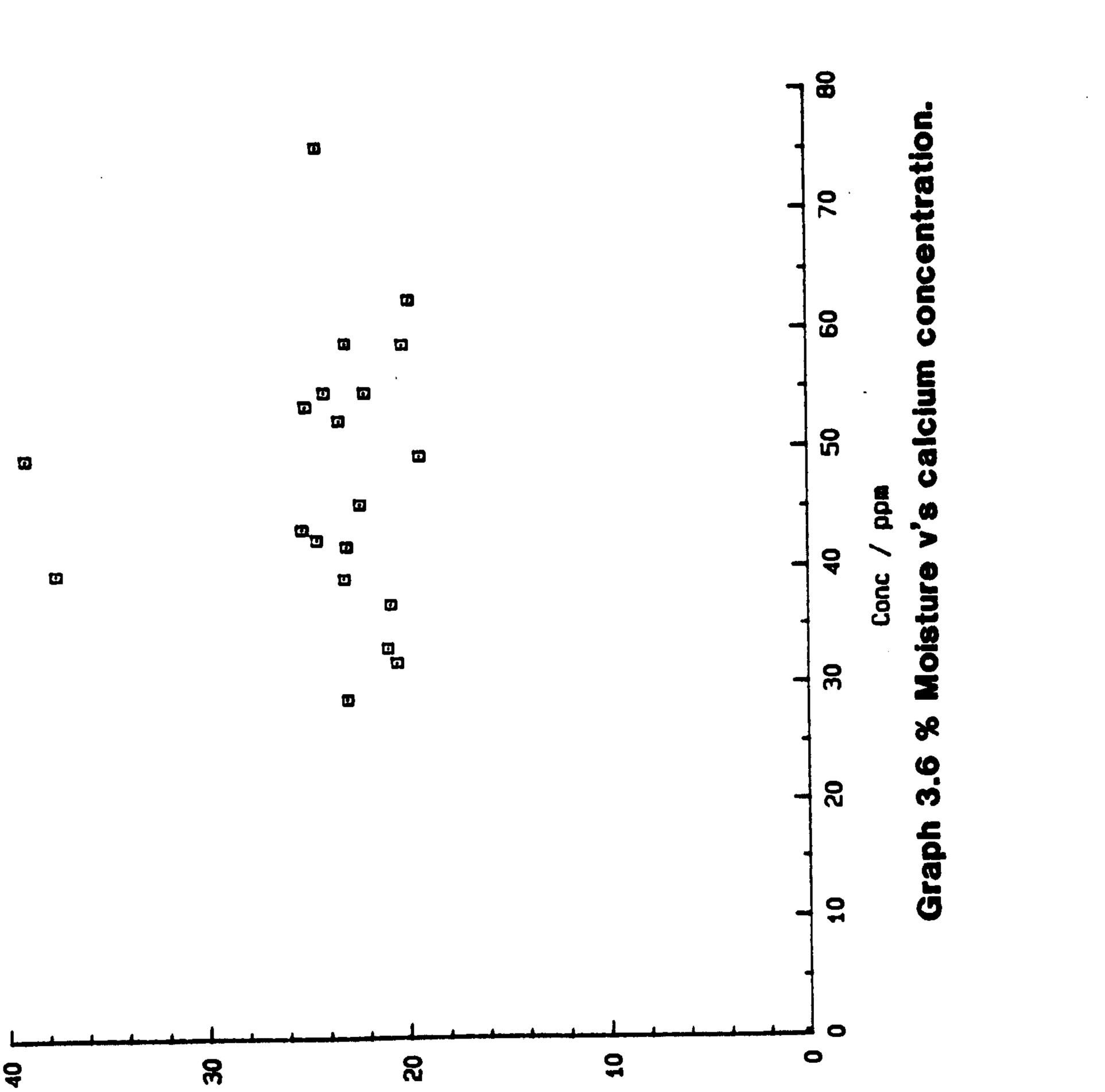

Graph 3.6 % Moisture v's calcium concentration.

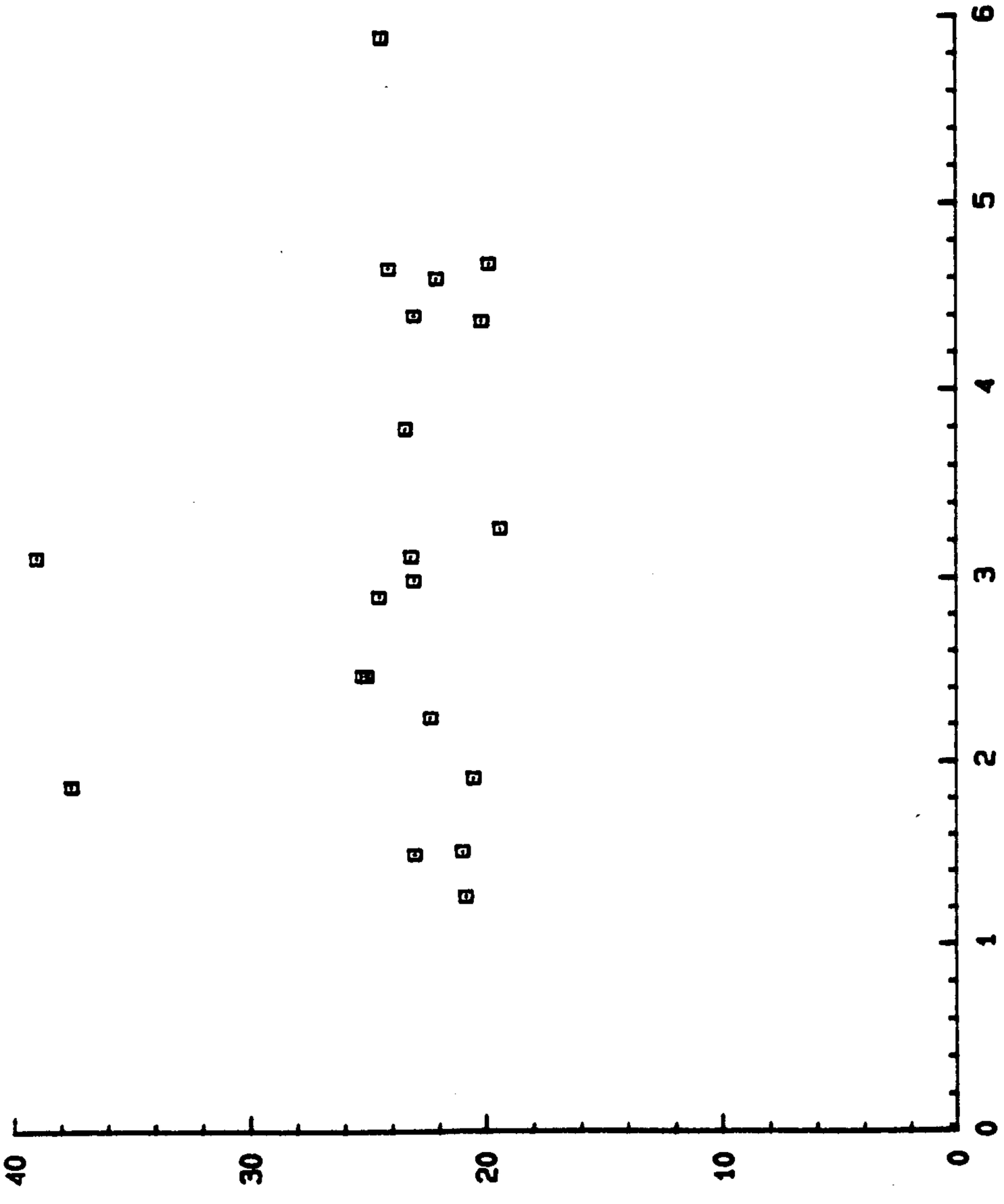

Graph 3.7 % Moisture v's magnesium concentration.

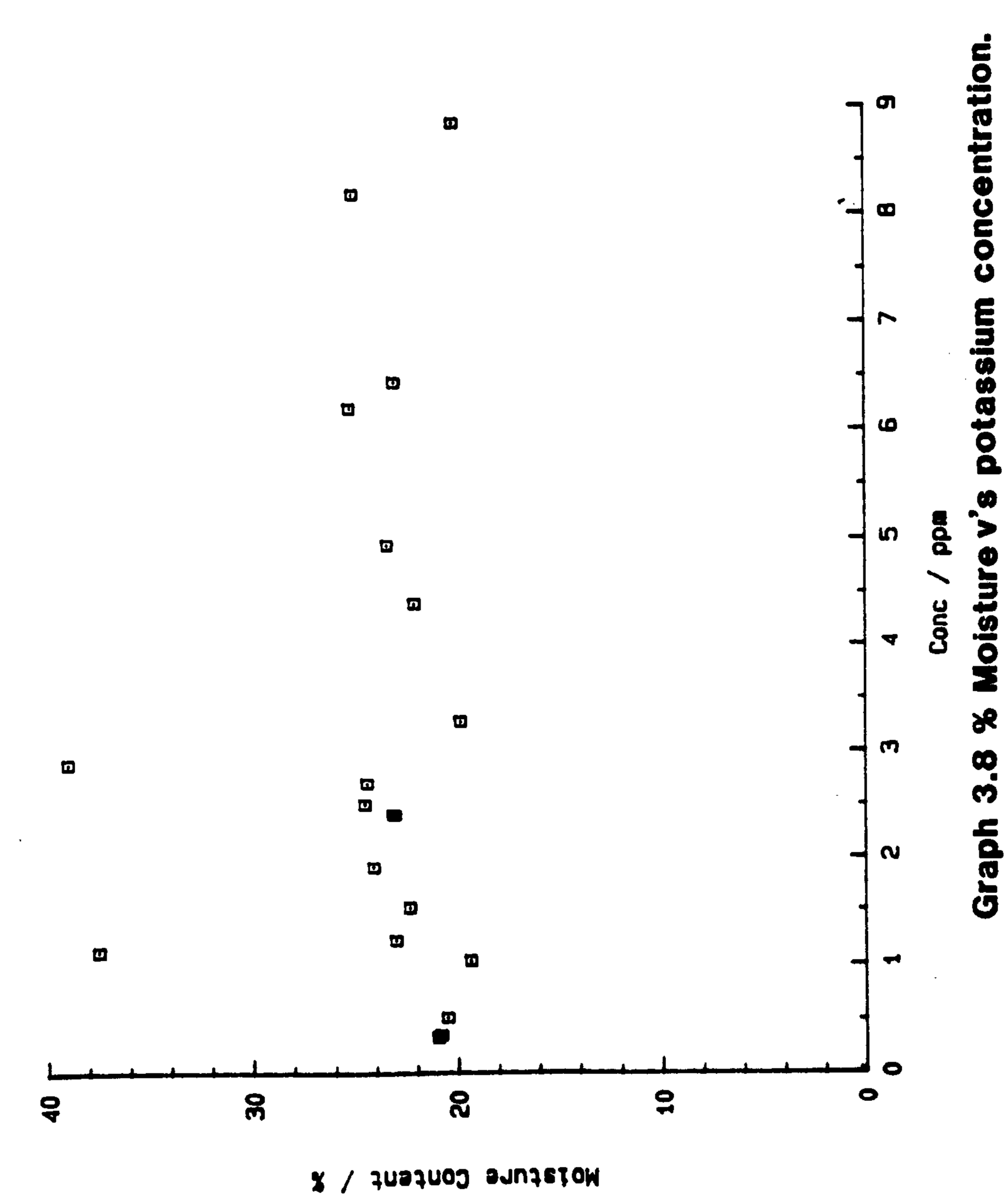

Graph 3.8 % Moisture v's potassium concentration.

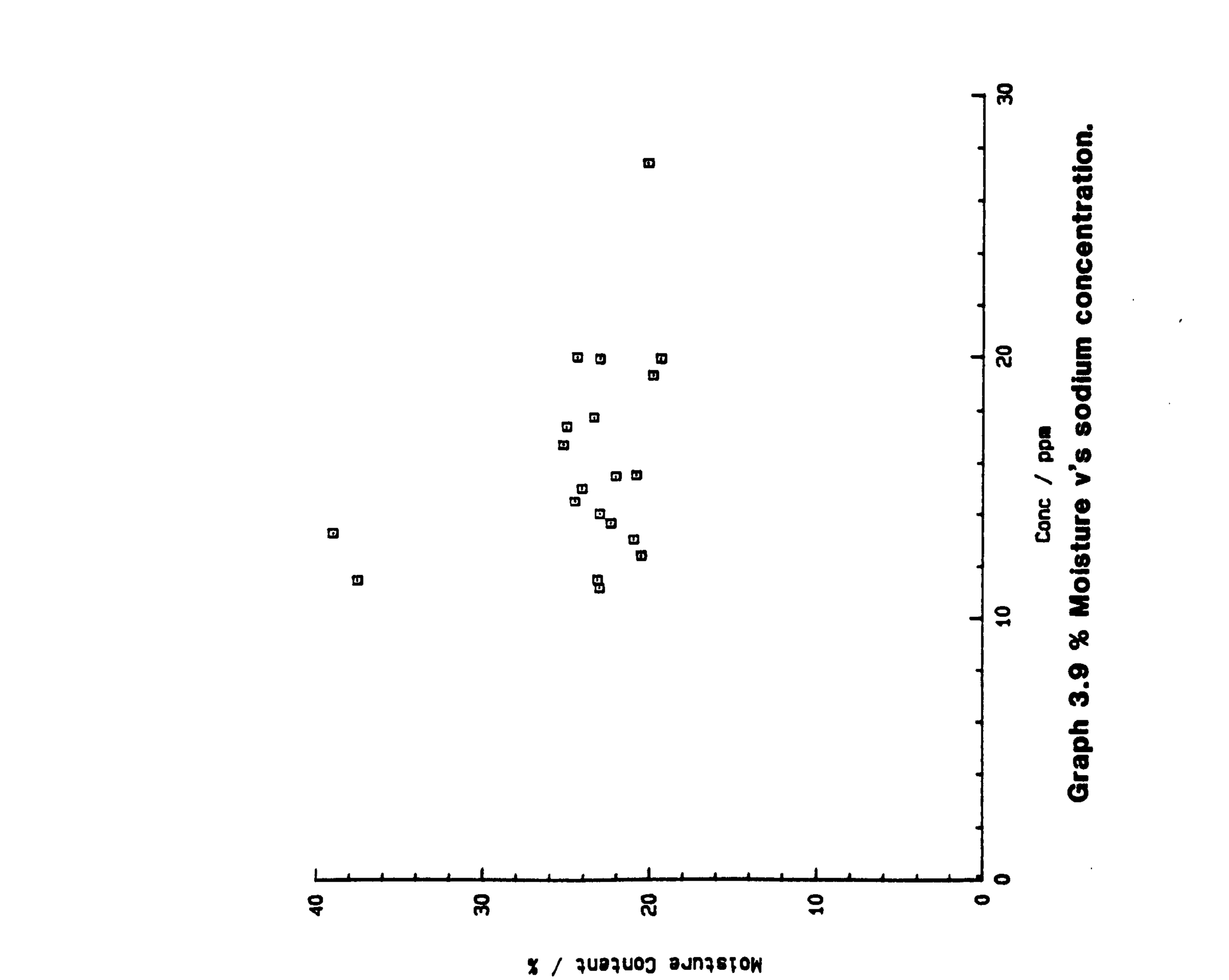
Graph 3.9 % Moisture v's sodium concentration.
Conc / ppm
0
10
20
30
Moisture Content / %
40
30
20
10
0

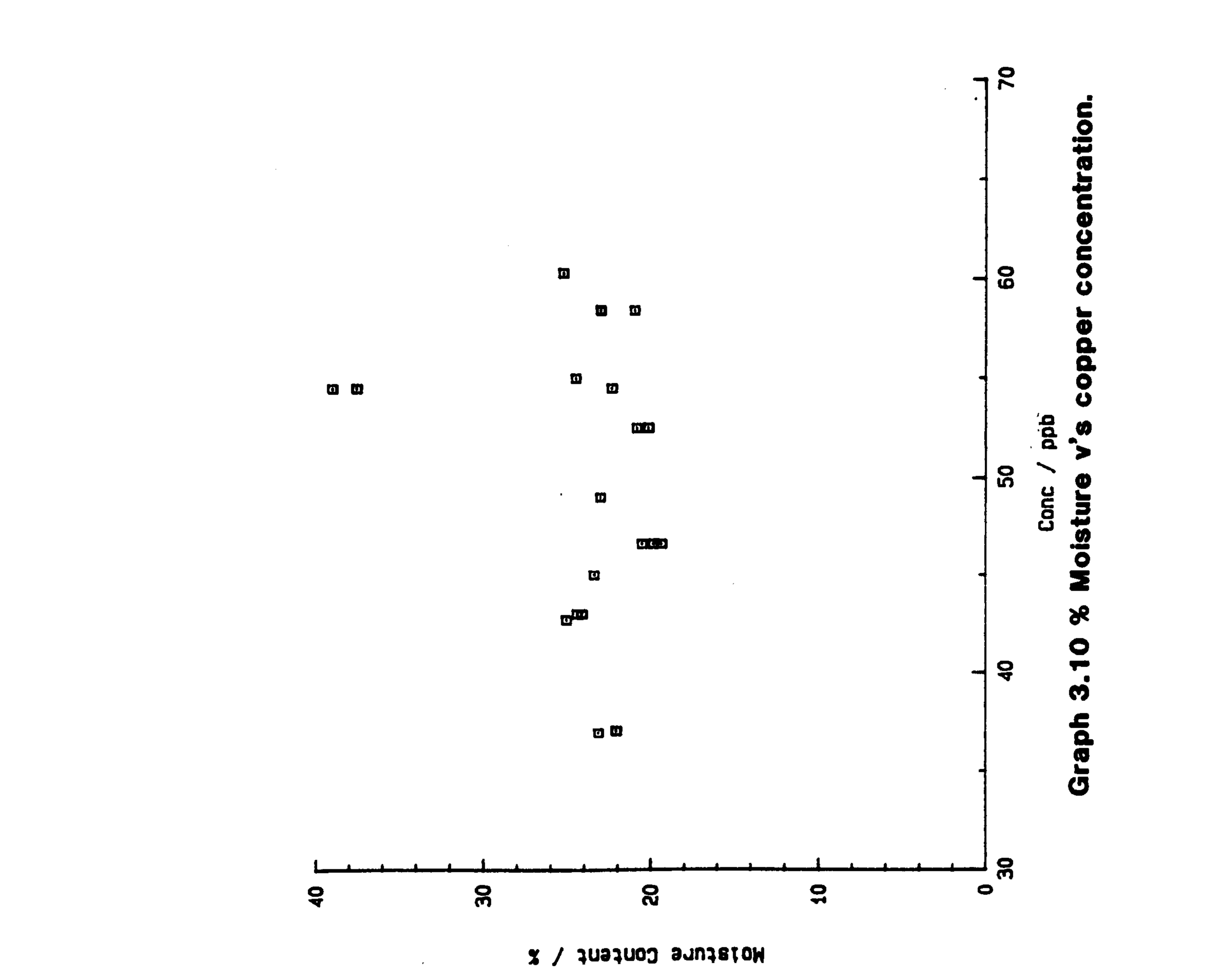

Graph 3.10 % Moisture v's copper concentration.

3.9.2.4 **Ionic Strength**

See Graph 3.11. As before there is no correlation between ionic strength and calculated from moisture content and % moisture content.

3.9.3 ***Discussion***

The results obtained are the opposite of those obtained by Edmeades, Wheeler and Clinton [5] who found that the concentrations of cations decreased with soil moisture content. The reason for this is due to different sampling procedures. The above workers used air dried soils to which they added distilled water and with such a procedure it seems obvious that the concentrations of the major elements would change depending on the amount of water added.

The soils in this study were treated in such a way that only the soil solution was extracted and the presence or absence of any correlation would suggest one of two possible situations:

(i) If a relationship between ionic concentrations and moisture content was found then it would suggest that the soil solution was isolated from the solid phase of the soil and the ionic concentrations would be solely dependant on the amount of moisture present.

(ii) If no relationship is apparent then it would suggest that there was substantial interaction between the soil solution and the solid phase.

In this instance the second situation seems to be the case and there is a substantion movement of ions between the solid and solution phase. This suggests that when more moisture enters the soil matrix there is an outflux of ions from the solid phase until equilibrium is reached.

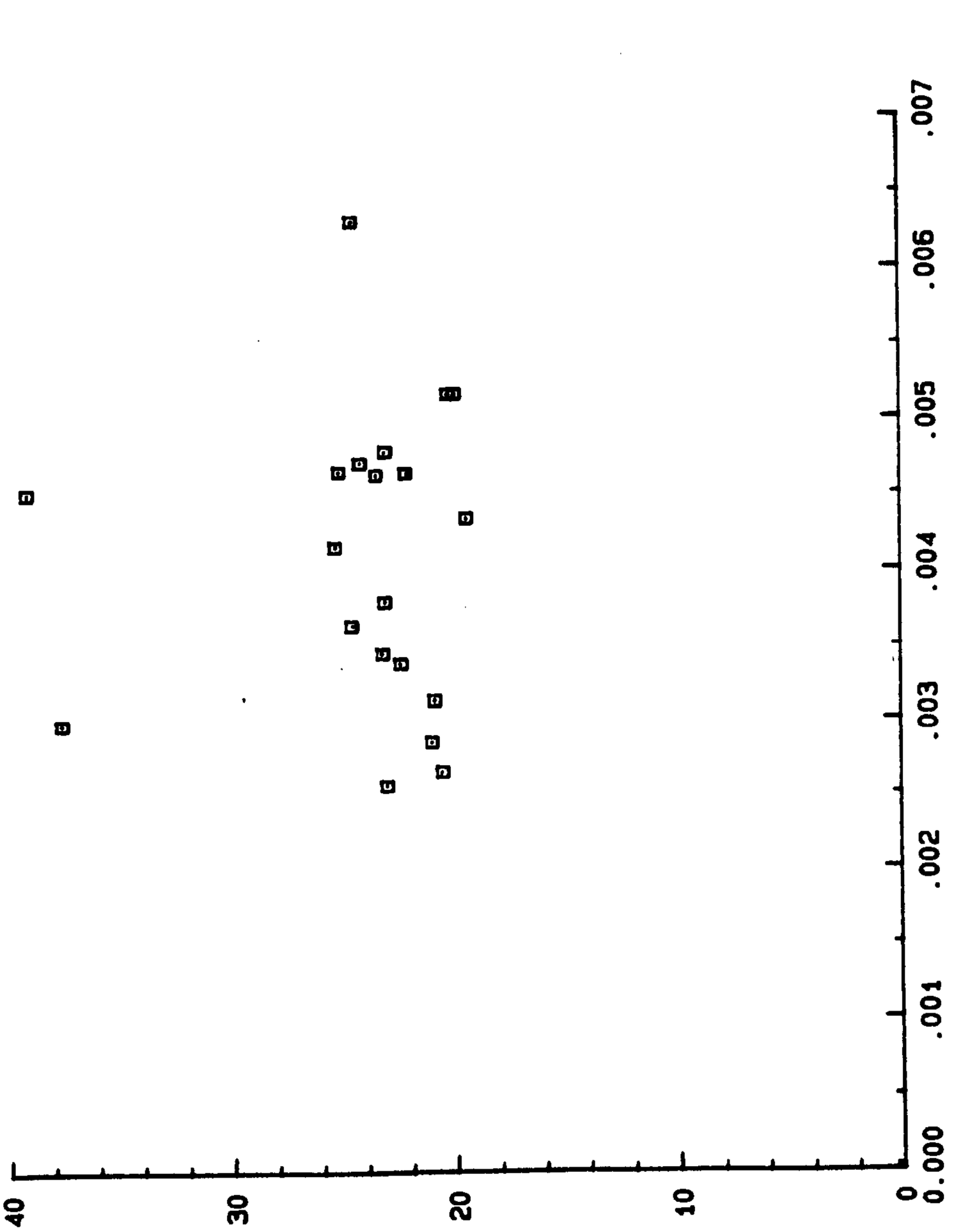

Graph 3.11 % Moisture v's Ionic strength.

REFERENCES

1. Hamilton E.I., 1980, Analysis for trace elements 1: Sample Treatment and Quality Control, in Applied Soil Trace Elements, Wiley, Chichester. Ed. Davies B.E., p 21-67.

2. Elkhatib E.A., Hern J.L. and Staley T.E., 1987, Soil Sci. Am. J., **51**, 578-583.

3. Sparling G.P., Whale K.N. and Ramsay A.J., 1985, Aust. J. Soil Res., **23**, 613-21.

4. Sparling G.P. and Berrow M.L., 1985, J. Agric Sci., **104**, 223-226.

5. Edmeades D.C., Wheeler D.M. and Clinton O.E., 1985, Aust. J. Soil Res., **23**, 151-165.

CHAPTER FOUR

THE APPLICATION OF HIGH PERFORMANCE SIZE EXCLUSION LIQUID CHROMATOGRAPHY TO THE STUDY OF COPPER SPECIATION IN WATERS EXTRACTED FROM SEWAGE SLUDGE TREATED SOILS

4.1 *INTRODUCTION*

It was apparent that size exclusion chromatography would be an ideal technique to use in copper speciation studies because, in theory, there should be no chemical interaction between the size exclusion column packing and the samples under study. In Chapters 2 and 3 an I vs EC relationship was established, which allowed a column eluent to be prepared with a similar pH and ionic strength to the soil solution under study. The use of SEC with such an eluent should allow a molecular weight separation to be obtained with a minimal disruption of the sample equilibria. Size exclusion chromatography is one of the newest of the liquid chromatographic techniques. It has also been referred to as gel filtration and gel permeation chromatography and it is a technique which has already been applied to the study of organic material in soils [1-3].

Much of this early work made use of Sephadex size exclusion gels. This type of packing is very soft and cannot be used with HPLC apparatus. Such columns tend to use low flow rates which results in a very long analysis time. Furthermore, particle sizes of the soft gels are large and less uniform, resulting in reduced column efficiency. Sephadex columns have been used in speciation studies with varying degrees of success [4-7]. These gels have associated with them some major problems due to gel-solute interactions which Swift and Postner [3] attributed to coulombic interactions and Van der Waals sorption. Coulombic repulsions arise due to ionic interaction between charged sites on the size exclusion gel and similarly charged test samples. The net result of such interactions is that charged species exhibit no retentions on the column and simply elute at the solvent front [2]. Van der Waals forces can result in an adsorption of organic material on to the column gel and in some cases this adsorption

may be irreversible. The above interactions render the use of traditional Sephadex gels almost useless in speciation studies due to the detrimental effects such phenomena are bound to have on the sample equilibria.

More recently gels have been developed which are more rigid and can be used to study humic materials and unlike Sephadex gels they exhibit minimal adsorption of organic matter. They do however suffer from coulombic repulsion and this has been overcome in the past by the use of high salt containing eluents e.g. 0.1 Mol dm^{-3} NaCl [8]. Such gels have not yet been used in speciation studies but it seemed that they would be useful in the separation of metal-organic complexes in soil solutions.

4.2 *PRINCIPLES OF SIZE EXCLUSION CHROMATOGRAPHY*

Packings for size exclusion chromatography consist of small (~10 μm) silica or polymer particles containing a network of uniform pores into which solute and solvent molecules can diffuse. Once the molecules enter the pores they are effectively trapped and removed from the flow of the mobile phase. The time a molecule spends in the pores is dependent upon the size of the solute molecule. Molecules that are too large to enter the pores are excluded and exhibit no retention. As a result these molecules are eluted at the solvent front. Molecules with effective diameters smaller than the pores take a long time to make their way through the pore maze and are eluted last. Molecules with a size between these two extremes spend varying amounts of time in the pores depending on their effective molecular size. Within this group fractionation occurs which is directly related to molecular size and to some extent molecular shape.

4.3 *THEORY OF SIZE EXCLUSION CHROMATOGRAPHY*

4.3.1 *The distribution coefficient*

The total volume V_t of a column packed with a porous polymer or silica gel is given by

$$V_t = V_g + V_i + V_o \qquad \ldots\ldots (1)$$

Where V_g is the volume occupied by the solid matrix of the gel, V_i is the volume of solvent held in the pores and V_o is the void volume outside the gel particles. If we assume that no mixing, or diffusion occurs then V_o corresponds to the theoretical volume of solvent required to transport through the column those molecules that are too large to enter the pore maze. In reality some mixing and diffusion does occur and as a consequence the non retained components appear as Gaussian-shaped peaks with a concentration maximum at V_o.

For components small enough to enter the pores, the peak maxima will occur at the end of the column corresponding to (V_i+V_o). Generally V_i, V_o and V_g are of the same order of magnitude; thus a gel column permits the separation of the large molecules from the small molecules with a minimal volume of eluate.

Molecules of intermediate size are able to transfer into some fraction K of the solvent held in the pores; the elution volume V_e for these retained molecules is:

$$V_e = V_o + KV_i \qquad \ldots\ldots (2)$$

Equation (2) applies to all of the solute on the column. For molecules too large to enter the pores, $K = 0$ and $V_e = V_o$; for molecules that can enter the pores unhindered, $K = 1$ and $V_i = (V_o + V_i)$. In deriving equation 2 the assumption made was that no interaction such as adsorption,

occurs between the solute molecules and the gel surfaces. If adsorption occurs then the amount of interstitially held solute will increase; with small molecules K will then be greater than unity.

The above equation can be rearranged to give

$$K = (V_e - V_o)/V_i = C_s/C_m \quad \ldots\ldots (3)$$

Where K is the distribution coefficient for the solute. Values of K range from zero for totally excluded molecules to unity for small molecules. The distribution coefficient is useful for comparing data obtained using different types of packing.

4.3.2 *Calibration Curves for SEC*

A calibration curve is by far the most convenient way to obtain a molecular weight calibration for a size exclusion packing. An example of such a curve is shown in Fig. 4.1, there the molecular weight of the molecules (which is directly related to molecular size) is plotted against retention volume V_R, where V_R is the product of the retention time t_R and the flow rate of the eluent (V_R is more commonly referred to as the elution volume). The exclusion limit defines the molecular weight beyond which no retention occurs. All species having a greater molecular weight than the exclusion limit are so large that they are not retained and co-elute (Peak A) at V_o. The permeation limit is the molecular weight below which the solute molecules can penetrate all the pores unhindered. All molecules of this volume coelute at V_i and are labelled D.

As molecular weights decrease from the exclusion limit, solute molecules spend progressively more time in the pores and thus move progressively more slowly. It is in this selective permeation region that fractionation occurs yielding individual solvent peaks such as B and C in the diagram.

Fig 4.1 SEC calibration graph.

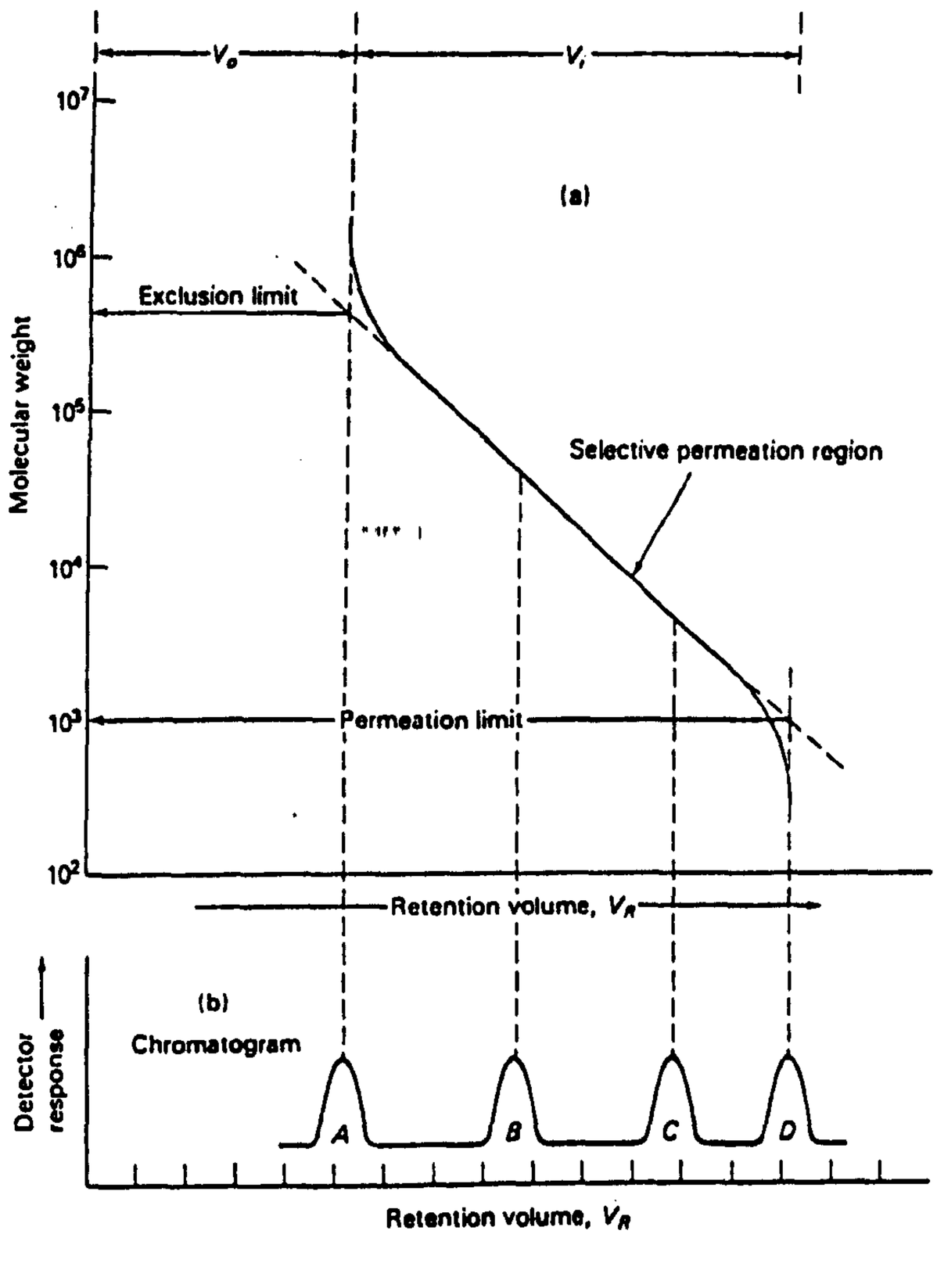

Experimental calibration curves are available in manufacturers literature and allow the selection of a column suitable for the molecules of interest.

4.4 *THE EFFECTS OF IONIC STRENGTH ON THE ELUTION VOLUME OF ORGANIC LIGANDS PERTAINING TO SOIL SOLUTIONS*

4.4.1 *Apparatus*

The HPLC separation was carried out with a TSK (Toyo Soda, Tokyo, Japan) G3000 SW SEC column (8 x 300 mm) fitted with a TSK GSW (8 x 40 mm) guard column. All HPLC apparatus used was manufactured by LKB (Bromma, Sweden) and consisted of the following: 2152 HPLC controller, 2158 U.V. cord SD detector (λ = 254 nm) 2150 HPLC pump and 11300 Ultograd mixer driver. Samples were injected via a Valco C6W injection valve fitted with a 200 μl injection loop.

4.4.2 *Reagents*

A few granules of Blue dextran (Pharmacia, Sweden) were dissolved in water and to this 2 drops of acetone were added. This solution was used in order to determine V_o and V_t.

A humic acid standard (50 mg dm^{-3}) was prepared by dilution of a 200 mg dm^{-3} stock solution prepared by dissolving 0.2 g of humic acid powder in 1 cm^3 of 0.2 Mol dm^{-3} NaOH and diluting with distilled water. This solution was then filtered through a Whatman 540 (Whatman Ltd., Maidstone, UK) to remove any particulate matter. A fulvic acid standard 50 mg dm^{-3} was prepared by dissolving fulvic acid powder in distilled water followed by filtration as above. The humic and fulvic acids were provided by Alan Hepburn (Soils Division, Macaulay Land Use Research Institute, Aberdeen, UK). The humic acids were extracted from a soil of the Insch Association sampled at Greenhall Farm, Insch. Unless stated otherwise all

other reagents were prepared from "Analar" grade (BDH Chemicals Ltd., Poole, UK) chemicals. All glassware was soaked overnight in 2% Decon, rinsed, washed three times with 1:4 HNO_3 and finally rinsed three times with water. All water used was purified by deionisation and distillation.

4.4.3 ***Experimental***

The TSK G3000 SW column chosen in this study has been used in the past to study humic materials. In all cases the authors have reported problems due to coulombic repulsion between the column packing and charged samples. This has been overcome by the use of high ionic strength eluents e.g. 0.1 Mol dm^{-3} NaCl. It was decided to investigate this phenomenon further by running test samples which were of importance in soil solutions using eluents of varying ionic strength. All samples were filtered using a Gelman LC3A 0.45 μm filter before loading into the sample loop. The samples were then injected on to the HPLC column with a carrier flow of 0.75 ml min^{-1}. The mobile phase consisted of 0.0058 Mol dm^{-3} Na_2HPO_4/NaH_2PO_4 buffer, pH 5.9 and varying concentrations of KCl to modify the ionic strength. At low ionic strengths comparable to soil solutions only NaH_2PO_4/Na_2HPO_4 was used in the eluent. A computer program "Buffer" was written (Appendix 1) which allowed the correct concentration of each of the components to be calculated so that the final eluent had a pH and total ionic strength similar to the soil solutions analysed in the previous Chapter.

Of the test samples blue dextran (a high molecular weight polysaccharide) was used in order to determine the column void volume V_o and acetone was used to determine the pore volume V_i. Samples of humic, fulvic and citric acid were run as substances representative of the ligands present in soil solutions.

4.4.4 *Results and Discussion*

The test samples were run with each eluent and the results obtained were then plotted as graphs of elution volume/ml versus ionic strength/Mol dm^{-3} (Graph 4.1).

When distilled water was used as an eluent the results obtained (Fig. 4.2 a,b,c & d) were similar to those obtained by other authors i.e. there was very little retention of charged molecules on the column with a distilled water eluent. Humic and fulvic acid both eluted at the void volume V_o (found from the blue dextran peak). This was most likely due to coulombic repulsion between the column packing and the test samples. This coulombic repulsion occurs between the covalently bound hydrophillic groups containing OH [13] and the similar hydroxyl groups on the humic, fulvic and citric acids. This made it impossible for the solute molecules to penetrate the pore structure of the size exclusion gel.

Citric acid did exhibit a little retention but the difference between its retention and those of the humic materials was very small when compared to the difference in molecular weight. The citric acid peak was also badly split. Analysis of the citric acid standard by reversed phase chromatography showed no impurity in the standard. The two peaks were labelled 1 and 2 in the figure. Peak 1 was initially thought to be the main citric acid peak. The reason for peak 2 is unclear but it could have been explained in terms of adsorption and desorption of some citric acid on to the gel. This seems unlikely as neither humic or fulvic acid showed any signs of secondary peaks due to adsorption. Both substances have exhibited extensive adsorption on Sephadex gels in the past due to the large aromatic content of these molecules. It is unlikely that citric acid would show a greater tendency to adsorb than humic or fulvic acids, so

Graph 4.1

Graph of elution volume v's ionic strength for various test samples.

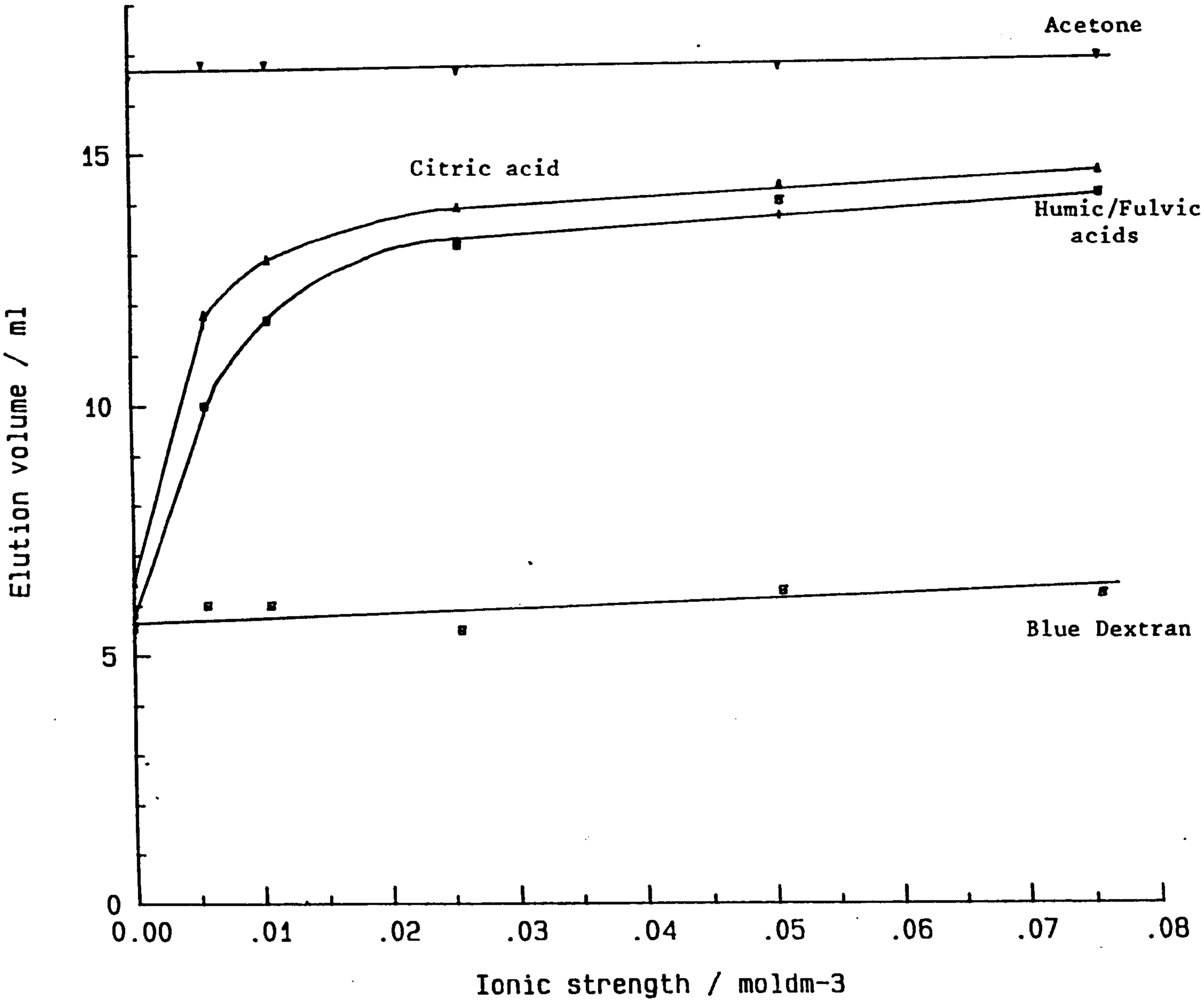

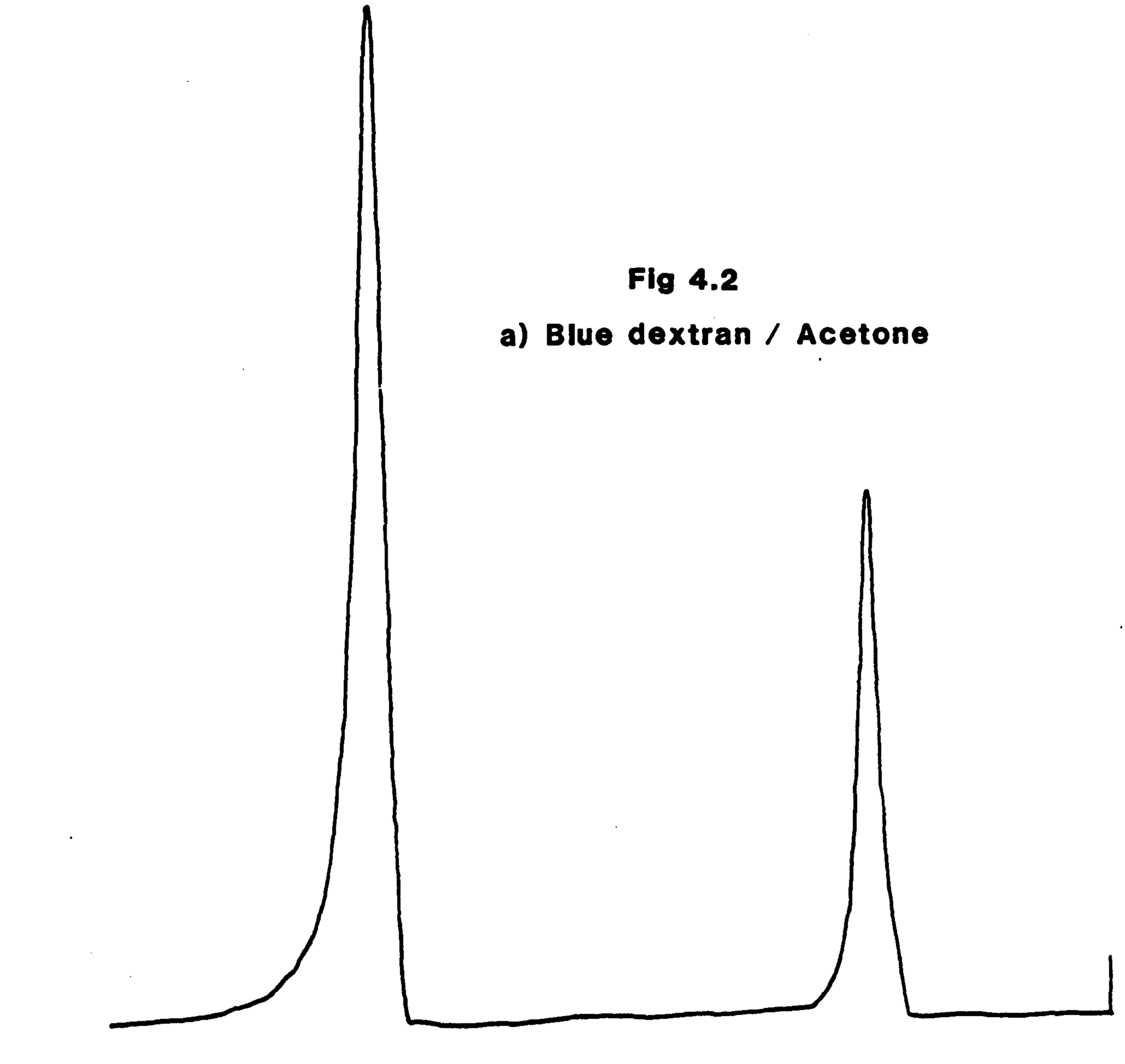

Fig 4.2

a) Blue dextran / Acetone

Fig 4.2

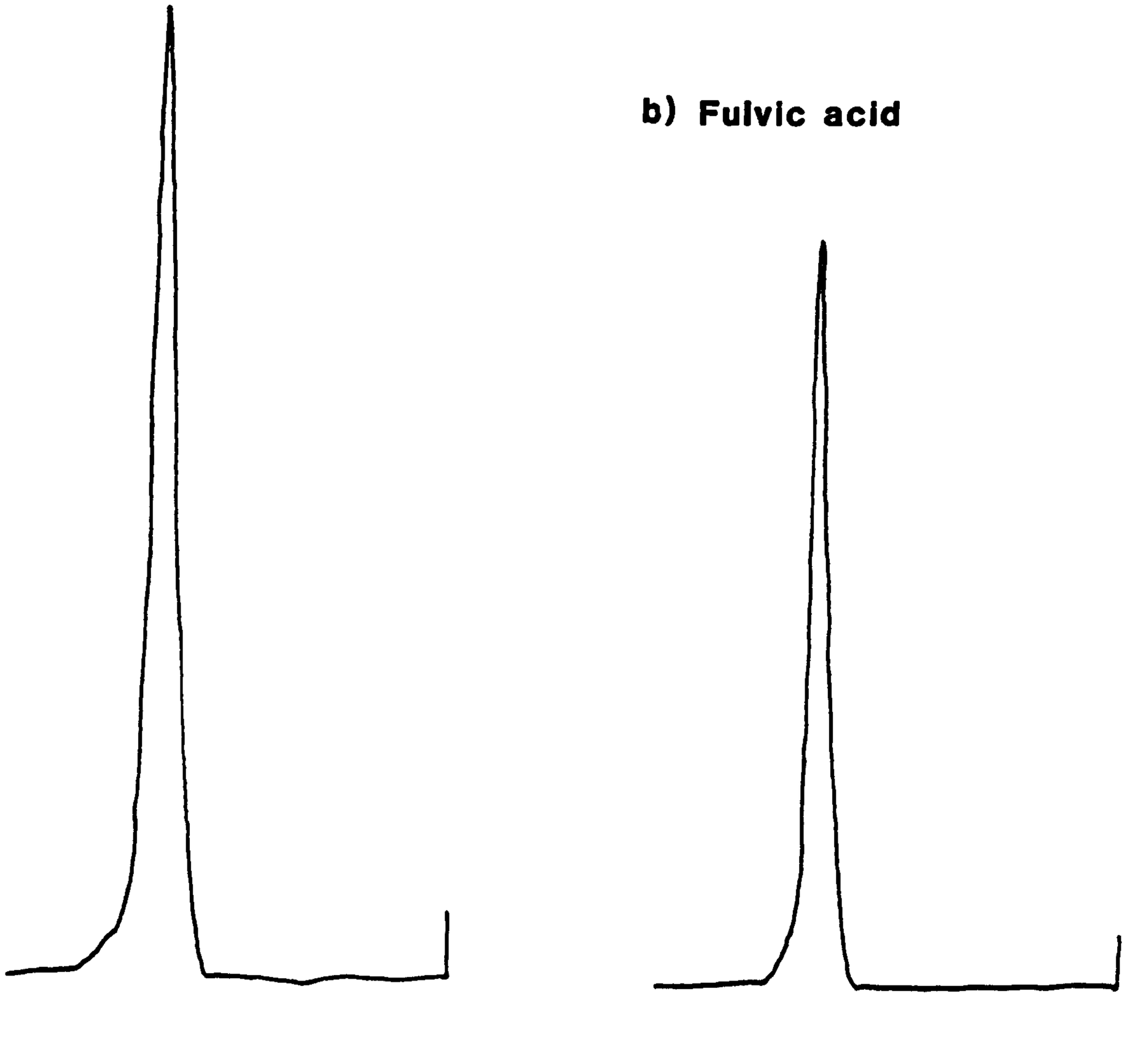
c) Humic acid
b) Fulvic acid
9
6
3
Elution Volume /ml
9
6
3
Elution Volume /ml

Fig 4.2 d) Citric acid

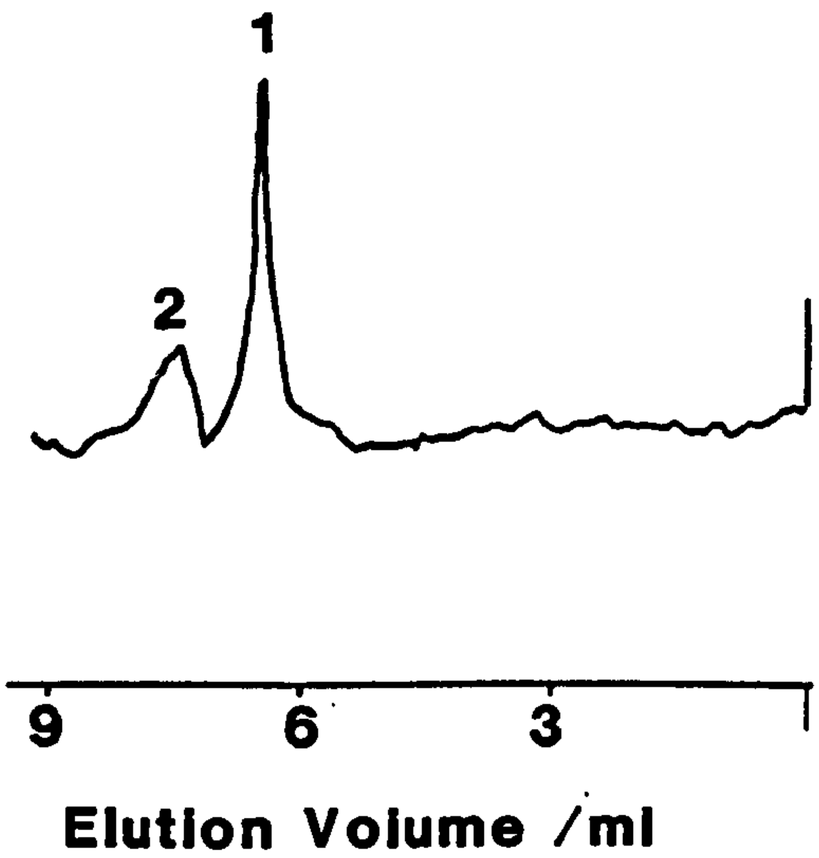

this explanation was discounted. It is possible that peak 2 was the main citric acid peak and the first peak (peak 1) could have simply been caused by the formation of the Na salt of citric acid due to interaction with the eluent.

Acetone exhibited a much larger retention on the column because it contains no hydroxyl groups which would cause repulsion and was therefore able to penetrate the whole pore matrix showing maximum retention (V_t). This was true at all ionic strengths.

At the highest ionic strength used (I = 0.0758 Mol dm^{-3}) the retention of all the organic acids was much increased (Fig. 4.3 a,b,c). At this ionic strength the coulombic repulsion was thought to have ceased to exist due to the higher concentrations of Na^+ and K^+ in the eluent. These actions would effectively block the repellant hydroxyl groups by the formation of $-O^-Na^+$ and $-O^-K^+$ species. Again the separation between the humic acids and citric acid was very poor.

It is evident from Graph 4.1 that as ionic strength is decreased the separation between citric acid and the humic materials increased. At ionic strengths comparable to soil solutions quite a good separation was achieved (Fig. 4.4 a,b & c).

Humic acid exhibited some unusual behaviour in that two peaks were observed. The first peak eluted at V_o and the second peak had an elution volume identical to that of fulvic acid. The peak ratios varied depending on the ionic strength of the eluent. At zero ionic strength only the peak at V_o was present but at higher ionic strengths only the second peak existed (Fig. 4.2c and 4.3b). As the ionic strength of the eluent was increased the height of peak 2 increased relative to the peak at V_o. In some ways these results are similar to those obtained on Sephadex gels [1]. By

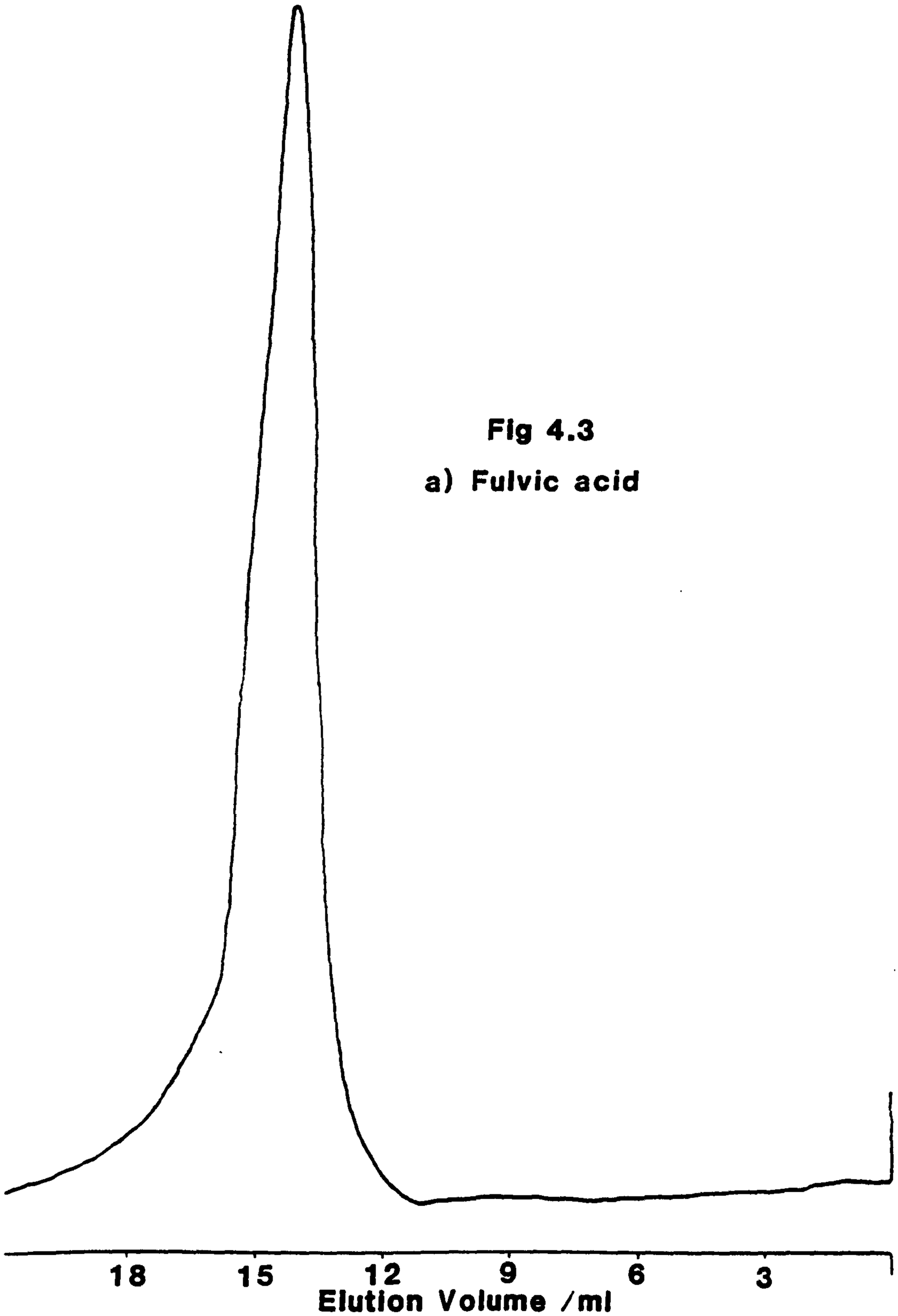

Fig 4.3

a) Fulvic acid

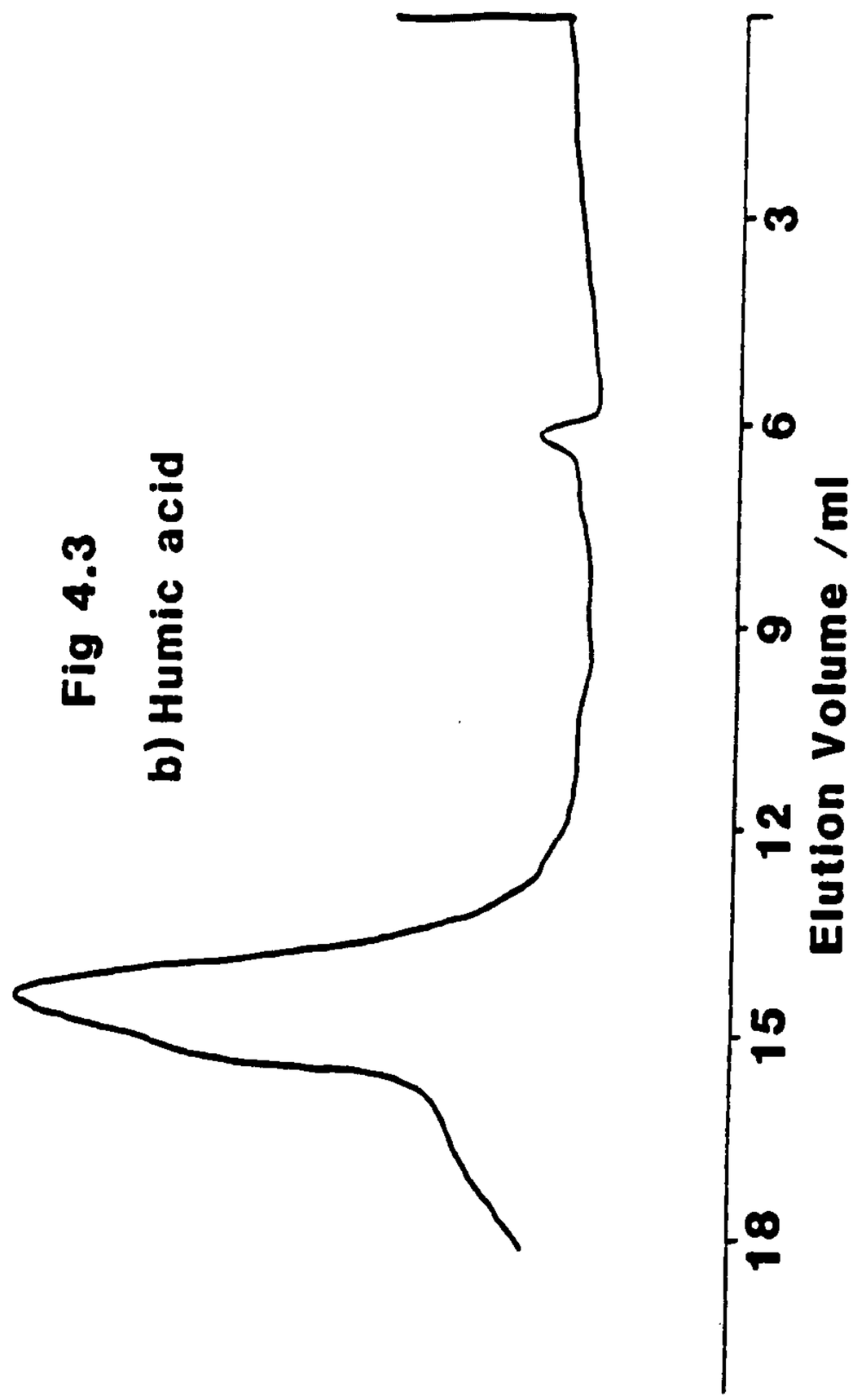

Fig 4.3
b) Humic acid

Fig 4.3 c) Citric acid

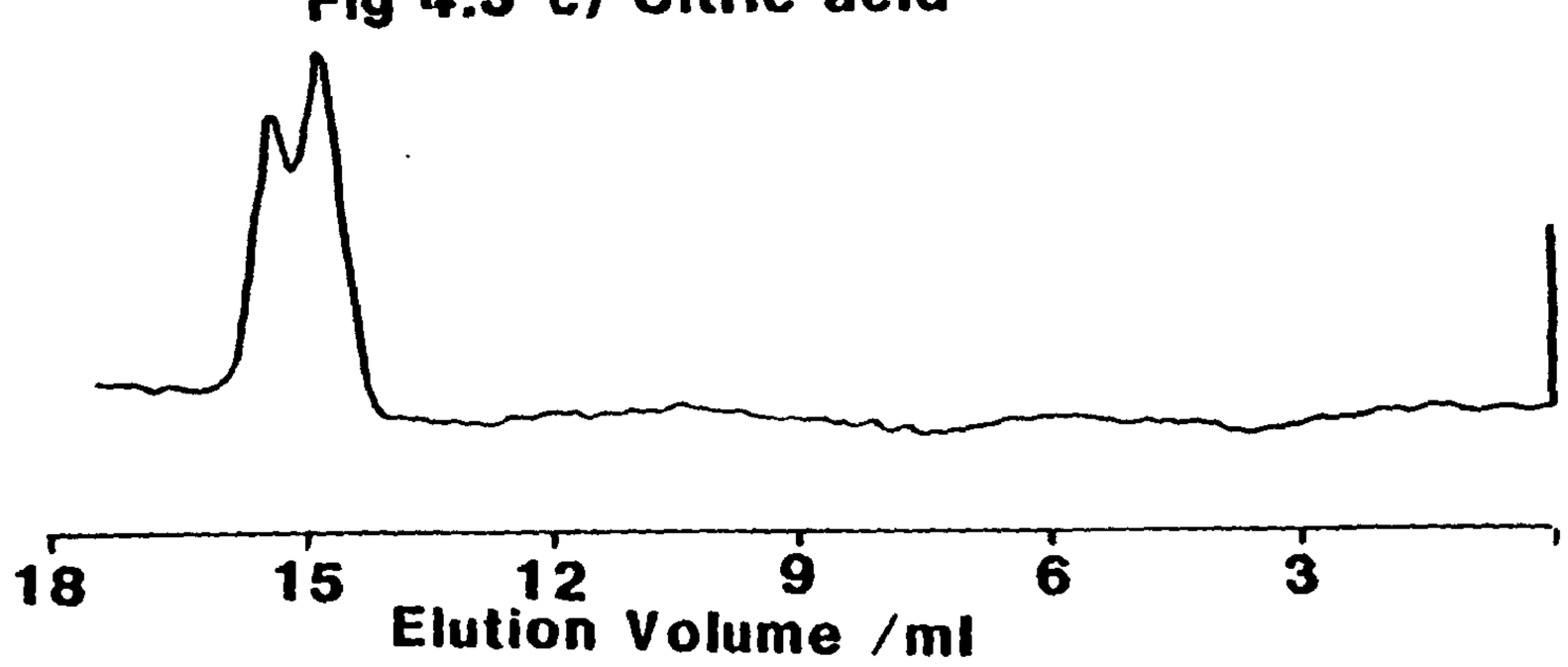

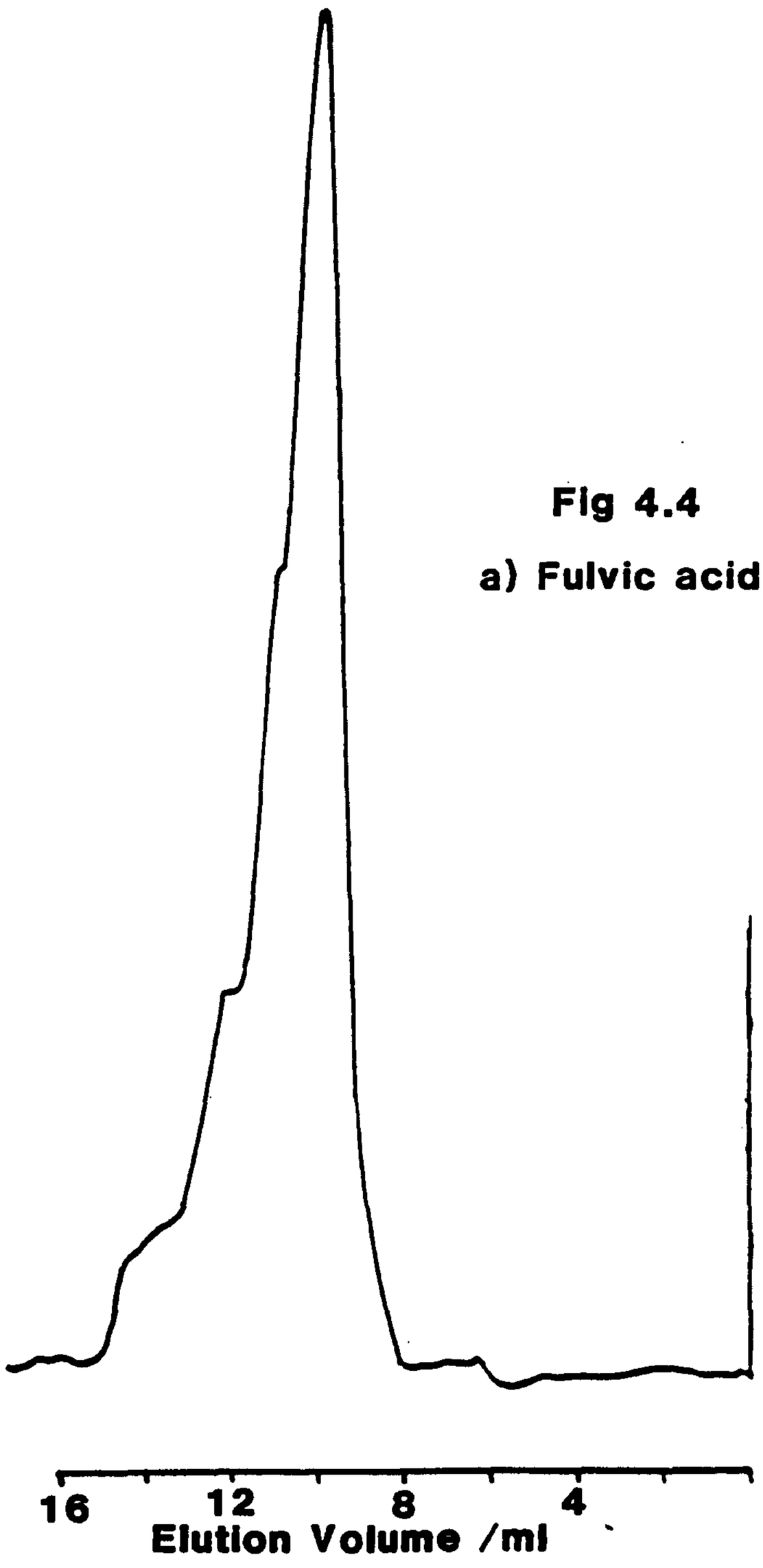

Fig 4.4

a) Fulvic acid

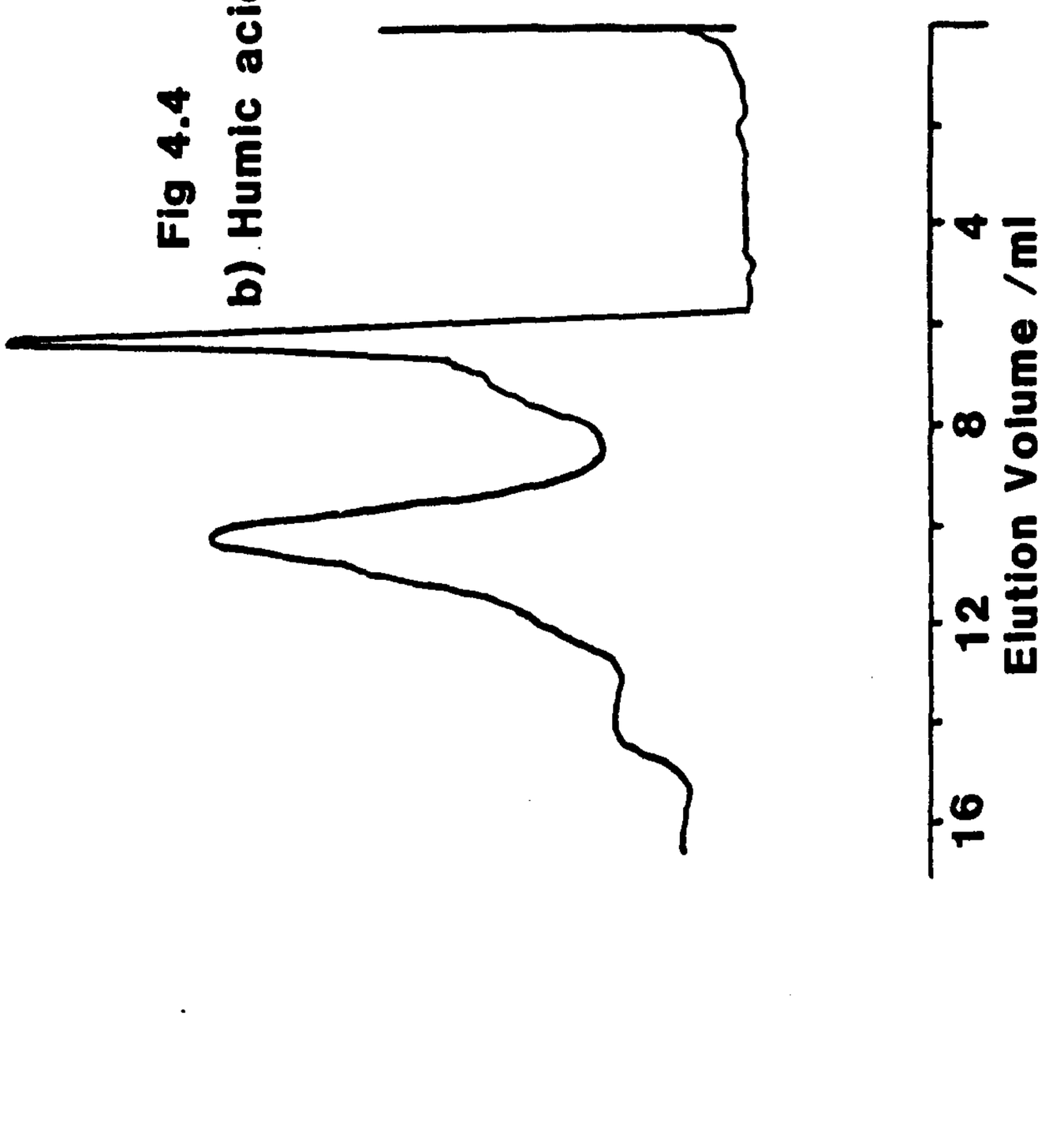

Fig 4.4
b) Humic acid

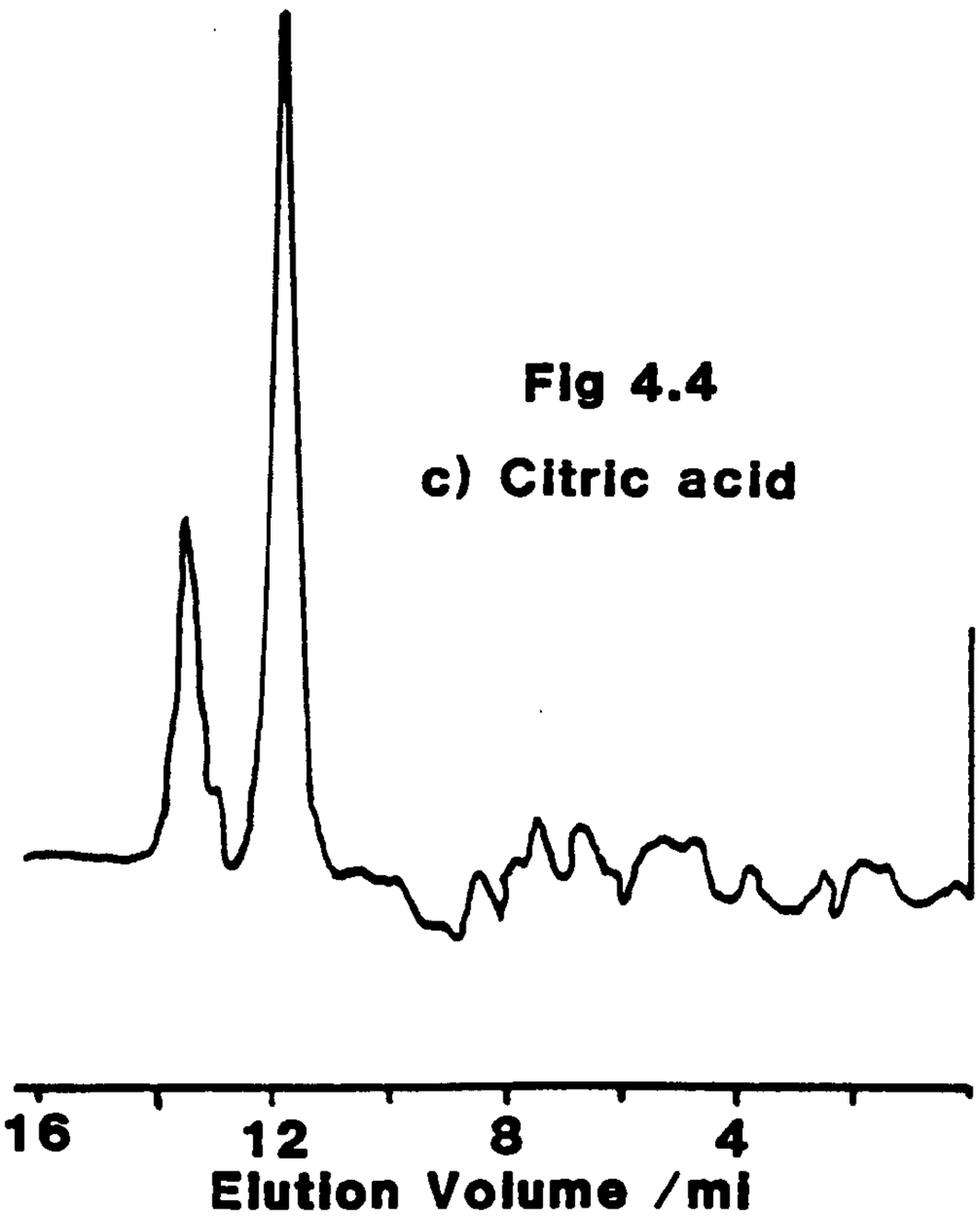

Fig 4.4

definition humic acid is soluble in dilute alkali only, whereas fulvic acid is soluble in both dilute acid and alkali. The existence of the second humic acid peak has in the past been attributed to a water soluble humic acid fraction with similar properties to fulvic acid [1]. The use of Sephadex gels in the study of humic materials was viewed more critically by Hine [2], who also found that increased salt concentrations caused a shift from a peak at V_o to a second peak with a greater elution volume. He also found that the addition of salt to the eluent resulted in a reversible adsorption of humic materials on to the sephadex gel similarly observed by Vaughan [1]. The existence of coulombic repulsion and adsorption on Sephadex gels casts doubt upon the conclusions reached in the past about molecular weight profiles of humic materials. It is difficult to accept that both adsorption and coulombic repulsion can be reduced simultaneously when it would be expected that since the two mechanisms work in opposition, conditions conductive to one would be detrimental to the other.

Earlier workers concluded that the existence of a peak at V_o suggested the presence of humic material with a molecular weight greater than the fractionation range of the gel and that the second peak was due to a water soluble humic acid fraction. This conclusion seems unlikely in the light of this work. The TSK G3000 SW column has not exhibited adsorption of humic materials in the past nor in this study and therefore at high ionic strengths coulombic repulsion is overcome and the only process taking place is that of size exclusion. At such ionic strengths all of the humic acid is eluted with fulvic acid suggesting that coulombic repulsion has been overcome and to the contrary of the results obtained

on Sephadex gels there is only one humic acid fraction. The fact that this is alkali soluble suggests that while it is structurally different from fulvic acid it is very similar in terms of molecular weight. If any high molecular weight fraction of humic acid existed then it is very unlikely that it would be able to penetrate the pores of the gel and would have eluted at V_o. This is simply not the case. Further evidence comes from the fact that the ratio of the two humic acid peaks is dependent on the ionic strength of the eluent. This suggests that at low ionic strengths there is not sufficient K^+ or Na^+ on the eluent to block the repelling hydroxyl groups of all the humic acid molecules and as a result the majority of the humic acid is eluted at V_o due to coulombic repulsion. As the concentration of the eluent is increased progressively more of the hydroxyl group on the humic acid are blocked by Na^+ or K^+ and the size exclusion process takes over until at high ionic strengths coulombic repulsion is overcome and only size exclusion is taking place.

At soil solution ionic strengths quite a good separation was obtained between citric acid and humic and fulvic acids. A possible explanation for this is that as I decreases so the effects of coulombic repulsion increase. The humic materials are more susceptible to coulombic repulsion due to the larger numbers of hydroxyl groups in the molecules, therefore, the separation at soil solution ionic strengths may occur as a result of both size exclusion and coulombic repulsion processes.

The humic acid peak at V_o provided further evidence that coulombic repulsion was still taking place.

4.5 *THE SIZE EXCLUSION CHROMATOGRAPHY OF SOIL SOLUTIONS*

4.5.1 *Apparatus*

The soil solutions were extracted by centrifugation with a MSE Mistral 3000 (Fisons Scientific Equipment, Loughborough, UK) Centrifuge. The HPLC apparatus was the same as used in Section 4.4.1.

4.5.2 *Experimental*

The soil samples were taken from Laverock Brae Farm as described in earlier Chapters. The soil solutions were extracted by centrifugation and stored in a cold room until required for analysis. The soil solutions were injected into the sample loop through a Gelman LC3A 0.45 μm filter to remove any particulate matter before analysis. The soil solutions were extracted from the soil samples taken on 5/5/89. It was decided to run the soil solutions with an HPLC eluent of 0.01 Mol dm^{-3} KCl + 0.0058 Mol dm^{-3} Na_2HPO_4/NaH_2PO_4 with a pH of 5.9 (similar to the pH's already encountered in this field). It was thought that this ionic strength would be representative of the highest ionic strength soil solutions likely to be encountered in the field of interest.

The soil sample taken from Lab 1-B was run at flow rates of 0.75 ml min^{-1} and 0.4 ml min^{-1} in order to investigate he effects of flow rate on the resolution of the peaks.

4.5.3 *Results and Discussion*

The chromatograms obtained from soil solution Lab 1-B are shown in Fig. 4.5 a,b. The chromatograms can be seen to consist of 5 distinct peaks. Peak 1 was most likely due to coulombic repulsion of humic materials but it could be due to genuine high molecular weight humic material. Peak 2 was thought to be due to the lower molecular weight humic

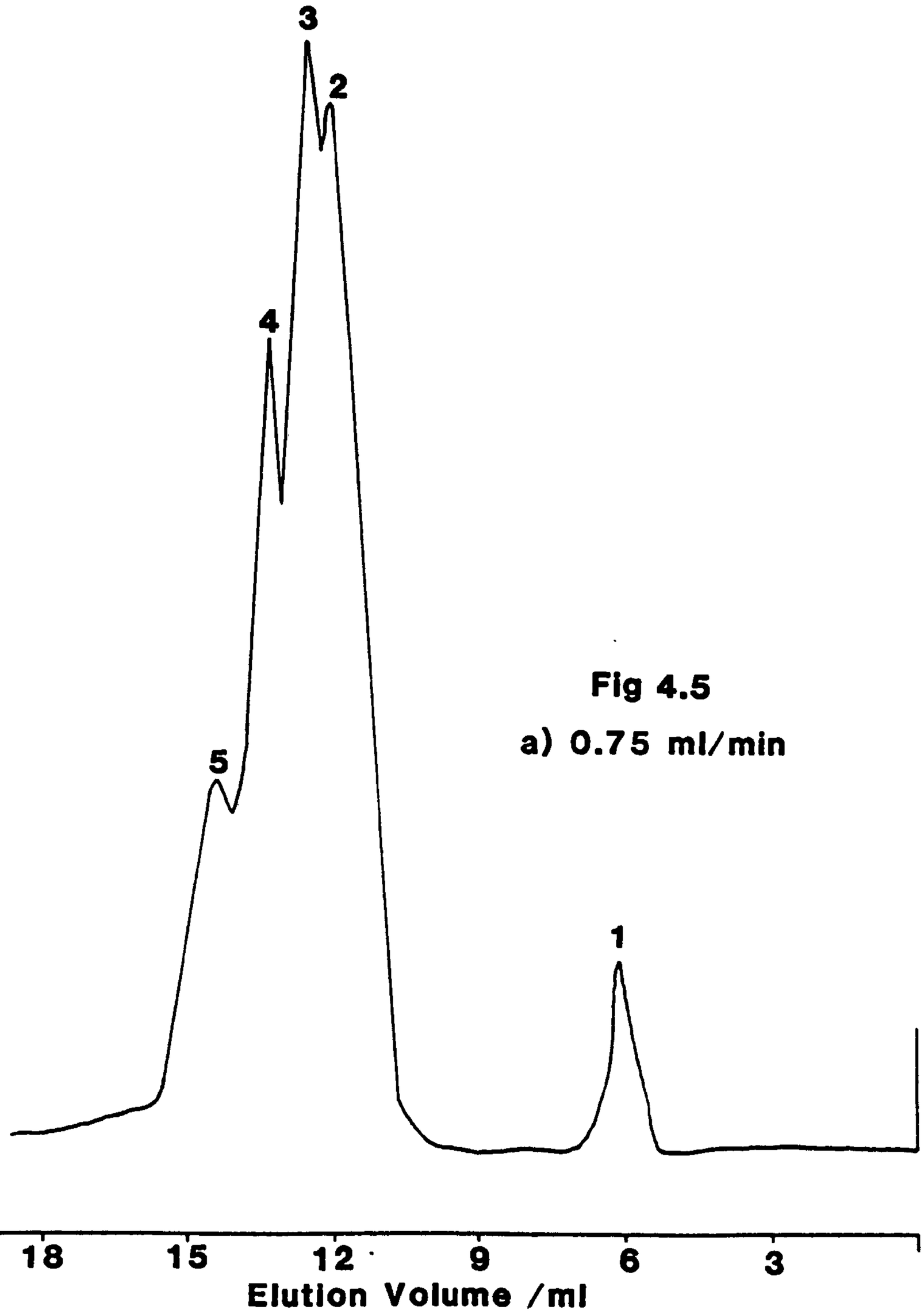

Fig 4.5

a) 0.75 ml/min

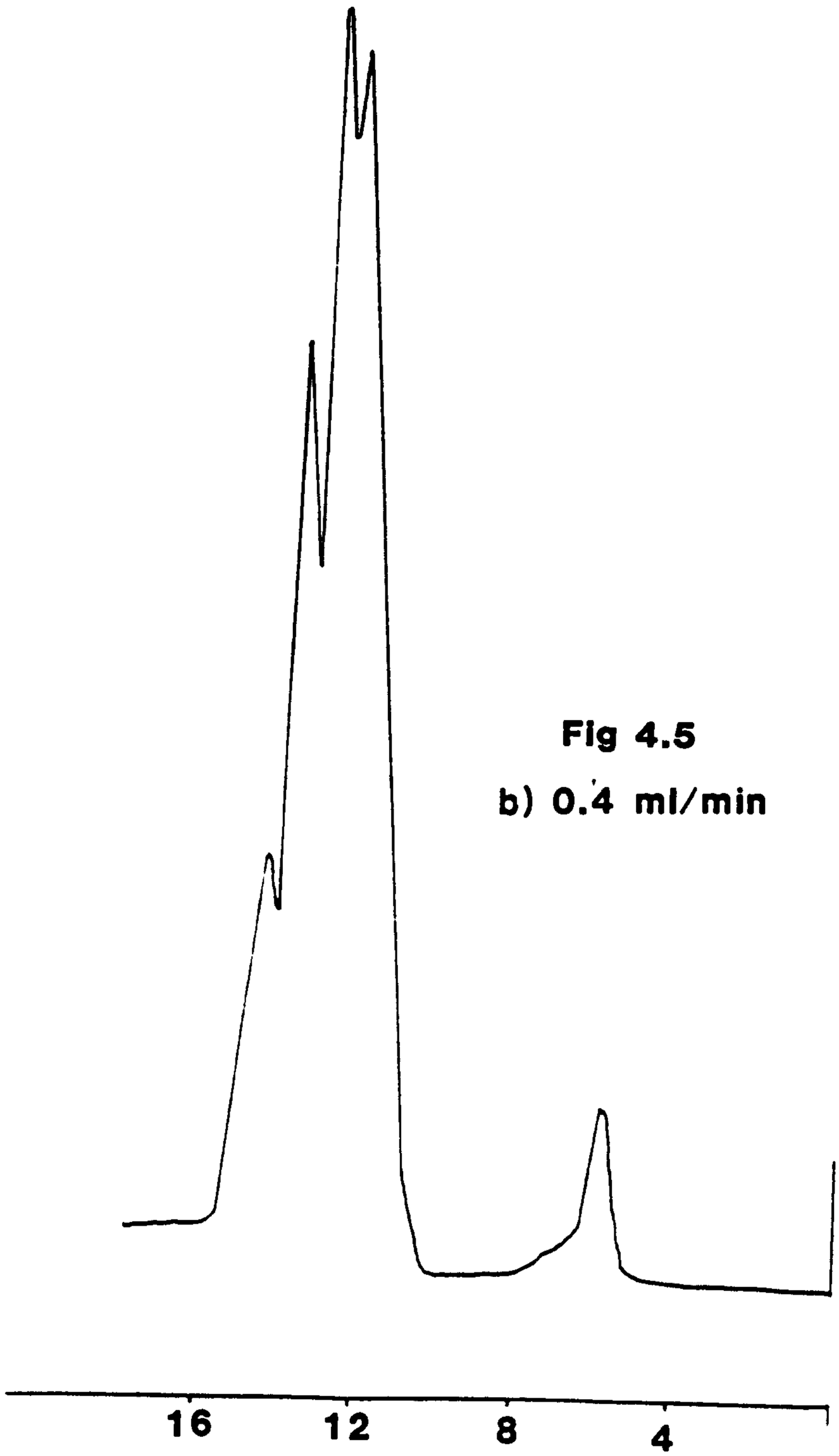

Fig 4.5

b) 0.4 ml/min

acid fraction and also fulvic acid as the elution volume was identical to those of the test samples. Similarly Peak 4 had an elution volume that was identical to citric acid and was therefore due to the low molecular weight organic ligands in the soil solution. Peak 3 lay in between those due to citric acid and the lower molecular weight humic substances and it is most likely due to a splitting of the latter peak. Peak 5 could have been due to either the second citric acid peak or U.V. absorbing inorganic ligands e.g. NO_3 which also elute at this volume. The same 5 peaks were present using both flow rates. The resolution was improved at a flow rate of 0.4 ml min^{-1} but it was not sufficiently better to warrant using such a low flow rate.

The conductivity measurements of the solutions extracted from the various sampling sites indicated that an eluent with an ionic strength of 0.0058 Mol dm^{-3} and pH 5.9 would be more closely matched to the ionic strength of the soil solutions. The soil solutions were all re-run with the above eluent and the results are shown in Figs. 4.6 a,b; 4.7 a,b and 4.8 a.b. From the chromatograms obtained it is noticeable that the resolution is much better than that obtained with the previous eluent. This may have been due to the increased effects of coulombic repulsion but if this had been the case one would have expected an increase in the size of Peak 1 which did not occur. The duplicate samples taken from sites Lab 1-A and 1-B were remarkably similar which seemed to indicate a reproducible sampling and extraction procedure. The duplicate sample taken at Site 1-CD was not quite as good but this may have been due to genuine differences in the organic content of the duplicate site.

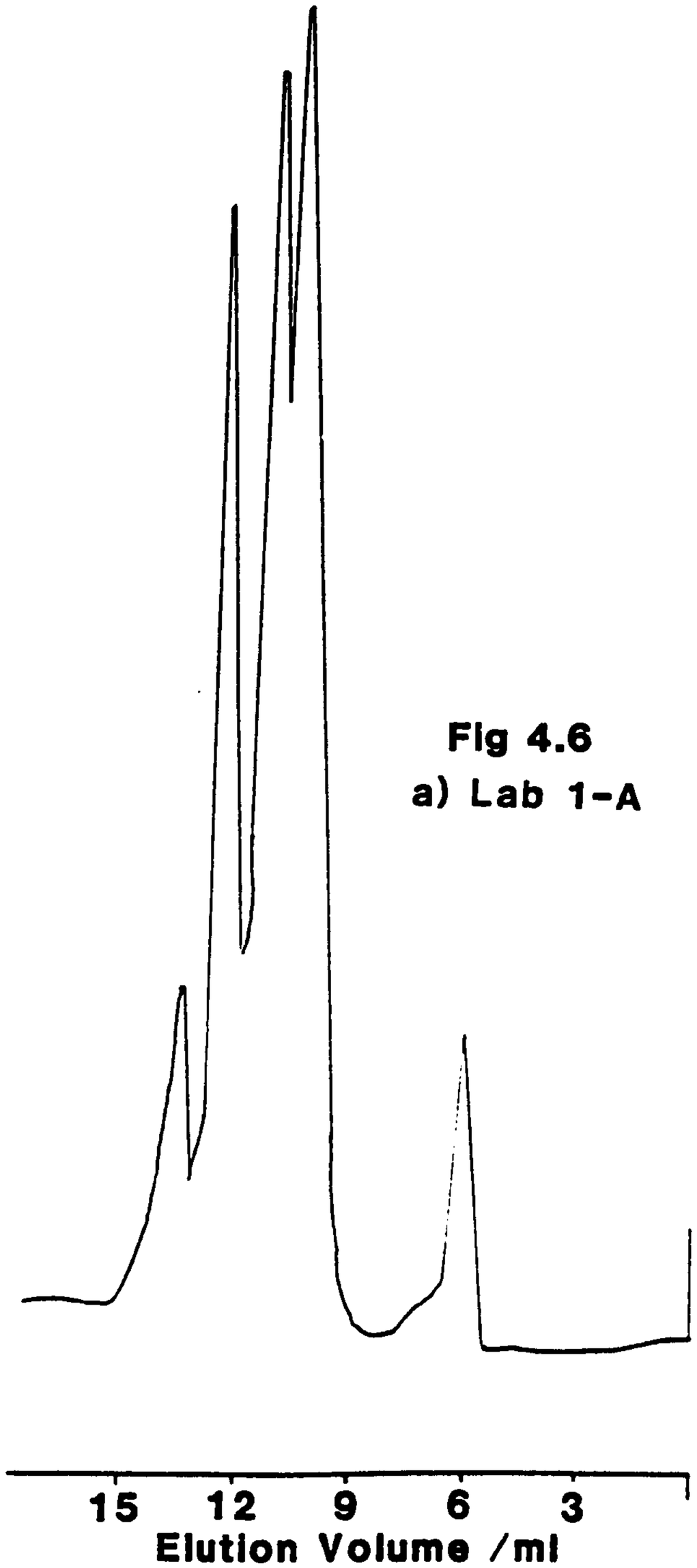

Fig 4.6
a) Lab 1-A

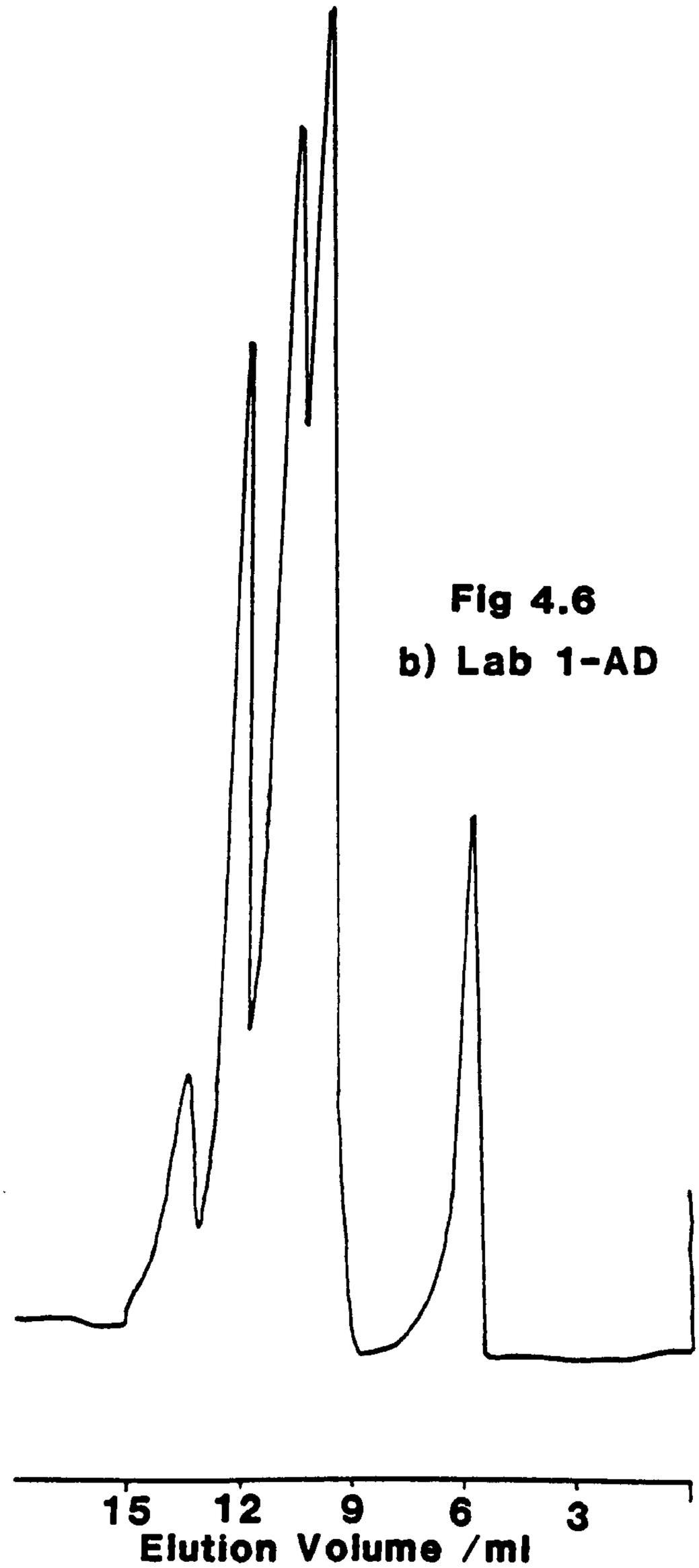

Fig 4.6
b) Lab 1-AD

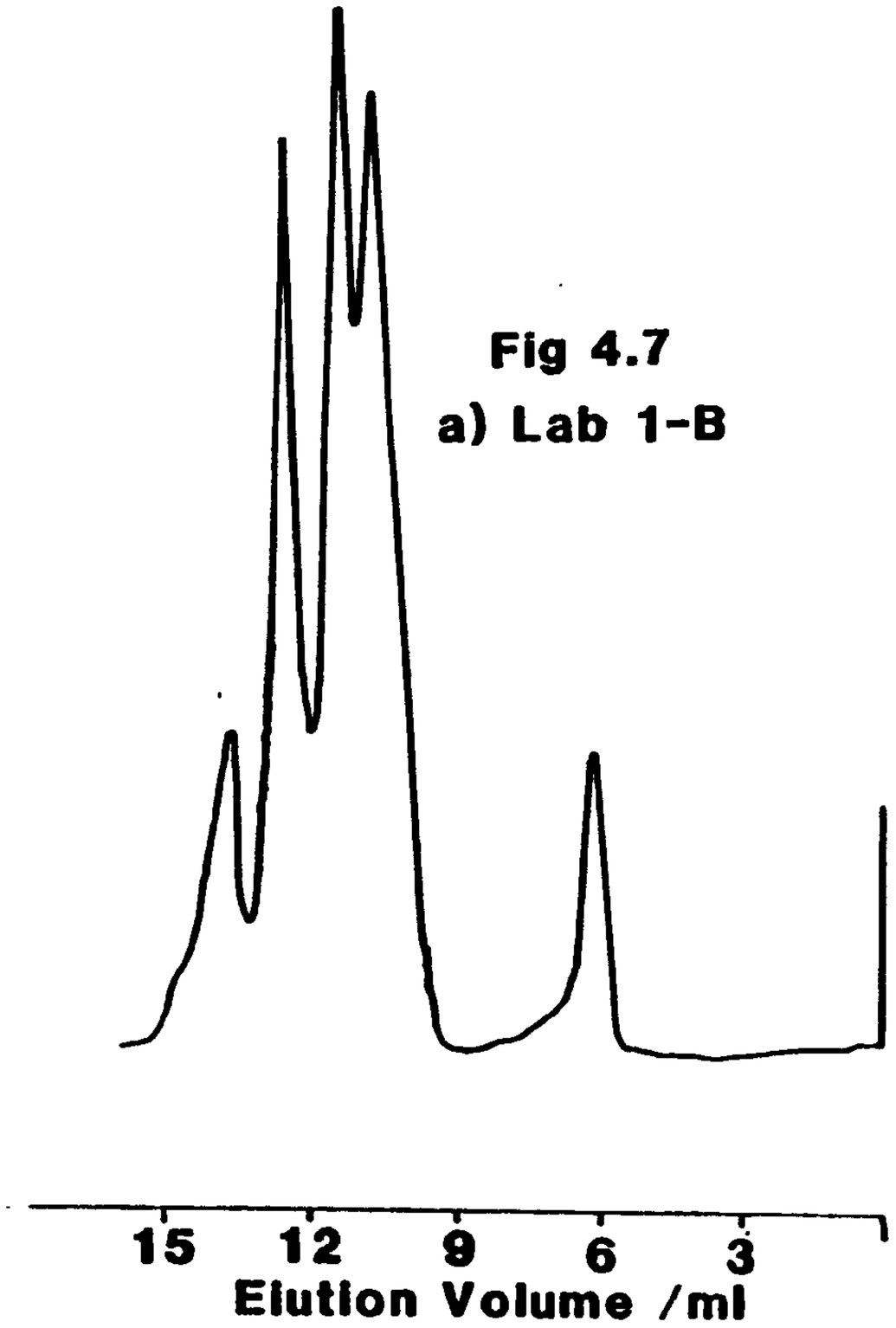

Fig 4.7
a) Lab 1-B

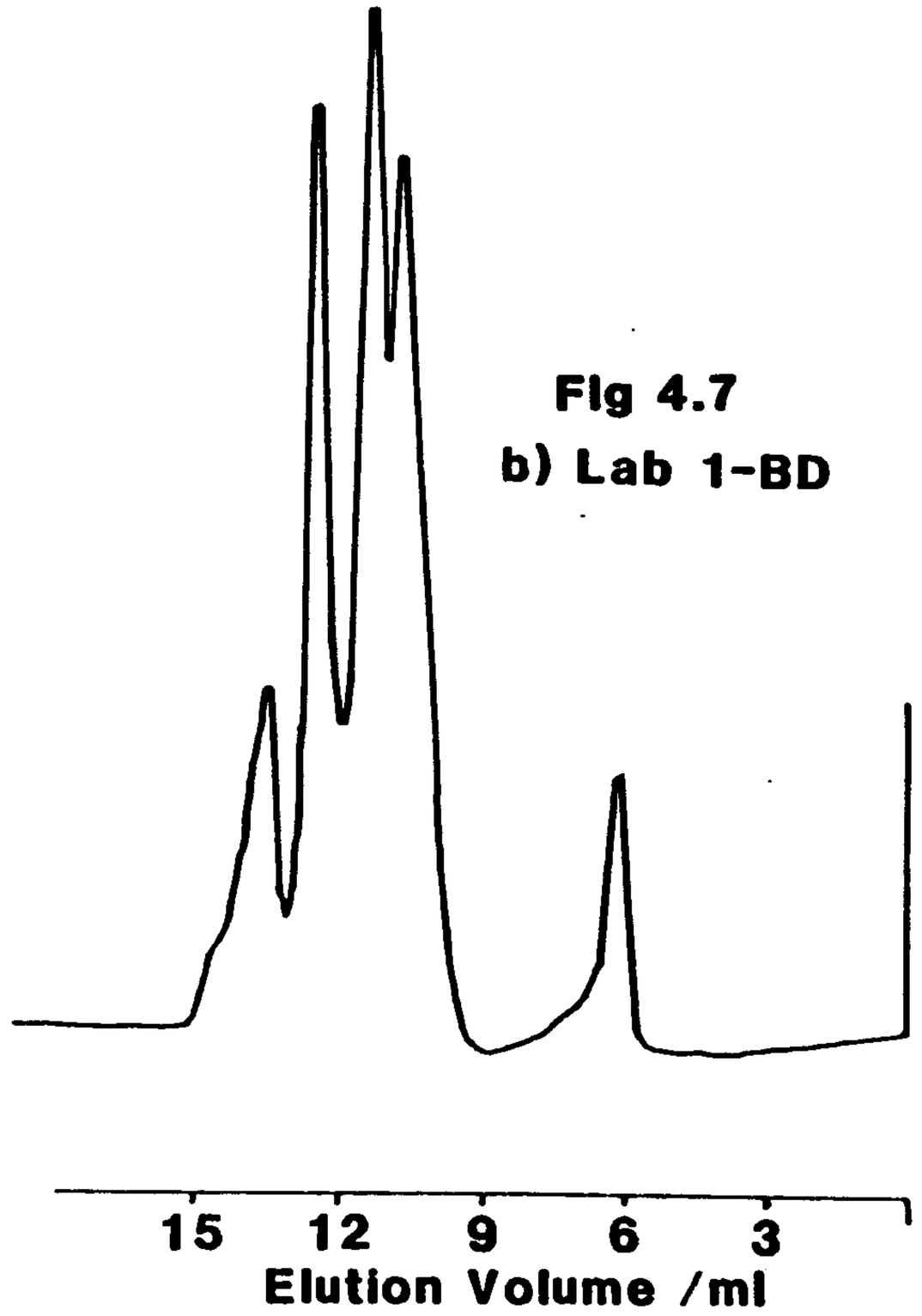

Fig 4.7
b) Lab 1-BD

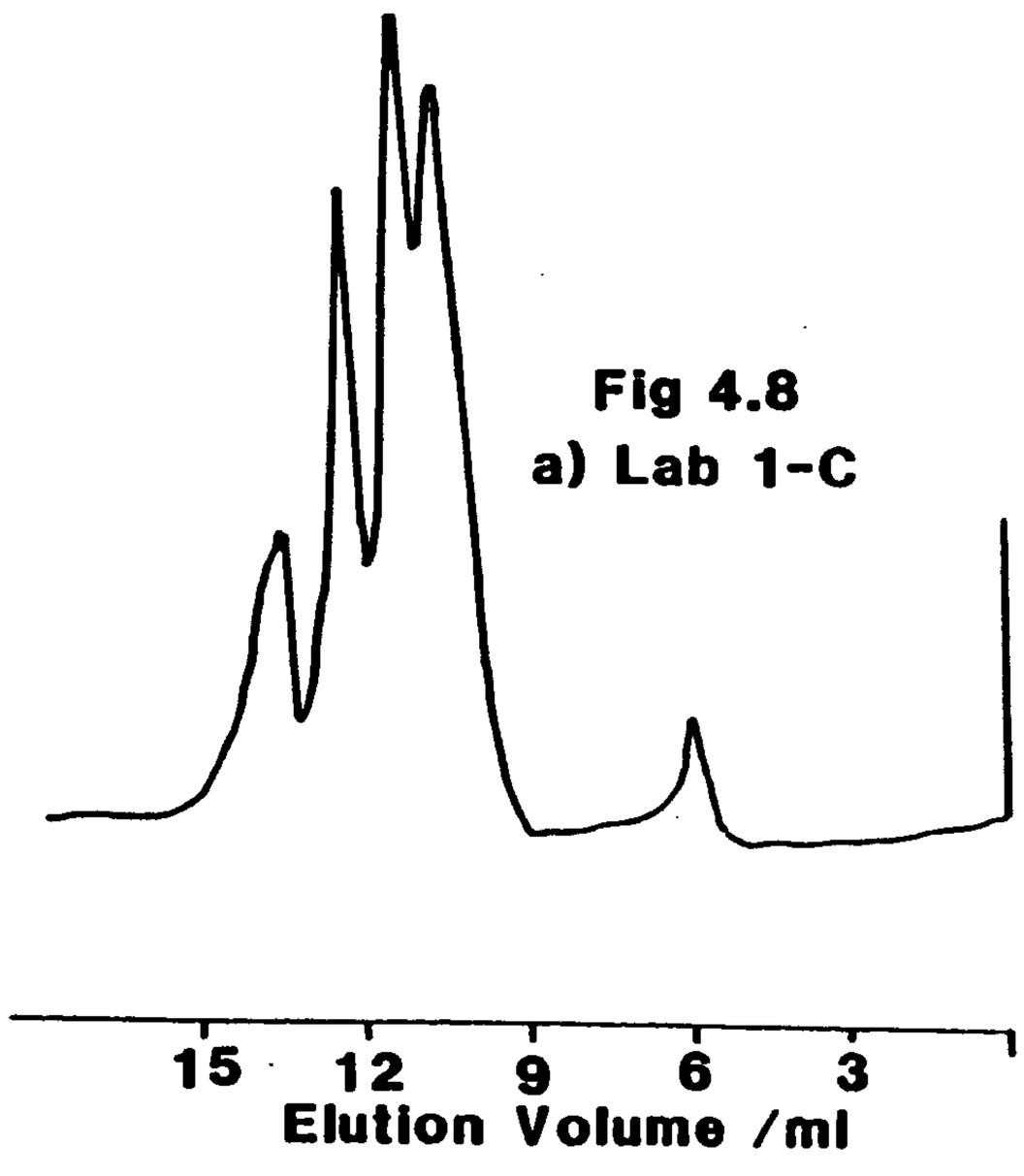

Fig 4.8
a) Lab 1-C

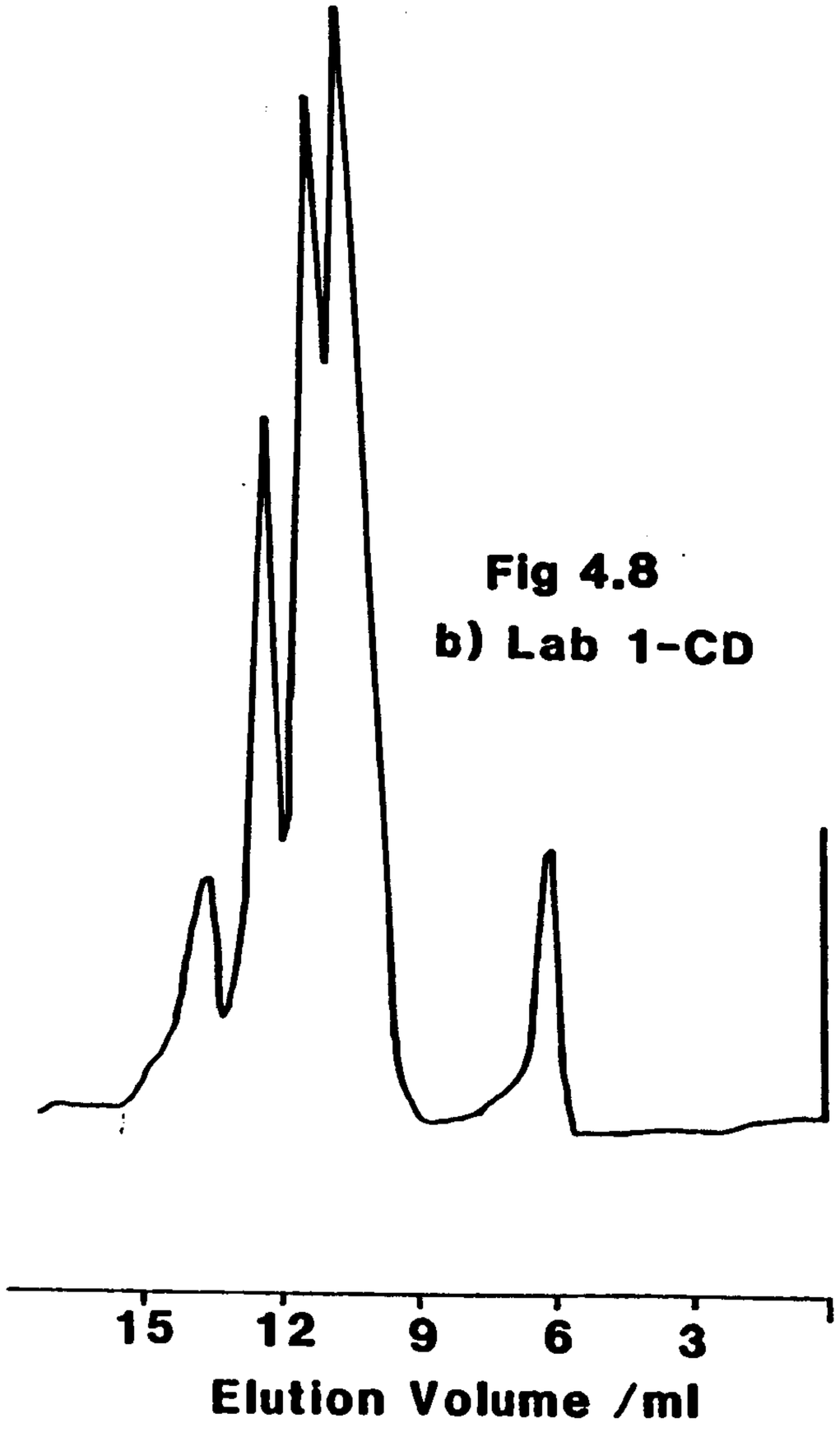

Fig 4.8
b) Lab 1-CD

4.6 *THE MOLECULAR WEIGHT PROFILE OF ORGANNOCOPPER SPECIES IN SOIL SOLUTIONS*

4.6.1 *Apparatus*

The HPLC apparatus was as mentioned previously. The copper in the eluent was detected by Graphite Furnace Atomic Absorption Spectrometry (GFAAS) using the following instrumentation: Pye Unicam SP9 Atomic Absorption Spectrometer fitted with PU 9090 data graphics system; PU Video Furnace Programmer and an SP9 Furnace Power supply. The furnace conditions employed were as follows and were identical to the conditions used by Brown *et al*. [14].

Wavelength 324.8 nm

Temperature/°C	75	100	350	700	1800	2630
Time/S	20	25	25	25	5	5

4.6.2 *Experimental*

Duplicate soil solutions from each sampling site were run under the same HPLC conditions used in the previous section. A fraction collector was used in order to collect 0.25 ml fraction of the eluent. These samples of eluent were transferred on to the GFAAS autosampler and 5 μl aliquots were run using the conditions mentioned in the previous section. The Cu results obtained for each soil solution were superimposed on the chromatograms and the absorbances corresponding to each peak were integrated manually. The total copper concentration of each site was determined by ICP-OES.

4.6.3 *Results and Discussion*

The chromatogram obtained for sampling site Lab 1-A is shown in Fig. 4.9. The Cu absorbances were integrated and then split into two categories

Fig 4.9 GFAAS Cu results superimposed on the SEC chromatogram.

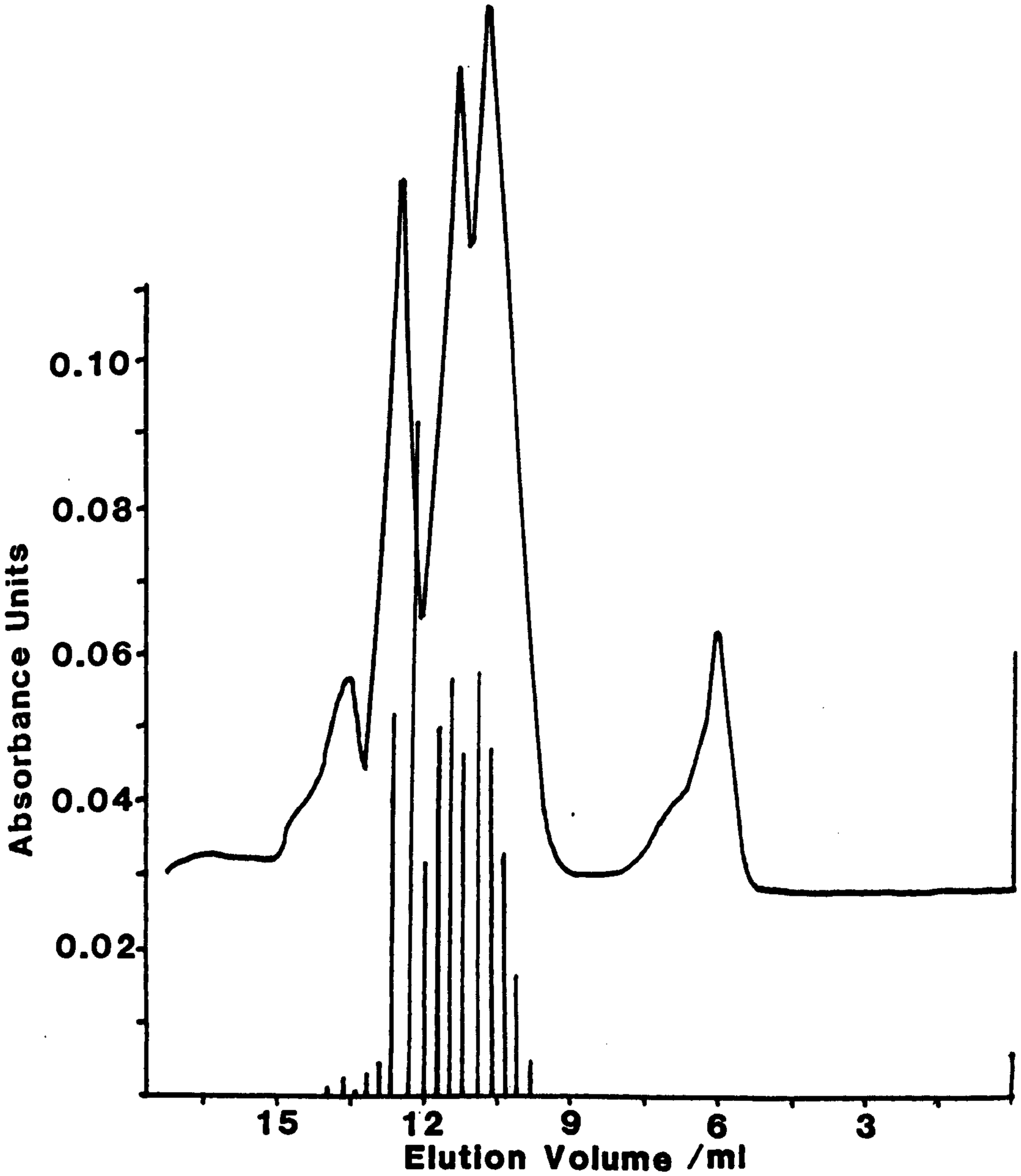

i.e. high molecular weight humic materials and low molecular weight organic ligands. These results were expressed in % of total Cu and ppm (for the ICP results) and are shown in Table 4.1.

TABLE 4.1

Soil Sampling Site	Humic Materials		Low molecular weight Ligands	
	% of total Cu	ppm	% of total Cu	ppm
Lab 1-A	67.0	(0.106)	33.0	(0.052)
Lab 1-B	63.2	(0.099)	26.8	(0.041)
Lab 1-C	83.0	(0.094)	16.6	(0.019)

It is apparent that in this soil the majority of the Cu is present as complexes with humic substances (63-83%) but a significant amount is in the form of complexes with low molecular weight ligands e.g. citric, malic and lactic acids. From these results it is evident that samples taken from sites Lab 1-A and Lab 1-B were similar in the amounts of copper bound by humic materials. Sampling site 1-C however, showed a much greater proportion of the Cu bound to humic material. This site was different from the previous two in that the soil here had a higher moisture content. In fact, this part of the field tended to collect water and was often waterlogged. In contrast Sites 1-A and 1-B were on a much greater gradient and subsequently water tended to drain off quickly. From these results it seems evident that if soil water is allowed time to equilibrate with the soil solution, copper will be predominately in the form of Cu-humic and Cu-fulvic acid complexes.

REFERENCES

1. Vaughan, D. and Ord, B.G., J. Experimental Botany, 1981, **32**, 679-687.

2. Hine, P.T. and Bursil, D.B., 1984, Water Res., **18**, 1461-1465.

3. Swift, R.S. and Postner, A.M., 1971, J. Soil Sci., **22**, 237-249.

4. Sterrit, R.M. and Lester, J.N., Environmental Pollution (Series A), 1982, **27**, 37-44.

5. Baham, J., Ball, N.B. and Sposito, G., J. Environ. Qual., 1978, **7**, 181-188.

6. Lawson, P.S., Sterrit, R.M. and Lester, J.N., Water, Air and Soil Pollution, 1984, **21**, 387-402.

7. Gregson, S.K. and Alloway B.J., J. Soil Sci., 1984, **35**, 55-61.

8. Saito, Y. and Hayano, S., J. Chromatogr., 1979, **177**, 390-392.

9. Gardner, W.S., Landrum, P.F. and Yates, D.E., Anal. Chem., 1982, 54, 1198-1200.

10. Adamic, M.L. and Bartak, D.E., Anal. Chem., 1985, **57**, 279-283.

11. Miles, C.J. and Brezonik, P.L., J. Chromatogr., 1983, **259**, 499-503.

12. Skoog D.A., in "Principles of Instrumental Analysis" (third edition), Chapter 27 'High Performance Liquid Chromatography', 1985, Saunders College Publishing, Philadelphia.

13. Wehr, C.T. and Abbott, S.R., J. Chromatogr., 1979, **185**, 453-462.

14. Brown, L., Haswell, S.J., Rhead, M.M., O'Neill, P. and Bancroft, K.C.C., Analyst, 1983, **108**, 1511-1520.

APPENDIX 4.1

```
'
'
'
'
10 CLS
PRINT "PLEASE INPUT THE CONCS (Mol/dm3) OF Na2HPO4 AND NaH2PO4"
INPUT L1#,L2#
NA#=(2*L1#)+L2# :PRINT"[NA] =";NA#
PRINT"[HPO4]= ";L1#
PRINT"[H2PO4#]=";L2#
INPUT "IS THIS DATA CORRECT";A$
IF A$="N" OR A$=="n" THEN GOTO 10
'
'
'
I#=0.5*(NA#+(L1#*4)+L2#)
PRINT"IONIC STRENGTH = ";I#
A#=0.509 :B#=0.329
Y#=A#*SQR(I#) : Z#=B#*SQR(I#)
SHPO4#=(4*Y#)/(1+(4*Z#))
SH2PO4#=(Y#)/(1+(4.5*Z#))
H#=(Y#)/(1+(9*Z#))
FHPO4#=EXP10(-SHPO4#)
FH2PO4#=EXP10(-SH2PO4#)
FH#=EXP10(-H#)
'
'
AHPO4#=FHPO4#*L1#
AH2PO4#=FH2PO4#*L2#
AH#=(6.3E-008#AH2PO4#)/AHPO4#
CH#=AH#/FH#
PH#=-LOG10(CH#)
PRINT "pH = " USING "#.##";PH#
INPUT "ANOTHER RUN ?";B$
IF B$="Y" OR B$="y" THEN GOTO 10
END
```

CHAPTER FIVE

THE LONG TERM PARTITIONING OF Cu IN WATER EXTRACTS OF SEWAGE SLUDGE AND DISTILLERY WASTE TREATED SOILS

5.1 *INTRODUCTION*

One major area of interest to soil scientists is how the speciation of heavy metals in soil changes with time. This is of particular interest in the case of polluted soils where the question is,

> does the speciation of pollutant metals change in the years after sludge application and what are the resulting effects on plant availability?

The speciation technique developed in the last chapter would be particularly useful in this type of study as it would allow the transformation of Cu from bonding by plant available low molecular weight ligands into the more stable, non plant available high molecular weight ligands to be studied. This type of study would normally take place over a long time period of about 20 years and would be obviously outwith the timespan of a Ph.D. study. Fortunately soil samples were available in the Macaulay Land Use Research Institute which had been sampled over a number of years before and after sludge application at a field experiment situated at Luddington near Stratford upon Avon. Samples were also available from sites in the North-east of Scotland at Pitglassie and Minmore which have a 70 year history of distillery waste application. These soils had already been well characterized and a great deal of data was available in the Institute. It was felt that the SEC/GFAAS method developed in Chapter 4 would yield more useful information especially about Cu speciation in this long term study.

5.2 *SAMPLING AND EXTRACTION OF SOILS*

The Luddington experiment was located on soil devised chiefly from coarse-sandy river-terrace drift deposits of Triassic material and drainage was slightly imperfect [1]. Three plots were selected for study:

I - Control Plot

II - High Cu Plot

III - Low Cu plot

No sludge was applied to plot I which served purely as a control. To plot II sludge was applied in one application of 125 tonnes dry matter/hectare with a Cu content of 4,700 mg/kg Cu (dry mass). This application took place in 1968 and in the same year sludge was applied to plot III at the same rate but with a Cu content of about half that of the high Cu plot (I).

The treated plots were sampled to a depth of 0-25 cm in 1968, 1972. 1976, 1981 and 1985 using a soil auger, some 25 cores being taken and bulked from each plot. These samples were air dried and then passed through a 2 mm sieve. 5g samples were obtained (in duplicate) by coning and quartering and to each 5 g sample 50 ml of distilled water was added. The samples were placed in an end-over-end shaker overnight in order to extract the Cu species. The resulting water extracts were filtered through Whatman 542 filters to remove all the particulate matter.

5.3 *THE ANALYSIS OF LUDDINGTON WATER EXTRACTS FOR CU BY AAS*

5.3.1 *Experimental*

The water extracts were analysed by Flame AAS using the instrumentation and conditions employed in Section 3.3.1.

5.3.2 *Results and Discussion*

The results obtained for the 3 test sites are shown in Table 5.1 below.

Table 5.1 AAS Cu analysis of Luddington plot soils

Sampling site/year	Copper conc/ppm (Results for duplicate extractions shown in parenthesis)
Block Soils	
1968 (before sludge application)	0.026 (0.026)
High Cu Plot	
1972	0.440 (0.520)
1976	0.404 (0.395)
1981	0.470 (0.470)
1985	0.440 (0.447)
Low Cu Plot	
1972	0.223 (0.247)
1976	0.229 (0.229)
1981	0.241 (0.271)
1985	0.205 (0.223)
Control (ppb)	
1972	19.9 (20.1)
1976	13.9 (15.8)
1981	13.9 (14.2)
1985	19.9 (18.6)

Over the 17 year experiment none of the three plots showed any real change in the Cu contents of the water extracts. One interesting fact was that the low Cu plot had half the concentration of Cu compared with the high Cu plot. This is in complete agreement with the amounts of Cu contained in the sludge applied to three sites.

5.4 *THE SEC/GFAAS ANALYSIS OF LUDDINGTON WATER EXTRACTS*

It was decided to continue to use an eluent with an ionic strength of 0.0058 Mol dm^{-3} as the question of sample equilibria did not arise in this case. The fact that the soils had been air dried and then

water extracted meant that the equilibria in the soil had already been disturbed, although air-drying of topsoils takes place naturally during hot, dry weather in summer. A water extract tends to contain higher Cu levels than would be found in the soil solution of the same sample in the field. This is because the addition of distilled water to any soil air-dried or moist results in a large concentration gradient between the sample and the distilled water. This tends to cause a flush of Cu species into the distilled water.

Although the sample equilibria had been disturbed it was felt that because all the samples had been treated in exactly the same manner that the results obtained would still provide an indication of how Cu speciation varies with residence time in polluted soils.

5.4.1 ***Experimental***

The HPLC conditions were exactly the same as those used in the previous chapter. The water extracts were filtered through a Gelman LC3A filter before analysis. 0.3 ml fractions of the eluent were collected and analysed using the furnace program listed in Section 4.6.1.

5.4.2 ***Results and Discussion***

The results obtained from the high Cu plot between 1968 and 1985 are shown in Figs. 5.1-5.5. The Cu peaks were integrated manually and split into two fractions. The high molecular weight fraction corresponds to the Cu-humic and Cu-fulvic acid species and the low molecular weight fraction consists of low molecular weight organo-copper species e.g. citric or malic acid Cu complexes. The results were tabulated and are shown in Table 5.2 below.

Fig 5.1 Block 1968 soils

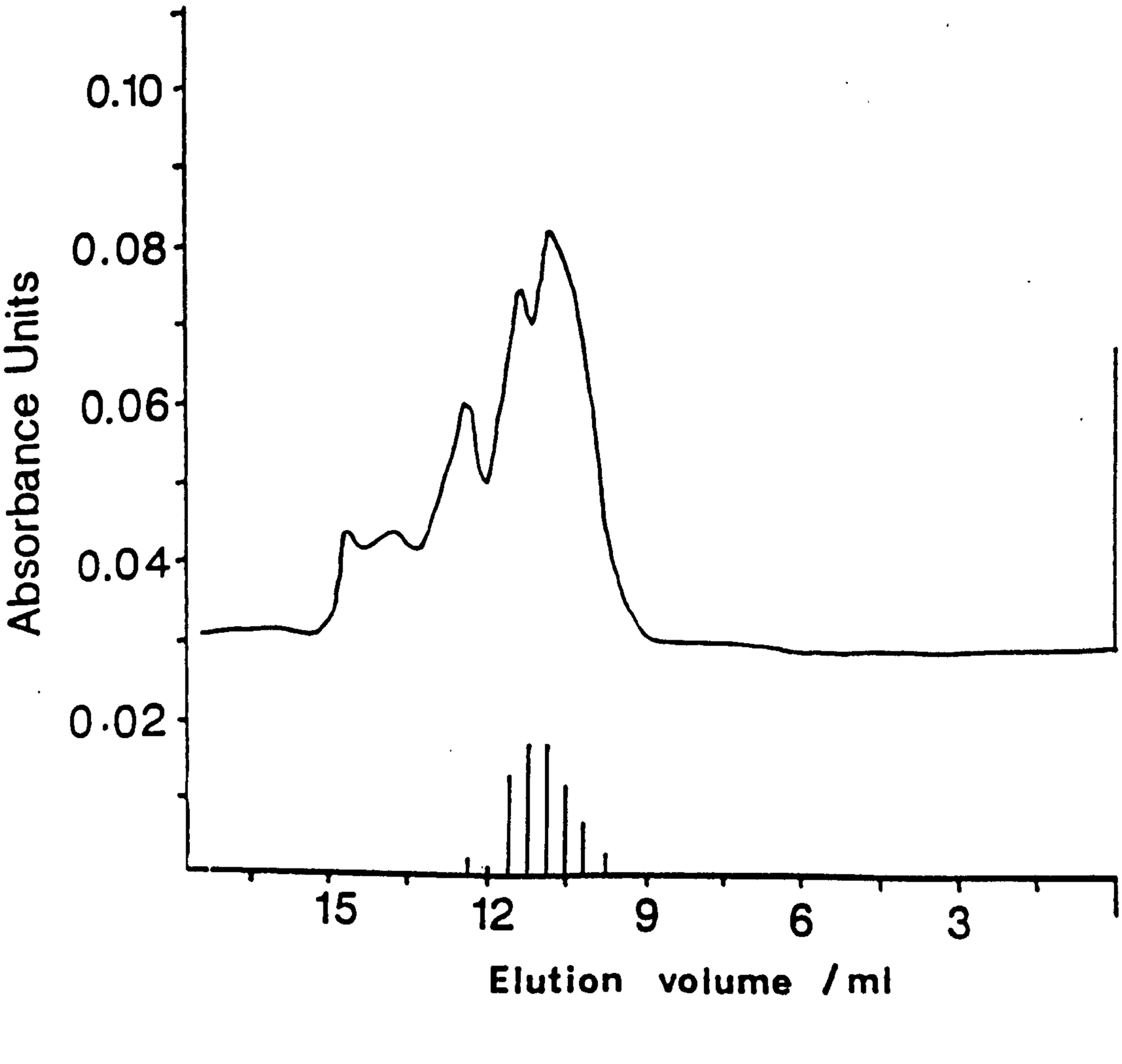

Fig 5.2 High Cu 1972

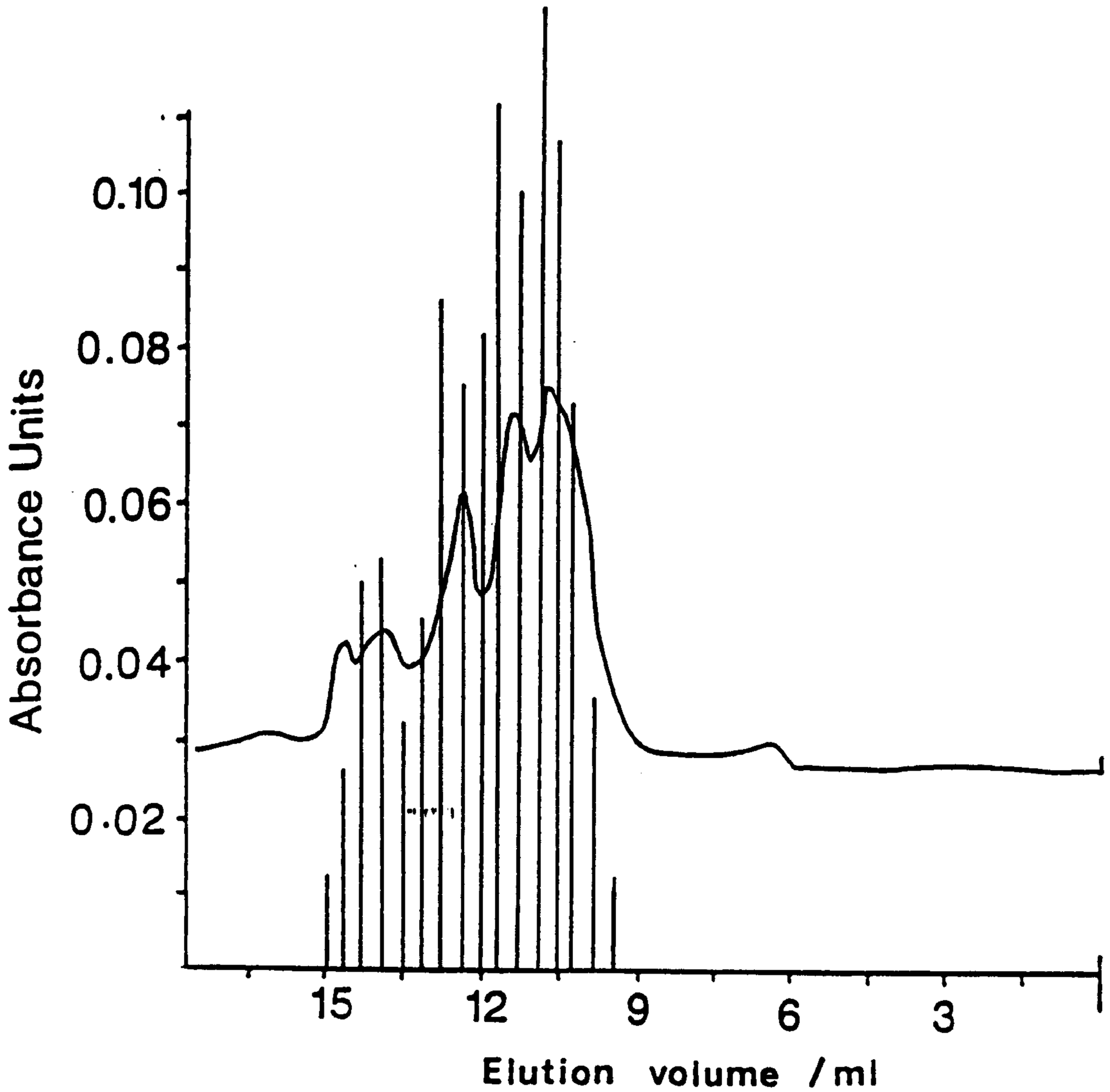

Fig 5.3

High Cu 1976

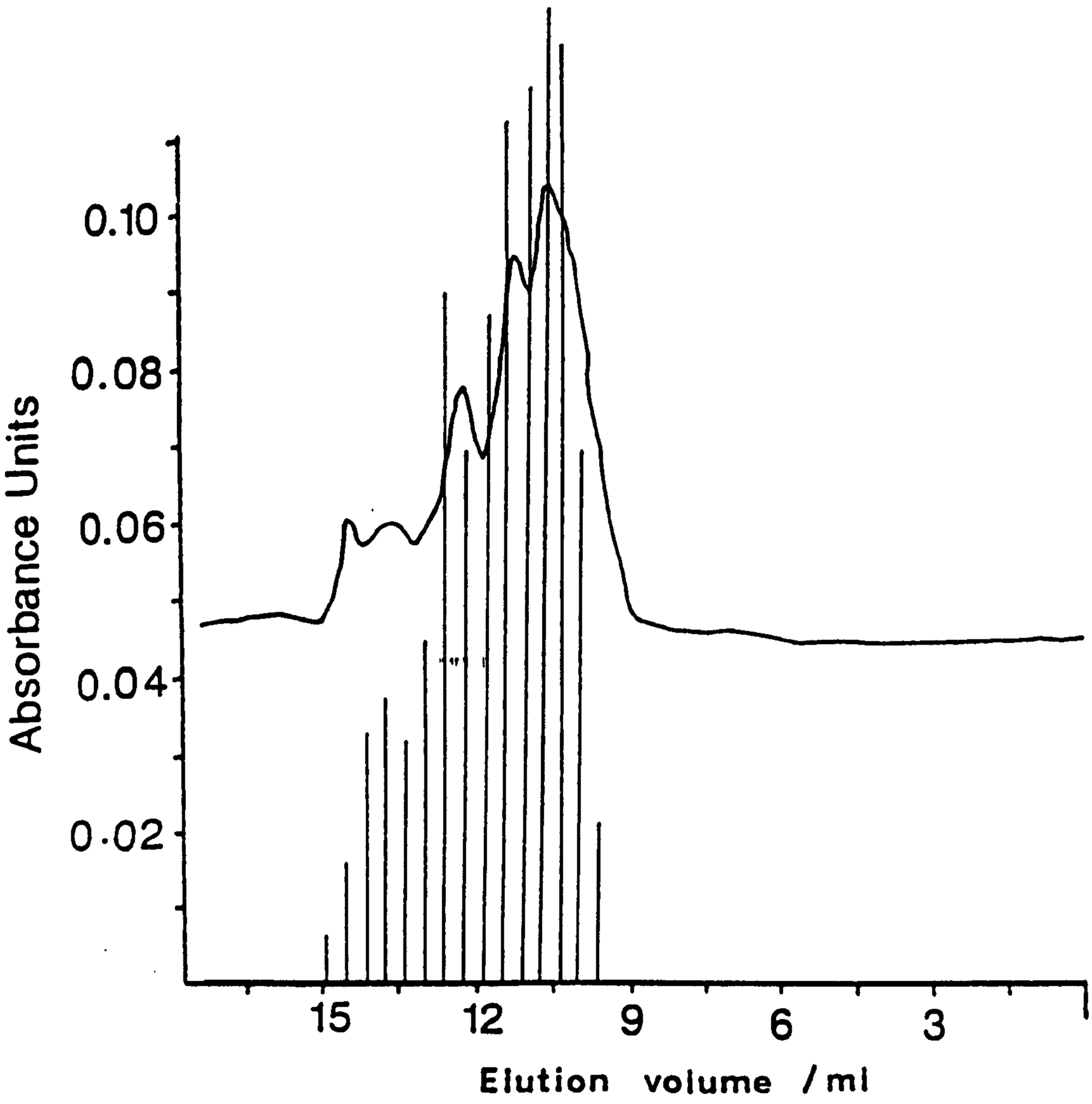

Fig 5.4

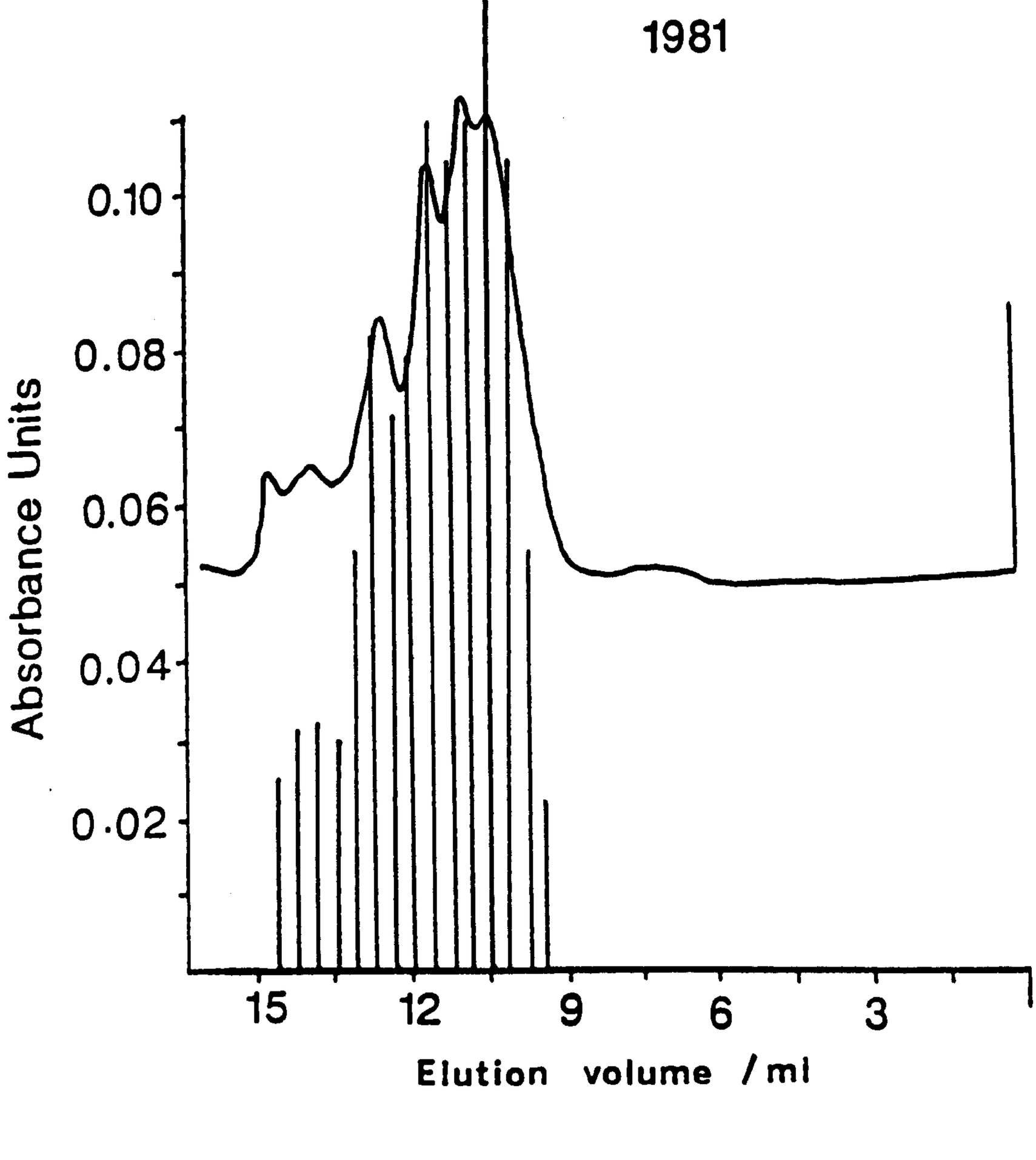
High Cu
1981
0.10
0.08
0.06
0.04
0.02
Absorbance Units
15
12
9
6
3
Elution volume / ml

Fig 5.5

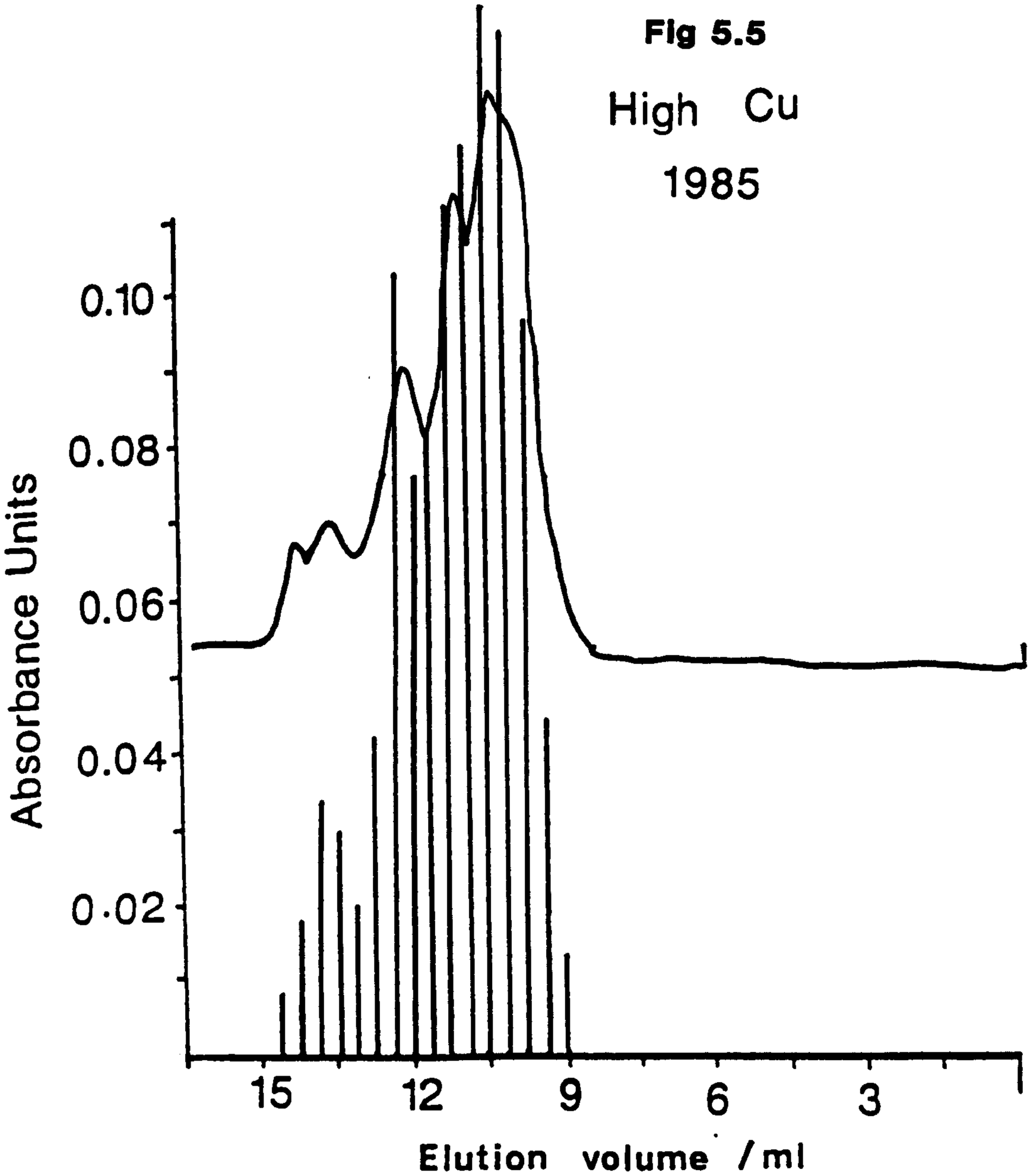
High Cu
1985
Absorbance Units
0.10
0.08
0.06
0.04
0.02
15
12
9
6
3
Elution volume /ml

Table 5.2 Cu speciation results from the high Cu plot at Luddington between 1968 and 1985

Year	High mwt		Low mwt	
	% of total	ppm	% of total	ppm
1968	96	0.025	4	0.001
1968D	95	0.025	5	0.001
1972	59	0.260	41	0.180
1972D	60	0.312	40	0.208
1976	62	0.256	38	0.147
1976D	65	0.257	35	0.138
1981	65	0.305	35	0.165
1981D	72	0.338	28	0.131
1985	65	0.286	35	0.154
1985D	65	0.291	35	0.156

It was noticeable that the duplicate extractions all gave very similar results typically within 2-5% of each other, that is except for 1981 and 1981D where there was a 7% difference. This was encouraging because in this type of analysis there is a great deal of scope for experimental error especially in the sampling and extraction stage; it was therefore surprising to find such a good degree of reproducibility between the duplicate samples.

Another area of difficulty arose in the processing of the results in that there was often difficulty in assigning the Cu results to the high or low molecular weight fractions. It was decided that whenever a Cu peak lay on the boundary of the two fractions that its height was divided by 2 and half assigned to each of the molecular weight categories. This was a major problem with this method because the fraction collector was programmed to collect 0.3 ml fractions. This meant that a sharp Cu chromatographic peak could be easily missed. A better method of analysis was devised and will be described later in

this chapter.

The results indicate an interesting trend in that in 1972, 4 years after sludge application around 40% of the Cu is in a form that is potentially available to plants i.e. the low molecular weight fraction. Between 1972 and 1981 the amount of Cu present in the low molecular weight fraction decreases to 35%. This may be due to genuine movement of Cu from less stable molecular weight complexes into the more thermodynamically stable humic or fulvic acid complexes. Alternatively, it may be the case that the low molecular weight complexes are more available to plants and that the removal of Cu from this low molecular weight fraction could be as a result of plant uptake. There is substantial evidence for the uptake of Cu by plants on this site. Berrow and Burridge [1] reported that the Cu contents of timothy grass grown on the high Cu treatment plot at Luddington was 11 mg/kg dry mass compared with 7 mg/kg on the control plot. This showed a clear increase in the amounts of plant available Cu eight years after application of sludge to the soil. This was not unexpected because the amount of Cu in the potentially available low molecular weight form had risen nearly 200 fold from 0.001 ppm to 0.182 ppm. This was interesting in that although there was a huge increase in plant available Cu it only resulted in a 2 fold increase in the Cu contents of timothy grass stems and leaves grown on the soil. On first inspection it may seem tempting to explain the decrease in the low molecular weight forms of Cu solely in terms of plant uptake but, unfortunately, it is well known that crops grown on polluted sites only have the ability to remove small amounts of Cu from the soil. Typically crop removal can only account for the removal of between 20-100 g/ha of B, Cu or Zn (ADAS, 1984) [2]. Assuming crop removal of 50 g/ha, this represents about 0.5%

of the water soluble Cu content of 4.5 ppm in this soil. It is therefore unlikely that plant uptake could account for a 4-5% difference in the amount of Cu present in low molecular weight forms. Looking back at Table 5.1 it was mentioned that there was little change in the total amount of Cu present in the water extract and if significant plant uptake had occurred one would have expected to see an overall decrease in the total Cu concentration of the water extracts with time, which did not occur.

It seems more likely that the 5% shift in Cu from the low molecular weight species to the high molecular weight species was due to an actual physical transfer of Cu between the two forms. This is backed up by the findings of Berrow and Burridge [3] who concluded that at the Luddington site it was the soil characteristics which controlled the final speciation of Cu, Ni, Zn and Cr. The Zn and Cu rich sludges showed a very marked increase in EDTA extractability over the first four years, followed by a decrease during the second four years, with little change in the acetic acid extractability. These results are remarkably similar to those obtained in this study in that the amount of Cu in the low molecular weight form increased rapidly in the first 4 years and then decreased rapidly over the next 4 years. Berrow and Burridge concluded that the changes in EDTA extrability [3] could be explained as a movement from less readily soluble material in the sludge (oxide or carbonate) to an initially more readily exchangeable form e.g. Cu-citrate to a more finely bound form e.g. Cu-fulvate or Cu-humate. This is exactly what was observed in this study. The reactions of Cu in this high Cu plot can be summarised as follows:

When the sludge is applied the breakdown of the sludge organic matter releases the copper in a readily soluble form. Some of this

copper immediately forms stable complexes with the soil humic materials, the remainder forms complexes with low molecular weight ligands e.g. citric acid. As time moves on there is a transfer of copper from these thermodynamically less stable low molecular weight complexes into the more thermodynamically stable Cu-fulvate and Cu-humate complexes. This change in speciation appears to stabilize after around 10 years probably as a result of saturation of the Cu complexing sites of humic and fulvic acids but a significant proportion of the Cu remains the low molecular weight form. This is a form which is potentially available to plants and not surprisingly herbage grown on this plot shows an increase in Cu content. The low uptake into the leaves of these plants means that a long period of time will pass before the copper is removed from these low molecular weight forms and the plant Cu contents decreases.

On the low Cu plot quite a different picture emerges. The results obtained are shown below in Table 5.3.

Table 5.3 Speciation results for the low Cu plot at Luddington sampled between 1968 and 1985

	High mwt		Low mwt	
Year	% of total	ppm	% of total	ppm
1968	96	0.025	4	0.001
1968D	95	0.025	5	0.001
1972	69	0.154	31	0.069
1972D	70	0.173	30	0.074
1976	69	0.158	31	0.071
1976D	67	0.153	33	0.076
1981	71	0.171	29	0.067
1981D	73	0.198	27	0.073
1985	70	0.143	30	0.062
1985D	69	0.154	31	0.069

These results seem to suggest that there is no change in the chemical speciation of Cu in the years after application at the low Cu plot. This was unexpected in the light of the previous results as one would have expected a movement from the low molecular weight complexes to the more stable high molecular weight species. Results produced in a later section with a modified method of analysis showed that this was indeed the case. The reason that it was not observed in this case could have been due to two reasons:

1) The fraction collector was collecting 0.3 ml fractions which meant that a sharp peak of lower concentration would have been subject to a large addition factor.

2) The fact that only a 5 μl fraction of eluent was analysed may have resulted in a detection limit that was not sufficient to pick up the lower concentrations of low molecular weight Cu species.

It was for both these reasons that the analytical method was modified and this is described in the next section.

5.5 *MODIFICATION OF THE ANALYTICAL METHOD TO IMPROVE RESOLUTION AND SENSITIVITY*

5.5.1 *Experimental*

It was felt that the previous procedure was both time consuming and lacking in sensitivity and it was hoped that this could be overcome by two modifications. Firstly, the method in its original form was a two stage process. The first stage was the HPLC analysis to determine the molecular weight profile of the soil solution organic matter, followed by fraction collection of the eluent.

The second stage involved transferring all the sample cups from the fraction collector into the furnace autosampler. These fractions were then analysed for Cu by GFAAS. It was hoped that the development of a continuous "on-line" interface between HPLC and GFAAS would provide a more rapid and automated method of analysis. It was decided to use the method proposed by Brinkman [4] whereby the HPLC eluent emerging from the detector was channelled through a flow-through cell and this was then analysed continuously by the furnace autosampler. A cell was designed for this purpose and is shown in Fig. 5.6. The cell was constructed from teflon and was made to fit the furnace autosampler turntable. It was decided to leave the teflon cup in position 1 of the autosampler and program the furnace to take something like 50 replicates. There were two problems with this. Firstly, the software of the PU 9095 Video furnace programmer only allowed 9 replicates to be taken. Secondly, the program insists on carrying out a wash of the pipette tip of the autosampler between replicates. This involved a movement of the autosampler turntable which was impossible when the teflon cup was in place. This meant the instrument just displayed an error message on the VDU. At first it was though that this may be overcome by modification of the instrument software but it was almost impossible to access. The problem was overcome by designing a new autosampler turntable. Figure 5.7 shows the original turntable alongside the newly designed version. The new design allowed the continuous analysis of the eluent without the need to change the instrument software. The teflon cup was placed directly under the sampling pipette of the furnace autosampler. The video furnace was then programmed to take 9 replicates of each sample. The absence of the sample cup receptacles on the autosampler turntable meant that the

Fig 5.6 Teflon flow cell

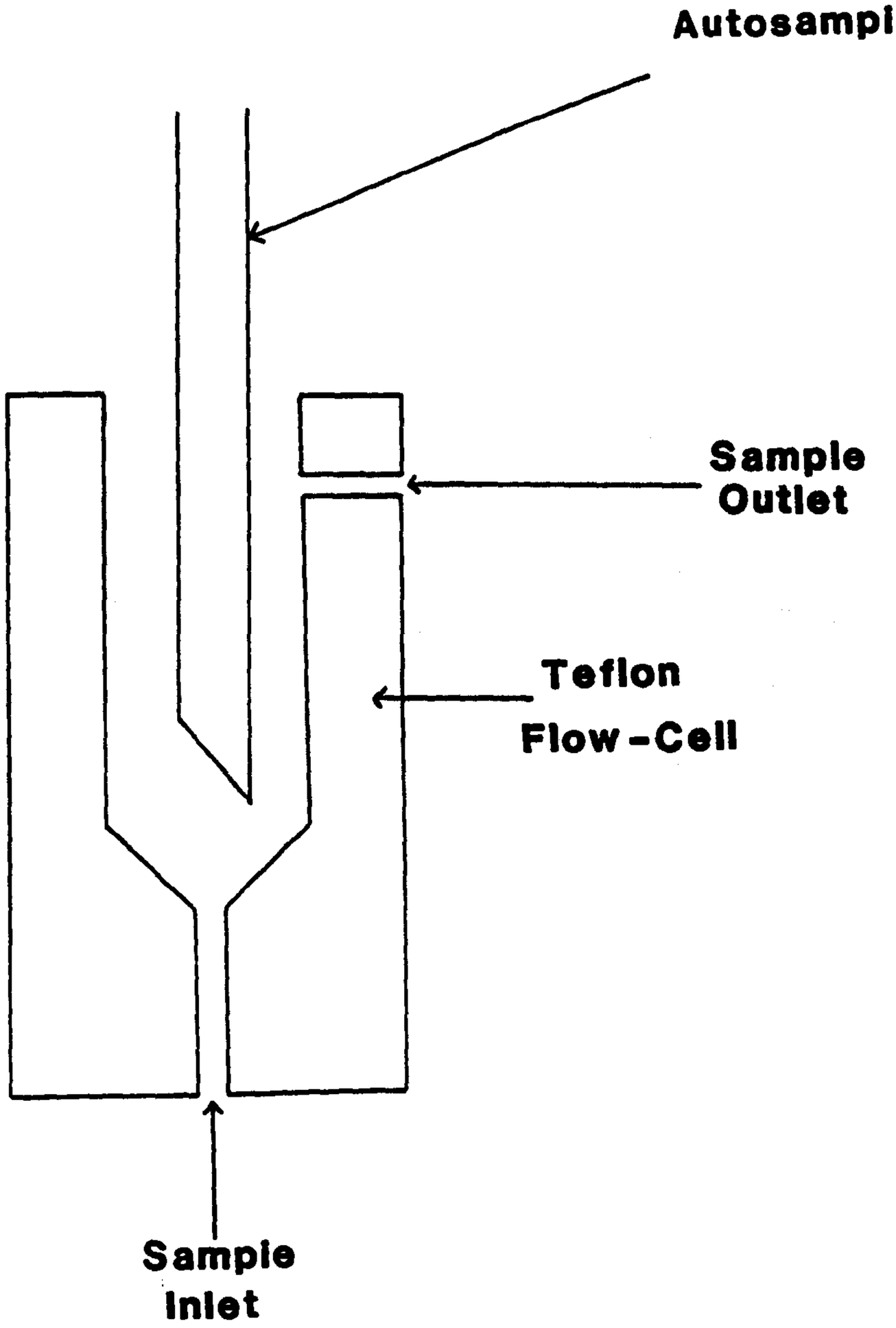

Fig 5.7 The two autosampler turntables used in this study.

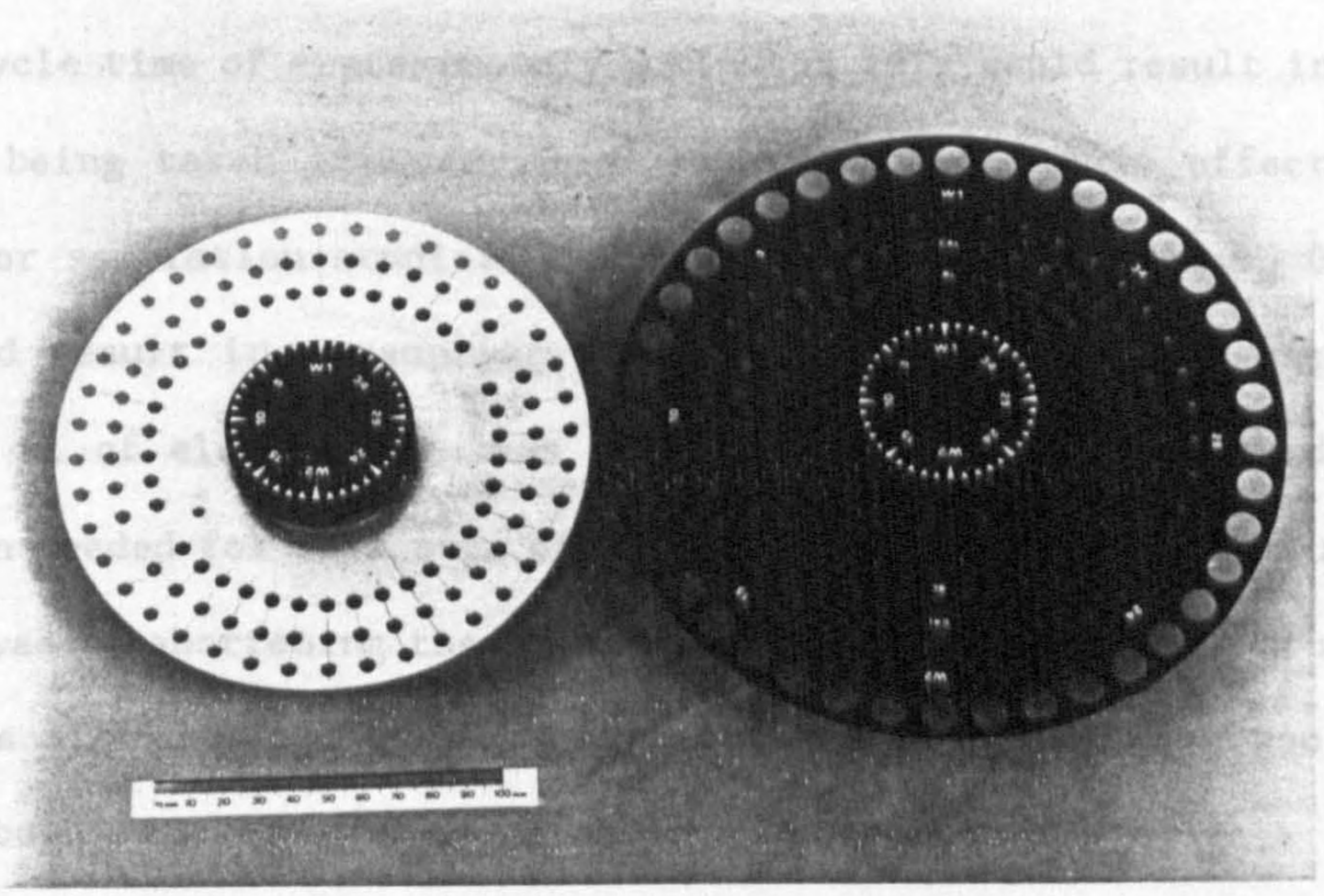

autosampler was able to wash the pipette tip between samples and also to move to different sample positions without moving the teflon sampling cup. This modification effectively "fooled" the autosampler into believing that it was taking 9 replicate samples from each consecutive sample position, when in fact it was only sampling the teflon flow through cell.

The next problem was due to the flow rate of the HPLC. In the previous section the flow rate used was 0.75 ml min^{-1}, but with a furnace cycle time of approximately 4 minutes this would result in only 1 sample being taken in every 3 ml of eluent which was effectively useless for speciation studies. Dropping the HPLC flow rate to 0.1 ml min^{-1} would result in a sampling of the eluent taking place once for every 0.4 ml of eluent. This was still not sufficient to provide the resolution needed for this type of analysis. The only way this could be overcome was by shortening the furnace cycle time. The modified furnace program is shown below. It was felt that the sample matrix would be simple enough to allow the use of a much shorter ashing stage.

Temperature/°C	225	800	1300	2600	2800
Time/s	15	10	15	5	5

The furnace cycle automatically includes a 40 second cool down time which meant that the overall time of analysis could only be halved to 2 minutes. This resulted in a sampling of the eluent every 0.2 ml which was the best that could be achieved without drastically increasing analysis time. The detection limit was also improved by injection 10 µl into the graphite furnace instead of 5 µl. Brown and Haswell [5] in their work had injected 100 µl into the furnace, but because heavily polluted soils were used in this study 10 µl was enough to provide a

suitable detection limit. The major problem with this modified method of analysis was that the actual analysis time was usually in the order of 3 hours and this would not be acceptable for a routine method of analysis. The time of analysis was drastically reduced by using two different flow rates. From Figs. 5.1-5.5 it can be seen that no Cu species elute between 0-8 ml, so it was decided to use a flow rate of 0.75 ml min^{-1} through this part of the chromatogram. The flow rate was then dropped to 0.1 ml min^{-1} in order to obtain good resolution when the Cu species eluted. The background reading was obtained by averaging the results before the Cu species started to elute and then this was subtracted from all subsequent copper peaks. As mentioned previously the Cu peaks were superimposed on to the HPLC chromatogram in the form of a histogram. The two sets of soil samples were re-analysed using this improved method.

5.5.2 ***Results and Discussion***

The duplicate samples from the high Cu plot and low Cu plot were rerun and the results obtained are shown in Table 5.4. The Chromatograms obtained from the high Cu plot with superimposed Cu results are shown in Figs. 5.8-5.12.

Compared with the last method these results indicate a larger proportion of high molecular weight material compared with the low molecular weight. The block soils 1968 have a higher % of lower molecular weight Cu than previously, this is because the newer method has the ability to detect Cu that was below the detection limit of the previous analytical method. The higher resolution of this modified method, i.e. the larger number of Cu fractions measured, made it much easier to align copper fractions with chromatographic peaks.

The results from the two plots, i.e. low Cu and high Cu, show a

Fig 5.8 Block soils 1968

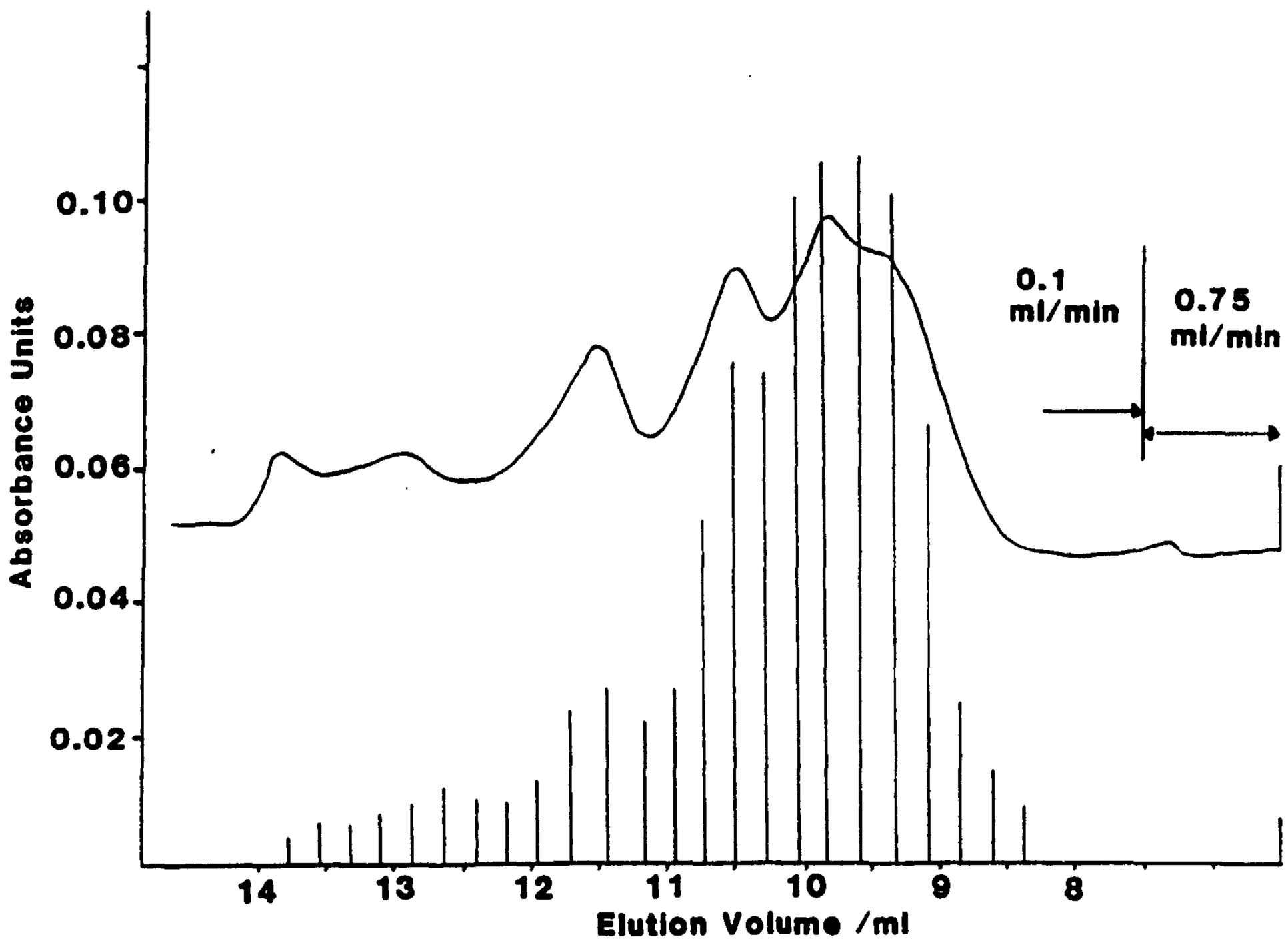

Fig 5.9 High Cu 1972

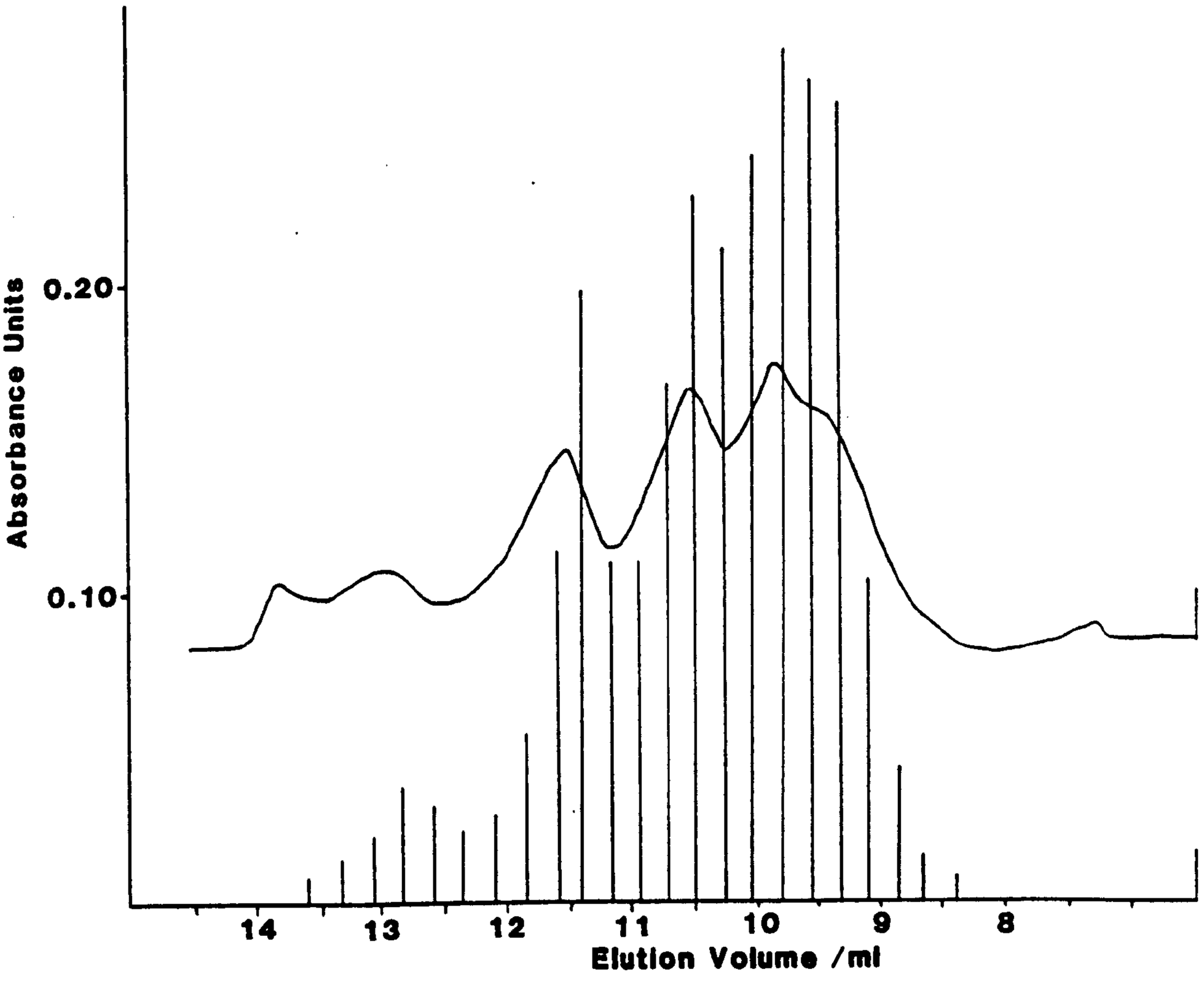

Fig 5.10 High Cu 1976

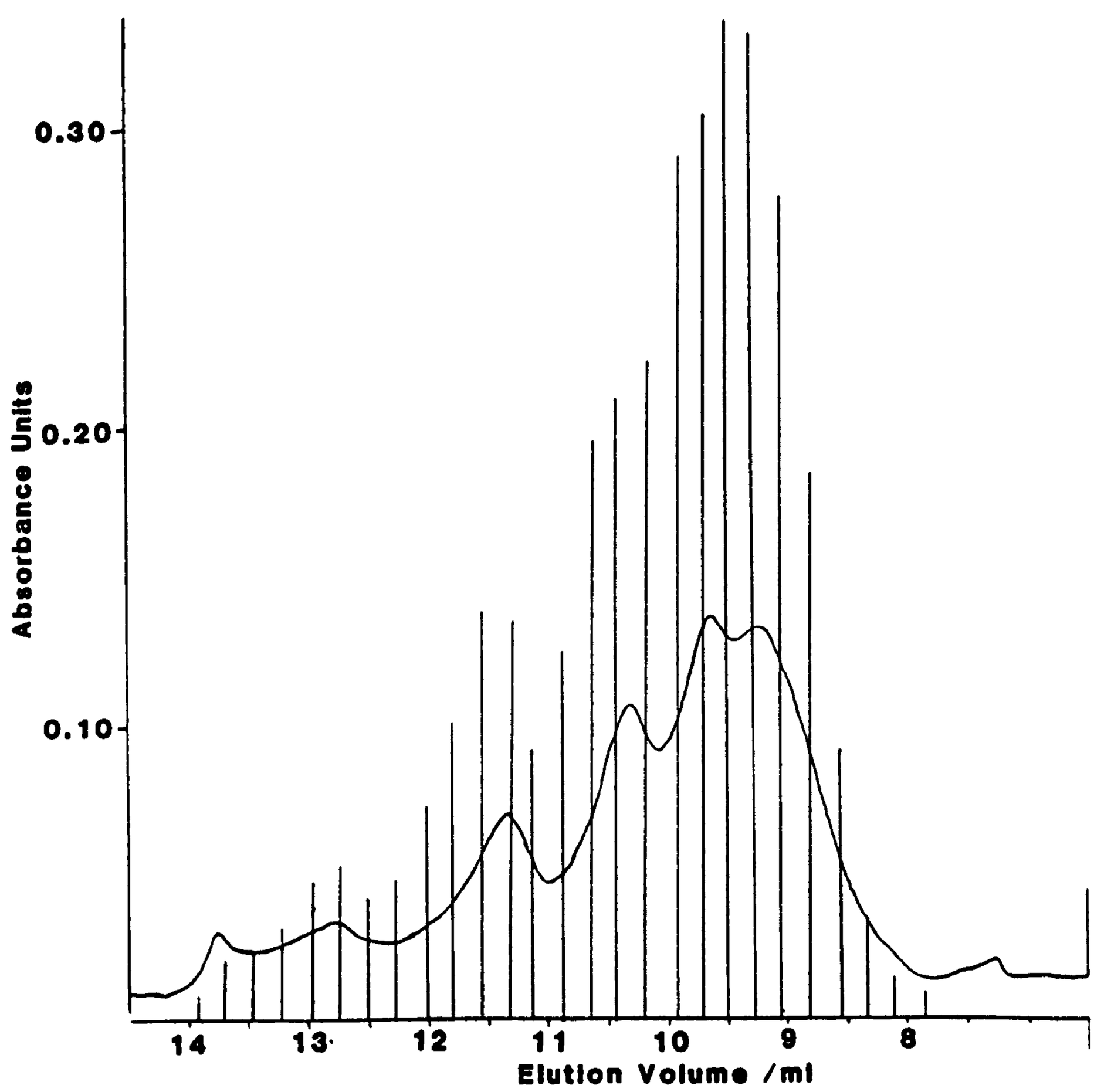

Fig 5.11 High Cu 1981

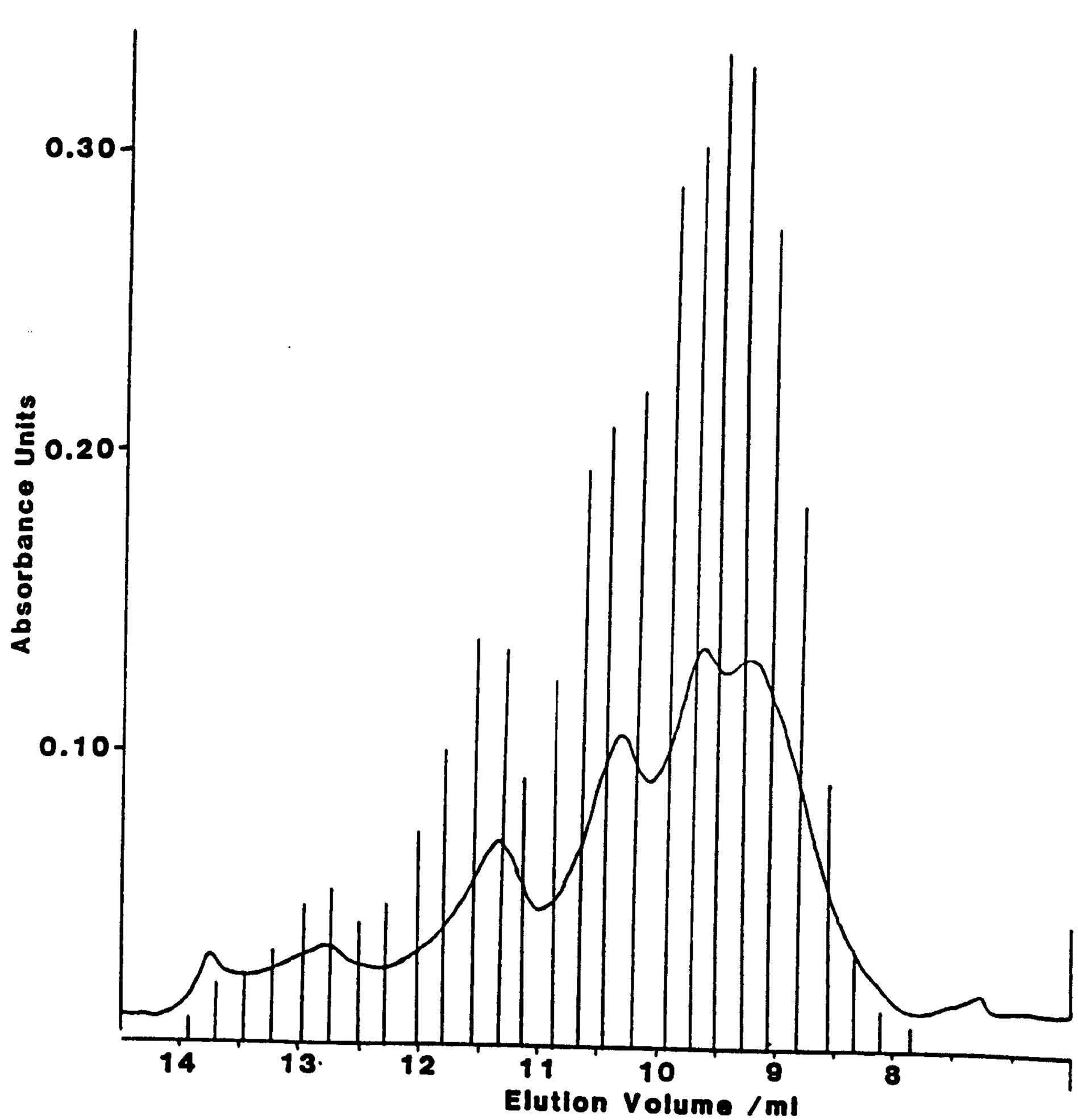

Fig 5.12 High Cu 1985

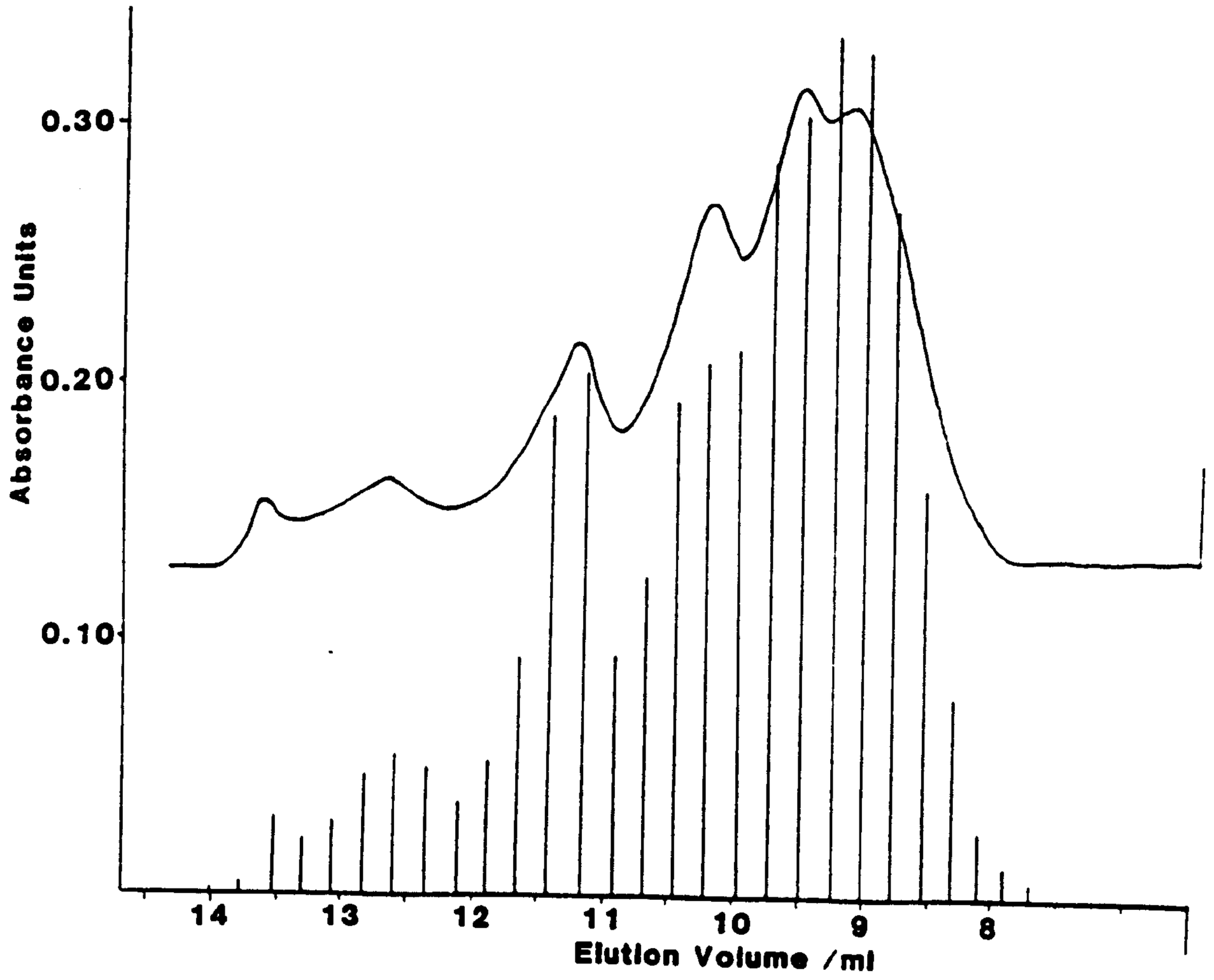

Table 5.4 Improved Cu speciation analysis of high and low Cu plots at Luddington between 1968 and 1985

Sample/year	High mwt		Low mwt	
	%	ppm	%	ppm
Block Soils				
1968	84.5	0.021	15.5	0.004
1968D	88.9	0.022	11.1	0.003
High Cu Plot				
1972	76.8	0.337	23.2	0.102
1972D	73.1	0.380	26.9	0.139
1976	82.0	0.331	18.0	0.072
1976D	81.1	0.320	18.9	0.075
1981	78.0	0.367	22.0	0.103
1981D	77.0	0.362	23.0	0.108
1985	76.0	0.334	24.0	0.106
1985D	81.7	0.365	18.3	0.082
Low Cu Plot				
1972	77.4	0.173	22.6	0.050
1972D	73.7	0.182	26.3	0.065
1976	77.7	0.178	22.3	0.051
1976D	78.0	0.179	22.0	0.041
1981	81.7	0.197	18.3	0.044
1981D	88.4	0.240	11.6	0.031
1985	81.8	0.167	18.2	0.037
1985D	84.1	0.187	15.9	0.035

great deal of similarity. In the unpolluted situation by far the majority of the copper is in a high molecular weight form. After sludge is added this value decreases and a significant amount of Cu appears in the low molecular weight form. In the case of the high Cu plot the results are very similar to those produced in the previous

section, graph 5.1, in that in the years after sludge is applied there is a 6% shift of Cu from the low molecular weight species present in the sludge to the high molecular weight humic materials prevalent in the soil. With this modified method a similar trend was observed in the low Cu plot. This is not what was observed with the previous method and it seems that the previous method was not sufficiently sensitive to detect such changes on the low Cu plot.

There is an important point to notice in the results from the two rates of Cu treatment in that there is almost twice as much transfer of Cu from the low molecular weight species to the high molecular weight species in the low Cu soil, Graphs 5.1 and 5.2. There are two possible reasons for this difference. In the low Cu plot the proportion of high molecular weight organic matter to copper is much larger and therefore there is much more chance of the low molecular weight copper complexes encountering a free complexation site on soil humic and fulvic acid molecules. The thermodynamic stability of such complexes mean that it is likely that the Cu will transfer from the low molecular weight species to the thermodynamically more stable high molecular weight species. In the high Cu soil the chances of an encounter between a low molecular weight Cu-species and a vacant complexation site on the humic materials is much decreased. This is because in the more polluted soil the majority of such complexation sites will already be occupied.

The second reason for the more rapid transfer of Cu from low molecular weight to high molecular weight species in the low Cu soil is that of microbial activity. The degradation of the sludge organic material is mainly carried out by microbiological processes e.g. bacteria etc. will use the organic matter present in the sludge as a food source. Table 5.5 below shows the changes in the % organic matter

Graph 5.1 Changes with time in the % of water soluble copper bound by a) high molecular weight and b) low molecular weight species in the high copper treatment soils.

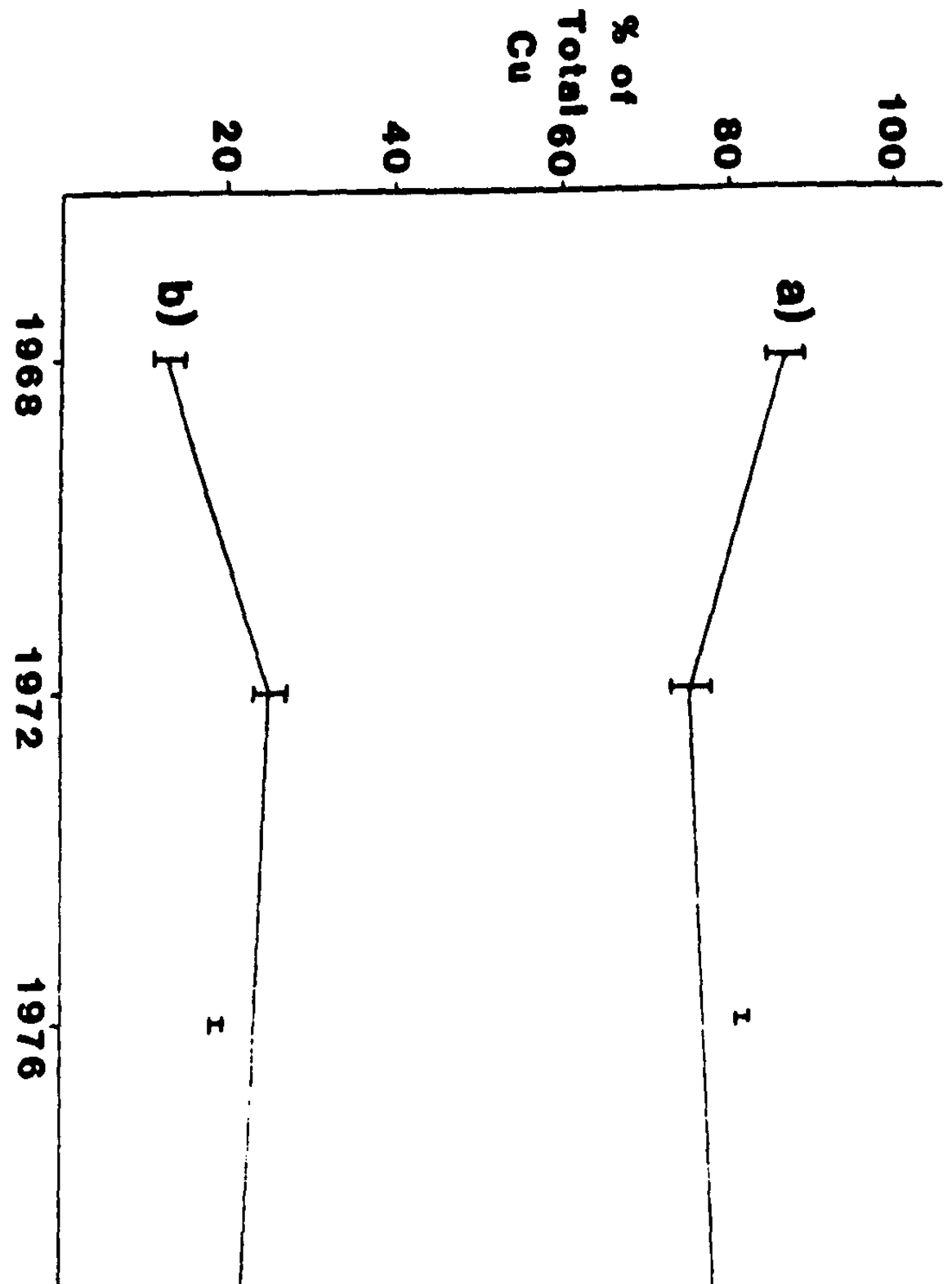

Graph 5.2 Changes with time in the % of water soluble copper bound by a) high molecular weight and b) low molecular weight species in the low copper treatment soils.

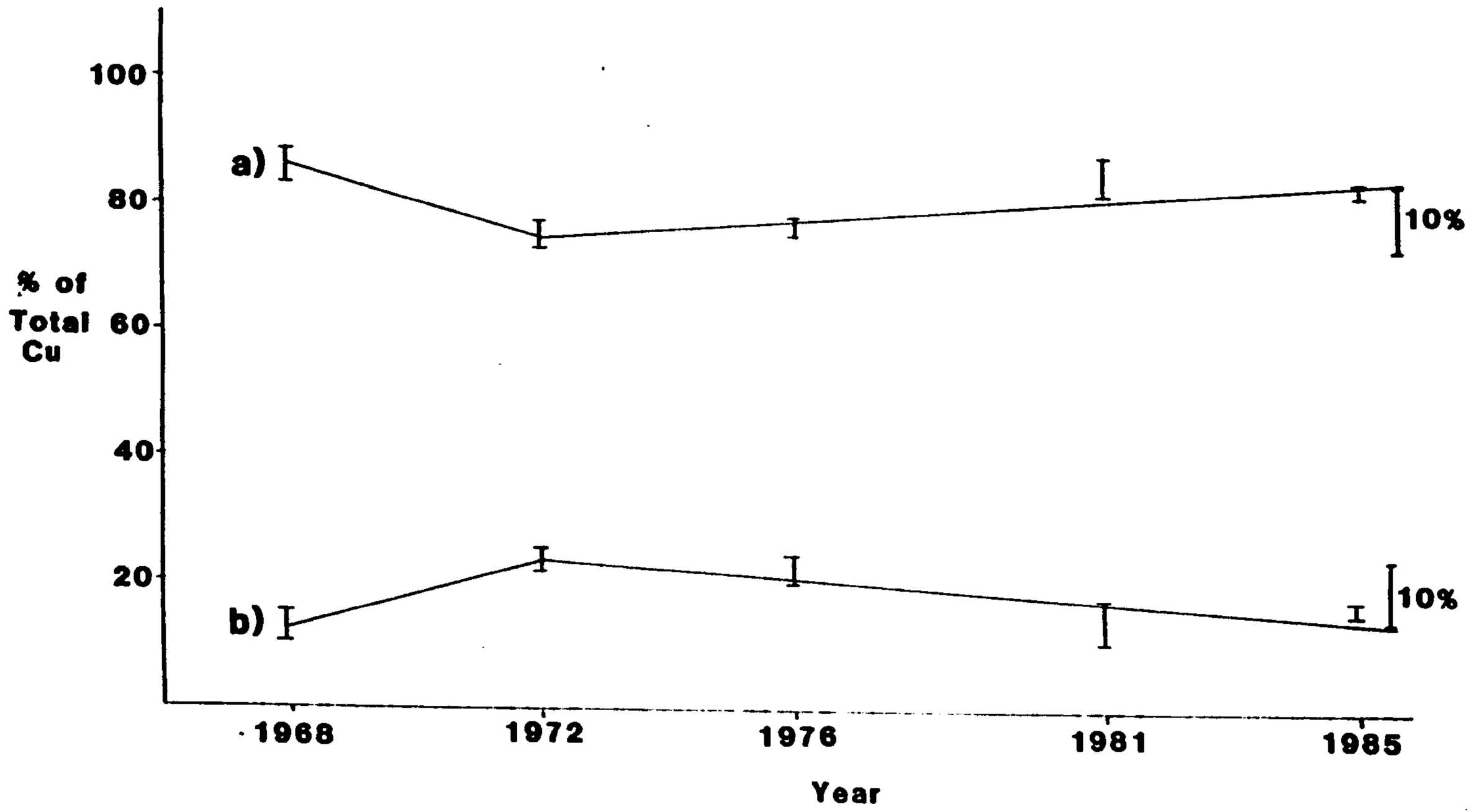

on a sludge treated plot with time at Luddington.

Table 5.5 Organic matter levels in Luddington soil

	1968	1972	1976
Control	1.8	1.8	2.0
125 T/Ha sludge	6.5	5.3	3.8

After 8 years 62% of the organic matter added in the sludge has been microbiologically degraded while there was no corresponding degradation at the control site and, if anything, an increase in the % organic matter occurred in 1976. This was due to grass/clover ley established on the site in 1972 which builds up the organic matter content of the soil. Microbial activity varies depending on the type of organic material in the soil. Bacteria first preferentially break down low molecular weight organic material due to its easier degradability and they will only degrade high molecular weight humic materials when the low molecular weight food supply is used up. This in part explains the movement of Cu from low molecular weight species into high molecular weight species. As the microbial activity proceeds the Cu in a low molecular weight form is released and then reacts with the humic material. The reason for the differences in the rate of transfer of Cu between the two molecular weight categories in the high and low Cu plots was explained earlier in terms of kinetics but can also be explained in terms of Cu toxicity. It is known that high Cu levels in soil can greatly reduce the enzymatic degradation of soil organic matter [6] due to the inactivation of soil enzymes. The levels of copper in the high Cu plot are sufficiently high to cause such a slow down of microbial and enzymatic activity. Since the bacteria etc. will

preferentially degrade the low molecular weight material. This will result in a slowdown in the rate of transfer of Cu to the high molecular weight species. This is the most likely explanation for the differences in the rate of Cu transfer to high molecular weight species between the high and low Cu plots.

This has important implications in the regulation of sludge disposal on land used for agriculture. If the sludge is highly contaminated with Cu then the chances are that this will result in a decrease in microbial activity. This will in turn result in a slower transfer of Cu into the less toxic high molecular weight species. The relatively slow Cu uptake rate of plants will mean that the Cu will remain in a plant available form for a long time after sludge application.

5.6 *COMPARISON OF CU SPECIATION RESULTS WITH OTHER LONG TERM STUDIES CONDUCTED AT THIS SITE*

5.6.1 *Introduction*

It was mentioned earlier that a great deal of experimental data was already available from this site. It was hoped that some of the trends observed in this work would be backed up by previous experiments on the same site. Data was available for various chemical extraction procedures and in particular aqua regia (total Cu concentration in soil), EDTA and acetic acid extractants.

5.6.2 *Results and Discussion*

Table 5.6 shows the results obtained by each of the above methods of extraction. The data seems to indicate an overall decrease in the extractable contents over the 15 year experiment. That is except for the 1976 results which are low for all the extractants. This decrease in extractability would suggest that plant availability had decreased

in the years after sludge application. However, the results presented in this work suggest that plant availability had only decreased very slowly indeed i.e. a maximum decrease of the plant available Cu by 10% on the low Cu plot over 15 years. Whereas the mildest extractant used in the previous work (acetic acid) showed a 40% decrease on the high Cu plot and a 50% decrease in plant available Cu on the low Cu plot. Although the overall trend is the same the use of chemical extractants to assess plant availability suggests a more rapid movement of Cu into non-available forms.

Table 5.6 Total and extractable copper in the plot soils from Luddington expressed as mg/kg in air dried <2 mm sieved soil

Sampling Date	Treatment	TOTAL Cu	EDTA Cu	HOAc Cu
1972	Control	19	8.9	1.9
	Low Cu	202	146	74
	High Cu	416	359	176
1976	Control	18	10	---
	Low Cu	113	116	63
	High Cu	198	254	177
1981	Control	22	6.8	---
	Low Cu	178	134	61
	High Cu	316	276	139
1985	Control	---	9.9	---
	Low Cu	---	91.3	38
	High Cu	---	216	103

The experimental procedure used in this study was a much milder process than used previously and should be more representative of the plant available forms in the soil. The mildest extractant used previously was acetic acid which would be able to solubilize Cu species not usually available to plants and hence give rise to misleading

results. This suggests that great care should be taken in interpreting data obtained by chemical extractant procedures.

5.7 *THE STUDY OF CU SPECIATION IN SOILS CONTAMINATED WITH DISTILLERY WASTE*

5.7.1 *Introduction*

In the North-east of Scotland there is concern over the disposal of distillery wastes on agricultural land [7]. These wastes have been applied to agricultural land for over a hundred years and although they can contain elevated Cu levels there are no regulations as to how much of this waste should be applied to agricultural land. The high Cu concentrations present in treated soils give rise to concern for the health of crops and livestock reared on contaminated land and there have been recent reports of sheep deaths due to Cu toxicity. It was decided to apply the analytical method devised earlier to study the Cu speciation in two highly polluted soils. One was at Minmore near Tomintoul and the other was from Pitglassie near Dufftown. Both sites had a 70 year history of distillery waste application and it was decided that it would be of interest to compare the speciation of Cu in these upland polluted soils with the Cu speciation in the Luddington sites.

Table 5.7 below shows the total concentration of Cu at each of the three chosen sites, one a Minmore and the other two at Pitglassie [8].

Table 5.7

Sampling site	Total Cu/mg/kg
Surface soil - Minmore	390
Surface soil - Pitglassie	300
Hilltop surface soil - Pitglassie	290

5.7.2 ***Experimental***

Water extracts of each of the soils were obtained as outlined earlier. These samples were analysed by AAS to determine the total Cu content of the water extracts. The samples were then analysed using the SEC/GFAAS method described earlier.

5.7.3 ***Results and Discussion***

The total Cu concentrations of the water extracts are shown below in Table 5.8.

Table 5.8 Cu contents of water extracts of distillery waste treated soils expressed as ppm. Duplicate results in parentheses.

Sampling site	Copper
Surface soil - Minmore	0.530 (0.517)
Surface soil - Pitglassie	0.475 (0.500)
Hilltop surface soil - Pitglassie	0.500 (0.536)

It was apparent that the Cu content of the water extracts was very small compared with the total concentration of Cu in the soil. This is because much of the Cu in a soil is strongly bound in the solid phase through adsorption/complexation reactions with particulate matter. A large proportion of the total Cu will also be strongly bound to humic materials which are adsorbed on to particulates. All of these forms are effectively removed from the solution phase. The same was true for the Luddington soils.

The results obtained for the Cu speciation analysis are shown in Figs 5.13-5.15 and in tabular form below.

Fig 5.13 Minmore surface soil.

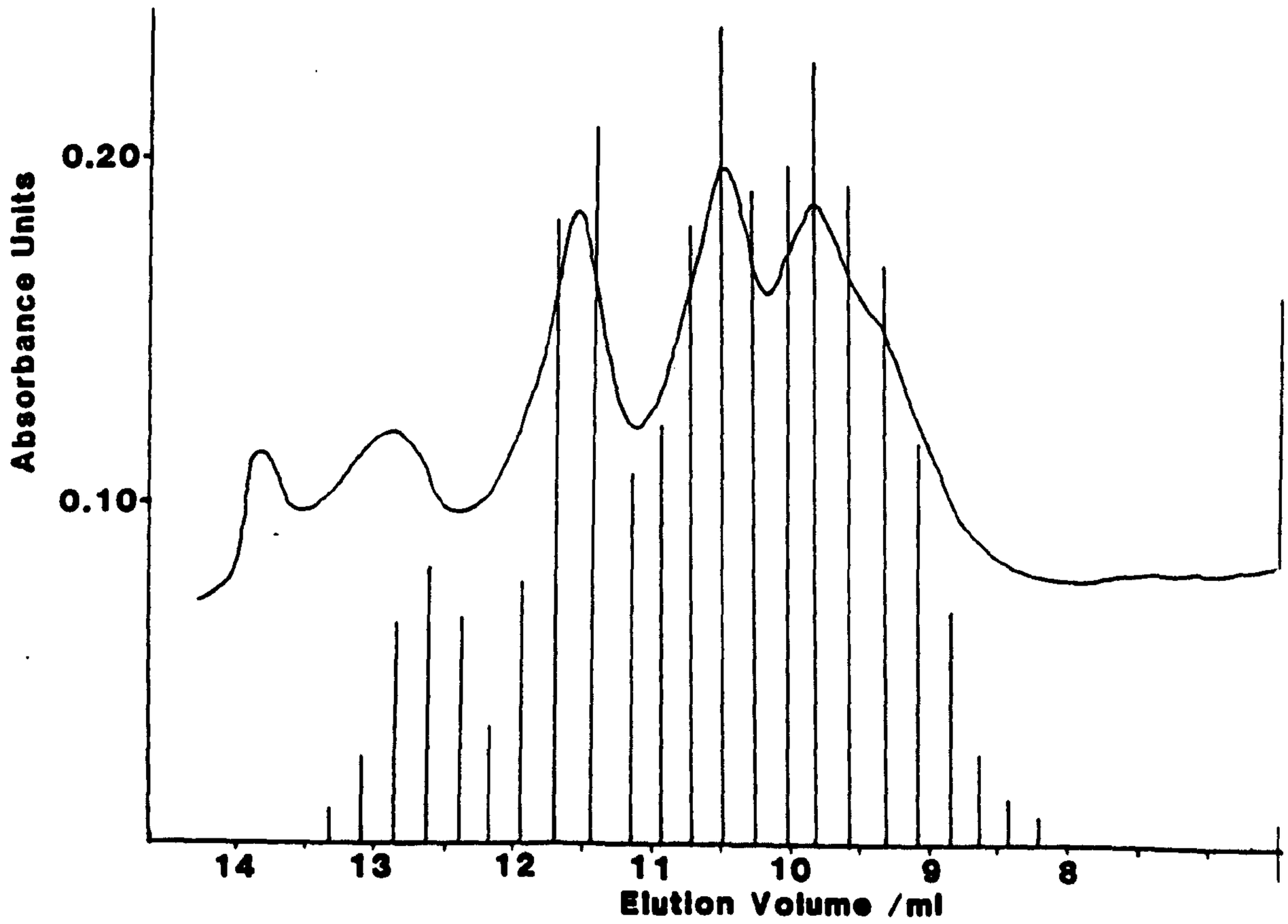

Fig 5.14 Pitglassie surface soil.

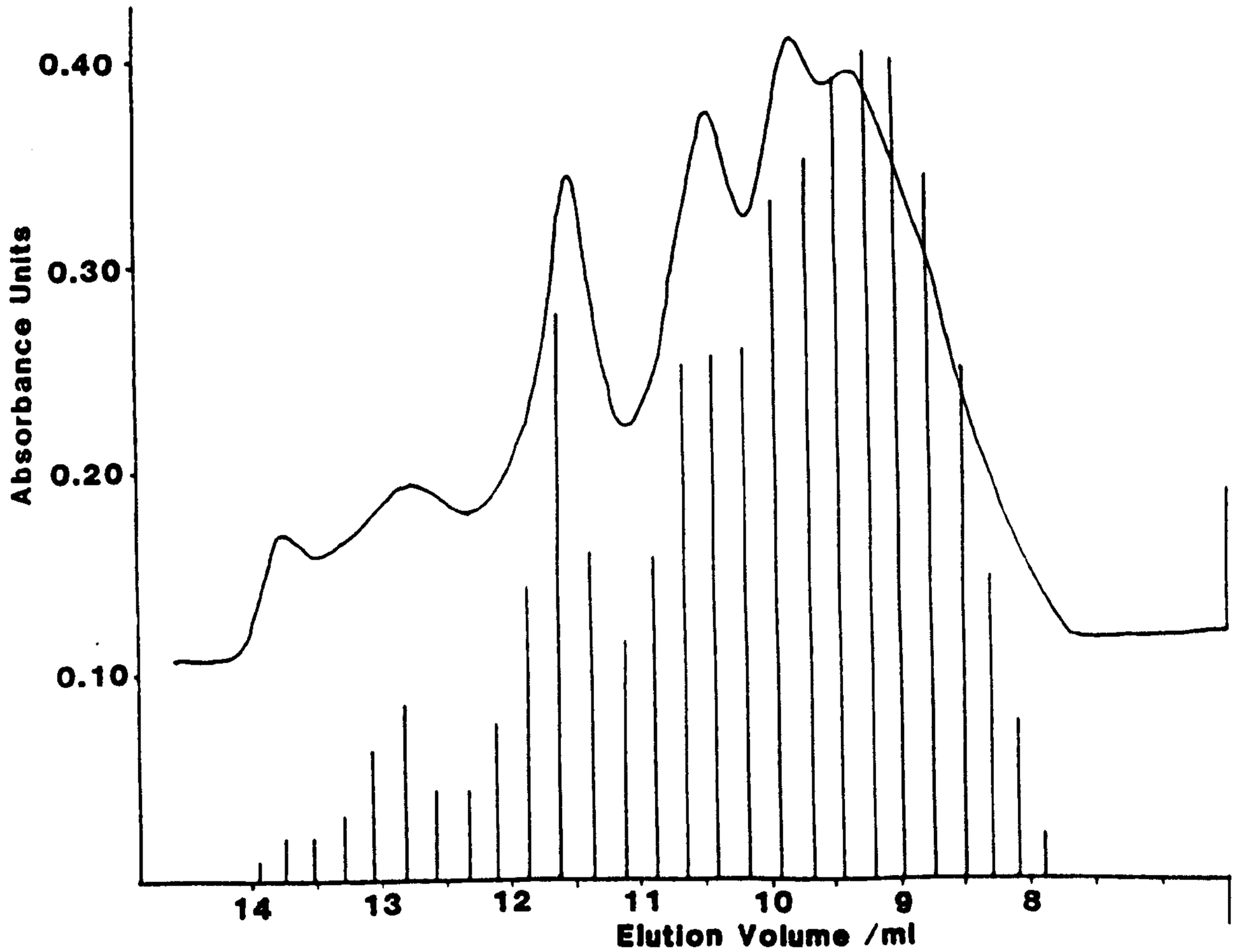

Fig 5.15 Pitglassie hill top soil.

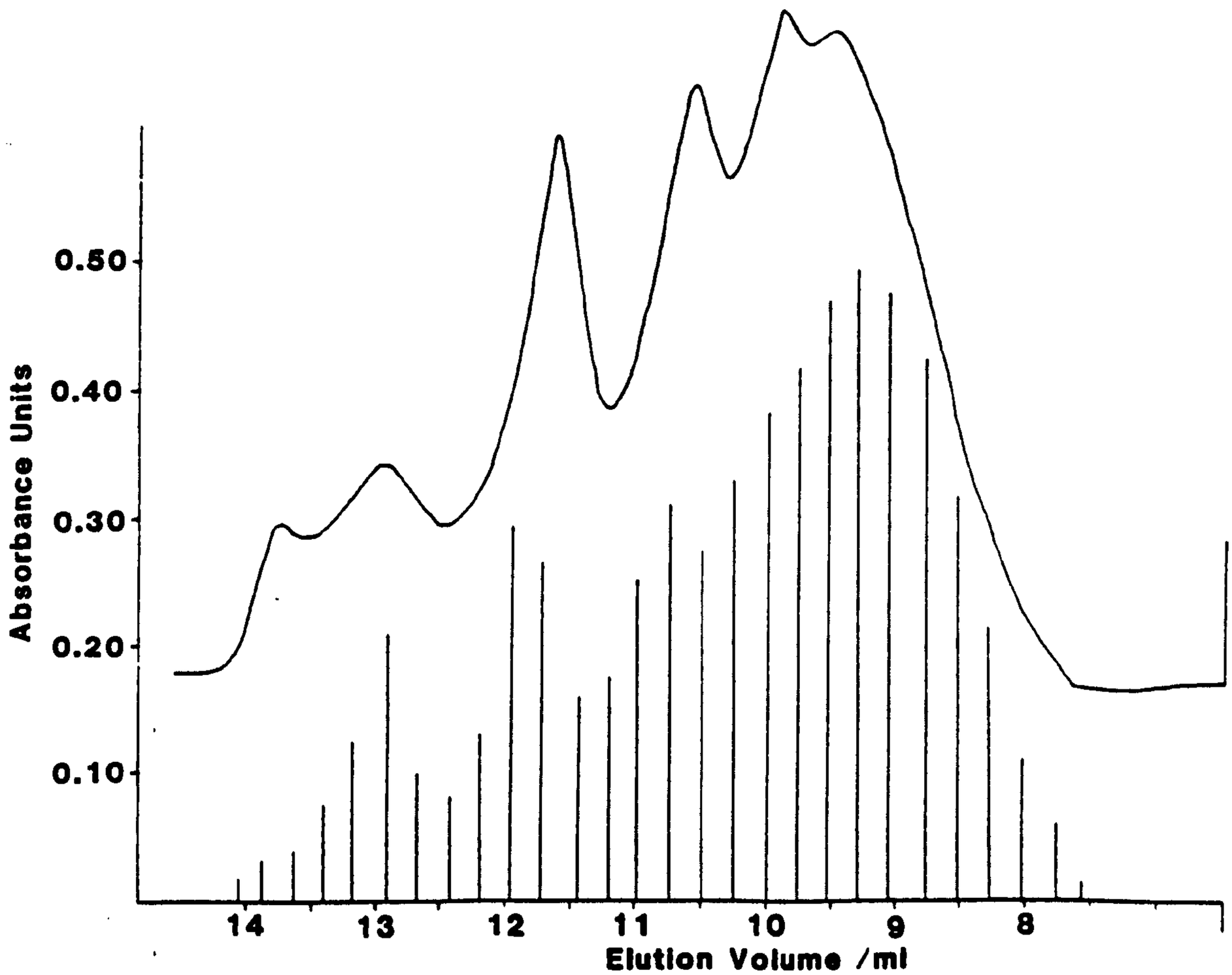

Table 5.9 Cu speciation results for distillery waste treated soils

	High mwt		Low mwt	
	%	ppm	%	ppm
Surface soil - Minmore	69.0	0.345	31.0	0.115
Surface soil - Pitglassie	76.7	0.364	23.3	0.110
Hilltop surface soil - Pitglassie	78.1	0.413	21.9	0.116

There are striking differences in Cu speciation between the two sampling sites. The speciation at the Pitglassie sites is similar in both the total Cu conc. in the soil and the distribution of Cu in the water extract, to the low Cu plot at Luddington. The Minmore site shows quite a different picture of Cu speciation. Quite a large proportion of the Cu at Minmore (31%) is in a low molecular weight, potentially plant-available form, much more than was found in a similar form in the Luddington or Pitglassie soils. This was very interesting in that there have been reports of toxic effects of Cu on rape plants grown on this site.

Table 5.10 shows the Cu contents of ryegrass and clover grown on the Minmore site.

These results indicate a three-fold increase in the Cu content of ryegrass and a 4-fold increase in white clover grown on the polluted soil. This compares with an increase of only 1.5 times for timothy grass grown at Luddington. These increases are to be expected in the light of the speciation results and further emphasise the need for speciation to be taken into account by regulatory agencies. The total

Table 5.10 Copper in herbage species grown on copper-polluted soils, as mg/kg in dry matter.

Location	Sampling date	Species	Untreated soil	Copper-polluted soil
Sewage sludge treated soils				
Luddington	June 1976	Timothy (Phleum pratense L)	6.8	10.9
Lee Valley	June 1977	Ryegrass (Lolium perenne L)	4.8	6.0
Lee Valley	June 1977	White clover (Trifolium repens L)	9.3	9.5
Distillery waste treated soils				
Site M	Aug. 1978	Ryegrass (Lolium perenne L)	6.5	17.1
Site M	Aug. 1978	White clover (Trifolium repens L)	6.0	25.6

concentration of Cu in the soil at Minmore (390 ppm) is similar to that of the high Cu plot at Luddington (416 ppm) shown in Table 5.6, yet the Cu speciation is very different. At Minmore a greater proportion of the Cu is in a low molecular weight form. It has already been stated that this molecular weight fraction is potentially available to plants and this is further substantiated by the observed increased in the plant Cu contents of ryegrass and clover grown on this site.

The speciation of Cu in the Minmore and Pitglassie sites was also very different. This was again reflected in the amounts of Cu found in plants grown on the site. Lucerne plants grown on the Pitglassie soil had about a quarter of the Cu content (13.4 mg/kg) of similar plants grown on the Minmore soil (45.2 mg/kg) [6] which is in line with what could have been predicted from the Cu-speciation results.

The striking similarities between the predictions of plant availability of Cu that can be made from the Cu speciation analysis and the actual levels of Cu found in plants grown on the sites indicates that the method does indeed present a true picture of the Cu speciation in polluted soils and that the method will be of use in future experiments on Cu speciation in polluted soils.

5.8 *SUMMARY AND CONCLUSIONS*

The analytical method described in the last chapter has been improved upon and used to study the long-term partitioning of copper in soils polluted with sewage sludge. The results produced have shown that the soil can modify Cu speciation in the years after sludge application. The copper is present initially in the form of low molecular weight complexes that are potentially toxic to plants but gradually transfers to higher molecular weight ligands e.g. humic and fulvic acids which are much less available to plants. This transfer of copper to high molecular weight ligands is due to two factors. Firstly, these complexes are much more stable than the low molecular weight organocopper species. Secondly, low molecular weight ligands are also a source of food for the various microbial gents present in soils. The degradation of the low molecular weight organic matter releases the Cu bound in this way and leaves it free to react with the humic material. It has been shown that the rate of Cu detoxification by microbiological pathways can be heavily influenced by the amount of Cu in the soil. Soil contaminated with large amounts of copper can cause such a decrease in microbial and enzyme activity due to Cu-toxicity that the detoxification process will take a significantly longer period of time than in less polluted soils. This further justifies the monitoring of copper speciation in soils as it will not only yield useful information

about plant availability, but will also give an indication of the affects of Cu toxicity on microbial activity in the soil.

The analytical method has also been used to study Cu speciation in soils which have a history of distillery waste application. When the speciation results were compared with plant uptake data obtained on the same site it was apparent that the amounts of Cu taken up by plants was in fact heavily dependent on the speciation in the soil. The striking similarities between Cu speciation and plant availability produced indicate that this analytical method isolates and quantifies plant available Cu species in soils and that this data and allow reliable predictions about plant availability to be made.

REFERENCES

1. Berrow M.L. and Burridge J.C., Proc. Int. Conf. Heavy metals in the Environment, Amsterdam, Sept 1981. CEP Consultants Ltd., Edinburgh, 1981, 202-205.

2. ADAS. Trace element deficiencies in field crops. MAFF Booklet 2197, (Revised 1983), 1984, 13 pp.

3. Berrow M.L. and Burridge J.C., Inorganic Pollution and Agriculture, MAFF Ref. Book 326, (HMSO, London), 1980, 159-183.

4. Brinkman, F.E., Jewett, K.L., Inverson, W.P., Irgolic, K.J., Ehrhardt, K.C. and Stockton, R.A., J. Chrom., 1980, **191**, 31-46.

5. Brown L., Haswell S.J., Rhead M.M., O'Neill P and Bancroft K.C.C., analyst, 1983, **108**, 1511-1520.

6. Mathur, S.P. The inhibitory role of copper in the enzymatic degradation of organic soils, Proc. Int. Symp., Bemidji, Minnesota (USA) 1981, 191-219.

7. Reith J.W.S., Berrow M.L. and Burridge J.C., Proc. Int. Conf. Management & Control of Heavy Metals in the Environment, London, 1979, CEP Consultants Ltd., Edinburgh, 537-540.

8. Berrow M.L. and Cheshire M.V., Proc. Int. Conf. Heavy Metals in the Environment, Athens, September 1985, Volume 2, CEP Consultants Ltd., Edinburgh, 1985, 397-399.

9. Berrow M.L. and Burridge J.C., Intern. J. Environ. Anal. Chem., 1990, **39**, 173-177.

CHAPTER SIX

THE DEVELOPMENT OF ICP-OES SAMPLE INTRODUCTION SYSTEMS EFFICIENT ENOUGH TO PROVIDE DETECTION LIMITS SUITABLE FOR SPECIATION STUDIES

6.1 *INTRODUCTION*

The use of ICP-OES as a detector in metal speciation studies has been widely reported in recent years. A number of workers have already demonstrated the use of plasma atomic emission sources in conjunction with liquid chromatography for the physico-chemical separation and detection of various metal-ligand species [1]. Much of this previous work has made little or no use of the multielement capabilities of this technique as most have utilized the plasma in a sequential mode [2]. Flame AAS could be used in such studies without any real loss in information. The strength of an ICP-OES lies in its multielement capability and this would be of great use in speciation studies. If the SEC separation technique described in previous chapters was interfaced to the ICP-OES then the amount of speciation data that could be obtained for a single sample would be enormous. It would allow the simultaneous determination of chemical speciation for over 20 elements, depending on the instrumentation used. The nebulisation systems commonly used in ICP-OES have very similar sample flow rates to HPLC and in some cases the interfacing requires no more than a simple connection of the HPLC eluent outlet to the sample intake tube of the nebuliser.

The method of detection used in previous chapters was GFAAS but it was a very time consuming method of analysis, 2-4 minutes per sample compared with the 10-20 seconds needed in flame AAS or ICP-OES. The use of ICP-OES would allow the continuous on-line monitoring of the eluent instead of the discontinuous sampling used in GFAAS. This would enable the detection of the sharpest chromatographic peaks.

The major problem that exists with ICP-OES is that the detection limits are not as good as those that can be obtained with GFAAS. The concentrations of Ca, Na, Mg and K are usually well within the detection

limits of ICP-OES. In the case of the heavy metals of interest in this study the levels normally encountered in even polluted soils are not sufficiently high to allow the use of ICP-OES as a detector. In the case of copper the total soil solution concentration encountered in the soil at Laverock Brae farm was typically in the region of 50 ppb. The physico-chemical separation and subsequent dilution of the Cu species would render a conventional ICP-OES system useless as a detector.

The Achilles heel of ICP-OES is the sample introduction system. Nebulisers and spray chambers used for ICP-OES are a good example of how empirical progress has been made without a genuine understanding of the physical processes involved. This has lead to a high price being paid in terms of reliable operation [3]. The two main problems associated with ICP nebulisers are unstable operation and salting up or even blockage. The efficiency of sample introduction (the ratio of analyte mass flux delivered to the plasma to the analyte mass uptake) is dreadfully poor. not usually exceeding 1%.

Pneumatic nebulisers were used as aerosol sources in flames for many years before ICP sources came into use and it was realised that placement of a spray chamber after the nebuliser could remove some of the large droplets produced and thereby enhance the stability of the spectral emission. The spray chamber and nebuliser were usually constructed from available pieces of laboratory glassware. So effective were these crude devices that apart from manufacturing refinement they are still used today in flame emission and atomic absorption spectrometers. The devices used for plasma spectrometry to-day have been produced by scaling down the devices used in flames. This was necessary because plasmas are much less forgiving than flames in terms of nebuliser operation and for ICP-OES the gas volumetric flow available for operating

the nebuliser was reduced to 0.5-1.5 l min^{-1}. This has resulted in the production of devices about which we have a very limited understanding of their mode of operation.

A recent review by Sharp [3] brought together the available knowledge from the fields of chemical, mechanical engineering and aeronautics to provide guidelines to designers of nebuliser/spray chamber systems. Some of the more novel ideas proposed in this review have been constructed in an attempt to increase the efficiency of sample introduction systems in ICP-OES.

6.2 *NEBULISERS AND SPRAY CHAMBERS COMMONLY USED IN ICP-OES*

This work was concerned with the evaluation of novel nebuliser spray chamber systems for ICP-OES. The nebuliser produces a fine aerosol from the bulk solution. Droplet sizes of about 1 μm would be ideal, but sizes of <10 μm are acceptable. There are a wide variety of nebulisers available commercially. The two main types used are pneumatic and ultrasonic, but the pneumatic type is by far the most common and is probably used for 99% of routine analysis. The main types of pneumatic nebuliser are the concentric, the crossflow (e.g. the MAK (200)), the Babington (e.g. V-groove) and the glass frit nebuliser [4].

A spray chamber is placed after the nebuliser the function of which is to remove the larger droplets >10 μm which are not completely atomised in the plasma. The reduction of aerosol concentration and modification in particle size distribution occur primarily through impaction of the aerosol on the internal surfaces in the spray chamber. Fig. 6.1 illustrates the particle motion and loss mechanisms in spray chambers. Impaction through motion induced by the bulk flows falls into the category of flow-line interception whereas deposition through random motion is commonly called turbulent deposition. Deposition will occur primarily

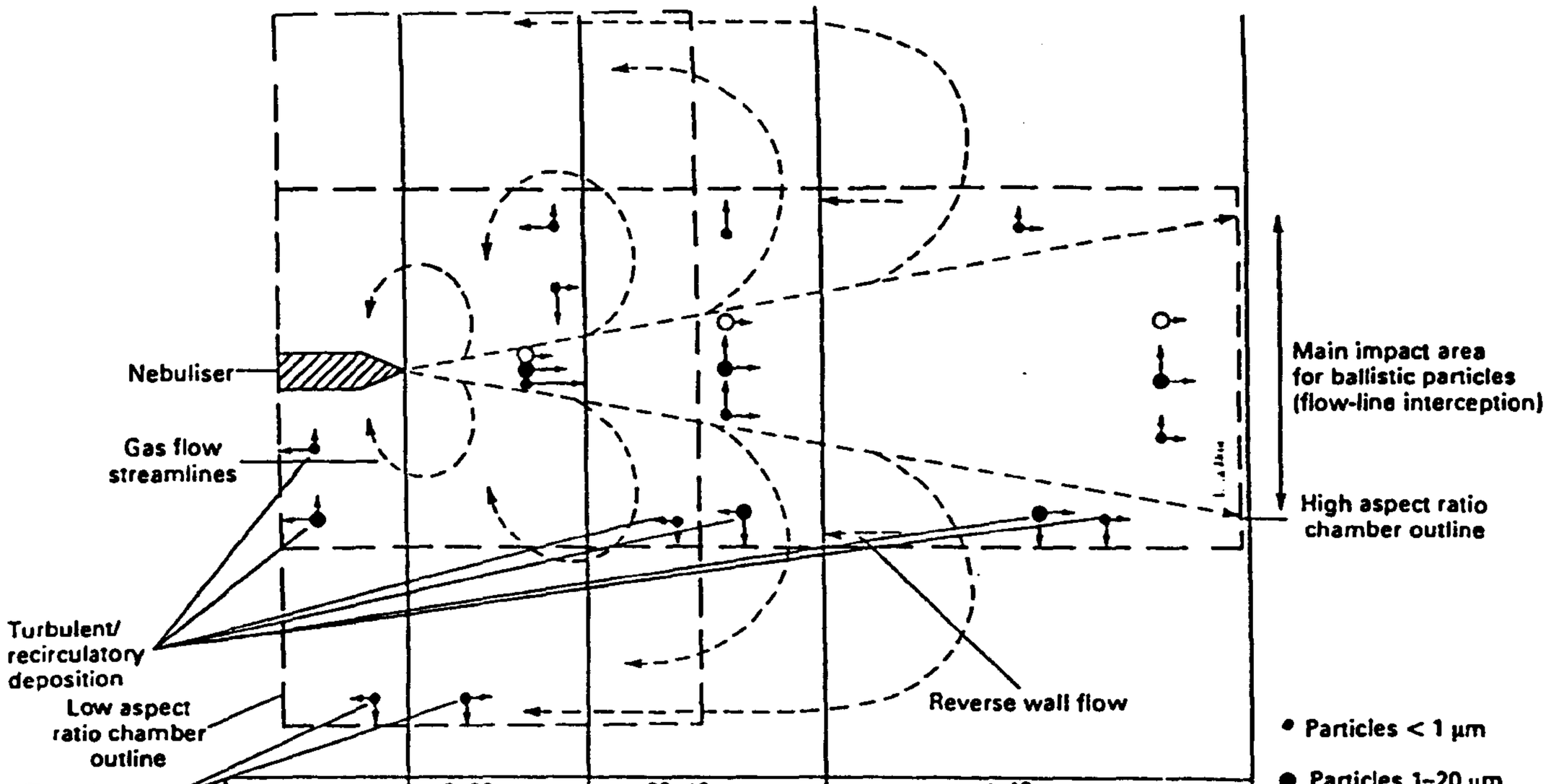

	0–20 mm	20–40 mm	>40 mm
Motion	All particles in ballistic phase	Small and medium sized particles acquire recirculatory/ turbulent motion	Large particles retain ballistic character Small and medium-sized particles fully entrained in recirculatory/ turbulent motion
Impaction process	Flow-line interception	Flow-line interception + recirculatory/ turbulent deposition	Large particles—flow-line interception Small and medium particles—recirculatory/turbulent deposition

Fig 6.1 Particle motion and loss mechanisms in ICP spray chambers.

on the side walls for high aspect ratio (length to width) chambers and on the end walls for low aspect ratios.

6.2.1 *Pneumatic Nebulisers*

The three main types of pneumatic nebuliser, concentric [4], cross-flow [4] and Babington [4] are shown in Figs. 6.2, 6.3 and 6.4 respectively. A typical ultra-sonic nebuliser is shown in Fig. 6.5.

6.2.2 *Spray Chambers*

The two most common types of spray chamber used in commercial ICP-OES systems are double pass spray chambers (Fig. 6.6) and impact bead spray chambers (Fig. 6.7).

6.3 *THE TESTING OF LINEAR CONESPRAY PROTOTYPES WITH VARIOUS SPRAY CHAMBER DESIGNS*

6.3.1 *Design of the Linear Conespray Nebuliser*

A radically new nebuliser design was proposed by Sharp which he named the Linear Conespray nebuliser. This device was a development of the patented Conespray nebuliser (Fig. 6.8) used in the ICP-OES at the Macaulay Institute. The Conespray nebuliser was not commercially viable as it was not compatible with the gas supply systems provided on commercial instrumentation. The Conespray nebuliser was able to produce a much finer spray than Meinhard nebulisers and could produce a 50% increase in signal to background ratio (SBR) compared with the SBR obtained using a Meinhard run under the same conditions. The Linear Conespray was an attempt to produce a nebuliser which provided a practical compromise between efficient gas-liquid interaction and universal sample handling and could be operated at pressures (<50 p.s.i.g.) available in commercial instrumentation. The design is shown schematically in Fig. 6.9 (a) and (b). The essential features of this design are:

(i) A 35 x 100 μm linear slot gas jet.

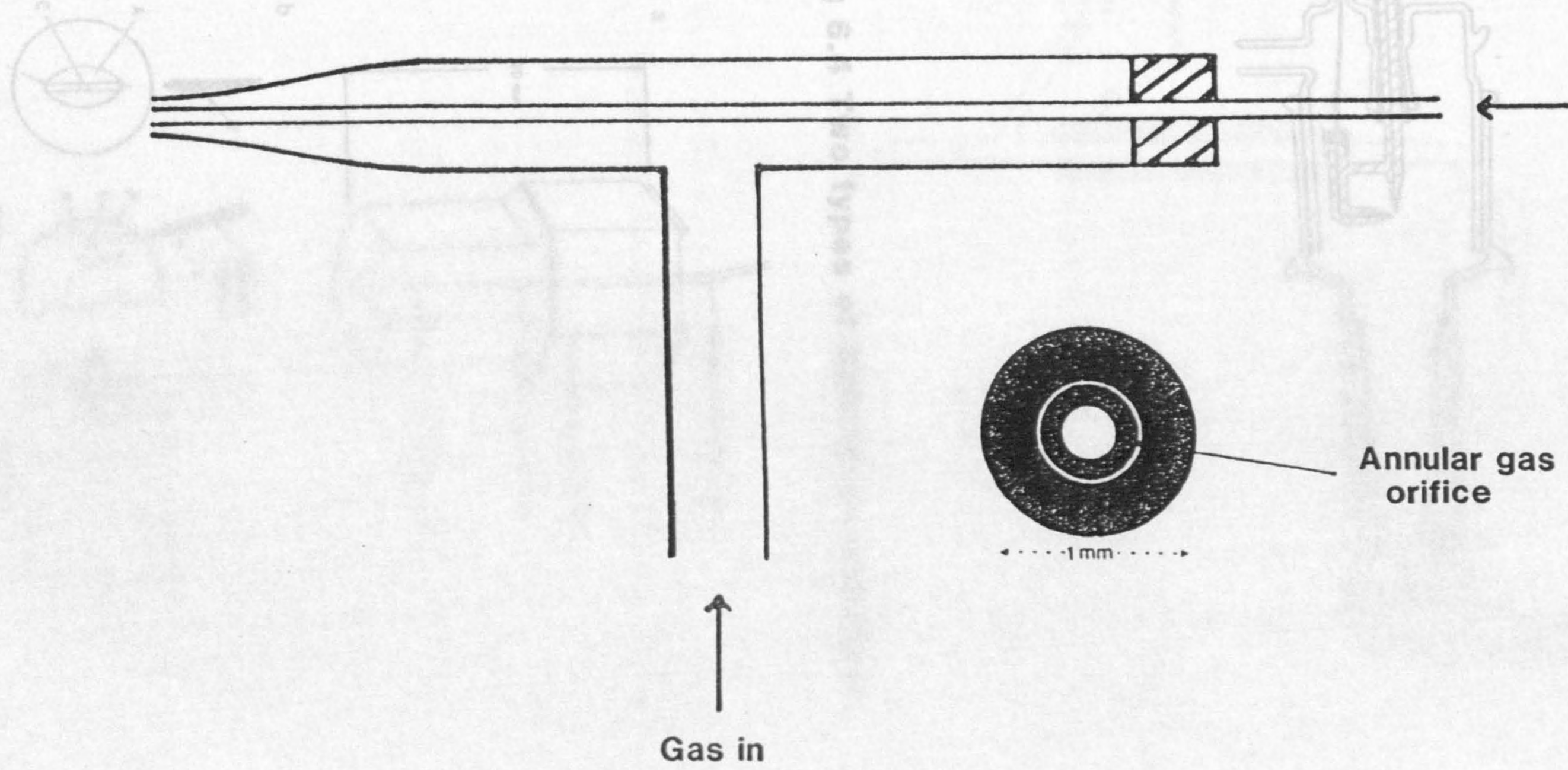

Fig 6.2 Schematic diagram of a meinhard nebuliser.

Fig 6.3 A cross flow nebuliser.

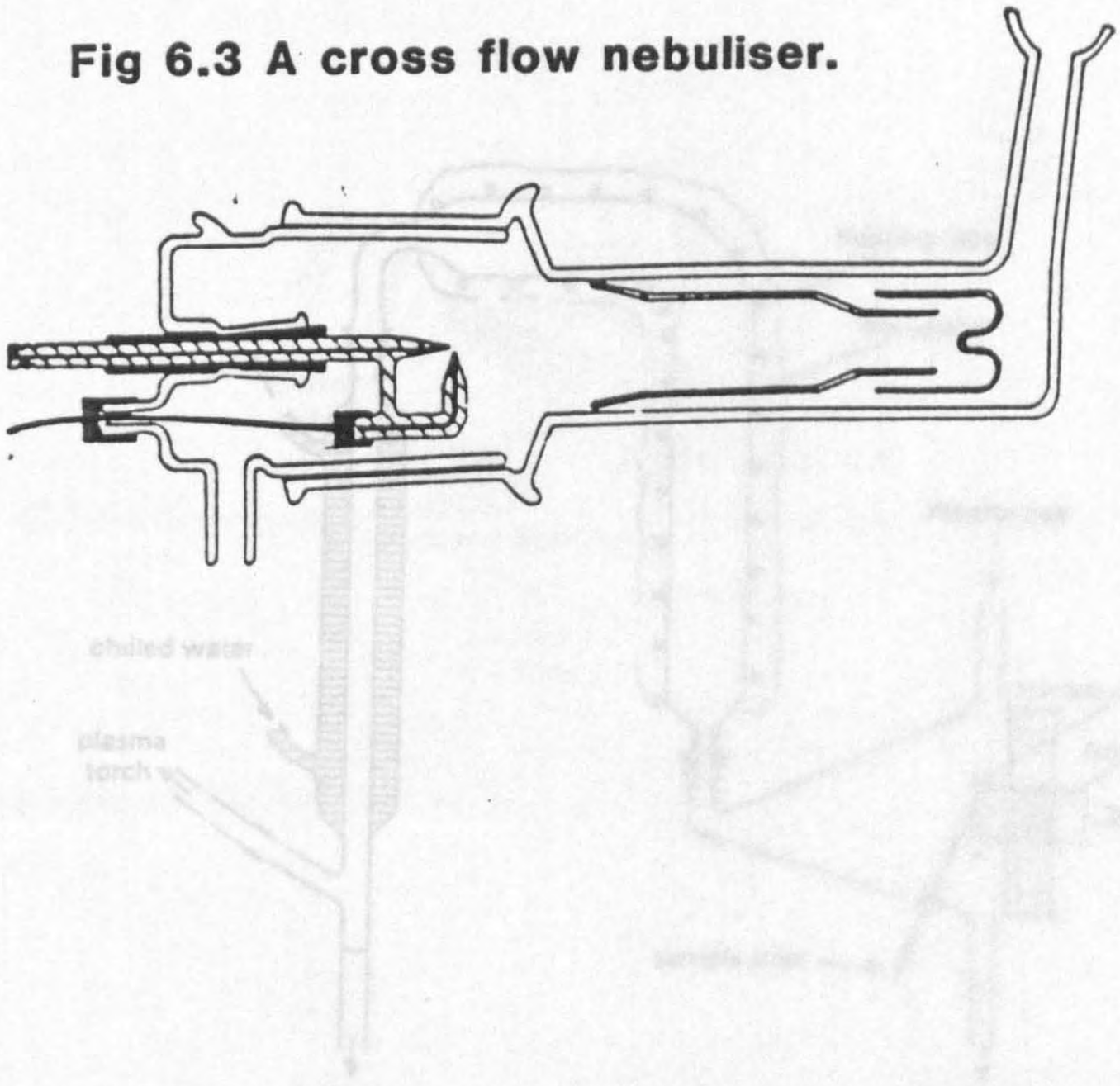

Fig 6.4 Two types of Babington nebuliser.

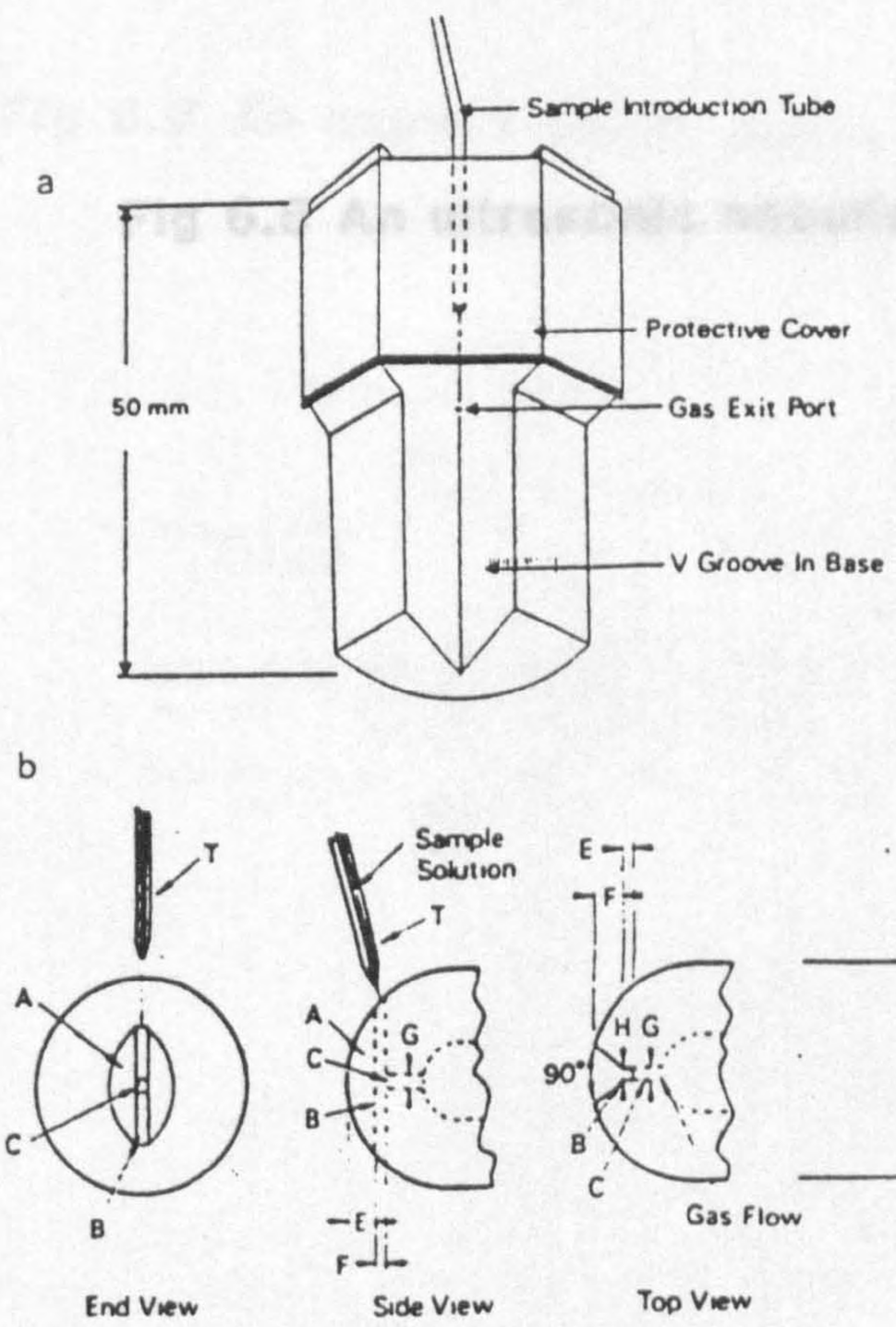

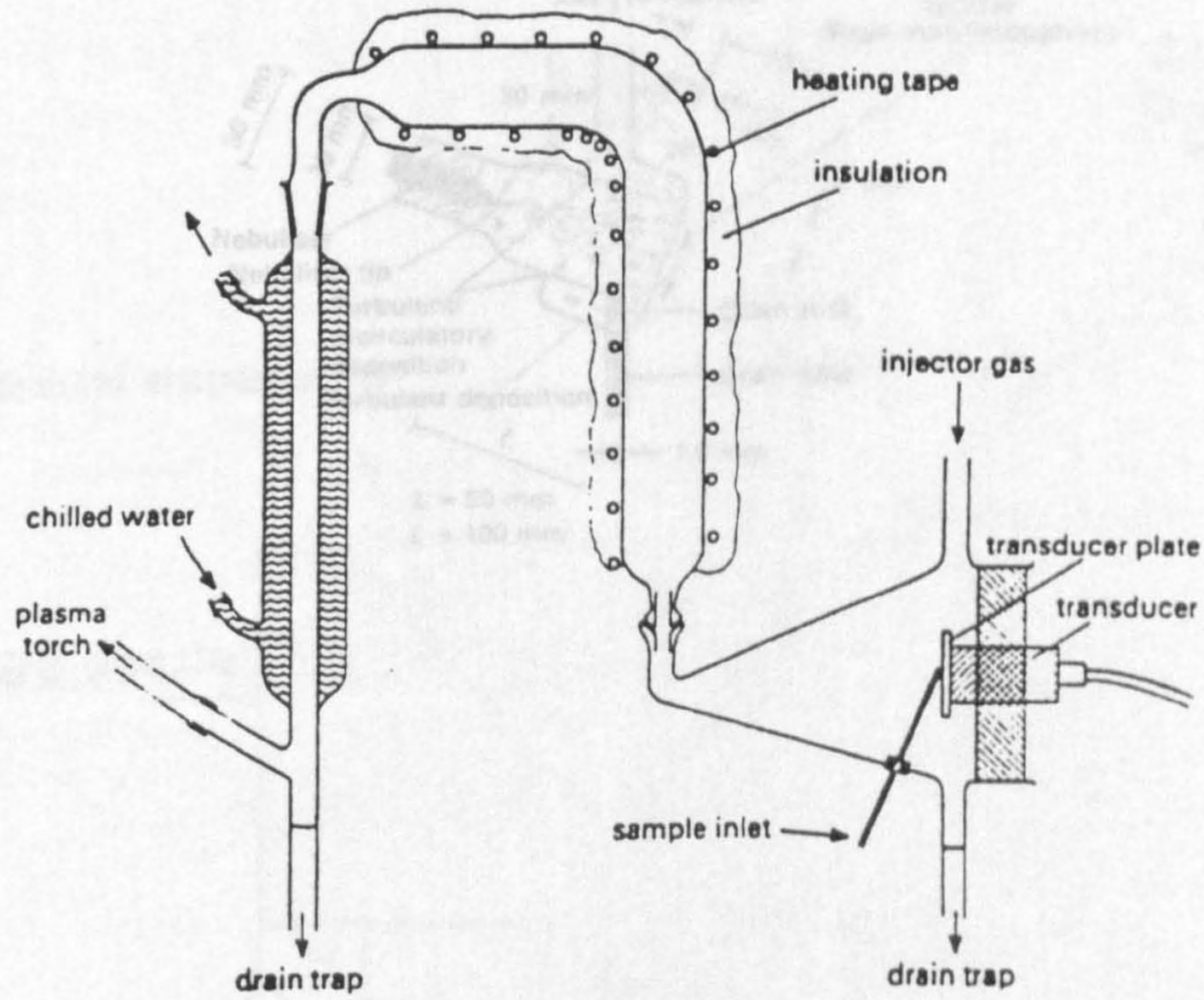

Fig 6.5 An ultrasonic nebuliser system.

Fig 6.6 A double pass spray chamber.

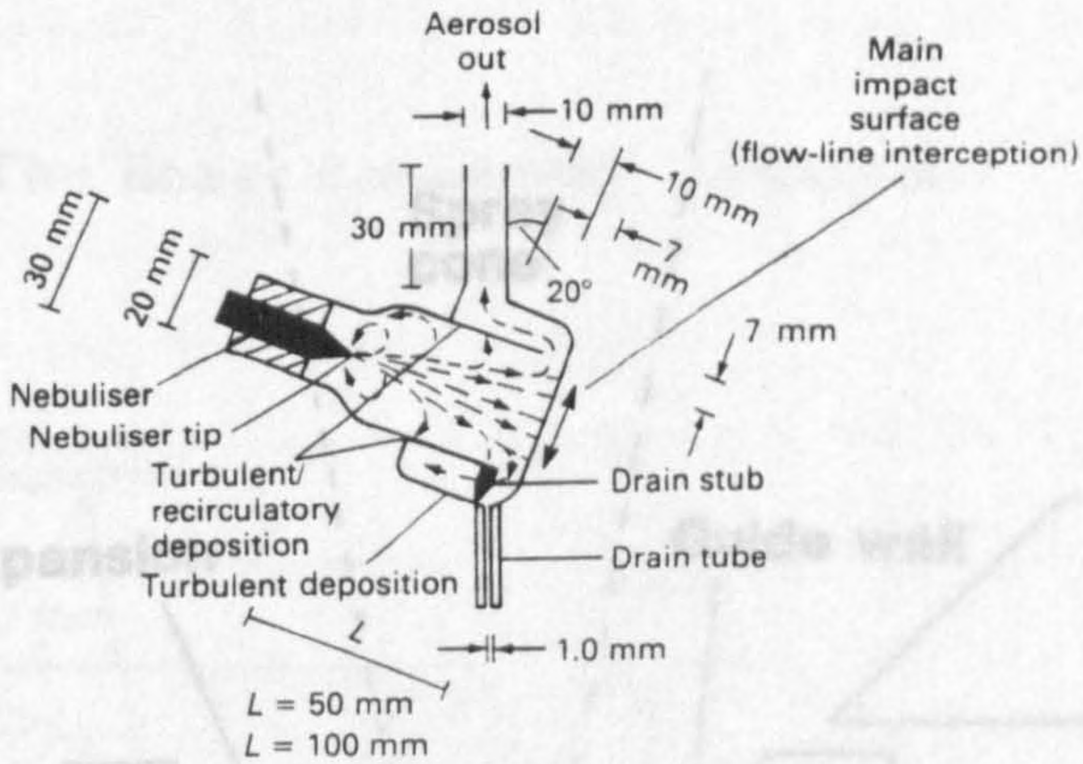

Fig 6.7 An impact bead spray chamber.

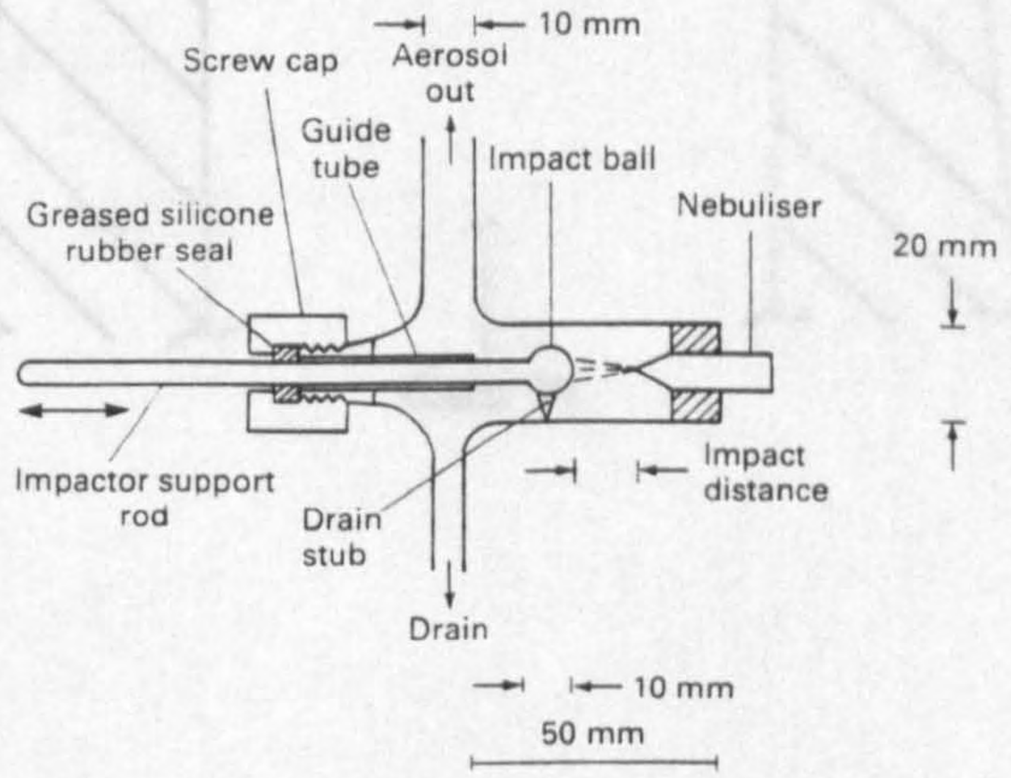

Fig 6.8 Conespray Nebuliser

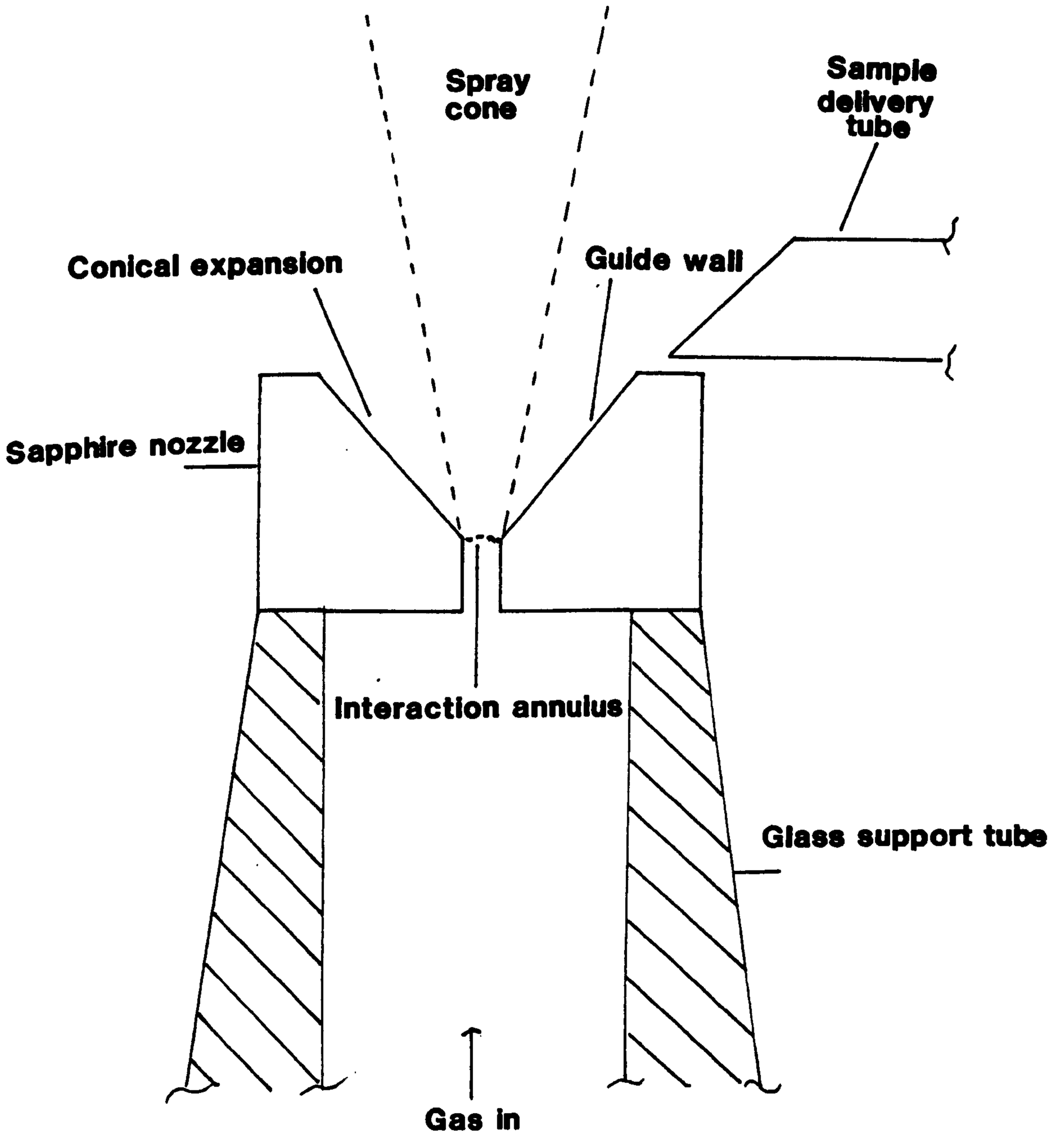

Fig 6.9 The linear conespray nebuliser.

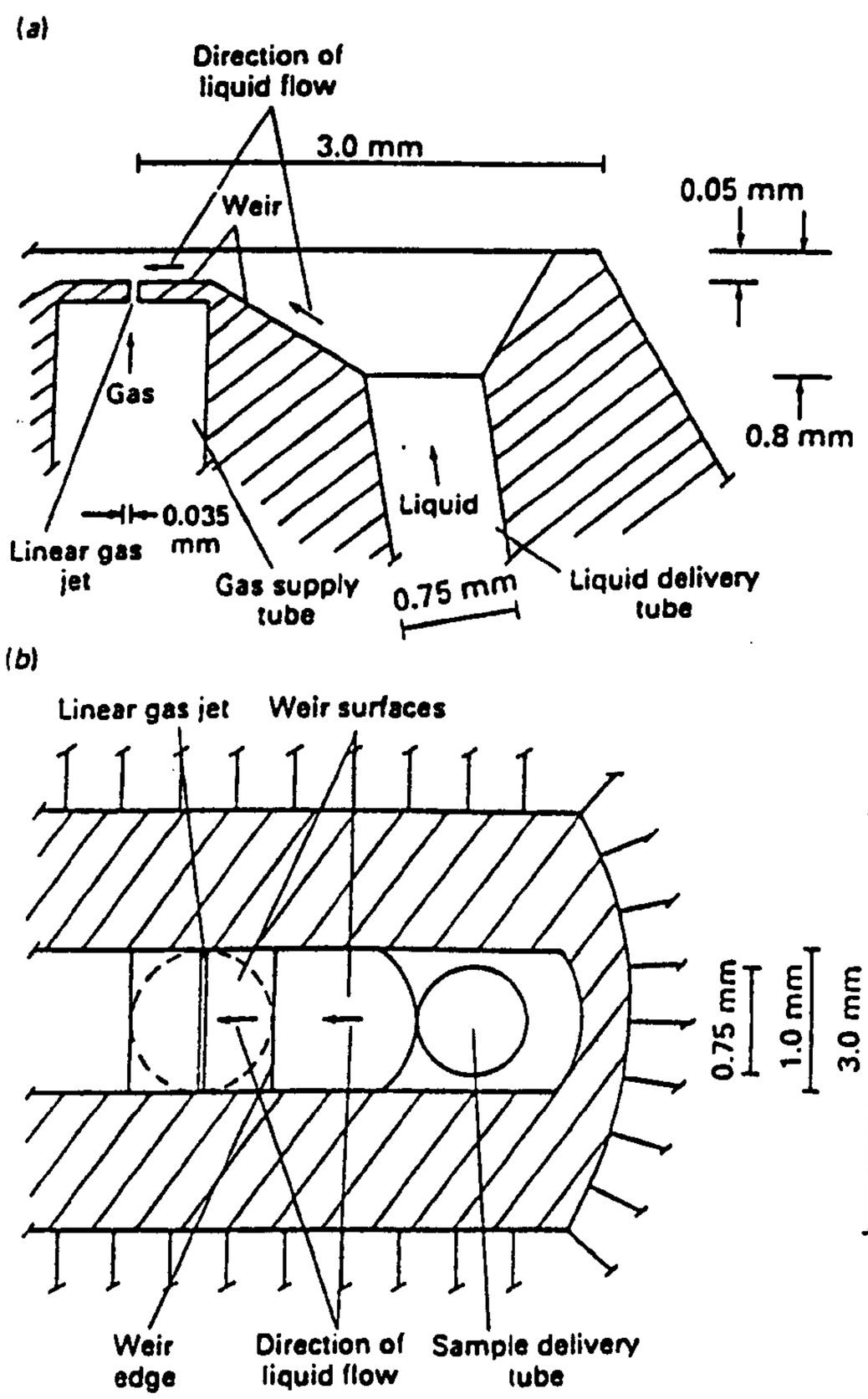

(ii) The liquid is introduced by two oppositely opposed supply ports coupled to the jet by weirs to produce a planar film of an appropriate depth.

(iii) Liquid introduction uses the entrainment principle but with a 180° cone angle for convenience of manufacture.

The nebuliser was constructed from polychlorotrifluorethylene (KCl-F). The slot jet was machined in the polymer which had been reduced to a depth of 100 μm. The use of a slot gas jet provides a large flow area enabling low pressure operation, but maximises the gas-liquid interaction area and its base-to-length ratio. The walls help to stabilize the film and set the maximum film depth that will be entrained into the gas jet. In practice upward entrainment of the leading edge of the liquid film produces a film thickness of ca. 200 μm which does not greatly exceed the 175 μm optimum depth predicted [3] for the 35 μm width slot jet. An essential feature of the device is that the film lifetime is short which aids stability and reduces unwanted evaporation. The surfaces adjacent to the gas jet are permanently subjected to a flow of fresh liquid which helps to prevent the formation of salt or particulate deposits. The use of a slot jet in preference to a row of holes, is based on the unproven assumption that a continuous slot will be less prone to blockage and slots down to 20 μm are well proven on concentric nebulisers.

The theoretical interaction area [3] of the Linear Conespray is 4×10^{-7} m^2 and the base to length ratio is ca. 10. The plume width at 400 μm is approximately 150 μm and so the minimum effective plume area is 1.2×10^{-7} m^2. The combined geometrical parameters therefore indicate that aerosol production should be superior to that produced by a conventional concentric nebuliser.

6.3.2 *The evaluation of the Total Transport Efficiency (TTE) of a Meinhard TR-30-C2 nebuliser in a 100 mm double pass spray chamber*

6.3.2.1 Experimental

The review by Sharp [3] made suggestions about the conditions for measuring the performance of nebuliser/spray chamber combinations and these have been adhered to whenever possible.

A Gilson Minipuls 2 (Gilson, Villers, France) pump was used to deliver distilled water at a rate of 2 ml min^{-1} to the Meinhard TR-30-C2 nebuliser (Meinhard & associates, California, USA). The flow rate of Ar used to run the nebuliser was 1 l min^{-1}. The nebuliser was allowed to equilibrate in the chamber and aerosol/vapour produced was collected using similar silica gel traps to those described by Ripsen and de Galan [5]. These silica gel traps consisted of a 10 cm glass tube packed with silica gel. Glass wool was placed at each end of the tube to hold the silica gel in position.

2 g samples of distilled water were sprayed and the resulting vapour collected in the silica gel traps and weighed by difference.

6.3.2.2 Results and Discussion

The results obtained are shown below.

Amount of H_2O collected /mg on silica gel after aspiration of 2 ml of distilled water

58.0	
57.1	Average
55.6	value = 57.2 mg
58.2	

The total transport efficiency was calculated as follows:

$$\frac{\text{wt of } H_2O \text{ collected}}{\text{wt of } H_2O \text{ sprayed}} \times 100 = \text{TTE\%}$$

$$\downarrow$$

$$\frac{57.2 \times 10^{-3}}{2} \times 100 = 2.86\%$$

This nebuliser/spray chamber combination is typical of those used in conventional ICP-OES systems and will therefore be used as a basis of comparison with the more novel nebuliser/spray chamber combination tested later.

6.3.3 *The TTE of a Prototype Linear Conespray in a 100 mm glass bulb recirculatory spray chamber*

6.3.3.1 Preparation of prototype Linear Conespray and Recirculatory Spray Chamber

A prototype nebuliser body was prepared "in house" and was sent to the University of Hull to have the slot jet laser machined. The final device was far from perfect firstly in that the slot was misaligned and secondly a number of shallow blind slots were present on one side of the slot jet due to test firings of the laser. Initially the weir was set at depth of 0.5 mm but this resulted in a very coarse aerosol. The reason for this is shown in Fig. 6.10. The film bypassed the high resistance of the weir edge and flowed in a vertical plane along the vertical wall of the groove. The results was that a large surface area of liquid was being exposed to a very small gas flow at the jet edge. The depth of the slot was gradually reduced and at a depth of 0.05 mm a sudden and noticeable improvement in aerosol production was obtained (Fig. 6.11). Aerosol was produced along about 50% of the length of the slot, but this increased and decreased with flow rate. This pattern of nebulisation could not be achieved on the

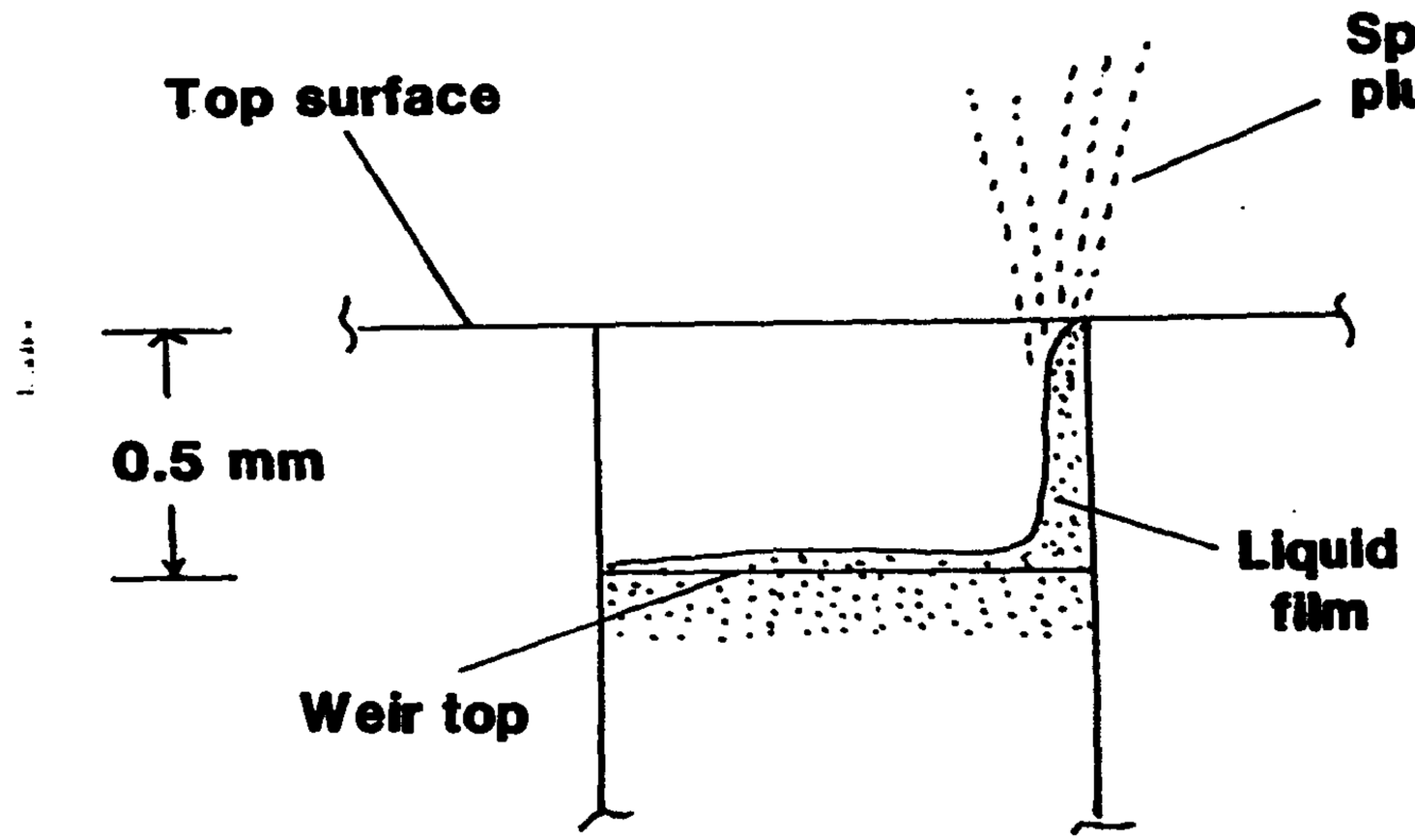

Fig 6.10 The nebulisation process observed with a 0.5 mm side wall.

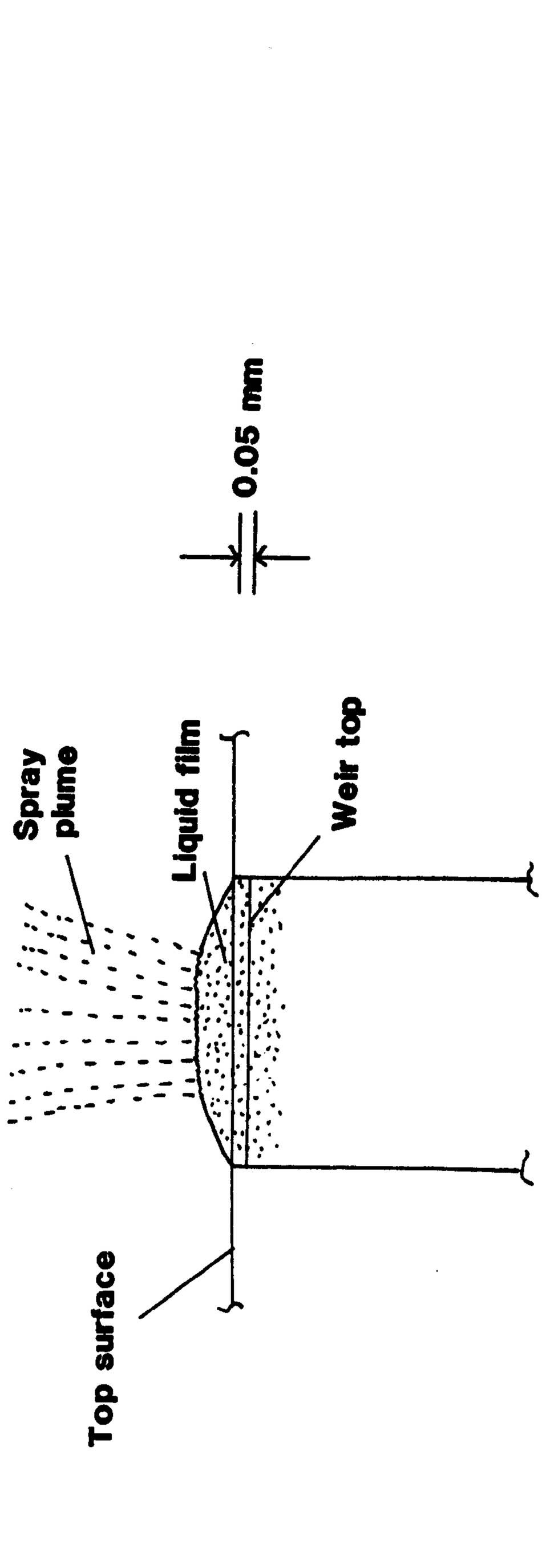

Fig 6.11 The nebulisation process observed with a 0.05 mm side wall.

damaged side of the device and attempts to run both sides simultaneously caused spray production on the good side to be pulled over to one side. The reason for the damaged side to so strongly favour nebulisation from one wall is shown in Fig. 6.12. The test slots were not in the centre of the groove, but were displaced to one side and therefore tended to conduct solution to the adjacent wall.

Total transport efficiency tests were carried out on this prototype in a glass bulb spray chamber (Fig. 6.13) and are shown in Table 6.1. The spray chamber was designed to try to allow the reintrainment of small droplets and to try to cut down the loss of small droplets through turbulent deposition on the spray chamber walls. At a gas flow rate of 1 l min^{-1}, the undamaged side of the nebuliser performed well (Table 6.1). The damaged side performed with a reduced efficiency and caused a decrease in the performance of the good side when both sides were operated simultaneously. When the gas flow rate was reduced nebulisation from the undamaged side tended to occur from the same sidewall. No visual reason for this could be detected. This resulted in little difference in the performance of the two sides of the device at reduced gas flow rates.

Table 6.1 Efficiency of Prototype (Ser. No. 001) Linear Conespray

Impact Distance (mm)	Liquid Flow Rate per side (ml min^{-1})	Liquid-to-Gas Ratio (V/V) x 10^3	Transport Efficiencies (%) Side 1	Side 2	Both sides
	Prototype 001	Gas Flow Rate = 1.0 l min^{-1}			
40	1.0	2.0	2.92	2.7*	1.38
75	1.0	2.0	3.90	3.5*	1.84
105	1.0	2.0	5.60	5.3*	2.63
	Prototype 001	Gas Flow Rate = 0.75 l min^{-1}			
40	0.5	1.33	3.70	3.6*	2.00
75	0.5	1.33	4.30	4.3*	2.40
105	0.5	1.33	7.00	7.0*	4.10

* Refers to results obtained on damaged side of nebuliser

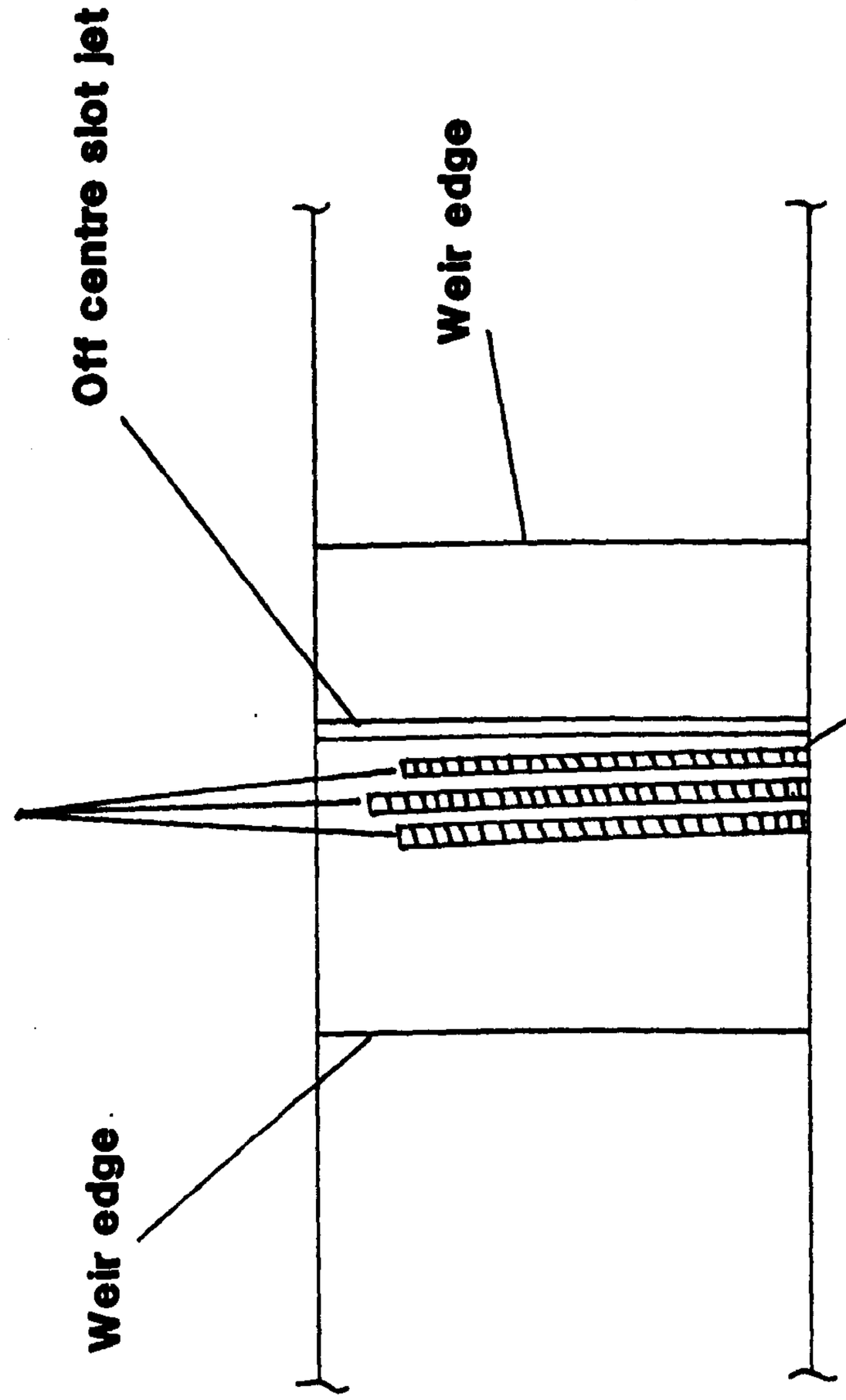

Fig 6.12 Top view of the prototype linear conespray.

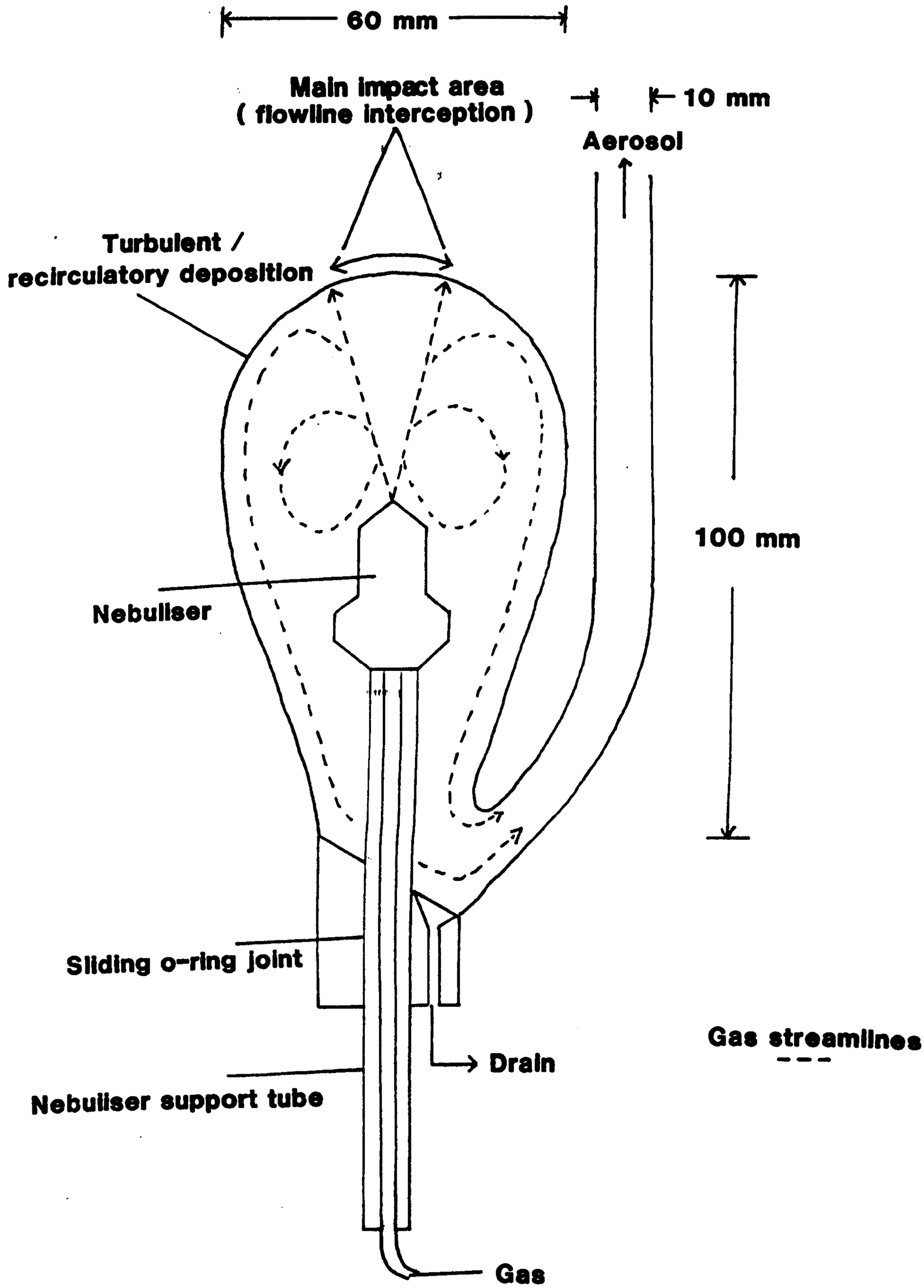

Fig 6.13 The glass bulb recirculatory spray chamber.

It was also noticeable that the TTE decreased with decreasing impact distance. This is because as the impact distance is decreased so progressively more of the smaller particles are lost due to flow line interception [6].

It was attempted to try to decrease the reintrainment of the smaller droplets through the use of baffles extending from the nebuliser tip. Various types of baffle design were tested but none showed any increase in the TTE. This is because any decrease in the reintrainment of small droplets was offset by the introduction of new surfaces on to which turbulent deposition could occur. It seemed that what efficiency increase was gained by avoiding reintrainment was simply negated through turbulent deposition.

Although this nebuliser was far from being the required design it compared favourably with the Meinhard nebuliser used in Section 6.3.2.2 indicating that it does have advantages not only in terms of efficiency but also in sample handling as the 30 μm slot is very unlikely to suffer from fibre blockage or "salting up".

6.3.4 *The testing of a new prototype with an improved recirculatory spray chamber*

A new prototype linear conespray was produced which more closely matched the paper design. It was decided to test this device in a newly constructed spray chamber (Fig. 6.14). This chamber was designed to allow free entrainment of small droplets but also to provide the aerosol with the easiest possible path to the ICP. This involved removing any sharp bends in the aerosol take off tubes as it had been noticed with the previous design, that droplets were impinging on the take off arm. In this new design the nebuliser was centrally located in the chamber. This was achieved through the use of a three pronged

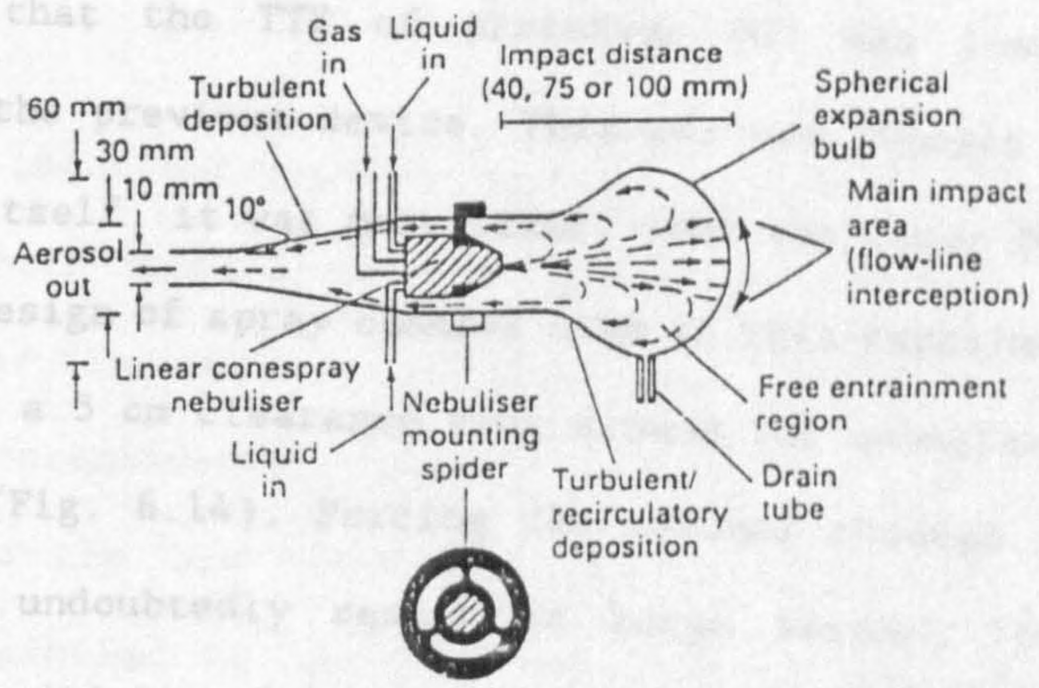

Fig 6.14 The redesigned glass bulb recirculatory spray chamber.

spider. The chamber was constructed from polypropylene and the glass bulb part of the chamber was interchangeable, this allowed the use of bulbs of different sizes which produced different impact distances.

6.3.4.1 Experimental

The TTE of this nebuliser/spray chamber combination was carried out using the same apparatus and procedure as described in previous sections.

6.3.4.2 Results and Discussion

This new prototype was better than the previous model in that its construction more closely matched the paper design. It was disappointing that the TTE of prototype 002 was lower than that obtained with the previous device. This was not thought to be due to the nebuliser itself, it was more likely that the lower TTE was due to the different design of spray chamber used in this experiment. This new design only had a 5 cm clearance ring around the nebuliser on the way to the plasma (Fig. 6.14). Forcing the aerosol through such a small aperture would undoubtedly result in large aerosol losses due to turbulent desposition. Although it is still believed that the philosophy of placing the nebuliser in the centre of the spray chamber is correct this particular design was inappropriate for the reason given above.

The spray produced by prototype 002 was much finer than had been observed with even the best Meinhard nebuliser. The total transport efficiency results are shown in Table 6.2, below.

Table 6.2 Efficiency of new prototype Linear Conespray

Impact Distance (mm)	Liquid-to-Gas Ratio (V/V) x 10^3	Transport Efficiencies (%) Side 1	Side 2	Both sides
Gas Flow Rate = 0.75 l min^{-1}		Liquid Flow Rate = 0.5 ml min^{-1}		
40	0.66	4.64	4.64	2.30
75	0.66	4.42	5.31	2.67
105	0.66	4.98	5.035	2.63
Gas Flow Rate = 1 l min^{-1}		Liquid Flow Rate = 2 ml min^{-1}		
40	2.0	3.64	3.86	1.93
75	2.0	3.49	3.75	1.82
105	2.0	2.88	3.01	1.54

The most important point to notice from these results is that the efficiency of both sides working in unison is not simply the additive value of their independent efficiencies. This demonstrates the importance of recombination in spray chambers as one of the factors contributing to the low efficiency of these devices. It was also noticed that, similar to the last experiment, transport efficiency increased with decreasing liquid to gas ratios which is in complete agreement with the results produced by Sharp [3].

It was unusual, in this study, that the TTE did not increase with increasing impact distance at a liquid to gas ratio of 2.0×10^{-3}. This was exactly the opposite of what had been observed in all the previous experiments. This seems to be in complete agreement with the visual observation that a much finer aerosol was produced by the second prototype. Increasing the impact distance only allows more of the larger droplets to make their way to the plasma. The fact that there was little difference in the TTE with increasing impact distance

indicated that the aerosol produced by 002 was indeed much finer than that produced by 001.

The main problem with this nebuliser was in its construction. It was never possible to produce a device which matched the paper specifications even after five attempts. The problem was in the alignment and shape of the slot gas jet. The shape of the slot varied between being convex and concave which had a great impact on the performance of the device. It was also difficult to place the slot in exactly the correct position and this often resulted in slots that were badly misaligned or in completely the wrong position. These experiments suggest a great deal of promise for the Linear Conespray but a more reliable method of manufacture will have to be found.

6.4 *THE USE OF A HEATED IMPACT BEAD IN ICP-OES*

It was described earlier that the main purpose of a spray chamber is to remove the larger droplets which cannot be completely atomised in the plasma. Impact beads are often incorporated into spray chambers because they can modify the spray in such a way that there may be an increase in the volume of particles in the smaller size ranges. Impact beads should ideally have a bluff shape, but the tangential surfaces must have a sufficiently gentle curve so that deposited solution can run to the rear without being renebulised. Spherical impact beads are most commonly used but the ideal impact bead would have a spherical front with a conical end section, to prevent flow separation [6].

Impact beads suffer from two main disadvantages, the renebulisation of deposited solution was mentioned above, but the actual deposition of solution on the impact bead can cause memory effects and extended washout times. The ideal impact bead would never be touched by the solution, this may sound implausible but it has been

achieved through the use of heated impact beads.

The process of heat transfer to droplets has been investigated by Wachters and Westching [7]. These authors investigated the heat transfer to droplets colliding with a hot surface and the observations made may be of use in the design of analytical devices.

For larger droplets (2.3 mm) they found that no bounce occurred until the surface of the hot plate reached a temperature of 170°C. At this temperature there is actual physical contact with the surface and the vapour produced at the interface beaks through the droplet and produces a fine spray from the surface of the trapped particle. As the temperature is increased so the vapour produced increases and this cushions the droplet. This results in a decrease in the degree of contact between the droplet and the surface until at 220°C the droplets bounce smoothly. As the temperature is increased bubbles of vapour continue to form within the droplets. This results in an explosive release of spray until at 350°C the vapour cushion is sufficient to prevent any contact with the surface and the intact particle behaves like a rubber ball.

They also found that for a heated surface (400°C) the behaviour of the droplet on impact was dependant on its Weber number We. We is given by

$$We = \frac{\rho_g U_r^2 L}{\sigma}$$

The Weber number expresses the ratio of the dynamic forces acting upon the droplet to the surface tension forces. At lower Weber numbers (We<30), the droplets bounce smoothly, but as the Weber number increases in the range 30-80, the bouncing process is accompanied by

severe body deformations that can lead to the ejection of daughter particles after the droplet leaves the surface. At We = 89 and above, the droplet spreads into a thin film above the heated surface and then disrupts into a fine spray. It is this process that is of potential use in analytical devices because it would provide a means of fragmentation of the larger droplets without physical contact of the liquid on the impact bead. Aerodynamic forces were absent in the work carried out by Wachters, but the presence of such forces would cause the flattening of droplets thereby increasing their Weber number which would undoubtedly encourage fragmentation. With all these facts in mind a heated impact bead spray chamber was designed and is shown in Figs. 6.15 and 6.16. In this case the heated impact bead was actually a Ta strip. This strip was mounted between two 5 mm Cu electrodes which had been gold plated. The electrodes were placed 20 mm apart and the Ta strip was held in place by two gold plated screws. The electrodes were held in place by a ceramic block. This whole assembly was then placed in the glass part of the spray chamber when in use.

6.4.1 *The temperature calibration of the Ta strip*

6.4.1.1 **Thermal Crayons**

The first attempt at calibration of the temperature of the Ta strip made use of thermal crayons (Thermochrom W. Faber-Catell, Germany). These crayons change colour at a set temperature and it was hoped to build up a resistance vs temperature calibration curve.

The heated impact bead was connected to a Variac and transformer so that a suitable current could be produced to heat up the Ta strip. The strip was connected to an ammeter and digital volt meter in order that the resistance of the strip could be monitored. Thermochrom crayons were then used to prepare a calibration line of resistance vs

Fig 6.15 The heated impact bead.

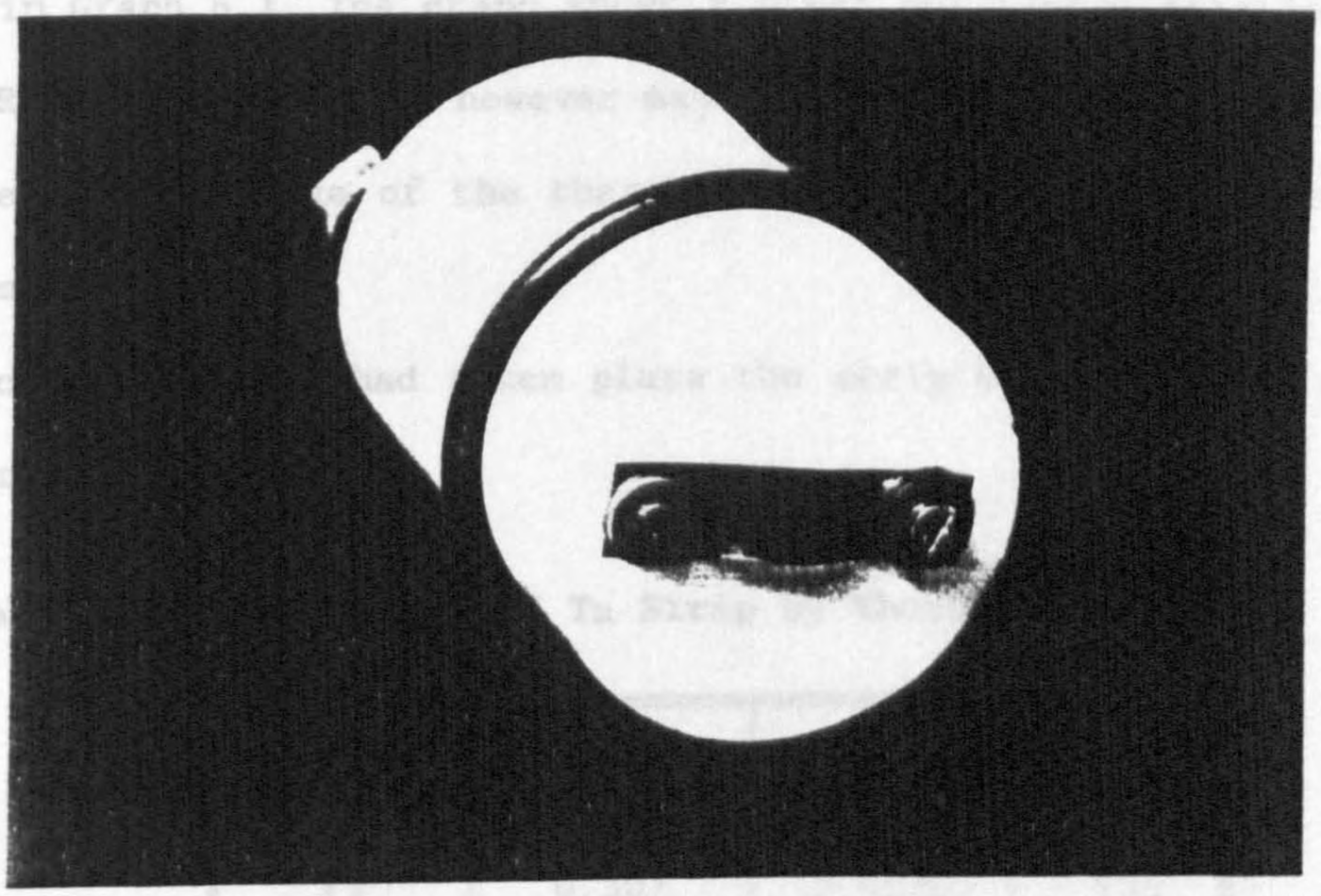

Fig 6.16 The heated impact bead spray chamber.

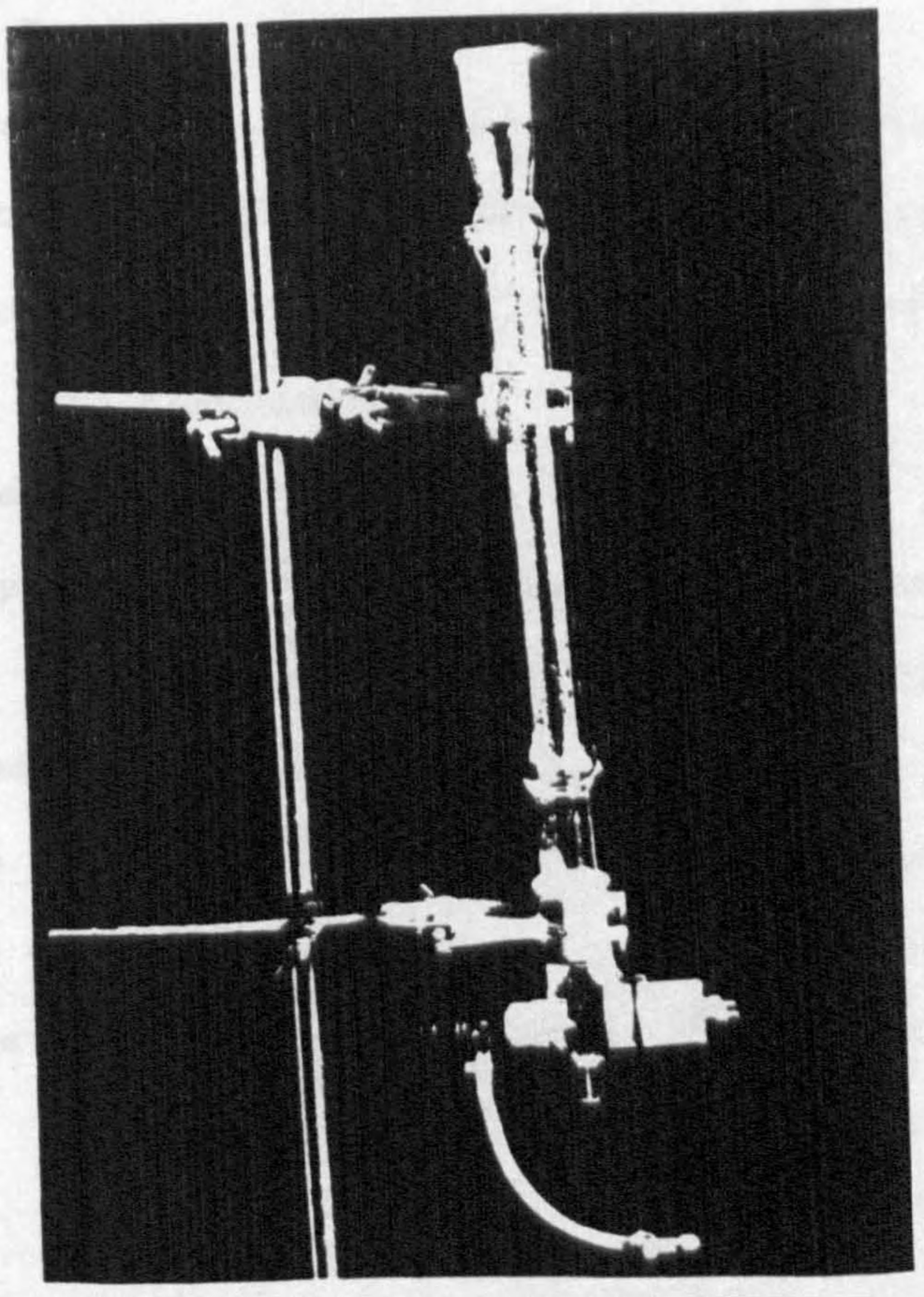

temperature at various power settings. The results are shown in Table 6.3 and in Graph 6.1. The graph shows a clear cut linear relationship between R and T, there were however major problems with this approach.

1) The colour change of the thermal crayons was not always easily observed.

2) Once calibration had taken place the strip was in no fit state for further work.

Table 6.3 Calibration of Ta Strip by Thermochrom Crayons

I (Amps)	V (Volts)	R (Ohms)	Temp (°C)
13	0.307	0.0236	150
15	0.362	0.0241	200
17	0.438	0.0258	280
19	0.518	0.0273	350
19	0.537	0.0283	375
20.5	0.617	0.0301	500
21	0.652	0.0310	600
27.5	0.718	0.0319	650

6.4.1.2 Optical Pyrometer

This device was not suitable at all owing to the fact that the strip had to be heated to 800°C for calibration to take place. Heating of the strip to this temperature caused rapid oxidation of the strip which shortened its life dramatically.

6.4.1.3 Thermocouple

The thermocouple (Type 1601, Comark, UK) probe was held against the Ta strip and the resistance of the strip measured as the temperature was gradually increased. The results of this experiment are shown in Graph 6.2. The calibration of the strip was repeated twice and the calibration curves superimposed on the previous graph. It is noticeable that the resistance of the strip increased after each

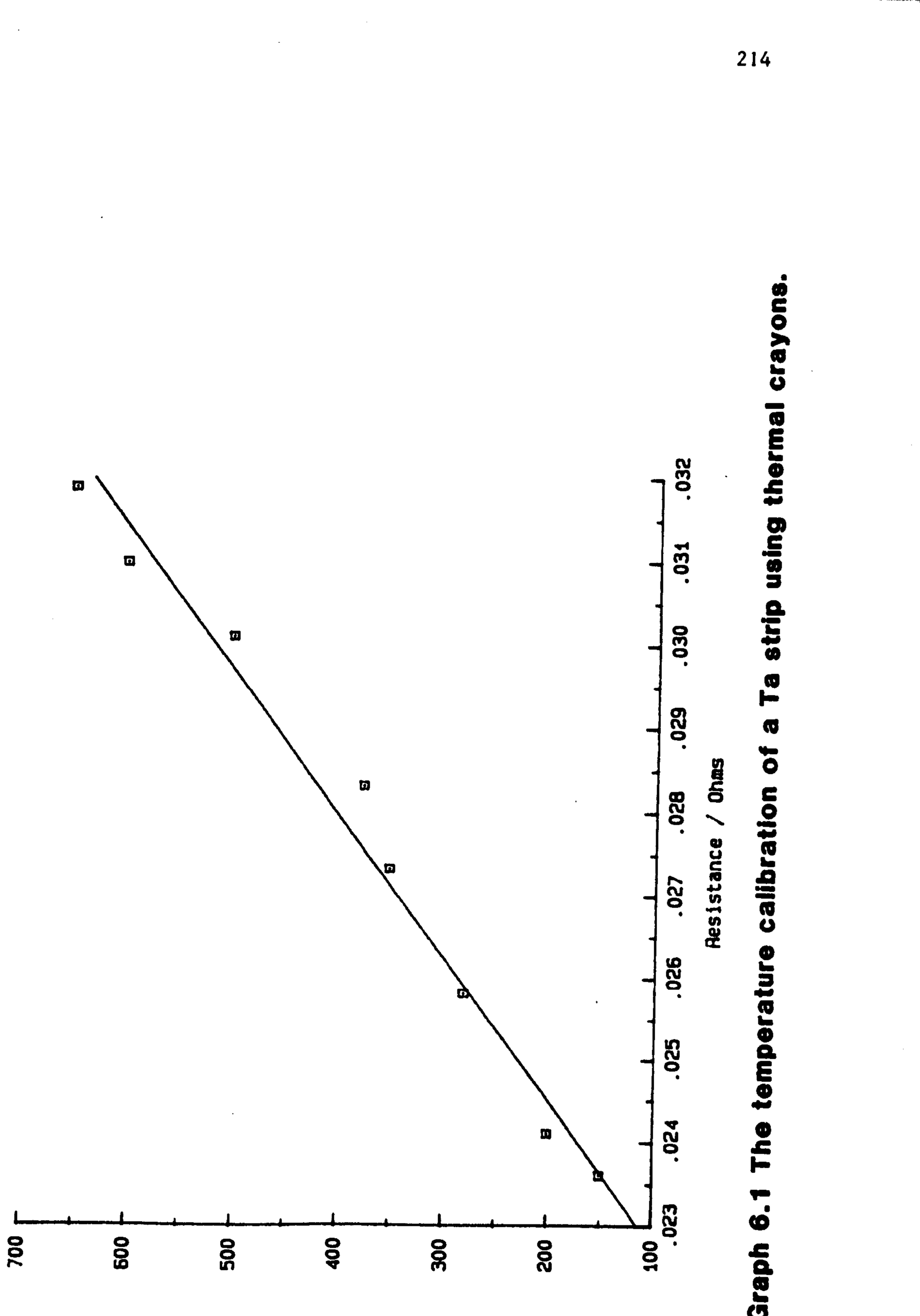

Graph 6.1 The temperature calibration of a Ta strip using thermal crayons.

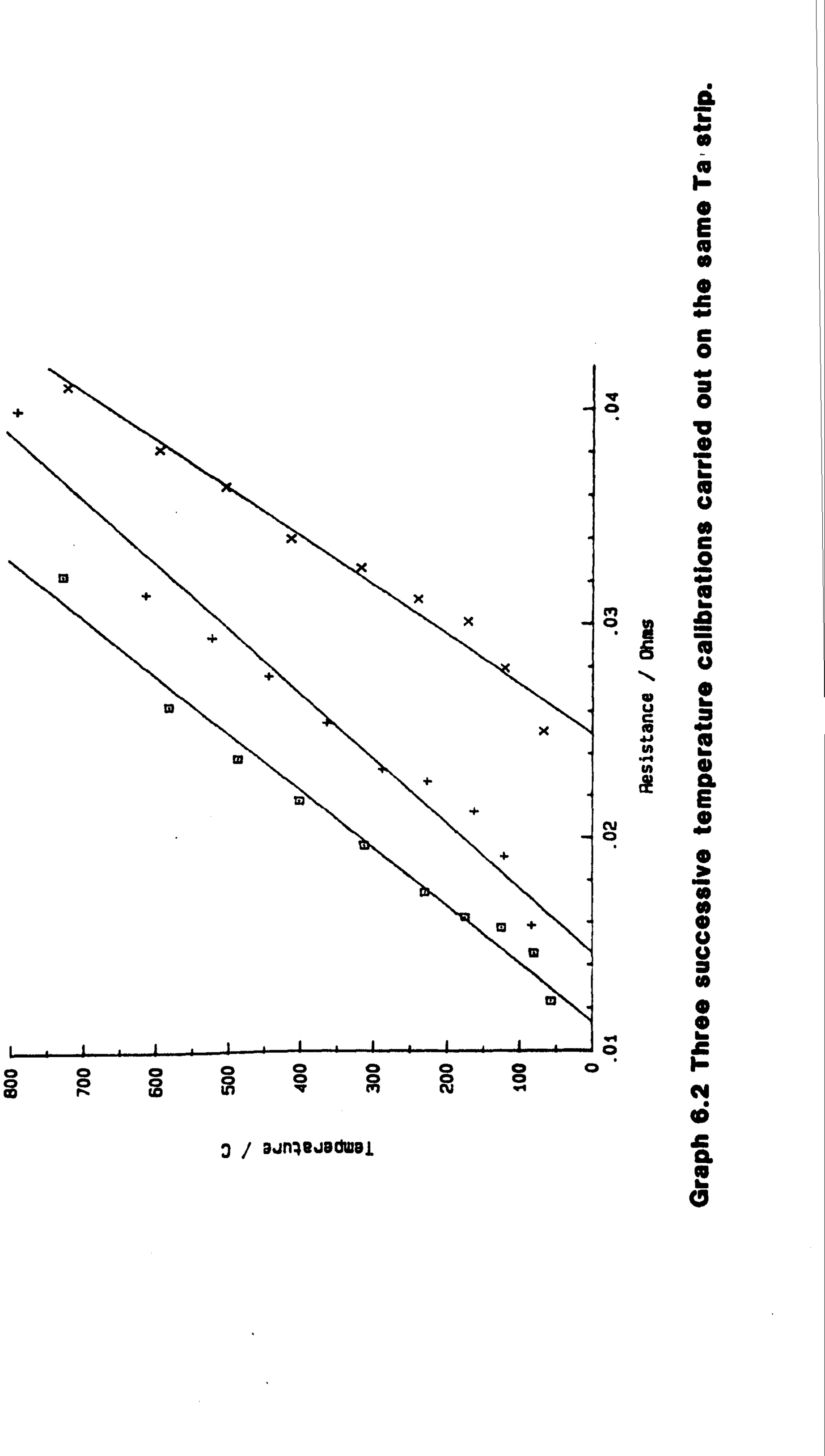

Graph 6.2 Three successive temperature calibrations carried out on the same Ta strip.

successive calibration. This was due to oxidation of the strip at higher temperatures i.e. in excess of 500°C.

The calibration procedure was repeated twice on a different strip but this time care was taken to ensure that the temperature of the strip never exceeded 550°. The resulting calibrations were plotted and can be seen in Graph 6.3.

From the two calibration lines it can be seen that there was no great difference between the two calibrations. This was useful in that it meant that Ta strips could be calibrated in air without oxidation as long as the temperature was kept below 550°C.

6.4.2 *The total transport efficiency of the Heated Impact Bead (HIB) spray chamber*

6.4.2.1 Experimental

A suitable Ta strip was selected and mounted on the copper electrodes. A resistance vs temperature calibration was carried out as before and the results are shown below in Table 6.4

Table 6.4 Calibration of new Ta Strip

I (Amps)	V (Volts)	R (Ohms)	Temp (°C)
12	0.16	0.0133	64
18.3	0.272	0.0149	139
24	0.429	0.0179	275
26	0.539	0.0207	390
27.75	0.632	0.0228	480

The calibration line obtained from these results is shown in Graph 6.4.

The total transport efficiency of the HIB chamber was measured at the chamber exit using the same silica gel traps that were used earlier. The nebuliser used in this study was a Meinhard TR-30-A3. This nebuliser was set at an impact distance of 10 mm from the heated Ta

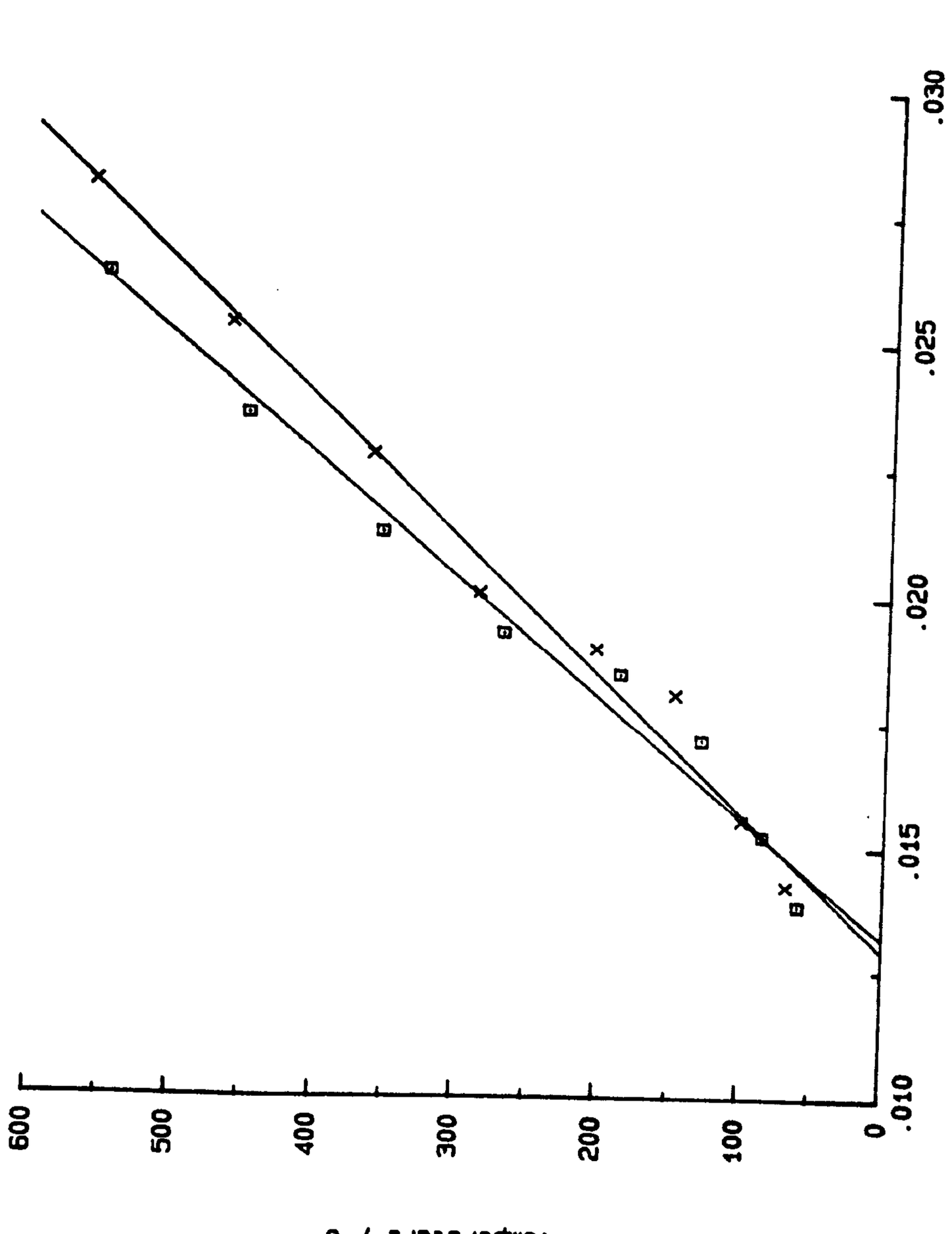

Graph 6.3 Duplicate calibration of a Ta strip.

Graph 6.4

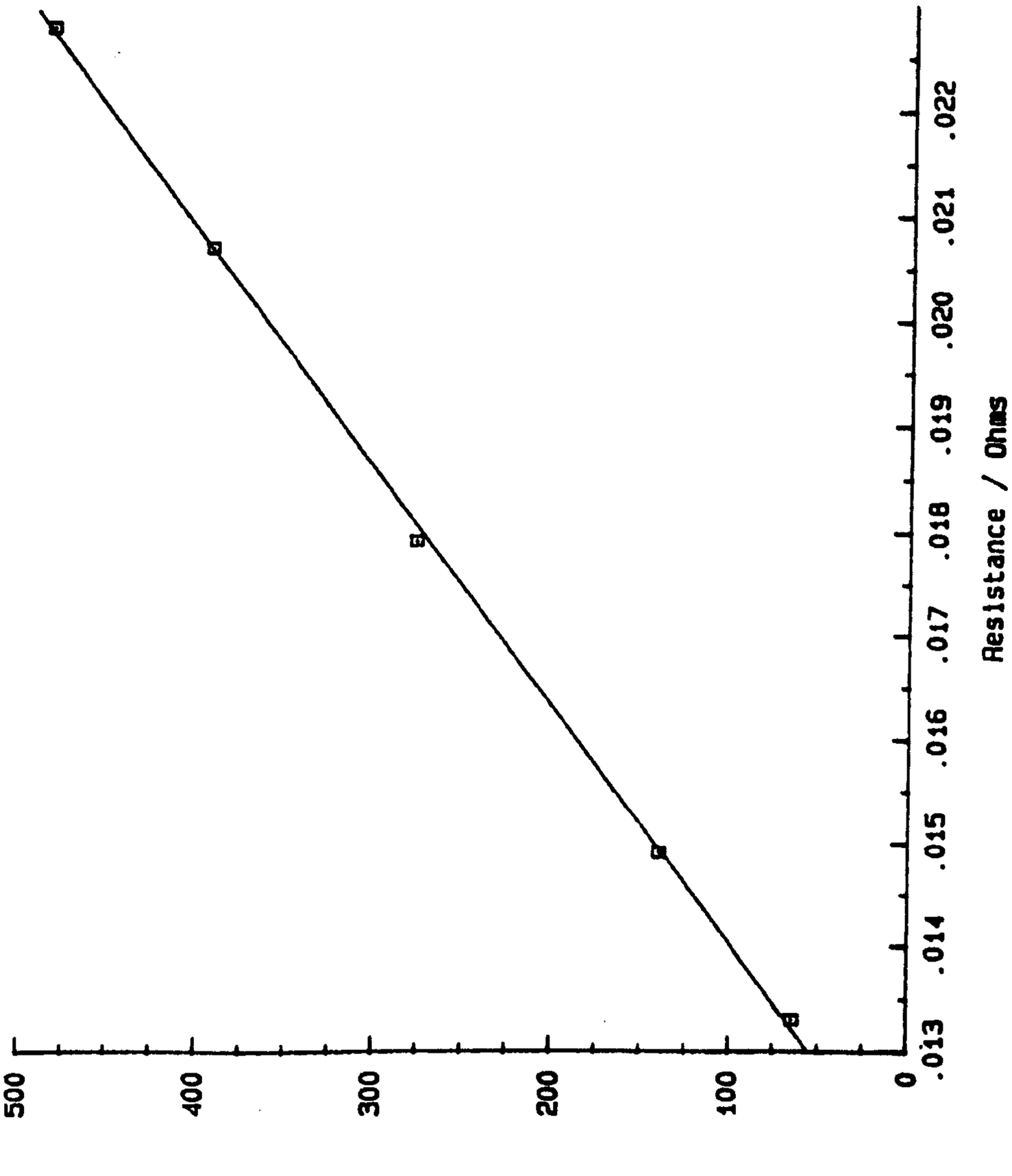
500
400
300
200
100
0
.013
.014
.015
.016
.017
.018
.019
.020
.021
.022
Resistance / Ohms
Temperature / C

strip and the gas and liquid flow rates were set at 1 l min^{-1} and 1 ml min^{-1} respectively. The total transport efficiency was then measured at various power settings on the Variac. The results obtained are shown in Table 6.5 below.

Table 6.5 The total transport efficiency of the HIB chamber measured at the chamber exit

Power Setting on Variac	V Volts	I Amps	R Ohms	P Watts	T1 °C	TTE %
0	0	0	0	0	23	1.46
5	0.119	9.75	0.0122	1.16	23	1.58
10	0.174	12.00	0.0145	2.09	23	1.92
15	0.225	14.25	0.0158	3.20	27	2.19
20	0.273	18.00	0.0152	4.91	31	3.30
25	0.321	21.75	0.0148	6.98	39	5.06
30	0.369	24.00	0.0154	8.86	43	5.56
35	0.414	27.00	0.0153	11.18	47	6.98
40	0.472	30.50	0.0155	14.40	51	8.49
45	0.518	32.25	0.0161	16.71	56	16.71

T1 = Temperature at the chamber exit

This experiment was repeated, but this time a condenser was fitted to the spray chamber exit port and the TTE was measured at the condenser exit.

Table 6.6

Power Setting on Variac	V Volts	I Amps	R Ohms	P Watts	T1 °C	T2 °C	TTE %
0	0	0	0	0	21	14	1.24
5	0.123	9.75	0.0126	1.20	21	14	0.98
10	0.174	12.00	0.0145	2.09	21	14	1.06
15	0.224	14.25	0.0157	3.19	21	14	1.12
20	0.274	18.00	0.0152	4.93	21	14	1.05
25	0.322	21.50	0.0150	6.92	22	14	1.17
30	0.377	24.00	0.0157	9.05	21	14	1.27
35	0.435	27.00	0.0161	11.75	21	14	1.66
40	0.483	30.25	0.0160	14.61	20	14	1.81
45	0.530	32.25	0.0164	17.09	21	14	1.76
50	0.579	35.00	0.0165	20.27	21	14	1.69

T1 = Temp. at the condenser exit T2 = Temp of water in condenser

6.4.2.2 **Results and Discussion**

Graphs were plotted of both sets of results and are shown in Graphs 6.5 and 6.6.

The very small changes in resistance in both experiments seemed to indicate that the temperature of the strip was not increasing significantly as the power was increased. The amounts of water vapour emanating from the chamber, however, did increase. The results taken at the condenser exit indicate that the increase in the TTE after vapour was removed was only very slight. This suggests that all the energy was being used simply to evaporate water deposited on the strip. The electical power required to vapourise 1 g of H_2O/min is 37 watts. For droplets to cease making contact with the strip the power would need to be greater than 37 watts. In neither experiment did the power exceed this value which explains why droplets were able to collect on the strip. This evaporation process caused such a cooling of the strip that the temperature never reached the critical 350°C mark where droplets no longer made contact with the strip. The R vs T calibration curve suggests that the temperature of the strip was around 150-200°C. There are difficulties in comparing the resistance of the strip during calibration and the resistance of the strip when in use. This is again due to the evaporative cooling which can be illustrated by referring to Fig. 6.14 a,b and c.

When the strip is heated it becomes visibly red in the middle and this area corresponds to the part of the strip with highest resistance and temperature. When aerosol is sprayed at the strip the resistance profile of the strip changes dramatically and the strip is cooled in the centre portion. The resistance calculated from the voltage and current measurements is the average resistance of the strip and takes

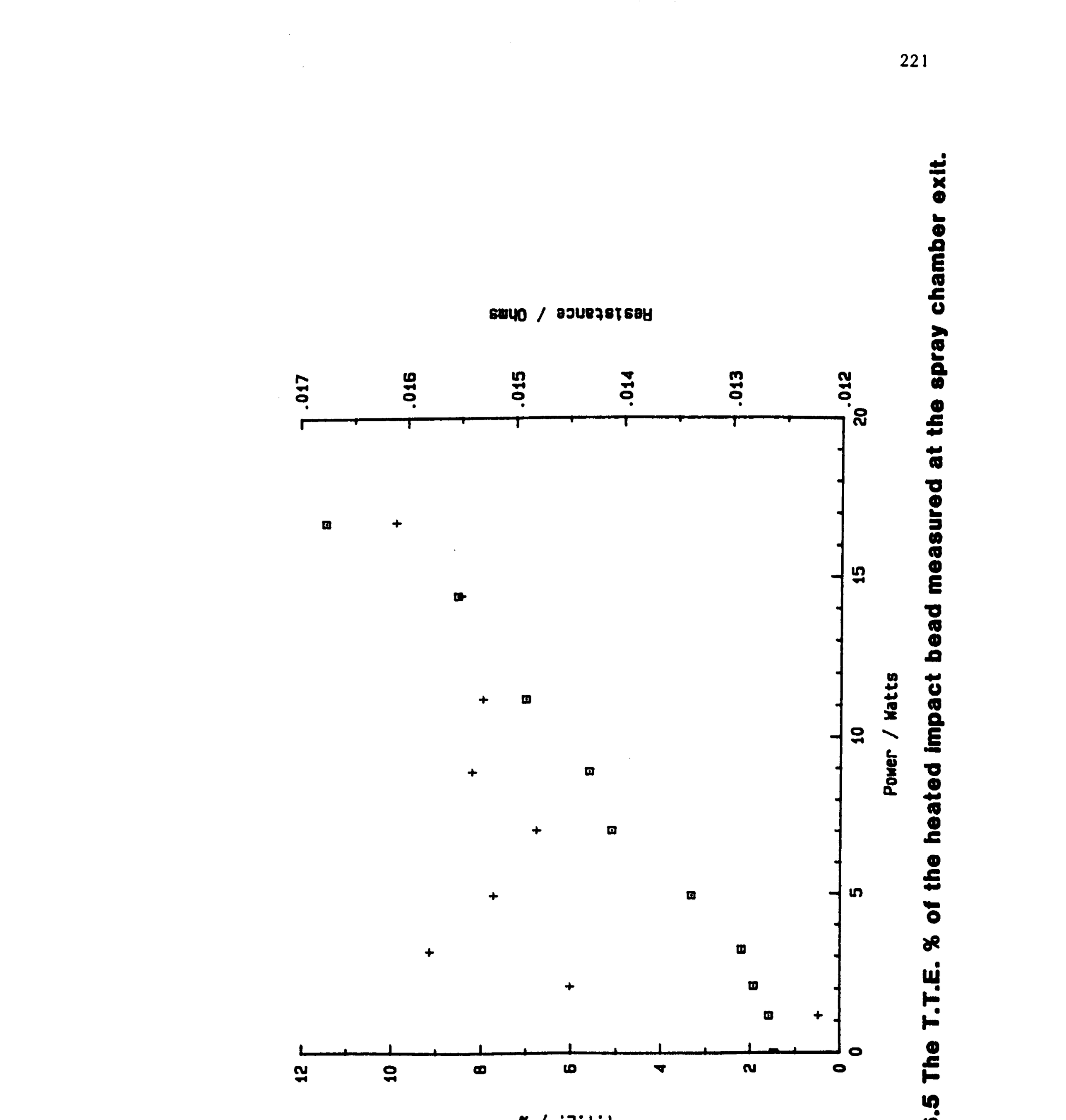

Graph 6.5 The T.T.E. % of the heated impact bead measured at the spray chamber exit.

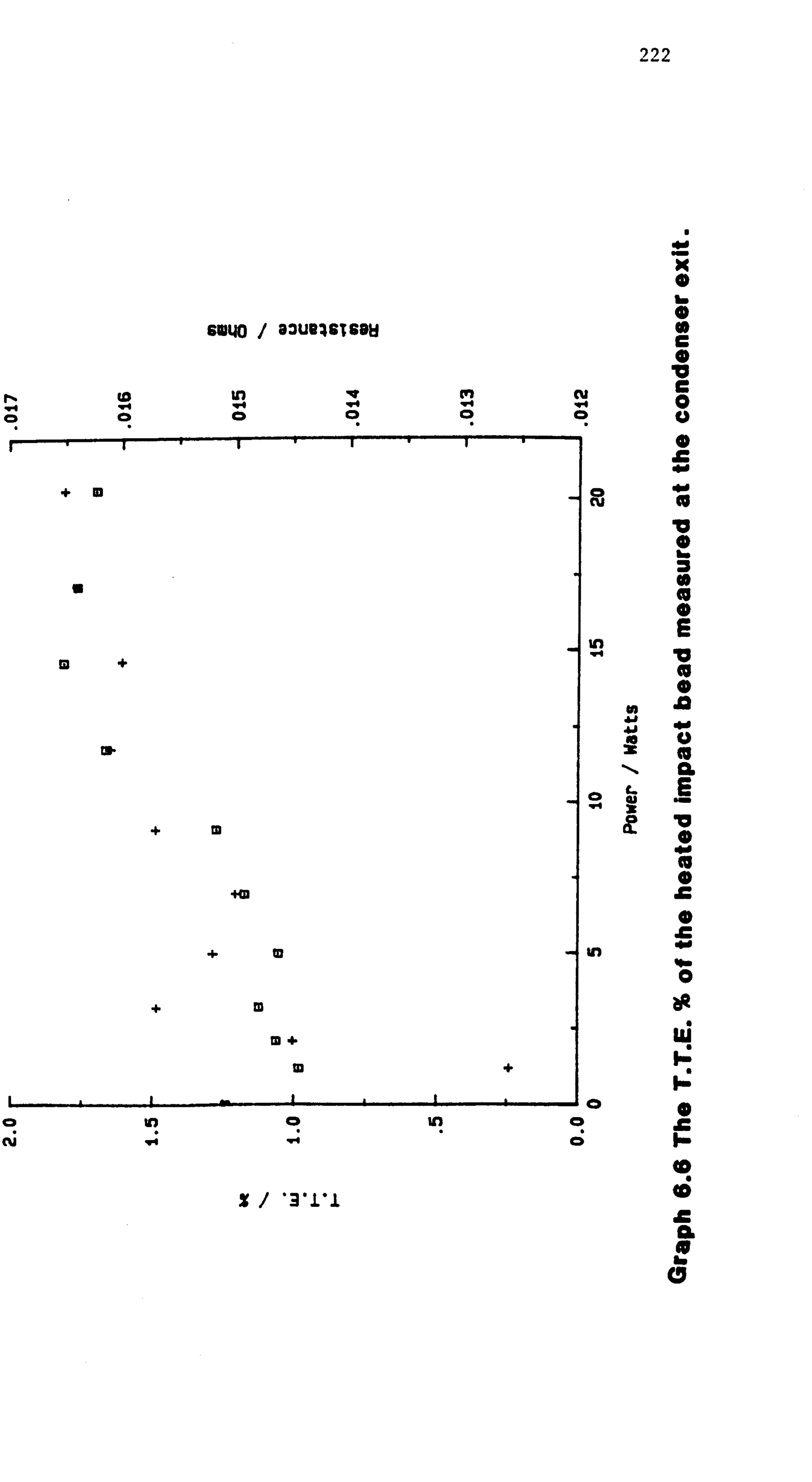

Graph 6.6 The T.T.E. % of the heated impact bead measured at the condenser exit.

Fig. 6.14 R & T Profile of Ta strip under various conditions

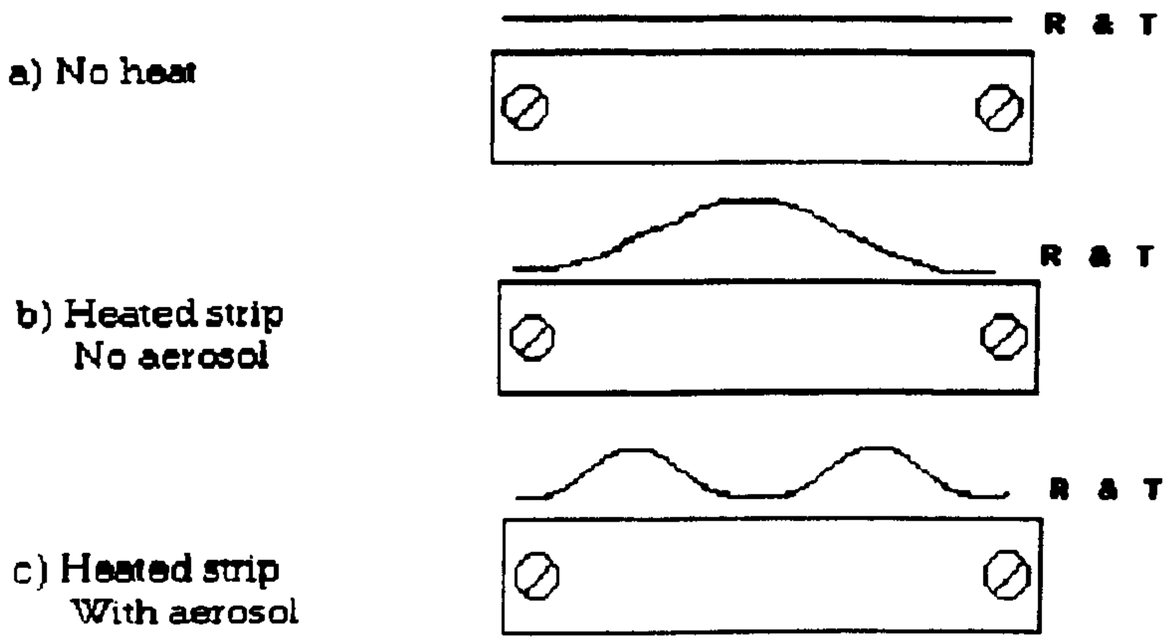

no account of the differences in the resistance profile. From (b) and (c) it is easily seen that the resistance profiles will be completely different in the working situation c.f. the conditions under which calibration of the strip was achieved. The resistance measured from the V and I of the strip only gives an indication of the average temperature of the strip and not the temperature at the point of impact of the aerosol.

This experiment was repeated but the liquid flow rate was dropped to 0.2 ml min^{-1}, it was hoped that this would reduce the evaporative cooling and allow some of the processes observed by Wachters and Westerling to occur. The impact distance was left at 10 mm and the gas flow rate was kept at 1 l min^{-1}. The total transport efficiency was measured at the spray chamber exit and the results are shown in Table 6.7 below and in the accompanying graph (Graph 6.7).

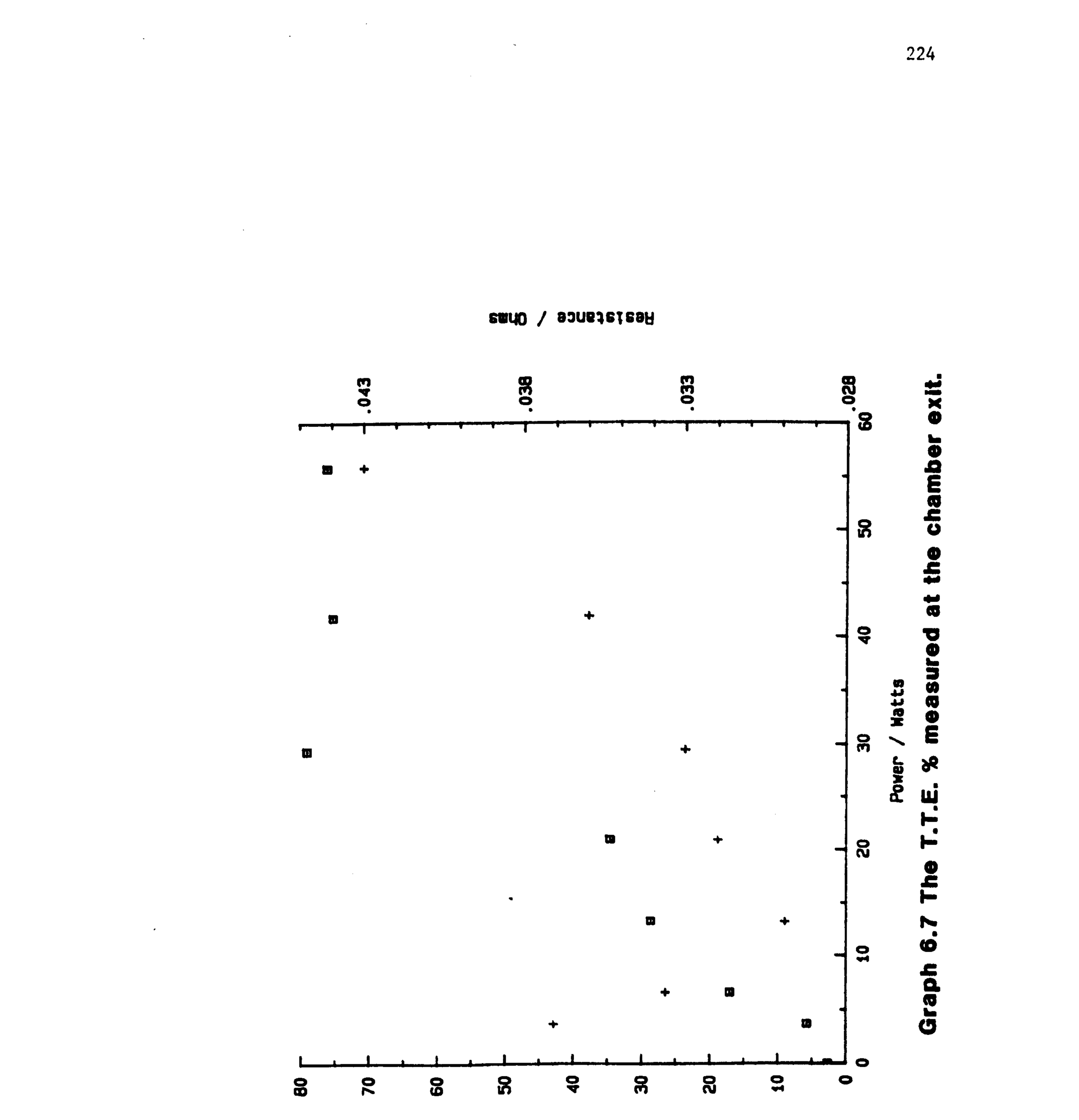

Graph 6.7 The T.T.E. % measured at the chamber exit.

Table 6.7 T.T.E. of HIB at the spray chamber exit

V Volts	I Amps	R Ohms	P Watts	T at exit °C	TTE %
-	-	-	-	21	2.68
0.371	10	0.037	3.71	29	5.77
0.471	14	0.034	6.59	39	17.02
0.627	21	0.030	13.17	48	28.54
0.817	25	0.032	20.85	61	34.48
0.980	30	0.033	29.40	66	79.00
1.231	34	0.036	41.85	66	75.08
1.550	36	0.043	55.80	70	76.00

The unreliability of the calibration curves is further confirmed because the resistance event at the lowest power setting was higher than any point on the calibration of this strip (Table 6.4). This was unexpected as it was through that the cooling effect of the water would result in a decrease in resistance. The reason for this high initial resistance is not clear and needs further investigation.

From the graph it can be seen that although initially high the resistance of the strip begins to fall as the power is increased. This can again be explained in terms of evaporative cooling because the extra power is just wasted through evaporation processes.

When the power was raised to 29.4 Watts an interesting phenomena occurred in that the chamber suddenly cleared i.e. there was no condensation in the chamber and the Ta strip appeared to be totally dry. At this point an increase in the power was accompanied by an increase in resistance suggesting that droplets were no longer making contact with the surface of the Ta strip. As the power was increased the strip became visibly hotter and could be brought to red heat. It was found that heating of the strip to red heat for long periods of

time caused oxidation and even failure of the strip. At these higher power settings, the transport efficiency of the chamber was between 75 and 79%. Such large amounts of water vapour would undoubtedly extinguish the ICP so the experiment was repeated with a condenser placed after the chamber to remove the excess vapour. The results obtained are shown in Table 6.8 below.

Table 6.8 The T.T.E. of the HIB at the Condenser Exit

V Volts	C Amps	R Ohms	P Watts	T1 °C	T2 °C	TTE %
-	-	-	-	23	15	6.17
0.324	10.00	0.034	3.24	20	15	3.48
0.415	14.75	0.028	6.12	21	15	4.29
0.541	22.75	0.024	12.03	21	15	6.73
0.655	27.00	0.024	17.68	21	15	6.18
0.830	31.75	0.026	26.35	21	15	6.51
1.140	34.00	0.033	38.76	21	15	6.92
1.525	32.00	0.048	48.80	21	15	*5.04

* Strip failed

T1 = Temp of condenser exit
T2 = Temp of water in condenser

The results were again plotted as a graph (Graph 6.8). The resistance followed exactly the same trend as in the previous experiment, but the total transport efficiency remained reasonably constant i.e. 6.0-6.9. This indicated that the condenser was sufficiently long to remove the excess vapour produced by the high temperature of the heated impact bead. These were a couple of low results but they were due to the cooling effect of water from the condenser falling back on to the Ta strip. The TTE started to rise at the higher temperatures and this may have been due to the occurrence of the processes described earlier causing the shattering of larger droplets. The evaporation of the daughter droplets could cause an increase in the signal observed in our

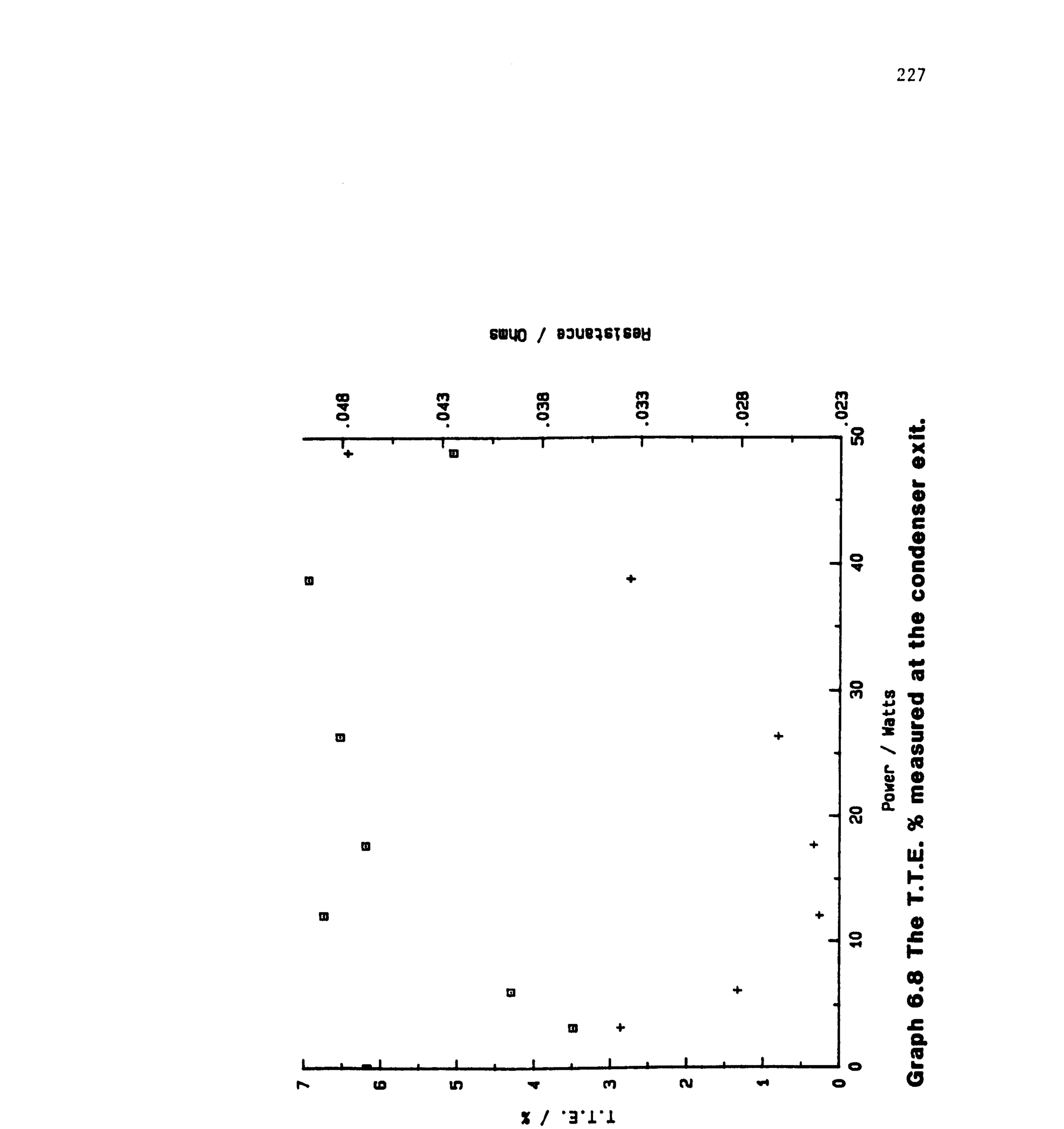

Graph 6.8 The T.T.E. % measured at the condenser exit.

ICP due to concentration of the analyte. This was investigated further in the next section.

6.4.3 *The analytical performance of the heated impact bead spray chamber*

The real test of any novel nebuliser/spray chamber is how well it performs as part of a conventional ICP-OES system. The ICP used in this study was an ARL 3580B ICP-OES and can be regarded as a standard commercial ICP-OES system. The heated impact bead chamber was set up as before and connected to the ICP-OES. The instrument was set up to read the Ca line at 317.93 nm and a blank solution was run at various power settings in order to obtain the background reading. A solution of Ca (10 ppm) was then run at various power settings and the intensity of the Ca line was measured. The results are shown in Table 6.9 below. The small change in background readings suggests that the water flux was not changing and that the condenser was effectively removing the excess vapour.

Table 6.9 The analytical peformance of the HIB Spray Chamber

Voltage V	Current A	Resistence Ohms	Power Watts	Signal	BG	S-BG	EIF
0	-	-	-	6.521	3.35	3.171	1
0.173	11.00	0.0157	1.903	6.120	3.190	2.930	0.92
0.281	18.25	0.0154	5.128	7.264	3.194	4.070	1.28
0.398	24.25	0.0164	9.650	9.435	3.083	6.352	2.00
0.531	30.25	0.0175	16.06	11.360	3.035	8.325	2.63
0.700	35.00	0.0200	24.50	14.140	3.032	11.108	3.50
0.870	40.00	0.0217	34.80	28.600	2.960	25.640	8.06
1.090	40.00	0.0270	43.60	30.770	3.220	27.550	8.69

where EIF = observed $\frac{\text{S-BG}}{\text{S-BG at power = 0 watts}}$

The graph of these results is shown in Graph 6.9. When the power was increased the EIF gradually increased due to evaporation of the larger droplets. When the power reached 34.8 watts the chamber cleared as reported earlier due to the complete evaporation of the water in the chamber. This was accompanied by a great increase in the EIF. Although the spray chamber was able to produce an improvement in the EIF the increase was not as large as had been hoped. This was because the nebuliser/spray chamber arrangement was not working as well as it should. Firstly the nebuliser had not been firing directly at the Ta strip. More importantly droplets formed in the condenser were falling directly on to the Ta strip. This caused the HIB to pulse and produced large clouds of vapour and as a result this caused instability in the plasma.

The experiment was repeated with more accurate positioning of the nebuliser and with the condenser fitted in such a way that droplets of condensation fell harmlessly down the spray chamber wall to the drain without making contact with the Ta strip. The results obtained were much improved and are shown in Table 6.10 below.

Table 6.10 The Analytical Performance of the HIB Under Improved Conditions

Voltage V	Current A	Resistence Ohms	Power Watts	Signal	BG	S-BG	EIF
-	-	-	-	4.888	3.236	1.652	1
0.405	10.00	0.0405	4.050	5.417	3.169	2.248	1.36
0.487	14.00	0.0348	6.818	6.413	3.146	3.263	1.98
0.640	21.00	0.0305	13.44	8.122	3.030	5.092	3.08
0.890	24.00	0.0371	21.36	10.249	3.055	7.194	4.35
0.985	30.00	0.0337	20.19	12.046	3.136	8.910	5.39
1.256	32.00	0.0392	40.19	29.987	4.340	14.920	14.92
1.470	35.00	0.0042	51.45	44.590	4.340	40.250	24.36

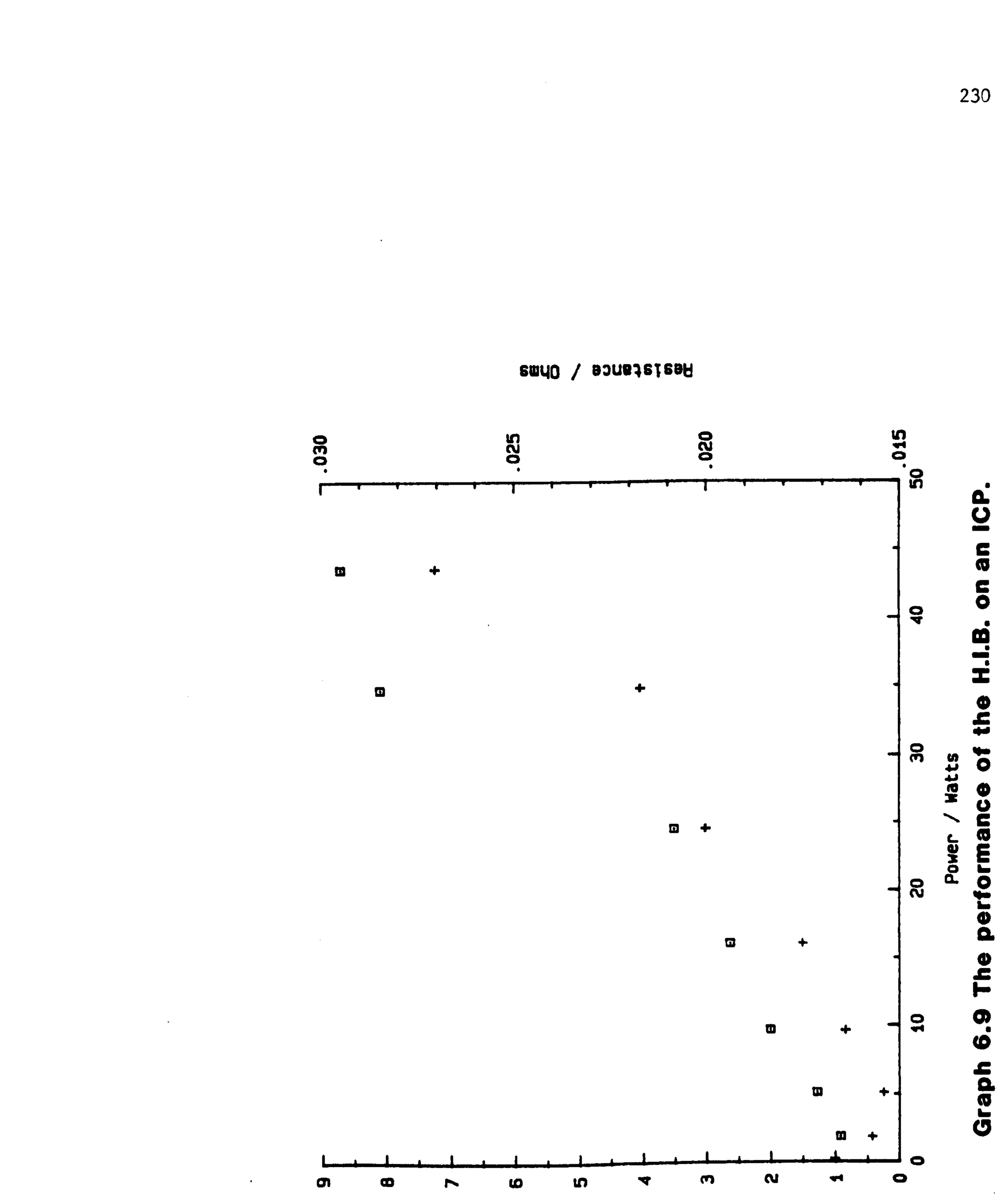

Graph 6.9 The performance of the H.I.B. on an ICP.

In this experiment the chamber behaved extremely well and the results are shown in Graph 6.10. The EIF increased gradually with power until at 40 Watts the chamber cleared as reported in earlier experiments and the EIF increased drastically. At the highest power setting used in this experiment the EIF was ~25. This compares favourably with the results obtained with heated spray chambers which have generally produced up to a 10 fold increase in nebuliser efficiency.

6.5 *CONCLUSIONS*

The use of the linear conespray nebuliser in free entrainment spray chambers has produced some very encouraging results when compared to conventional nebuliser spray chamber combinations. The main problem with this device is that it is incredibly difficult to manufacture in its present form and it has so far been impossible to produce a good example of the paper design.

The heated impact bead produced very promising results which compare favourably with other attempts to improve the efficiency of sample introduction systems for ICP-OES. The only problem that exists with the current design is that it is nowhere near robust enough for routine operation. The Ta strips used in the device break far too easily and a way round this will have to be investigated.

One possible design would utilize a quartz disc heated by a device of very high thermal mass e.g. an HT Firerod (Whatlow Electric Mfg. Co., Missouri, USA).

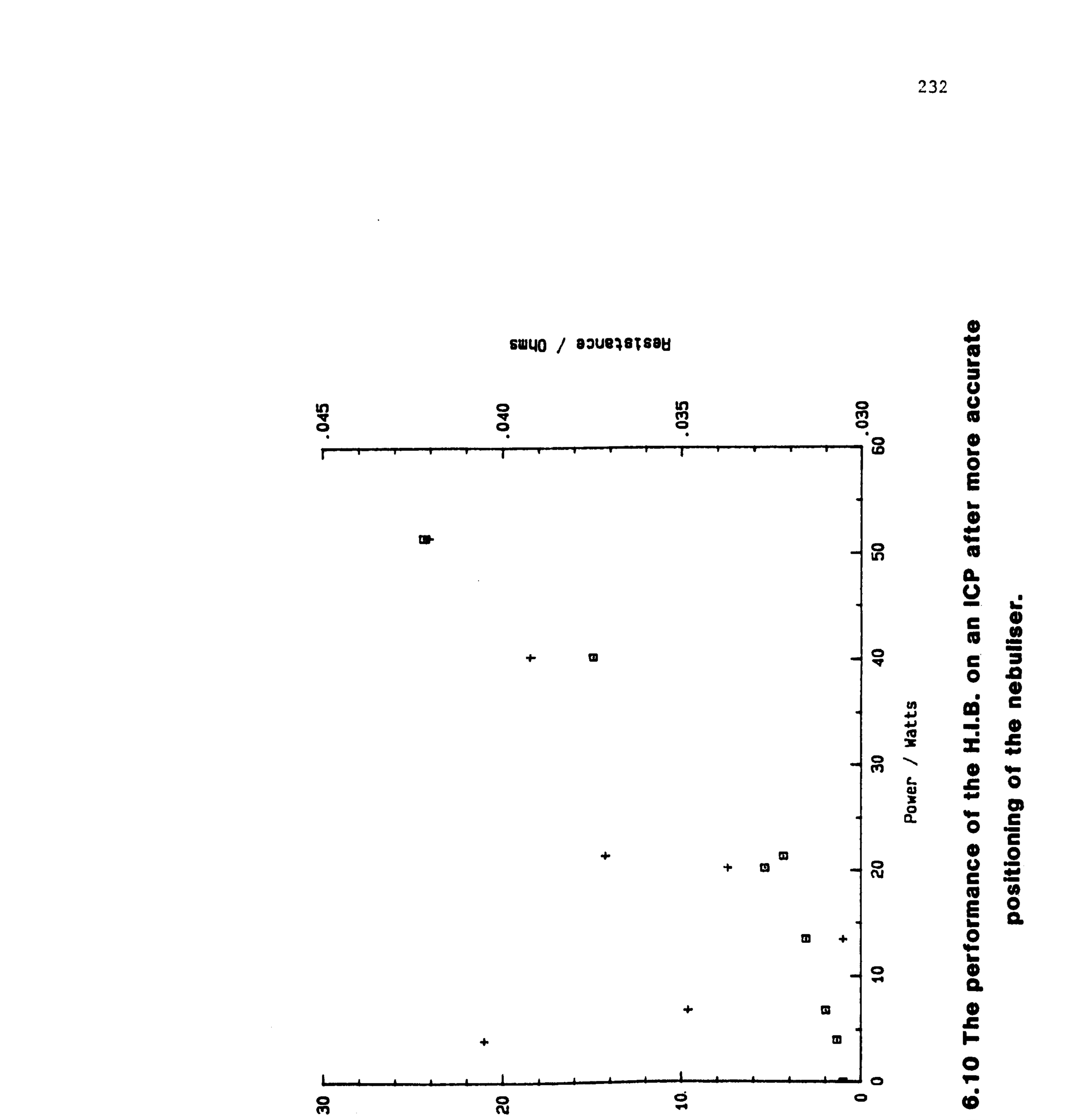

Graph 6.10 The performance of the H.I.B. on an ICP after more accurate positioning of the nebuliser.

REFERENCES

1. Ebdon L., Hill S. and Ward R.W., Analyst, 1987, **112**, 1-15.

2. Gardiner P.E., Braetter P., Gercken B. and Tomiak A., JAAS, 1987, **2**, 375-378.

3. Sharp B.L., JAAS, 1988, **3**, 613-651.

4. Thompson M. and Walsh J.N., 'A Handbook of Inductively Coupled Plasma Spectrometry', Blackie, Glasgow, 1983, 1st edn.

5. Ripsen P.A.M. and de Galan L., Spectrochim Acta, 1981, **36B**, 71.

6. Sharp B.L., JAAS, 1988, **3**, 939-963.

7. Wachters L.H.J. and Westerling N.A.J., Chemical Engineering, Science 1966, **21**, 1047-1056.

CHAPTER SEVEN

SUGGESTIONS FOR FURTHER WORK

7.1 *SUGGESTIONS FOR FURTHER WORK*

There is a great deal of scope for further research in many of the areas investigated during this work. The first area where further research would be useful is to investigate in more detail the temporal variation in the speciation of copper at the Laverock Brae farm site. The temporal variation in the speciation of Zn, Cd and Pb could also be studied as the sewage sludge applied to the above site is also contaminated with these three heavy metals. It would be of interest to combine the speciation results obtained with parallel field experiments on plant uptake of heavy metals as this would confirm whether or not changes in metal speciation in soil solutions affects the plant uptake of heavy metals.

While the HPLC separation has been largely successful there is still scope for improvement. The resolution of the separation could be improved by placing various columns with different molecular weight fraction ranges in series, although this would have the disadvantage of greatly increasing the analysis time. The best improvement to the HPLC analysis would be to completely eliminate the effects of coulombic repulsion. This could be achieved through the use of alternative size exclusion packings to the silica packing used in this study. This silica based packing was particularly prone to the effects of coulombic repulsion. There are currently available packings which are based on polymers and should therefore be much less affected by coulombic repulsion. The complete elimination of coulombic repulsion would ensure that the sample equilibria is maintained during analysis, especially if the HPLC eluent is identical to the sample under study in terms of both pH and total ionic strength.

This question of the preservation of sample equilibria could be further tested through the use of computer models e.g. Soilchem by Garrison Sposito. This would involve the preparation of model soil solutions with ligand and metal concentrations similar to the field of interest. These concentrations could be entered into soilchem which would then calculate the theoretical concentration of each metal ligand pair based on thermodynamics. These results could then be compared with those produced by running the same model solution with the SEC-GFAAS method. Major differences between the two sets of results would indicate that there were transfers of metals between ligands during the analysis.

Finally the concept of a heated impact bead to improve the detection limits of ICP-OES was tested in this research and the results indicate that this is indeed a very promising concept that could prove extremely fruitful with further development. It is possible that such a device could produce ICP-OES detection limits more akin to those obtainable with GFAAS. This would make ICP-OES more useful as a detector in speciation studies.